NASA CONTRACTOR REPORT

NASA CR-2177

NASA CR-2177

EFFECTS OF VIBRATION AND SHOCK ON THE PERFORMANCE OF GAS-BEARING SPACE-POWER BRAYTON CYCLE TURBOMACHINERY

II - Sinusoidal and Random Vibration

by J. M. Tessarzik, T. Chiang, and R. H. Badgley

Prepared by
MECHANICAL TECHNOLOGY INCORPORATED
Latham, N.Y. 12110
for

NATIONAL AERONAUTICS AND SPACE ADMINISTRATION • WASHINGTON, D. C. • MARCH 1973

1. Report No.	2. Government Accession No.	3. Recipient's Catalog No.
NASA CR-2177		

4. Title and Subtitle	5. Report Date
EFFECTS OF VIBRATION AND SHOCK ON THE PERFORMANCE OF GAS-BEARING SPACE-POWER BRAYTON CYCLE TURBOMACHINERY II - SINUSOIDAL AND RANDOM VIBRATION	March 1973
	6. Performing Organization Code
7. Author(s) J. M. Tessarzik, T. Chiang, and R. H. Badgley	8. Performing Organization Report No. MTI-71TR66
	10. Work Unit No.
9. Performing Organization Name and Address Mechanical Technology Incorporated 968 Albany-Shaker Road Latham, New York 12110	11. Contract or Grant No. NASw-1713
	13. Type of Report and Period Covered Contractor Report
12. Sponsoring Agency Name and Address National Aeronautics and Space Administration Washington, D.C. 20546	14. Sponsoring Agency Code

15. Supplementary Notes

Project Manager, Henry B. Tryon, Power Systems Division, NASA Lewis Research Center, Cleveland, Ohio

16. Abstract

The vibration response of a gas-bearing rotor-support system has been analyzed and experimentally documented for sinusoidal and random vibration environments. The NASA Brayton Rotating Unit (BRU), 36,000 rpm, 10 KWe turbogenerator, was subjected in the laboratory to sinusoidal and random vibrations to evaluate the capability of the BRU to (1) survive the vibration levels expected to be encountered during periods of nonoperation and (2) operate satisfactorily (that is, without detrimental bearing surface contacts) at the vibration levels expected during normal BRU operation. Test results indicated the onset of journal and thrust bearing surface contacts at relatively low random vibration input levels. Chrome oxide bearing surface coatings were found to operate satisfactorily, permitting multiple contacts without evidence of degradation. Analysis of axial random vibration response of the BRU was accomplished by using a linear three-mass model. Response power spectral density was calculated for specified input random excitation, with particular emphasis upon the dynamic motions of the thrust bearing runner and stator. A three-mass model with nonlinear representation of the engine isolator mounts was used to calculate axial rotor-bearing shock response.

17. Key Words (Suggested by Author(s))	18. Distribution Statement
Shock and vibration Gas bearings Brayton cycle Space power	Unclassified - unlimited

19. Security Classif. (of this report)	20. Security Classif. (of this page)	21. No. of Pages	22. Price*
Unclassified	Unclassified	266	$3.00

E7112

* For sale by the National Technical Information Service, Springfield, Virginia 22151

Page Intentionally Left Blank

CONTENTS

TABLE OF CONTENTS (Concluded)

LIST OF FIGURES

Figure

Figure

Figure

Figure

Figure

Figure

SUMMARY

The axial vibration response of a gas bearing system representative of the NASA A-engine turbocompressor simulator mounted on isolators with nonlinear characteristics has been analyzed. The equations of motion for a three-mass model were integrated numerically using a fourth-order Runge-Kutta method and the computations were programmed for solution on a digital computer. The types of vibration input that can be dealt with by the computer program include the following: sinusoidal vibrations, half-sine or haversine shock pulses, or any arbitrary shock or vibration expressed in tabular form in terms of displacement of acceleration versus time. The vibration analysis of the A-engine turbocompressor simulator given in this report represents an extension of previously reported work in Part I where a three-mass model was used which had mounting isolators represented by constant stiffness and constant damping coefficients.

The axial random vibration response of the NASA Brayton Rotating Unit (BRU) was analyzed with the BRU represented by a three-mass linear system. From the equations of motion, the relationship between the response power spectral density (PSD) and the input random vibration PSD was derived and expressed in terms of transfer functions. A computer program was written to calculate the PSD's and the mean squared values of the responses from specified input random excitations. The calculated response based on this linearized lumped-parameter model was found to be generally smaller than the measured values. A parametric study using the computer program was carried out to investigate the dependence of the random vibration response on various elements of the system, for example, the stiffness of the connectors between the BRU and the shake table, the stiffness of the gimbal support, the combined mass of the gimbal and thrust bearing, and the stiffness and damping coefficients of the thrust bearing gas film. It was found that the root-mean-square value of the gas-film thickness variation in the thrust bearing decreases significantly with increasing stiffness of the engine mounts, but is relatively insensitive to changes in mass and stiffness of the thrust bearing gimbal support. High values of gas-film dynamic stiffness and damping are desirable to achieve low thrust bearing gas-film thickness variations in a random vibration environment.

Vibration testing of the BRU was conducted, with both sinusoidal and random vibrations applied both along and across (one axis) the shaft axis of rotation. Tests were conducted with and without shaft rotation. Proximity probes and accelerometers were used to observe the response of the BRU components to the externally-imposed vibrations, and representative data has been extracted from the large quantity recorded and is presented herein. Complete data reduction is scheduled for a future effort.

In summary, further efforts to increase the ruggedness of the BRU bearing system were found to be necessary because of the onset of journal and thrust bearing surface contacts at relatively low random vibration levels (NASA Specification 417-2 Rev. C for Electrical Generating System Components - Operating). Sinusoidal vibration inputs to the BRU in the frequency range 5 to 35 Hz (according to the same aforementioned specification) did not produce any noticeable bearing system resonances and rotor-bearing operation was generally satisfactory in that operating region. However, significant bearing-system resonances were observed in the frequency range 60 to 400 Hz. Chrome-oxide bearing surface coatings were found to be instrumental in permitting multiple bearing surface contacts without evidence of degradation.

INTRODUCTION

The steadily progressing development of Brayton Cycle Systems for space-power generation has now reached the stage where adaption of the equipment to space environmental and launching conditions must be accomplished.

Brayton Cycle power systems consist basically of a closed gas loop in which an inert gas is heated in a heat source (reactor or isotope) and then, through one or more turbines, drives an alternator and a compressor before being cooled again in a recuperator and radiator. The rotating parts of this equipment are supported by gas bearings which utilize the working gas from the system. The utilization of gas as a medium for the separation of moving surfaces in the bearings eliminates most of the problems associated with other methods of lubrication at the high temperatures and speeds involved. Considerable attention must, however, be given to preventing motions between rotating and nonrotating parts that might result in sustained contacts between the parts, leading to bearing performance degradation or possibly even catastrophic failure.

Under Tasks I and II of this contract, an analytical and experimental study was conducted on the effects of shock and sinusoidal vibrations upon the performance of a gas bearing machine representative of the type then under consideration for space-power applications, (Reference 1). Since then, equipment specifically built for a space-power system of approximately 10 KWe maximum output has successfully undergone steady-state testing at the NASA Lewis Research Center, and components of this system became available for vibration environment testing. For the tests, the turbine and compressor wheels were replaced by rotor masses of similar weight (BRU simulator configuration).

In the analytical portion of this investigation a computer program previously developed (Reference 1) for the calculation of axial rotor responses under sinusoidal vibrations and shock was extended from linear to nonlinear representation of the isolator mounts. In addition, a computer program was developed for analytical prediction of the axial rotor response under random vibrations.

DEVELOPMENT OF ANALYTICAL METHODS

Analytical methods for vibration analysis have been developed for prediction of the following vibration characteristics of gas-bearing turbomachinery dynamically similar to the BRU:

1) Axial vibration response of the turbomachine to specified shock and sinusoidal vibration excitation with the turbomachine supported on nonlinear isolator mounts.

2) Axial response of the turbomachine to specified random excitations.

Nonlinear Element Shock and Sinusoidal Vibration Calculation Methods

A schematic of the turbocompressor simulator mounted on the test stand with its axis of rotation vertical is shown in Figure 1, which is reproduced from Figure 1 of Reference 1. The axial vibration response of this turbocompressor simulator was analyzed in Reference 1 by using the three-mass model shown in Figure 2, except that linear isolator stiffness and damping properties were assumed in Reference 1.

The three masses shown in Figure 2 represent the lumped masses of the following turbocompressor elements, starting with the base and proceeding upward:

1) The turbocompressor simulator casing;

2) The thrust bearing housing, flexure and thrust plate;

3) The rotor.

The nonlinear properties of the isolators are represented by a nonlinear stiffness $k_1(x)$ and a nonlinear damping coefficient $c_1(x)$. The equivalent stiffness and damping coefficient of the thrust bearing housing and flexure are both constant values and are represented by k_2 and c_2 respectively. The nonlinear gas film force is represented by $G(h,\dot{h})$.

An improved analysis of a more general three-mass model, shown in Figure 3 and including nonlinear isolator properties, is presented in Appendix A. This analysis is an extension of that presented in Reference 1. The computer program

implementing the analysis reported in Reference 1 has also been modified, and is presented in Appendix B. The flow chart which describes the modified computer program is shown in Figure 4. Note that when the calculation type is "isolators", there are three choices:

1) Linear Isolator (analysis and computer program of Reference 1)

2) Isolator represented by prescribed nonlinear functions

3) Isolator represented by table inputs.

The thrust bearing gas film load capacity and damping coefficient characteristics can be represented by either of the following two types of nonlinear functions:

a) An exponential function of the form:

$$Ae^{-Bh}$$

where h = mean thickness of thrust bearing gas film,

e = base of natural logarithms,

and A and B are constants selected by the user to give the best practical approximation to the nonlinear characteristics of the thrust bearing gas film as calculated from rigorous lubrication theory, and

b) A power function of the form:

$$Ch^{-D}$$

where C and D are arbitrary constants used to obtain a curve fit.

The actual nonlinear functions for the load capacity and damping coefficient for the NASA A-Engine turbocompressor simulator thrust bearing gas film are shown in Appendix A.

The extended computer program will handle each of the four different types of base forcing functions shown in Figure 4. These functions may be expressed either as base displacement or base acceleration and include sinusoidal vibration and three types of shock pulses.

Figure 5a shows the measured response of the thrust bearing gas film thickness to the applied shock pulse shown in Figure 5b. These are the measured data shown in Figure 41 of Reference 1. In the same figure calculated thrust bearing

film thickness data is shown as a function of time for the case in which the simulator was mounted on linear isolators. Calculated results compare poorly with measured results (it should be noted that good agreement was reported in Reference 1 when the measured acceleration function above the isolators was used as input to the calculation.)

The calculations were repeated using the extended analysis and improved computer program and with the isolators represented by their measured static stiffness curve, as shown in Figure 6 and an estimated constant damping value of 13.0 lb.sec/in. The circulated points in Figure 5a are the calculated responses using the improved program. Relatively poor correlation with measured results was obtained.

In order to investigate further possible reasons for this poor correlation it was decided to determine the sensitivity of the calculated response values to variations in the isolator properties, and thus to indicate the areas in which the stiffness and damping values may differ significantly from actual values. First, damping was held constant and stiffness was varied successively to half, twice, and four times nominal. Different results were noted, but none resembled the measured values. Next, stiffness was held constant and damping was varied. With damping equal to one-quarter of the nominal value, the calculated data denoted by squares in Figure 5a were obtained. While the calculated peak film thickness occurs somewhat earlier than the corresponding measured peak, the relative peak sizes are comparable. While no reasons exist for good correlation subsequent to the apparent thrust-runner impacts, the physical system appears to have settled down quickly enough after the impacts such that response to the imposed shock is reasonably close to the calculated results. While these results are promising, it appears that the least-known element of the system is still the isolator, and that a more complete understanding of the elastomeric damping would be highly desirable.

In summary, a vibration analysis has been developed and incorporated in a computer program for predicting the thrust bearing gas film thickness as a function of time for a general class of gas-bearing turbomachinery, mounted on nonlinear isolators and subjected to shock and sinusoidal vibration. The computer program has been verified to the limits within which the isolator dynamic stiffness and damping properties are known.

Random Vibration Calculation Methods

Gas-bearing space-power Brayton-cycle turbomachinery will be subjected to various vibration and shock conditions during its normal operating cycle. Reference 1 and the previous section deal with the response of this class of power-generating equipment to half-sine shock and sinusoidal vibrations. This section of the report presents an analysis of the response of this type of turbomachine, particularly the Brayton Rotating Unit (BRU), to specified random vibration excitations. General information on the design and fabrication of the BRU was reported in References 2 and 3. A schematic of the BRU with its shaft axis vertical is shown in Figure 7.

For purposes of the present study we distinguish at the outset between two basically different types of vibration: deterministic and random. Deterministic vibration is characterized by the fact that its amplitude can (in principle at least) be predicted as a function of time providing that enough of its time history is available to an observer. The amplitude of a random vibration record cannot be predicted, regardless of how much of its past history is known. Random vibration can only be analyzed in a statistical manner. That is, the more data that we have on the time history, the more precisely we can predict the probability that the amplitude will lie within specified values.

These probabilities are customarily described in terms of the Power Spectral Density (PSD) of Random Vibration. The PSD has a precise mathematical definition which is used in random vibration analysis but this section will try to introduce the concept and some associated implications in a descriptive manner, temporarily without regard for the more precise mathematical tools which will be needed later.

Figure 8 introduces the concept of PSD by means of a schematic based on one which appears on Page 30 of Reference 4. Consider the acceleration time history, $a(t)$, as the input to the system, the first element of which represents a narrow band filter with a center frequency, f, and a bandwidth, Δf (f might be 20 Hz for example and Δf might be the 1-Hz band between 19.5 and 20.5 Hz). The output of the first element would then be the time history of the acceleration at the frequency 20 Hz, represented by $g(t)$. Let the second element be a

squaring device. The input to the third element would therefore be $g^2(t)$. The third element yields the time average of the function $g^2(t)$ by integrating and dividing it by the total time. The fourth element takes the output of the third and divides it by the filter bandwidth, Δf (which is 1-Hz in this simple example). The four elements in series have converted an accelerometer record into the acceleration power spectral density (PSD) at 20 Hz. If the filter is subsequently retuned to 21 Hz with a bandwidth of from 20.5 Hz to 21.5 Hz, another PSD value is obtained for the 21 Hz frequency setting. By repeating this process, the entire frequency range of interest may eventually be covered, and a complete PSD curve obtained. In obtaining the PSD by this method, two precautions are usually observed:

1) The averaging time, T, should be long, compared to the longest vibration period of interest; and

2) The filter bandwidth, Δf, should be small, compared to the center frequency f.

Because of this latter assumption, analysis time is often saved by using a wider bandwidth filter to measure the PSD at higher frequencies. This is, in fact, done in practice. The reader wishing to gain a more thorough description of this process is referred to Reference 6. References 5, 6, 7 and 8 are brief introductory presentations on random vibration theory and practice while References 4, 10, and 11 are texts on random vibration and noise.

Figure 9, based on Reference 6, illustrates in a simple manner the basic difference between the types of mechanical response that one might expect for random and for sinusoidal vibration. This figure shows two cantilever beams attached to a rigid base lying in the plane of the paper. The beams project upward from the paper and are of sufficient length to permit them to vibrate along the lines AC and BC respectively. For purposes of discussion, one might assume that we apply sinusoidal vibration as shown at a very low frequency and start to sweep upward in frequency while maintaining a constant amplitude. Eventually we reach a frequency at which beam A goes into resonance and swings along line AC at large amplitudes, assuming that the first natural frequencies of the beam are separated. Beam B does not vibrate much while A is in resonance. At some higher frequency the resonance of beam A dies out, and eventually B executes wide swings along BC as we approach the natural frequency of B. Since A and B

resonate at different frequencies, sinusoidal vibration testing of the system should reveal that beams A and B do not collide. If we were conducting a random vibration test on the same system then we would simultaneously subject the system to a wide range of frequencies. Hence if the natural frequencies of both beams lie within the bandwidth of applied random vibration, it is conceivable that the beams resonate simultaneously resulting in a collision somewhere below the point C. The likelihood of this occurring would, of course, depend upon the specific system properties as well as the applied vibration characteristics. The point is that there is a difference in the actual response and not just a conceptual difference between sinusoidal and random vibration.

The actual dynamic environment associated with spacecraft operation is primarily random rather than deterministic. The origin and nature of this dynamic environment is presented in Reference 12.

The random vibration test specification of principal concern here is in Section 3.5.1.2.2 of Reference 13. This paragraph of the reference specification applies to the electrical generation system (EGS), and is quoted below for easy reference.

> The EGS shall withstand random noise excitation over a frequency range of 20 - 2000 Hz for 3 minutes in each of three mutually perpendicular axis, as specified below.
>
> | | |
> |---|---|
> | 20-100 Hz | 3 db/Octave increase |
> | 100-2000 Hz | .015 g^2/Hz |
>
> These are to be input levels at the interface between the EGS structure and the flight vehicle structure.

Figure 10 is a graph of the above PSD specification. Note that the unit of this PSD is g^2/Hz. Therefore, the area under this curve has the dimensions of g^2. The square root of this area represents the value of an acceleration in g - units. The equation for determining this area may be found in References 14 and 15 which are brief magazine articles devoted entirely to the subject of calculating the area under random vibration test specifications of the type under consideration. The square root of the area under the PSD curve can be interpreted physically as the root mean square of the accelerometer reading in g's.

Figures 11 and 12 represent additional sections of the Reference test specification. They are included in this report because the analysis techniques and computer program were developed with sufficient generality to treat any structure subject to any input PSD specification, as long as the structure can be adequately represented by a 3-mass vibrational model similar to the one presented in Figure 13.

The Brayton Rotating Unit (BRU) may be represented by a linear, discrete-parameter system which converts a particular input into a specific output in accordance with the system properties. Suppose that the PSD specified in Figure 10 is chosen to be the input. The output could then be expressed in various ways, and the coordinates most likely to be of value to the designer should be selected.

For the Brayton Rotating Unit, the relative displacements between the various mass points shown in Figure 13 are considered to be the most important output parameters. This is because the film thickness of the gas thrust bearing is of primary concern in this program of study; the relative displacement between m_2 and m_3 shown in Figure 13 would yield information on the gas film thickness variation due to random vibration excitations.

In Appendix C, the equations of motion for the system shown in Figure 13 are derived. The transfer functions between the input and output PSD's are also derived, based on the known system properties as described in the equations of motion. The PSD's of the relative displacements between various mass points can then be calculated from the transfer function and the input PSD.

Appendix D contains a complete listing of the computer program based on the analysis given in Appendix C. The input acceleration PSD of Reference 13 is included in the program as a sub routine. The values of the masses, stiffnesses and dampings are inputs as to the computer program and can be specified by the user. Also included in Appendix D are instructions for preparing input data cards, sample input and sample printed output.

Results of Axial Random Vibration Response Calculation for Brayton Rotating Unit

The foregoing analysis was applied to the Brayton Rotating Unit for the case of axial random vibration applied to the BRU with shaft rotation. Before giving the results of the random vibration response calculations, it is appropriate to describe the inputs to the program.

Inputs

m_1 = mass of the BRU housing structure = 96 lb.

m_2 = mass of the gimbal and thrust bearing = 7 lb.

m_3 = mass of the rotor = 21 lb.

k_1 = stiffness of connector between the BRU and shake table
= 300,000 lb./in.

k_2 = stiffness of the gimbal support
= 250,000 lb./in. (from page 79 of Ref. 3)

k_3 = stiffness of the gas thrust bearing
= 113,500 lb./in.

c_1 = damping coefficient of connector = 0.02 $\frac{\text{lb sec}}{\text{in}}$

c_2 = damping coefficient of gimbal support = 0.02 $\frac{\text{lb sec}}{\text{in}}$

c_3 = damping coefficient of gas thrust bearing = 84 $\frac{\text{lb sec}}{\text{in}}$

The above values of the masses, stiffnesses and damping coefficients are the nominal values and are summarized in Table I.

Table I. Nominal Values of the Lumped Masses, Stiffnesses, and Damping Coefficients of an Axial Vibration Model of the Brayton Rotating Unit

Element	m (lb)	k (lb/in)	c(lb sec/in)
1	96	300,000	0.02
2	7	250,000	0.02
3	21	113,500	84.00

It should be noted that the values of k_1, k_3 and c_3 are only nominal values. With respect to the stiffness k_1, there are three connectors between the BRU and the shake table. Each is bolted down at one end to the shake table. When the unbolted end of the connector tends to move up, the connector behaves like a cantilever with a calculated stiffness of 75,000 lb/in. at the BRU mount point. But for downward motion the cantilever arm is considerably shorter and thus much stiffer. This stiffness is calculated to be about 1,200,000 lb/in. For the purpose of this analysis, a nominal value of k_1 = 300,000 lb/in. is chosen.

The stiffness and damping characteristics of the gas thrust bearing are functions of frequency and bearing clearance. They have been calculated by an existing gas-bearing computer program and tabulated in Tables II and III. It is seen that they both vary widely with frequency and bearing clearance. Since the random vibration analysis is limited to a linear, time-invariant system, the stiffness and damping coefficients must have fixed constant values. The nominal values of k_3 and c_3 are chosen at a frequency of 100 Hz and with a film thickness of 0.0005 inch (the total axial clearance in the thrust bearing is 0.0021 inch).

The test objective power spectral density S_o is shown in Figure 10. During actual testing of the BRU, to be described below, it was found that frequent touching of the gas thrust bearing surfaces (possibly to the point of failure) would have occurred if it had been attempted to subject the BRU to the full level of this vibration specification. Tests were therefore performed with reduced input PSD values (i.e, the shape of the PSD was preserved, but the magnitude of the PSD was reduced by a constant factor, α, across the whole spectrum). From the definitions of the power spectral density and the root-mean-square value, the root-mean-square value is reduced by a factor of $\sqrt{\alpha}$ when the power spectral density is reduced by a factor of α across the whole spectrum.

Table II. Dynamic Stiffness (lb/in) of Double-Acting Gas Thrust Bearing

h(in) / ω(Hz)	.0002	.0005	.00105
100	477,000	86,900	18,900
500	523,000	93,700	20,000
1,000	652,000	113,500	22,700
2,000	950,000	166,000	33,600

Table III. Dynamic Damping Coefficient (lb sec/in) of Double-Acting Gas Thrust Bearing

h(in) / ω(Hz)	.0002	.0005	.00105
100	413	92	33
500	392	90	33
1,000	338	84	33
2,000	191	66	32

Now the root mean square (RMS) acceleration of the PSD in Fig. 10 is 5.4g. Testing was performed on the BRU at reduced PSD with the same shape of Fig. 10 but with several RMS acceleration levels including 0.54g. The response PSD is calculated based on this 0.54g RMS acceleration. Thus, $\sqrt{\alpha} = \frac{0.54}{5.4} = 0.1$ and $\alpha = 0.01$.

With the above input values of masses, stiffnesses and damping coefficients, and input PSD of Fig. 10 with $\alpha = 0.01$, the response PSD's Sy_1, Sy_2 and Sy_3 were calculated and are shown in Fig. 14, 15 and 16 respectively. Note that y_1, y_2 and y_3 are the relative displacements between m_1 and base, m_2 and m_1, and m_3 and m_2 respectively. The area underneath the PSD curve represents the mean square value of the respective quantity.

$$E(y_1^2) = \text{mean square value of } y_1 = 9.125 \times 10^{-8} \text{ in.}^2$$

$$E(y_2^2) = \text{mean square value of } y_2 = 1.753 \times 10^{-8} \text{ in.}^2$$

$$E(y_3^2) = \text{mean square value of } y_3 = 5.164 \times 10^{-8} \text{ in.}^2$$

The square root of the mean square value is the root mean square (RMS) value. Thus,

$$\text{RMS of } y_3 = 0.226 \times 10^{-3} \text{ in.}$$

The RMS of y_3 is the statistical average of the response of the gas thrust bearing film thickness. This is to be compared with the measured value of 0.35×10^{-3} in.

The power spectral densities shown in Figures 14, 15 and 16 and the RMS value of thrust bearing gas film variation are for the nominal case of the Brayton Rotating Unit with values of the lumped masses, stiffnesses and damping shown in Table I. In order to determine the sensitivity of the results to changes in these quantities, a parametric study was carried out by varying k_1, k_2, m_2, k_3 and c_3 individually from their nominal values. Variation of the RMS value of the gas film thickness with changes in the above parameters was sought.

The first parameter to be varied was the connector stiffness k_1. The RMS value y_3 was calculated for various k_1 values and is plotted against k_1 in Fig. 17. It is seen that the RMS value of y_3 increases with decreasing k_1. Therefore, any attempt to install a softer connector between the shake table and the BRU should increase the RMS value of the gas film variation. When k_1 = 100,000 lb/in, for example, the RMS value of y_3 is 0.359×10^{-3} in. The PSD of y_3 is shown in Fig. 18 for this case. Note that the peak value is considerably higher than that of the nominal case shown in Fig. 16.

Using the nominal values of Table I but varying the gimbal stiffness, k_2, the RMS value of y_3 was next calculated and is plotted in Fig. 19. It is clear that the RMS value of y_3 is insensitive to the gimbal stiffness in the range being studied. In another study, the variation of the RMS value of y_3 with changes in gimbal and thrust bearing mass m_2 was studied. The results are presented in Fig. 20.

The gas film dynamic stiffness and damping characteristics vary considerably with the frequency and the film thickness as shown in Tables II and III. In the nominal case the gas film stiffness and damping values were chosen at a frequency of 1,000 Hz and a gas film thickness of 0.0005 inch (with a total thrust bearing clearance of 0.0021 inch as indicated earlier). The gas film characteristics were next varied using the values of Tables II and III. The resulting calculated RMS values of the gas film variations are tabulated as follows:

Gas Film		RMS Value of Gas Film Thickness Variation (in)
Dynamic Stiffness (lb/in)	Dynamic Damping Coefficient (lb-sec/in)	
20,000	33	0.391×10^{-3}
168,000	66	0.254×10^{-3}
113,500	84	0.226×10^{-3}
86,900	92	0.218×10^{-3}
523,000	392	0.103×10^{-3}

Response calculations were performed for five sets of gas film characteristics. The first and the last sets correspond, respectively, to film thicknesses of 0.00105 and 0.0002 in. (with ω = 500 Hz). Since the total gap of the double-acting gas thrust bearing is 0.0021 in., a film thickness of 0.00105 corresponds to the thrust runner at its central position (zero load), and a film thickness of 0.0002 in. corresponds to the thrust runner at its highly loaded position. This is reflected by the fact that they have, respectively, very low and very high stiffness and damping values. Obviously, they will not necessarily be representative values for the gas film characteristics for all operating conditions. The three cases in the middle in the above table are at a film thickness of 0.0005 in. (corresponding to a moderately loaded thrust bearing). It is interesting to note that the RMS values of the gas film variation for the above three cases have a narrow range from 0.218×10^{-3} to 0.254×10^{-3} inch.

DESCRIPTION OF TEST HARDWARE

Test Apparatus

A schematic of the BRU simulator with the rotor in the vertical orientation is shown in Figure 21. The rotor, from the top down, consists of the following components:

1) The (simulated) compressor wheel, containing the cold gas simulator drive turbine
2) The thrust runner
3) The compressor end journal
4) A center section, (homopolar generator rotor)
5) The turbine end journal
6) The (simulated) gas turbine wheel.

The three-pad configuration of the gas film journal bearings is shown in cross-section in Figure 21. The pads are individually supported by pivots, with one of the pivots in each bearing assembly mounted on a mechanical flexure. The flexure, which has a radial stiffness of approximately 2000 pounds per inch, permits the bearing to accommodate radial centrifugal growth of the journal and differential, radial, thermal expansion between the various bearing parts.

The double-acting thrust bearing is supported by a gimbal assembly with two sets of gimbals 90° apart. These permit the thrust bearing to align itself with the thrust runner of the rotor. The surface geometry of the thrust plates consists of nine equal sectors of 39° each with narrow radial grooves separating the sectors. Each sector in turn consists of a slightly depressed sector of 15° arc followed by the raised part in the direction of rotor rotation. Design details for the complete journal and thrust bearing assemblies are given in Reference 3.

The journal bearings, as well as both thrust bearing plates, have hydrodynamic and hydrostatic operating capabilities. For hydrostatic operation, each journal bearing pad and each raised thrust plate sector is equipped with a small gas supply hole, connected to an outside gas source. Hydrostatic bearing operation is normally employed to separate the bearing and rotor surfaces at start-up until rotor speed is high enough to produce a sufficiently large gas film for safe bearing operation. At the design speed of 36,000 rpm and above, the rotor operates hydrodynamically. The BRU design also requires hydrostatic bearing operation at shutdown to prevent rubbing contact between the rotor and the bearing surfaces at speeds too low to provide hydrodynamic film separation of the bearing surfaces. Prior to the vibration tests described in this report, all bearing and corresponding rotor surfaces had been coated by MTI with chrome oxide and refinished to the original dimensional specifications. This was done to improve the tolerance of the bearing surfaces against accidental rubs which might occur in the course of the vibration tests. Figure 22 shows a photo of one of the unassembled chrome oxide coated thrust plates after grinding and lapping.

Figure 23 is a photograph of the BRU simulator in the vertical support fixture mounted on the vibration table ready for testing. The simulator is held in the support fixture without isolators by three mounting brackets extending radially outward from the simulator casing and resting on the rim of the vertical support fixture. The flexible air hoses visable in Figure 23 serve to pressurize separately each of the journal bearings, the thrust bearing plates, the bearing cavity, the thrust loader chamber and the cold gas drive turbine. Nitrogen at room temperature was used for hydrostatic bearing operation and to provide the ambient gas atmosphere during all hydrodynamic tests.

Figure 24 is a photograph of the BRU simulator in the transverse test fixture which is attached to the shake table surface. The shake table has been rotated into a horizontal position so that the direction of vibration is perpendicular to the vertically oriented axis of rotation of the BRU. The same three mounting brackets without isolators are used for connecting the BRU simulator to the transverse test fixture as were used on the vertical fixture.

A small-scale schematic of the BRU simulator in the transverse test fixture is shown on all data graphs obtained for this arrangement. As the schematic

indicates, the direction of applied vibration is in line with the instrumentation turret and thus passes also through the pivot of the flexibly mounted pad in each journal bearing.

Instrumentation

The dynamic response measurements on the rotor-bearing system were made with capacitance probes. These probes may be divided for convenience into two categories: those measuring displacements of the rotor or some bearing component relative to the simulator casing, and those measuring gas film thickness variations between the rotor and the thrust bearing or between the rotor and any of the journal bearing pads. From a total of four probes measuring thrust bearing film thickness variations, only two data signals from two probes 90° apart circumferentially have generally been recorded. These two probes were axially in line with probes recording motions of the gimbaled thrust bearing relative to the casing.

Gas film thickness variations between the rotor and individual journal bearing pads were measured with capacitance probes built into each pad. These probes, which were installed by MTI prior to tests, were located next to the pivot on the inboard side of each bearing pad (a total of six).

Two sets of two probes were used to measure rotor displacement relative to the simulator casing at two locations inboard of the journal bearings. (The angular orientation of these capacitance probes is indicated in Figure 25). The radial motions of the two flexures supporting each one of the three pads of each journal bearing were measured near the pivot location relative to the casing. Pad motions at the pad leading edge were recorded for one solid mounted and one flexure mounted pad.

A schematic of the probe locations in relation to the rotor is shown in Figure 25.

Figure 26 provides a listing of all capacitance probes used for data recording. Most of the significant capacitance probe signals obtained in any given test were permanently recorded on a multichannel tape-recorder. In addition to one direct-record channel each for voice and rotor speed, twelve frequency-

modulated (FM) channels were available for dynamic signals on two separate recording heads. The two recording heads on the tape recorder are not phase-tied, therefore, one accelerometer signal (the vibration table input signal) was recorded on one channel of each of the two recording heads to permit later phase correlation between vibration input and response signals. Two more tape channels were assigned to a second accelerometer signal from one of the BRU mounting brackets on the casing and to a logarithmic frequency indicator (to be used later for driving the X-Y plotter). This left eight channels available for data signals from the capacitance probes, necessitating a repeat run on each of the tests to be performed for sufficient coverage. All recording was done at 30 inches-per-second tape speed insuring a flat response of the FM channels from DC to 10 KHZ.

Crystal accelerometers were used to check acceleration levels on the BRU simulator mounting brackets and at locations on the support fixtures directly adjacent to the mounting brackets. The acceleration input level to the BRU simulator was monitored by an accelerometer located on the rim of the vertical support fixture for the vertical vibration tests. For the lateral vibration tests the input control accelerometer was located on the horizontal support fixture near the BRU mounting bracket opposite from the instrument turret, as shown in Figure 27. Accelerometer locations on the vertical support fixture and the BRU simulator are shown in the schematic in Figure 28. For the lateral vibration tests, accelerometers were monitored at the locations shown in Figure 29.

The BRU simulator was equipped with a number of thermocouples on the journal bearing pads, the thrust bearing and the internal support structure. Temperatures from nine locations, including both flexure-mounted journal pads, one solid-mounted pad at the compressor-end journal, and one thrust plate were recorded by automatic print-out throughout the tests.

Figure 30 shows the test control station. The control panel on the left contained the pneumatic controls for the operation of the BRU simulator. Rotor speed was manually regulated by controlling air flow through the simulator drive turbine via a regulating valve located in the panel. Speed was indicated by an electronic counter on the panel.

Other pressure regulators and gages served to control the gas pressure to the bearings at start-up and shutdown and to regulate the bearing cavity pressure. The center panel of the control station shown in Figure 30, holds the sinusoidal vibration control console. Sinusoidal vibrations with constant acceleration over the test frequency (5-2000 Hz) were programmed on this instrument prior to the start of actual shake table motions. A closed-loop control circuit including the accelerometer mounted on the BRU simulator mounting fixture held the acceleration level at that point constant despite table or fixture resonances that might occur. The time required to traverse the test frequency range from 5 to 2000 Hz could be varied within wide limits, with a 10 to 15 minute sweep preferred to match the length of one test run to the running time (16 minutes) of one reel of magnetic tape on the tape recorder. The frequency sweep on the sinusoidal vibration control console may be either a linear or a logarithmic progression. A logarithmic progression was used exclusively in these tests for better resolution in the low frequency range.

The console on the right in Figure 30 contains the analyzer and equalizer for the random vibration tests. Basically, the analyzer consisted of 45 narrow bandwidth filters which broke down the incoming random signal from the shake table control accelerometer into narrow frequency bands (50 Hz wide above 100 Hz center frequency, less at lower frequencies) and then determined the power spectral density in each range. The equalizer portion of the console compared a pre-set power spectral density level for each of 45 channels with the level of the incoming signal from the shake table and automatically adjusted the level of the signal going out to the power amplifier (which in turn drove the shake table) to make it conform to the pre-set values. "Shaped" power spectra with decreasing power density towards the ends of the frequency spectrum, such as are required by NASA Spec 412-2-C-3, could easily be set up on this control instrument. A graphic representation of the random vibration test levels from NASA Spec 412-2-C-3 for operating and non-operating electrical components (BRU simulator) is shown in Figures 31 and 32, respectively. During testing the level of the random vibrations at the shake table could be increased gradually in steps from 20 db below the set value to full value, while maintaining the originally set shape of the spectrum. Shake table response to changes in the spectral density power level was nearly instantaneous, inviting visually monitored operation of the random tests with immediate vibration level reductions when danger of excessive rotor-bearing contacts seemed imminent.

Oscilloscopes and temperature recorder were arranged opposite from the control panels shown in Figure 30. The vibration shake table with the BRU simulator mounted on it was easily observable through a glass door from the test control station.

DESCRIPTION OF TESTS

The BRU simulator was tested under sinusoidal and random vibration input conditions. Both types of vibrations were applied separately and no combined sinusoidal-random testing was performed. Identical sinusoidal vibration levels were applied to the simulator with and without shaft rotation. Under random vibration conditions the specified levels of power spectral density were lower with the shaft rotating and more severe with the shaft stationary. All tests were performed with the shaft in the vertical position (compressor end up), conducted with the direction of applied vibration along the rotor axis and then repeated with vibration applied in a direction perpendicular to the rotor axis. For the latter tests the shake table was turned by 90° into the horizontal position and the simulator was mounted in a different support fixture. During the lateral vibration tests the simulator was so oriented that the direction of vibration passed through the flexure-supported journal pads.

All vibration tests were conducted according to NASA Spec 417-2-C*. However, since these tests were not intended as qualification tests, it was attempted to hold vibration levels below threshold values above which the BRU simulator rotor-bearing assembly might seriously have been endangered. During the sinusoidal vibration tests in the frequency range between 35 and 2000 Hz where no particular input level was specified, the danger zone for the gas bearings was generally assumed to start at a minimum film thickness of 0.0001 inch or less. Shake table acceleration levels around 0.12 g peak were found to permit generally safe operation in this frequency range. There was, however, an exception where even this low input led to sustained rubbing of the rotor in one of the journal bearings**

During the random vibration tests, where visual observation of minimum gas film thicknesses was much more difficult due to the erratic nature of the rotor excursions, the danger zone was considered to start at the point where intermitent

---

* Environmental Specification of SNAP-8 Electrical Generating System, dated March 31, 1967.

**Upon disassembly of the BRU simulator, the failure of the compressor end journal bearing to operate hydrodynamically was found to be failure of the brazed joint between journal bearing pad and pivot seat in four of the six pads.

rotor-bearing contacts could be recognized. A rapid rise in bearing temperatures or a slow-down in rotor speed were taken as certain indicators of repeated brief contacts between rotor and bearings.

The following vibration schedule from NASA Spec 447-2-C was used as a goal for these exploratory tests:

Sinusoidal vibration, with shaft rotation:
5-35 Hz - 0.25 g peak
35-2000 - Identification of resonances only

Sinusoidal vibration, without shaft rotation:
5-35 Hz - 0.25 g peak

Random vibration, with shaft rotation:
20-100 Hz - 3 db/Oct. increase
100-2000 Hz - 0.015 g^2/cps

Random vibration, without shaft rotation:
20-100 Hz - 3 db/Oct. increase
100-600 Hz - 0.4 g^2/cps
600-2000 Hz - 6 db/Oct. decrease

A graphic representation of the random specifications is shown in Figures 31 and 32.

For those vibration tests where shaft rotation was required, the BRU simulator bearings were operated hydrodynamically in a nitrogen atmosphere of 38 to 40 psia at room temperature. Initially it had been desired to operate the simulator bearings at an ambient pressure of 43 psia, however, apprehension about a rather small steady state thrust bearing gas film thickness with a fully vented thrust loader chamber led to the arrangement where the vent from the thrust loader chamber was closed and leakage gas from the bearing cavity was allowed to build up to some pressure in that chamber. The resultant upward force on the rotor, together with the drive turbine reaction force, exceeded the rotor gravitational force at bearing cavity pressures above approximately 30-32 psia. Any further increase in bearing cavity pressure caused a smaller increase in the thrust loader chamber pressure and consequently an increased loading on the upper thrust plate.

In the interest of maintaining a reasonably large thrust bearing gas film thickness, the bearing cavity pressure was not increased above the 38-40 psia level. (Replumbing of the exhaust line and regulator from the thrust bearing loader chamber with a larger line and more sensitive exhaust regulator would probably have been satisfactory for reducing the thrust loader chamber pressure by one or two psi and thus allowing a bearing cavity pressure increase by 3 to 5 psi.) For a better perspective on the concern for a sufficient bearing gas film, it must be noted that the BRU simulator bearings were operated at off-design conditions, to their disadvantage. The viscosity of the He-Xe mixture in the bearing cavity of the operating BRU at a temperature of 400°F would be 0.47 lb.sec/in.^{2}. This compared with 0.31 lb.sec/in.^{2} for nitrogen at 250°F, the steady-state temperature of the BRU simulator bearings without external heating.

BRU simulator rotor speed was 36,000 rpm for hydrodynamic bearing operation. The rotor was not driven whenever vibration tests were conducted with all bearings hydrostatically pressurized. However, hydrostatic bearing pressurization alone, (drive turbine inactive) caused the shaft to rotate at approximately 2500 rpm, but opposite to the normal direction of rotation. For tests with nominal hydrodynamic bearing operation conducted after the initial failure of the compressor journal bearing, hydrostatic supply pressure had to be supplied to the compressor journal bearing to maintain contact-free operation.

DESCRIPTION OF RECORDED DATA

Test data was obtained and recorded with vibration applied to the BRU simulator along the rotor axis and at right angles to it. The test results are generally recorded in the same sequence the tests were completed, except for the axial non-rotating tests, which were conducted last.

Preliminary Axial Vibration Tests

The BRU simulator is a complex and sensitive machine, which requires careful control for satisfactory operation even under normal steady-state operating conditions. To avoid possible damage to the simulator from excessive acceleration loads caused by either support fixture resonances or responses of simulator bearing system components, two sets of preliminary tests were performed prior to the specified vibration test under rotating shaft conditions.

First, the acceleration levels at various external points on the BRU simulator were determined while a constant input acceleration was maintained on the support fixture at a point close to one of the mounting brackets of the simulator. In addition, measurements were made of the response of various internal BRU simulator parts (by means of proximity probes) under representative vibration levels. In all preliminary tests, the simulator gas bearings were pressurized at 150 psia and the shaft was not driven. (Some shaft rotation at approximately 2500 rpm was present when the bearings were pressurized due to turbining torque produced by the gas jets leaving the external pressurization holes in the bearing surfaces.)

Axial vibration input level tests

The shake table vibration level control system features a servo loop which continuously measures acceleration at the table and appropriately adjusts the power level input to the table to maintain a predetermined shake table acceleration level.

Electrical and mechanical resonances of the bare table necessitate this automatic adjustment, even without the presence of mounting fixtures or test specimen. With mounting fixtures and test specimen present, the shaker servo loop maintains the preset acceleration level at that particular spot to which the control accelerometer is attached. Other locations on the test fixture or the test specimen will, of course, exhibit vibrations peculiar to their own mass-stiffness relationships.

The initial vibration input level tests were conducted with a dummy mass so that more sensitive parts in the BRU simulator might not be damaged by excessive vibration inputs during the table programming and adjustment phase. Following the initial equipment and specification familiarization phase, the BRU simulator was placed in the vertical mounting fixture and, with all gas bearings pressurized, subjected to the specified 0.25 g sinusoidal vibration in the direction of the vertical vector axis. Figures 33 through 41 document the acceleration levels on various points along the circumference of the rim of the vertical support fixture and on the BRU simulator itself.

The shake table control accelerometer was mounted on top of the vertical support fixture at a location approximately 3 inches away circumferentially from the BRU mounting bracket located counterclockwise next to the instrumentation turret, as seen from the BRU compressor end. The location of the other accelerometers on or next to the BRU is indicated in Figure 28.

Inspection of the acceleration plots indicate the following important conclusions to date:

1) The input acceleration to the BRU, as indicated by both the table control accelerometer and the test accelerometer next to it, (Figures 33 and 34), was nearly constant over the frequency range from 5 to 2000 Hz.

2) The acceleration levels on the BRU mounting brackets are noticeably affected by the dynamic characteristics of the BRU structure and components. The frequency range over which resonances occur extends from 70 to 300 Hz. (Figures 35, 37, and 39.)

3) The acceleration levels on the BRU mounting brackets are not identical for all three brackets. (Equal torque was applied to all three mounting screws prior to the vibration test.) (Figures 35, 37, and 39)

4) Accelerometers T-4, T-6, and T-8 (Figures 36, 38, and 40) appear to indicate the "bouncing" of the BRU mounting brackets on the vertical support fixture. At a distance of approximately 4.5 inches (circumferentially along the top of the support fixture) this "bouncing" effect in the fixture seems to have been damped out, as evidenced by data from accelerometer T-2. (Figure 34)

5) The top of the BRU simulator (part number 32, nozzle and seal assembly) exhibts several pronounced vibration peaks. These are at approximately 100 Hz, 260-290 Hz, and 1400 Hz. Oscilloscope photographs obtained during testing indicate that above 260 Hz the vibration of the top of the BRU is out-of-phase with that of the top of the support fixture. At high table frequencies (around 1800 Hz) the top of the simulator exhibits primarily a low frequency vibration of approximately 350 Hz. (Figure 41)

Axial sinusoidal vibration response tests - hydrostatic operation

As discussed earlier, amplitude measurements were also made to determine the dynamic response of the internal parts of the simulator with hydrostatic bearing operation. The response of the BRU simulator bearings and their support structures to externally applied vibrations was recorded from capacitance-type displacement sensors, using both existing probes and also those installed by MTI to measure film thickness above the pivot location in the journal bearing pads. Only that part of the monitored signals which signified dynamic part motion was recorded. Base line changes - as e.g., minimum gas bearing film thicknesses were kept under observation on oscilloscopes for BRU simulator safety without being recorded. All of the preliminary tests recorded here were made at a shake table vibration input of 0.25 g. The sweep time was 15 minutes for the frequency range from 5 to 2000 Hz, with a logarithmic increase in shake table frequency.

The vibration amplitude graphs, which are presented in Figures 42 through 52, indicate the presence of resonances (vibration peaks) in the same general frequency ranges as previously shown by the signals from accelerometers mounted on the BRU simulator. A summary of the frequencies at which the most pronounced vibration peaks occurred for most of the bearing parts is given in Table IV below.

Table IV
Measured Vibration Peaks in BRU Simulator Hydrostatic Operation With External Axial Vibration (No Rotation)

Approx. Freq. Hz	Flex. Mounted Pads	Flexure	Solid Mounted Pads	Casing-to-Shaft	Thrust Brg. Film	Thrust Brg. Gimbal	Mounting Bracket	Top of BRU
70		XX	XX	X		X	T3	
110	X	X	XX	XX	XX	XX	T7 T5	X
150			X	X				
190	X	X	X	X	X			
260/290	XX	X	X	X	X	X	T3 T7	XX
1350								X

The notation XX indicates the frequency at which the largest vibration peak was observed. However, it must be noted that not necessarily all parts of the same type, as e.g., solid mounted bearing pads, exhibit the largest vibration peak at the same frequency. Also, when there are peaks of nearly equal magnitude at two different frequencies either one of them may become the largest in successive test runs. The underlined accelerometer designations in the mounting bracket column indicate the frequency at which each of the three mounting bracket accelerometers exhibited the largest response peak.

Axial Sinusoidal Vibration Tests With Hydrodynamic Bearing Operation

Subsequent to the preliminary tests described above, sinusoidal vibration tests were undertaken in partial fulfillment of the vibration test requirements.

With the BRU simulator in the vertical orientation, the bearings were operated hydrodynamically for a shaft speed of 36,000 rpm. Cavity gas pressure was 40 psia (nitrogen). In this configuration two sinusoidal vibration tests were conducted:

a) with vibration frequencies varying between 5 and 35 Hz, an input acceleration level of 0.25 was applied along the direction of the rotor axis, and

b) in the frequency range between 35 Hz and 2000 Hz system resonances were identified.

The BRU simulator withstood the low frequency (5 to 35 Hz) sinusoidal vibrations up to the specified level of 0.25 g (peak) without apparent ill effect. Bearing temperatures ranged between 230 and 250°F.

The typical vibration amplitude curve depicting the response of individual bearing parts to vibration input in the frequency range up to 35 Hz was quite flat. No sample plots are shown in this report, however, this information is available on magnetic tape.

Attempts to continue the frequency scan above 35 Hz at the input level of 0.25 g were not successful. Observed minimum gas film thickness decreased to 0.0001 inch or less even before any resonance peaks in the 70 to 300 Hz range were traversed. Therefore, the vibration input level was decreased to 0.12 g, which is near the minimum at which the vibration system would operate and still produce a low frequency acceleration with a nearly sinusoidal wave shape. (The minimum noise level guaranteed by the manufacturer for this particular vibration system is stated as "below 0.1 g"). At the vibration input level of 0.12 g (peak), two scans between 5 and 2000 Hz, each lasting 15 minutes, were successfully completed

and recorded. The resultant vibration amplitude response curves as monitored by the capacitance probes are shown in Figures 53 through 63. A subsequent attempt to repeat the test under identical test condition led to sustained rubbing of the compressor journal bearing. Rubbing of the shaft in the bearing began at a vibration frequency of 190 Hz and did not subside until the external vibration was removed. By that time the vibration frequency had increased to 290 Hz and the rotational speed of the BRU had fallen from 36,000 rpm to approximately 19,000 rpm. Up to the time the vibration was removed, and jacking gas applied to all bearings, the affected journal bearing had not regained hydrodynamic operation. Later attempts to operate the compressor journal bearing in a fully hydrodynamic mode were not successful. However, a jacking gas supply pressure of 20 psi above cavity ambient pressure was sufficient to prevent journal contact.

The above described occurrence becomes apparent from inspection of Figures 64 through 74. In these figures the onset of the rub can be recognized for all affected bearing pads by the large fluctuations in amplitude. The sharp drop in the rotor speed curve, shown on some of these figures, shows very dramatically the occurrence of the rub. Furthermore, temperature recordings (Figure 74) for one solid mounted pad and the flexibly mounted pad on the compressor journal bearing confirm the momentary breakdown of the bearing gas film.* The photographs in Figure 72 picture the variations in pad-to-shaft film thickness of the compressor journal bearing pads which were caused by the rubbing. In Figure 73, photos show dynamic motion of the compressor and turbine journal flexures and of one of the compressor journal casing-to-shaft probes. These photos were obtained through signal playback from magnetic tape and thus accurately describe the changes that occurred at approximately 190 Hz in the compressor journal bearing. It cannot be overemphasized that the chrome-oxide coating on all mating bearing parts was instrumental in preventing a serious system failure at this point in the tests.

* Upon disassembly by NASA-Lewis of the BRU simulator at the conclusion of the vibration tests it was found that failure of the brazed joint between journal bearing pad and pivot seat had occurred in all three compressor-end journal bearing pads and in one of the turbine-end pads.

It must be noted here that between the two "successful" tests and the test at which the journal rub occurred, the BRU had been subjected to some low level random vibration testing (vertical mounting, axial vibration) with hydrostatically pressurized bearings (rotor not driven) and at levels not exceeding 13 db below 5.4 g (RMS). This input is even far below the specified random input level of 5.4 g (RMS) for hydrodynamic bearing operating conditions.

Axial Sinusoidal Vibration Tests Without Rotor Operation

For these tests no hydrostatic bearing gas was supplied. The rotor was therefore held radially in a clamped position by the spring loaded journal bearing pads and axially restrained by the friction force resulting from the radial shaft loading. When subjected to the specified sinusoidal vibration of 0.25 g (peak) over the frequency range 5 to 35 Hz, the BRU simulator rotor and bearing parts did not exhibit any measurable motion relative to each other.

Axial Random Vibration Tests With Hydrodynamic Bearing Operation

With the BRU simulator in the vertical position and with bearings operating hydrodynamically (except for the compressor end bearing which was pressurized with nitrogen at 20 psi above cavity ambient), random vibrations were applied along the rotor axis. Beginning at a power spectral density level 20 db below the NASA specification* for random vibration under BRU operating conditions, the input vibration level was increased by 0.5 db steps until the BRU simulator bearings were judged to be close to cessation of hydrodynamic operation. At the highest attained random vibration level a slow drop in rotor speed and increasing bearing temperatures were considered to be good indications of intermittent brief contacts between rotor and bearings, particularly in the thrust bearing. (The irregularity of the random response motions of the rotor and bearing parts makes visual observation of intermittent contacts between

* NASA environmental specifications 417-2-C-3.5 for random vibration under operating conditions read as follows:

Frequency				
- 20 -	100 Hz:	3 dB/Oct. increase
- 100 -	2000 Hz:	0.015 g^2/Hz

These specifications amount to approximately 5.4 g (RMS). Initial shake table operation of 20 db below the specified full level is then equivalent to approximately 0.54 g (RMS).

rotor and bearings very difficult). Figure 75 demonstrates the dramatic changes in rotor orbits which occur with progressing time, even though the random vibration input level is held constant. Figure 76 indicates a similar observation for other bearing system component parts, with a very noticeable difference in response characteristics between the flex-mounted and solid-mounted journal bearing pads.

The maximum level of random vibration in the axial direction applied to the BRU simulator under hydrodynamic operation was 8 db below the specified full level. This is the equivalent of approximately 0.0024 g^2/Hz in the frequency range 100 to 2000 Hz with a 3 db/Octave decrease between 100 and 20 Hz. The full level of the specified random vibration corresponds to 5.4 g (RMS). The maximum attained level of 8 db below specification thus corresponds to approximately 2.15 g (RMS), which is about 40 percent of the specification input level. The vibration amplitude response of all monitored bearing parts has been recorded on magnetic tape.

Within the capabilities of the available instrumentation, a simple presentation has been prepared of the RMS values of the random vibration response of those bearing parts monitored by capacitance probes. In Figures 77 through 89, RMS vibration amplitude levels are shown as they occurred during the course of the test (test-time shown in minutes) and as they increased with increasing table vibration input.

Most of the amplitude curves show step increases for each step increase in table vibration level. Notable exceptions may be seen in Figures 86 and 88 which show the axial vibration amplitude of the thrust runner. At random vibration input levels greater than approximately 1.20 g (RMS) the thrust runner response does not increase significantly with increasing input vibration levels. As nearly as can be determined, the runner axial vibrational amplitude at this point is very nearly equal to the available thrust bearing clearance. Figure 90 shows clearly the increasing magnitude of larger and larger rotor amplitudes between thrust plates as the vibration level is increased. In the final photo of the series shown in Figure 90 the rotor moves back and forth almost all the way between the two thrust plates nearly every time it reverses its direction of axial motion.

Figure 91 is a replot of the measured temperatures obtained for three journal bearing pads and one thrust plate during application of the random vibrations to the operating BRU simulator. Except for what appears to be a momentary rub of the compressor-end solid mounted pad at less than the full random vibration input level, a general, gradual rise in bearing temperatures is evident, indicating a rising frequency of brief contacts between the rotor and all bearing parts.

Axial Random Vibration Tests Without Rotor Operation

These tests were conducted without hydrostatic gas supply to the BRU simulator bearings. The rotor remained clamped by the flexure supported journal bearing pads and restricted in the axial direction by the friction force resulting from the clamping action.

The random vibration specifications for the nonoperating BRU are rather severe, with bearing pad-rotor separations and axial rotor motions occurring at levels far below the specified maximum. By NASA project manager direction, tests were discontinued at the input vibration levels indicated in Figure 32. Data from the capacitance probes has been recorded on magnetic tape. No sample plots are shown in this report.

Preliminary Transverse Vibration Tests

The transverse vibration tests were conducted with the BRU simulator in the vertical position (rotor axis coincidental with gravity vector) and the shake table turned to the horizontal position, as shown in Figure 24. For these tests the simulator gas bearings were pressurized at 150 psia and the shaft was not driven.

Transverse vibration input level tests

The objective of the transverse vibration input level tests was the determination of the vibration levels at the BRU simulator mounting points on the support fixture. Since the design of the transverse support fixture suggested the possibility of vibrational cross-coupling between the transverse and the axial

directions at the location of two of the three simulator support brackets, acceleration levels were measured on various points of the fixture in both the transverse and the axial directions.

The location of the control accelerometer was considered a suitable starting point for mapping of acceleration levels on the mounting fixture. At that location the acceleration level should very nearly correspond to the pre-set table input value over the full frequency range. Figure 92 offers proof of satisfactory acceleration control near the mounting location for the BRU simulator support bracket opposite the instrumentation turret. With the BRU simulator in place, the acceleration input at that same location is still satisfactory (Figure 95), even though two or three small resonances clearly show the effect of the simulator upon the vibrational behavior of the support fixture.

At the location of the other simulator support brackets on the support fixture a high frequency (1200 Hz) resonance is apparent without the simulator in place, (Figure 93).

The effect of this resonance, an increase in acceleration level to the BRU simulator at this frequency, is of no importance because it occurs above all significant resonances in the simulator itself.

With the simulator mounted in the fixture, an additional small resonance is noted between 300 and 400 Hz (Figure 96). This may be a thrust bearing (gimbal) related resonance which, either on its own strength (Figures 97 and 98) or through a coincident fixture resonance (Figure 94), is transmitted back to the BRU simulator support points in both the direction of table motion (Figures 97 and 98) and perpendicular to it (Figures 100, 101, 102, 103, and 104). In the latter direction, which coincides with the BRU rotor axis, the vibration peaks seem to be more pronounced, but then the minor fixture resonance, as indicated in Figure 94 may provide a boost.

Another important observation from this preliminary test series is the occurrence of the vibration peak of the transverse support fixture at 90 Hz in the vertical direction (perpendicular to the shake table motion). The effect of this (unwanted) input to the BRU simulator at a frequency close to where in earlier

testing most of the axial resonances were observed, should be carefully assessed in the evaluation of all transverse vibration test results.

Transverse sinusoidal vibration response tests - hydrostatic operation

The amplitude response measurements in this preliminary test series were made under very similar conditions and for a similar purpose as those described under the heading "Axial Sinusoidal Vibration Response Tests - Hydrostatic Operation". However, the transverse tests were all made with a 0.12 g (peak) vibration table input and a sweep time of 10 minutes for the frequency range from 5 to 2000 Hz.

The resultant amplitude graphs, which are shown in Figures 105 through 116 are similar to those obtained for vertical vibration table input. Internal BRU simulator part resonances are most pronounced in the frequency range between 60 and 400 Hz. A summary of the frequencies at which vibration peaks occurred for most of the bearing parts is given in Table V below.

TABLE V

Measured Vibration Peaks in BRU Simulator, Hydrostatic Operation, with External Transverse Vibration

Approximate Frequency Hz	Flexure Mounted Pads	Flexure	Solid Mounted Pads	Casing-to-Shaft	Thrust Bearing Film	Thrust Bearing Gimbal
70	XX	XX	XX	XX	X	X
110		X	X	X	XX	XX
150			X			
350	X		X	X	X	X

The notation XX indicates the frequency at which the largest vibration peak was observed Noteworthy differences between the axial and transverse vibration results are the absence of the 190 Hz resonance from the transverse test case, and the shifting of the 260/290 Hz resonance in the axial test case to 350 Hz in the transverse tests for all journal bearing pad and rotor-to-casing measurements.

Transverse Sinusoidal Vibration Tests With Hydrodynamic Bearing Operation

The transverse sinusoidal vibration tests with the BRU simulator operating (hydrodynamically) at 36,000 rpm, were conducted similarily to the axial sinusoidal tests.

The BRU simulator withstood the low frequency (5 to 35 Hz) sinusoidal vibrations at 0.25 g (peak) without noticeably fluctuating responses or difficulties.

The frequency range 35 to 2000 Hz, was scanned for resonances at 0.12 g (peak) vibration table input. The response of various bearing components and of the rotor relative to the simulator casing is plotted in Figures 117 through 129. It is noted on all of these plots that the compressor-end journal bearing was operated hydrostatically, due to its previous failure during the axial sinusoidal vibration test series.

Transverse Random Vibration Tests With Hydrodynamic Bearing Operation

The transverse random vibration tests with the rotor operating at 36,000 rpm (hydrodynamically, except compressor-end journal bearing) were essentially a repetition of the axial random vibration tests, with the direction of vibration now perpendicular to the rotor axis and in-line with the instrumentation turret on the BRU simulator. The maximum level of random vibration applied laterally to the BRU simulator was 10 db below specified full level, or 1.7 g (RMS). Response graphs similarly to those obtained and described for the axial random vibration tests are shown in Figures 120 through 142. Figure 143 shows a plot of bearing pad and thrust bearing plate temperatures obtained during the transverse random vibration tests.

Transverse Random Vibration Tests Without Rotor Operation

For these tests the rotor was clamped by the flexure supported journal bearing pads (no hydrostatic gas bearing supply). Random vibrations were applied up to a level of approximately 8 1/2 db below the specified maximum (or 1.97 g -RMS), but were not increased beyond this level upon NASA project managers directive. Separation of the journal bearing pads from the rotor (or vice versa) had

started to occur before test termination. Capacitance probe signals have been recorded on magnetic tape, however, none are shown in this report.

CONCLUSIONS

The primary objective of the work reported in this volume was continued assessment of the effects of environmental vibration on the mechanical performance of gas-bearing space-power Brayton cycle turbomachinery. This objective was achieved via the following specific steps:

1. The previously-developed analysis and computer program for the calculation of axial shock and vibration response of a gas-bearing-supported rotor system was extended to include nonlinear supporting elements (i.e., passive isolators).

2. An analysis and computer program were developed for calculating the response of the Brayton Rotating Unit (BRU), in the axial direction, to externally-imposed random-type vibrations.

3. Experimental tests were conducted to assess the effects of external vibrations on a newly developed space-power turbo-compressor-alternator (the Brayton Rotating Unit, or BRU). The tests included both sinusoidal and random vibration inputs.

The following paragraphs describe the conclusions pertaining to the three areas of investigation listed above. Conclusions relating to the experimental part are still incomplete and tentative, because a thorough evaluation of the recorded data has still to be performed. Such an evaluation will constitute a separate study.

Analysis of Response of Nonlinear System to Externally-Imposed Shock and Sinusoidal Vibration

Nonlinear elements were added to the axial shock and sinusoidal vibration analysis reported in Reference 1. The extended analysis was implemented in a modified version of the computer program reported in that reference. The improved program permits specification of either linear or nonlinear spring-damper elements, with nonlinear elements describable in terms of functions or tabular input.

Comparisons of calculated and measured axial response to shock inputs for the NASA A-Engine turbocompressor simulator yield reasonably good correlation to the accuracy within which the elastomeric isolator dynamic stiffness and damping properties are known.

Analysis of Response of Linear System to Externally-Imposed Random Vibration

An analysis was developed for the linear three-mass axial response model reported in Reference 1. This model is applicable to a wide range of single-shaft gas-bearing rotor systems. The analysis considers random acceleration, specified as a power spectral density of arbitrary shape over an arbitrary frequency range, to be applied along the shaft axis of ration to that element of the dynamic model which supports the rotor-bearing system. Since primary interest centers about the behavior of the gas-lubricated thrust bearing, the axial response of the system is presented in terms of displacement power spectral density. Thus, the dynamic behavior of the thrust bearing film, in terms of both power spectral density and RMS values, may be examined as a function of other system design parameters.

Such calculations and studies of the axial response of the Brayton Rotating Unit (BRU) have been performed and are reported herein. Preliminary comparisons between calculated and measured thrust bearing response, on an RMS basis, give reasonably good correlation.

Experimental Tests

Sinusoidal and random vibration tests were conducted on the Brayton Rotating Unit (BRU) with NASA environmental specification 417-2-C, as a goal for the upper limits of the externally-applied vibration levels. In the sinusoidal mode, the imposed vibrations were relatively light and had little effect upon the gas bearing system. In the low frequency range (5-35 Hz), for which a vibration input level of 0.25 g peak was prescribed (BRU operating and non-operating) no system resonances were encountered. Exploratory investigations in the frequency range 35-2000 Hz revealed strong resonances between 60 and 400 Hz. This regime could only be traversed (BRU operating) by reducing the shake table input to 0.12 g peak so as to maintain reasonably safe gas bearing film thicknesses of 0.0001 inch and larger. Generally, intermittant rotor-bearing

contacts were not observed during sinusoidal testing. A failure of the compressor-end journal bearing to maintain hydrodynamic operation was noted during sinusoidal testing; the bearing lost permanently its ability to function hydrodynamically. Upon disassembly of the BRU simulator at the NASA Lewis Research Center subsequent to testing, it was found that all three pivot seat-to-journal bearing pad joints had broken on that bearing. Since it is unlikely that all three brazed joints broke at the same instant, no particular significance should be ascribed to the frequency (190 Hz) at which the failure became apparent. This may have been the instant at which the last of the three joints broke, because this type of journal bearing is capable of operating with at least one broken joint, as evidenced by the fact that at disassembly the brazed joint of one of the turbine-end journal bearing pads was also found to be broken. No degradation of turbine-end journal bearing performance had been observed during vibration testing at MTI.

One of the most striking observations made during sinusoidal vibration testing, with the BRU simulator bearings operating hydrodynamically, was the absence of resonances of the flex-mounted journal pads relative to the shaft surfaces. The ratio of spring stiffnesses of the gas film between the journal bearing pad and the rotor on the one hand, and that of the flexure which supports one pad in each journal bearing on the other hand, appears to permit those pads to "track" the rotor under hydrodynamic operating conditions. Relative motions due to rotor or bearing support excursions are accommodated by the flexure supporting the pad. This fact indicates that the provision of damping in the flexure may be a viable method for introducing an energy dissipation mechanism into the system.

The random vibration requirement contained in NASA Environmental Specification 417-2-C is more severe than the sinusoidal requirement. For the operating mode 5.4 g RMS is specified, and for the nonoperating mode 19.7 g RMS. Momentary breakdowns of the gas bearing film were observed at less than half the desired random vibration input value of 5.4 g RMS. This is not surprising in view of the numerous resonance peaks observed in the BRU for relatively small vibration table inputs at discrete frequencies during sinusoidal testing.

The short duration rubs which occurred at the higher vibration input levels during random testing were evidenced by a fairly rapid rise in measured temperatures of the affected bearings. However, these rubs did not seem to cause noticeable permanent hydrodynamic bearing performance degradation, because rotor operation at the conclusion of all tests appeared normal (except for the failure of the compressor journal bearing, described earlier) and the chrome oxide bearing surface coatings were found to be in good condition after simulator disassembly at the NASA Lewis Research Center.

The electromagnetic shaker which was obtained for the BRU tests, proved well suited to the task. It has a 15,000-pound sine vector and 9,000-pound RMS (random) force rating. Testing at such levels has not yet been conducted, of course, for the BRU.

LIST OF REFERENCES

1. Spencer, P.R., Curwen, P.W. and Tryon, H.B., "Effect of Vibration and Shock on the Performance of Gas Bearing Space Power Brayton Cycle Turbomachinery, Part I-Half-Sine Shock and Sinusoidal Vibration", NASA CR-1762, Prepared for NASA by Mechanical Technology Incorporated under Contract NASW 1713, July 1971.

2. Brown, W.J., "Brayton-B Power System --- A Progress Report", Appearing in 4th Intersociety Energy Conversion Conference, pg. 652-658, Washington, D.C. September 22-26, 1969, Statler Hilton Hotel.

3. Davis, J.E., "Final Report --- The Design and Fabrication of the Brayton Rotating Unit (BRU)", APS-5334-R, Prepared by Airsearch Manufacturing Company of Arizona for NASA, March, 1971.

4. Crandall, S.H. and Mark, W.D., "Random Vibration in Mechanical Systems", Academic Press, New York, London, 1963.

5. Wise, J.H., "Elementary Concepts in Vibration Analysis", Institute of Environmental Sciences, 1966, Tutorial Lecture Series, Dynamics, pp. 11-22.

6. Tustin, W., "Random and Complex Vibration Testing", Institute of Environmental Sciences, 1964 Proceedings, pp. 53-63.

7. Curtis, A.J., "Random and Complex Vibration Theory", Institute of Environmental Sciences, 1964 Proceedings, pp. 35-52.

8. Miles, J.W. and Thomson, W.T., "Statistical Concepts in Vibration", Chapter 11 of Shock and Vibration Handbook, Vol. 1, Ed. Harris and Crede, McGraw-Hill, 1961.

9. Kozin, F., "A Brief Introduction to Some Basic Ideas on the Topic of Random Functions", Publ. in Stochastic Processes in Dynamical Problems, Presented at the 1969 Winter Annual Meeting of the American Society of Mechanical Engineers.

10. Bendat, J.S. and Piorsol, A.G., "Measurement and Analysis of Random Data", John Wiley & Sons, New York, 1966.

11. Papoulis, H., "Probability Random Variables and Stochastic Processes", McGraw-Hill, New York, 1965.

12. Lyon, R.M., "Random Noise and Vibration in Space Vehicles", The Shock and Vibration Information Center, Monograph SVM-1, Department of Defense, 1967.

13. NASA, Lewis Research Center, "Environmental Specification for SNAP 8 Electrical Generating System", Specification No. 417-2, Revision C, June 1, 1969.

14. Visek, A.J., "Accurate Determination of Grms Through Spectrum Analysis", Published in the Journal of Environmental Sciences, pgs. 20-23, December 1965.

15. Pratt, J.S., "Random Acceleration: RMS Value", Published in Test Engineering, March 1970.

16. Crede, C.E., and Ruzicka, J.E., "Theory of Vibration Isolation", Chapter 30, of Shock and Vibration Handbook, Vol. II, Ed. Harris and Crede, McGraw-Hill, 1961.

17. Thomson, W.T., "Vibration Theory and Applications", Chapter 11, Random Vibrations, Prentice Hall, 1965.

APPENDIX A

NONLINEAR-ELEMENT SINUSOIDAL VIBRATION AND SHOCK AXIAL RESPONSE ANALYSIS

The three-mass vibration model developed in Reference 1 was used in this study with the implementation of nonlinear isolator properties. The lumped masses m_1, m_2 and m_3 are those of the turbocompressor simulator casing, the thrust bearing housing-flexure combination and the rotor respectively. The nonlinear isolator properties are represented by a nonlinear stiffness $k_1[x]$ and a nonlinear damping coefficient $c_1[x]$. The thrust bearing housing and the flexure are represented by a stiffness k_2 and a damping coefficient c_2. Both are constants. Denoting the displacements of the three masses and the base as x_1, x_2, x_3 and x_b, the equations of motion can be written as:

$$m_1\ddot{x}_1 = k_2(x_2 - x_1) - k_1[x](x_1 - x_b) - c_1[x](\dot{x}_1 - \dot{x}_b) - m_1 g \quad (A.1)$$

$$m_2\ddot{x}_2 = -G[h, \dot{h}] - k_2(x_2 - x_1) - c_2(\dot{x}_2 - \dot{x}_1) - m_2 g \quad (A.2)$$

$$m_3\ddot{x}_3 = G[h, \dot{h}] + F_a - m_3 g \quad (A.3)$$

where F_a = aerodynamic force acting on m_3.

g = gravitational acceleration.

$G[h,\dot{h}]$ = gas film force.

The gas film force can be resolved into a load capability component $W_3(h)$ and a damping component. Thus,

$$G[h,\dot{h}] = W_3[h] - \dot{h}\ B_3[h] \quad (A.4)$$

where h = gas film thickness = $x_3 - x_2$.

It is convenient to write the nonlinear isolator restoring force $-k_1[x](x_1 - x_b)$ as:

$$W_1[x_1 - x_b] = -k_1[x](x_1 - x_b) \tag{A.5}$$

With the substitution of (A.4) and (A.5), Equations (A.1), (A.2) and (A.3) can be rewritten as:

$$m_1\ddot{x}_1 = k_2 (x_2 - x_1) + W_1[x_1 - x_b] - c_1 (\dot{x}_1 - \dot{x}_b) - m_1 g \tag{A.6}$$

$$m_2\ddot{x}_2 = -G[h,\dot{h}] - k_2(x_2 - x_1) - c_2(\dot{x}_2 - \dot{x}_1) - m_2 g \tag{A.7}$$

$$m_3\ddot{x}_3 = G[h,\dot{h}] + F_a - m_3 g \tag{A.8}$$

These equations can be expressed in a form amenable to laboratory measurement by some redefinition. First of all, the position under static equilibrium can be obtained from Equations (A.1), (A.2) and (A.3).

$$0 = k_2(\bar{x}_2 - \bar{x}_1) + W_1 [\bar{x}_1 - \bar{x}_b] - m_1 g \tag{A.9}$$

$$0 = - W_3[\bar{h}] - k_2 (\bar{x}_2 - \bar{x}_1) - m_2 g \tag{A.10}$$

$$0 = W_3[\bar{h}] + F_a - m_3 g \tag{A.11}$$

where $\bar{x}_1$, $\bar{x}_2$, $\bar{x}_3$ and $\bar{x}_b$ are the values of coordinates at static equilibrium and $\bar{h}$ is the equilibrium gas film thickness. Obviously, $\bar{h} = \bar{x}_3 - \bar{x}_2$. Now, if we measure the displacements of the masses from their respective equilibrium position, and denote them by y_1, y_2, y_3 and y_b, then

$$\begin{aligned} y_1 &= x_1 - \bar{x}_1 & \qquad y_3 &= x_3 - \bar{x}_3 \\ y_2 &= x_2 - \bar{x}_2 & \qquad y_b &= x_b - \bar{x}_b \end{aligned} \tag{A.12}$$

In terms of the y coordinates, the equations of motion can be written as

$$m_1\ddot{y}_1 = k_2(y_2-y_1) + W_1[y_1-y_b+\bar{x}_1-\bar{x}_b] - W_1[\bar{x}_1-\bar{x}_b] - c_1(\dot{y}_1-\dot{y}_b) \quad (A.13)$$

$$m_x\ddot{y}_x = - W_3[h] + W_3[\bar{h}] + (\dot{y}_3-\dot{y}_2)\, B_3[\bar{h}] - k_2(y_2-y_1) - c_2(\dot{y}_2-\dot{y}_1) \quad (A.14)$$

$$m_3\ddot{y}_3 = W_3[h] - W_3[\bar{h}] - (\dot{y}_3-\dot{y}_2)\, B_3[\bar{h}] \quad (A.15)$$

Note that by definition

$$h = x_3 - x_2 = y_3 - y_2 + (\bar{x}_3 - \bar{x}_2)$$

$$= y_3 - y_2 + \bar{h}$$

$$\dot{h} = \dot{y}_3 - \dot{y}_2$$

The square bracket is used here to denote functional dependence. For example, $W_3[h]$ should be read as "W_3 as a function of h".

The isolation system consists of four individual shock and vibration isolators connected in parallel to support the turbocompressor simulator. The load-deflection characteristics of an individual isolator were measured and the results were plotted in Figure 4. The ordinate in Figure 4 is the total load on the isolation system which is four times the load on each individual isolator.

The right-hand sides of Equations (A.13), (A.14) and (A.15) are discussed as follows. The stiffness k_2 and damping coefficient c_2 are known constants. The damping coefficient of the isolator c_1 can be a quantity varying with the isolator deflection. In this analysis, c_1 will be taken as a constant because no further information is available at the present time. The isolator load deflection characteristic W_1 can be read from Figure 2. The nonlinear load capacity and damping coefficient of the thrust bearing gas film can be approxi-

mately represented by either an exponential function or a power function of the film thickness as indicated on page 17 of Reference 1. As shown in Figure 18 and 19 of Reference 1, the load capacity and the damping coefficient of the thrust bearing gas film can be approximately represented by

$$W_3[h] = 105 \exp(-1555h) \text{ lb}$$

$$B_3[h] = 9.73\, h^{-1.5} \text{ lb sec/in.}$$

Note that h should be expressed in inches in the above two formulas.

Equations (A.13), (A.14) and (A.15) can be expressed as a set of six simultaneous, first-order, nonlinear differential equations. The shock or vibration forcing function to the simulator is fed in through y_b. If the system is started from its static equilibrium position, then the initial conditions of the differential equations are homogeneous, i.e., at $t = 0$, $y_1 = y_2 = y_3 = \dot{y}_1 = \dot{y}_2 = y_3 = 0$. These equations and inital conditions were programmed on a digital computer using a fourth-order, Runge-Kutta integration technique supplemented by an error control method which continuously adjusted the integration step size to maintain solution accuracy within prescribed limits.

APPENDIX B

NONLINEAR-ELEMENT AXIAL RESPONSE COMPUTER PROGRAM

This appendix presents a complete listing of the computer program which calculates the axial response of the turbocompressor simulator. This program is a modification of the axial response program of Reference 1 to include nonlinear isolator properties. Also presented in this appendix are instructions for preparing input data cards, sample input and sample printed output. The lumped-mass model used for the nonlinear-element computer program is shown in Figure 6.

PROGRAM INPUT CARDS

Card 1 - FORMAT (I5, 75H)

This card contains a case number and descriptive text for the users convenience.

Set NCAS = Any nonzero numerical digit to sequentially identify the case being computed (a blank here will stop the program)

Title = Any descriptive identification for case being computed. If computer graphs are requested, this descriptive identification will automatically appear at bottom of graph.

Card 2 - FORMAT (I5, 10X, 4I5, 3(I5, F10.4))

This is a control card which contains the following control variables. MODEL, IFOFT, ICC, MOTION, NONLIN, ITYP1, TAB1, ITYP2, TAB2, ITYP3, TAB3

These variables dictate options as follows:

Physical Model

MODEL = 1. Complete system as shown in Figure 2.

MODEL = 2. Complete system on rigid mounts ($k_1 = \infty$) with flexible lower casing.

MODEL = 3. Simple model, gas film with nonlinear stiffness and damping; rigid casing and mounts ($k_1 = k_2 = \infty$).

Type of Excitation Function

IFOFT = 8 Continuous sine function

IFOFT = 9 Shock function half sine

IFOFT = 10 Shock function haversine

IFOFT = 11 Shock function (table)

Calcomp desired?

ICC = 12 yes

ICC = 13 no

Is forcing function described in terms of displacement or acceleration?

MOTION = 0 if forcing function input represents displacement in inches.

MOTION = 1 if forcing function input represents acceleration in g's.

NONLIN = 1 This is a control integer which causes the program to utilize the nonlinear element analysis described in this report rather than the previous analysis described in Reference 1 which permitted nonlinearities only in the gas film.

NONLIN = 0 This input will cause the program to utilize the analysis published in Reference 1.

ITYP1 = 1 and TAB1 = 0. For the case that K1 and C1 are linear values to be read in as constants.

ITYP1 = 2 and TAB1 = 0. For the case that K1 and C1 are nonlinear functions which can be completely arbitrary, but must be supplied by the user as function subprograms called by "FK1" and "FC1".

ITYP1 = 3 For the case that K1 and C1 are to be read in as tabular values.
TAB1 = 0. If table increment of relative displacement is irregular.
TAB1 = Table increment of relative displacement between the mass 1 and the base for which the load and damping values will be specified.

ITYP2 and TAB2 are the same as ITYP1 and TAB1 except that they relate to K2 and C2 and the relative displacement between mass 2 and mass 1.

ITYP3 and TAB3 similar to above but apply to K3 and C3 and the relative displacement between mass 3 and mass 2.

Card 3a, and 3b - FORMAT (8 E10.4) and (2E 10.4)

This card describes the values of the masses, stiffnesses, and damping coefficients associated with the three degree of freedom vibration model. Read M1, M2, M3, K1, K2, K3, C1, C2, C3, HINIT

M1, M2, M3 = Weights (in pounds) of the lumped-masses shown in Figure 3.

K1, K2, K3 = Stiffnesses (in pound per inch) shown in Figure 3.

C1, C2, C3 = Damping coefficients (lb-sec/in.) shown in Figure 3.

HINIT = Initial equilibrium film thickness of gas film. This quantity need only be furnished if linear stiffness and damping are assumed for this gas film.

NOTE: Any pair(s) of the stiffness and damping elements may have been declared

nonlinear by the variables specified on Card 2. If this is done, the corresponding values on Card 3 are ignored by the program.

Card 4 - FORMAT (3E10.4)

This card contains constants which affect the conditions of the initial equilibrium conditions of the gas film. It also contains a variable, ELIM, which serves to prevent the nonlinear thrust bearing gas film properties from becoming infinitely large at zero film thickness.

GL = Local gravitational acceleration in "g's" (GL = 1.0 on earth's surface)

FA = Net aerodynamically induced axial force (in pounds) on rotor (positive, if force is upward).

ELIM = Nonlinear load and damping functions are held constant at film thicknesses less than "ELIM" inches.

Cards 5A, 5B, 5C, 5D - FORMAT (8E10.3)

These cards contain, in tabular form, the nonlinear properties required to specify the various spring and damping characteristics of the system. The use of these cards depends upon the values of ITYP1, TAB1, ITYP2, TAB2, ITYP3, and TAB3 specified on Card 2. If ITYP1 = 3, ITYP2 = 3, or ITYP3 = 3, then the tables must be supplied. Otherwise, OMIT Cards 5A, 5B, 5C, 5D entirely.

For the spring and damping coefficients k_1 and c_1:

Card 5A

Submit all values of relative displacement (inches) for which load values are specified. In each card, the values are punched in successive fields of ten, (8 values per card). The last value may not be 0.0, and the last card of this set is followed by a blank card.

Card 5B

The second set of values consists of the nonlinear load characteristic (lb) for which the displacements were specified above. The values are submitted in the same manner. The last card of this set is followed by a blank card.

Card 5C

The third set of values specifies displacement values for which damping is specified. The values are submitted in the same manner. The last card of this set is followed by a blank card.

Card 5D

The fourth set of values specifies values of the nonlinear damping characteristic. The values are submitted in the same manner. The last card of this set is followed by a blank card.

If TAB1 $\neq$ 0, then the table increment of the relative displacement is regular and given by TAB1. In this case, omit the first and third sets and replace set 1 by a card containing the starting value of the relative displacement (column 1-10). The starting value applies to both displacement values for both load and damping characteristics. The same procedure is used for quantities k_2, c_2 and for k_3, c_3 if required, with a separate set of cards 5A, 5B, 5C, 5D for each.

NOTE: All tables for K1, K2 and C1, C2 must be formulated with respect to the conditions of static equilibrium to remove any preload effects.

Card 6

This card specifies the parameters of the system forcing function: amplitude and frequency, if the system is under a steady-state vibration; or pulse amplitude and pulse duration if the forcing function is a closed-form shock pulse. Data is dependent upon options chosen for IFOFT and MOTION.

There are four distinct possibilities depending upon the control variable IFOFT specified on Card 2.

If IFOFT = 8 Read AMPLD, FREQ

FORMAT (2E10.4)

AMPLD = amplitude of sinusoidal forcing function.
If MOTION = 0, AMPLD = displacement in inches.
If MOTION = 1, AMPLD = acceleration in g's.
FREQ = frequency of forcing function in Hz (cps).

If IFOFT = 9 Read PEAKS, PDURS

FORMAT (2E10.4)

PEAKH = peak value of half sine shock pulse.
If MOTION = 0, PEAKS = displacement in inches.
If MOTION = 1, PEAKS = acceleration in g's.
PDURS = duration of half sine shock pulse (seconds).

If IFOFT = 10 Read PEAKH, PDURH

FORMAT (2E10.4)

PEAKH = peak value of haversine (shock machine half sine) pulse.
If MOTION = 0, PEAKH = displacement in inches.
If MOTION = 1, PEAKH = acceleration in g's.
PDURH = duration of haversine shock pulse (seconds)

If IFOFT = 11 Read NINC, TINCP

FORMAT (15, F10.4)

NINC = number of evenly-spaced intervals in pulse.
TINCP = time interval of each of the above increments.

This data card must be followed by as many data cards, 6A, 6B, etc., as are necessary to represent the shock pulse.

Cards 6A, 6B, etc. Read PUVAL (only if IFOFT = 11)

FORMAT (8E10.4)

PUVAL = values of the shock pulse at each increment specified above. Values

must be contiguous starting with the first increment.

If MOTION = 0, PUVAL = displacement in inches.
If MOTION = 1, PUVAL = acceleration in g's.

NOTE: If more than one increment size is desired, a different case may be run for each step size by using the conditions at the change point as restart values.

Card 7 - FORMAT (415, 6E10.4)

This card controls the precision and duration of the internal computation and output. It contains the following ten variables: IPSTEP, M, MAXINC, NCYCLS, TPRINT, TMAX, H, E, HM, RERR

IPSTEP = ratio of printed to plotted output points. In most cases IPSTEP = 1.

M = number of integrations performed internally before step size is automatically adjusted. Usually M = 2. This will usually result in the best trade off between precision and economy.

MAXINC = the maximum number of internal integrations before program shuts itself off. This is a safety control to prevent exorbitant computer charges due to unforeseeable misbehavior of the solution. Recommended MAXINC = 3000.

NCYCLS = the number of cycles for which the solution will be calculated beyond the first minumum and maximum after the shock pulse ceases to act. NCYCLS has meaning only for shock pulses. This variable is ignored if IFOFT = 8.

TPRINT = output control which establishes the step size of printed and plotted output (seconds). May be any convenient interval into which the time range of the solution is to be divided, generally a few hundred points or so. Example: If the range of interest is expected to be between 0 and 2 seconds, and 200 solution points are adequate to describe the system behavior in detail:

$$\text{TPRINT} = \frac{2 \text{ seconds}}{200} = 0.01$$

This will cause results to be printed at 10 milliseconds, 20 milliseconds, etc.

TMAX = maximum time value (seconds) for which solutions will be computed. This is another safety feature designed to prevent excessive computational charges resulting from some unforeseeable characteristic of the solution. Normally, this value should be twice as large as the solution is expected to run.

H = time increment (seconds) at which to begin computations.

E = maximum absolute error permitted in internal computation. A value of 0.002 is suggested for this quantity.

HM = minimum step size (seconds) for internal calculation. This parameter is another safety measure which keeps the internally-set step size from approaching zero in the attempt to achieve greater accuracy. A value of 0.000001 is suggested for this quantity.

RERR = comparable to E, except that RERR represents relative error, whereas E represents absolute error. This quantity should normally be set equal to 0.01.

Card 8 - FORMAT (7E10.4)

Initial value of restart card. Values need only be given if the initial conditions of the case being computed are unequal to zero. Otherwise, a blank card will suffice here. The values read are: TINIT, Y1IN, Y2IN, Y3YN, V1IN, V2IN, V3IN.

TINIT = initial or restart time (seconds).

Y1IN = initial value of Y_1 (inches).

Y2In = initial value of Y_2 (inches).

Y3IN = initial value of Y_3 (inches).

V1IN = initial value of V_1 (inches/sec).

V2IN = initial value of V_2 (inches/sec).

V3IN = initial value of V_3 (inches/sec).

Repeat all above cards for each case.

Insert a blank card as the last data card in order to stop the program.

```
  116 REPEAT OF TEST CASE NO. 116 - SIGN CHANGE ON FORCES   5/12/71
    1    0    0   11   13    1    1    3   0.          1                2
109.          .9      10.5                 53000.                        .01

  1.         0.          .00005
  1.00       .98         .96         .94         .92         .90         .88         .86
   .84       .82         .80         .78         .76         .74         .72         .70
   .68       .66         .64         .62         .60         .58         .56         .54
   .52       .50         .48         .46         .44         .42         .40         .38
   .36       .34         .32         .30         .28         .26         .24         .22
   .20       .18         .16         .14         .12         .10         .08         .06
   .04       .02         .01         .00        -.01        -.02        -.03        -.04
  -.05      -.06        -.07        -.08        -.09        -.10        -.11        -.12
  -.14      -.16        -.18        -.20        -.22        -.24        -.26        -.28
  -.30      -.32        -.34        -.36        -.38        -.40        -.42        -.44
  -.46      -.48        -.50        -.52        -.54        -.56        -.58        -.60

  -4290.    -4210.      -4120.      -4040.      -3950.      -3870.      -3790.      -3710.
  -3630.    -3540.      -3460.      -3380.      -3300.      -3220.      -3130.      -3050.
  -2970.    -2880.      -2800.      -2710.      -2630.      -2550.      -2470.      -2390.
  -2300.    -2220.      -2140.      -2050.      -1970.      -1880.      -1800.      -1710.
  -1620.    -1540.      -1450.      -1370.      -1300.      -1200.      -1130.      -1040.
   -950.     -820.       -780.       -720.       -616.       -536.       -452.       -364.
   -264.     -120.        -35.          0.         24.         32.         36.         40.
     48.       52.         56.         60.         64.         72.         76.         80.
     88.       96.        108.        120.        132.        144.        156.        168.
    180.      196.        212.        228.        240.        260.        280.        300.
    328.      360.        390.        436.        516.        628.        780.       1000.

  1.00       .98         .96         .94         .92         .90         .88         .86
   .84       .82         .80         .78         .76         .74         .72         .70
   .68       .66         .64         .62         .60         .58         .56         .54
   .52       .50         .48         .46         .44         .42         .40         .38
   .36       .34         .32         .30         .28         .26         .24         .22
   .20       .18         .16         .14         .12         .10         .08         .06
   .04       .02         .01         .00        -.01        -.02        -.03        -.04
  -.05      -.06        -.07        -.08        -.09        -.10        -.11        -.12
  -.14      -.16        -.18        -.20        -.22        -.24        -.26        -.28
  -.30      -.32        -.34        -.36        -.38        -.40        -.42        -.44
  -.46      -.48        -.50        -.52        -.54        -.56        -.58        -.60

     3.25      3.25        3.25        3.25        3.25        3.25        3.25        3.25
     3.25      3.25        3.25        3.25        3.25        3.25        3.25        3.25
     3.25      3.25        3.25        3.25        3.25        3.25        3.25        3.25
     3.25      3.25        3.25        3.25        3.25        3.25        3.25        3.25
     3.25      3.25        3.25        3.25        3.25        3.25        3.25        3.25
     3.25      3.25        3.25        3.25        3.25        3.25        3.25        3.25
     3.25      3.25        3.25        3.25        3.25        3.25        3.25        3.25
     3.25      3.25        3.25        3.25        3.25        3.25        3.25        3.25
     3.25      3.25        3.25        3.25        3.25        3.25        3.25        3.25
     3.25      3.25        3.25        3.25        3.25        3.25        3.25        3.25

   20 .001
  -.01415    -.0283      -.04245     -.0565      -.0565      -.0848      -.113       -.1415
  -.157      -.160       -.159       -.156       -.145       -.1272      -.113       -.099
  -.113      -.1272      -.1415      -.170
    1    2 3000    0      .0005       .02         .0001       .002        .000001     .01


000000000000000000000
```

PN457. RESPONSE OF VERTICAL THRUST BEARING TO AXIALLY-APPLIED SHOCK OR VIBRATION

116 REPEAT OF TEST CASE NO. 116 - SIGN CHANGE ON FORCES 5/12/71 07/27/72

PROGRAM OPTIONS
OPTIONS SELECTED FOR THIS PARTICULAR RUN ARE DESIGNATED BY
OPTION

CHOICE OF VIBRATION MODEL

1 = THREE-DEGREE OF FREEDOM SYSTEM USING ISOLATORS

2 = THREE-DEGREE OF FREEDOM SYSTEM USING RIGID MOUNTS

3 = SIMPLE MODEL, ENTIRELY RIGID EXCEPT FOR GAS FILM

NON-LINEAR LOAD AND DAMPING FUNCTIONS ARE HELD CONSTANT AT FILM THICKNESSES LESS THAN 5.000E-05 INCHES.

EQUILIBRIUM FILM THICKNESS IS .9012 MILS

ASSUMING STEADY-STATE AERODYNAMIC FORCES ON THE ROTOR OF 0. LB
AND A LOCAL GRAVITATIONAL FIELD OF 1.0000 TIMES STANDARD

PARAMETERS OF THE SYSTEM ON RIGID MOUNTS ARE AS FOLLOWS

M1 (LB)	M2 (LB)	M3 (LB)	K1 (LB/IN)	K2 (LB/IN)	K3 (LB/IN)	C1 (LB-SEC/IN)	C2 (LB-SEC/IN)	C3 (LB-SEC/IN)
109.0	.9000	10.50		5.3000E+04			1.0000E-02	

****

TYPE OF EXCITATION FUNCTION

8 = STEADY SINUSOIDAL INPUT

9 = HALF SINE SHOCK

10 = HAVERSINE SHOCK

---

11 = ARBITRARY SHOCK (TABLE)

****

IS CALCOMP OUTPUT DESIRED-

12 = YES

---

13 = NO

****

****

THE STIFFNESS AND DAMPING PROPERTIES ARE SPECIFIED AS FOLLOWS

K1 AND C1	TABLES
K2 AND C2	CONSTANT
K3 AND C3	USER SUPPLIED FUNCTION

THE NONLINEAR LOAD VALUES BETWEEN M1 AND BASE ARE AS FOLLOWS

RELATIVE DISPLACEMENT BETWEEN M1 AND BASE (IN)	FORCE BETWEEN M1 AND BASE (LB)	RELATIVE DISPLACEMENT BETWEEN M1 AND BASE (IN)	FORCE BETWEEN M1 AND BASE (LB)	RELATIVE DISPLACEMENT BETWEEN M1 AND BASE (IN)	FORCE BETWEEN M1 AND BASE (LB)	RELATIVE DISPLACEMENT BETWEEN M1 AND BASE (IN)	FORCE BETWEEN M1 AND BASE (LB)
1.00000	-4290.00000	.56000	-2470.00000	.12000	-616.00000	-.18000	108.00000
.98000	-4210.00000	.54000	-2390.00000	.10000	-536.00000	-.20000	120.00000
.96000	-4130.00000	.52000	-2300.00000	.08000	-452.00000	-.22000	132.00000
.94000	-4040.00000	.50000	-2220.00000	.06000	-364.00000	-.24000	144.00000
.92000	-3950.00000	.48000	-2140.00000	.04000	-264.00000	-.26000	156.00000
.90000	-3870.00000	.46000	-2050.00000	.02000	-120.00000	-.28000	168.00000
.88000	-3790.00000	.44000	-1970.00000	.01000	-35.00000	-.30000	180.00000
.86000	-3710.00000	.42000	-1880.00000	0.00000	0.00000	-.32000	196.00000
.84000	-3630.00000	.40000	-1800.00000	-.01000	24.00000	-.34000	212.00000
.82000	-3540.00000	.38000	-1710.00000	-.02000	32.00000	-.36000	228.00000
.80000	-3460.00000	.36000	-1620.00000	-.03000	36.00000	-.38000	240.00000
.78000	-3380.00000	.34000	-1540.00000	-.04000	40.00000	-.40000	260.00000
.76000	-3300.00000	.32000	-1450.00000	-.05000	48.00000	-.42000	280.00000
.74000	-3220.00000	.30000	-1370.00000	-.06000	52.00000	-.44000	300.00000
.72000	-3130.00000	.28000	-1300.00000	-.07000	56.00000	-.46000	328.00000
.70000	-3050.00000	.26000	-1200.00000	-.08000	60.00000	-.48000	360.00000
.68000	-2970.00000	.24000	-1130.00000	-.09000	64.00000	-.50000	390.00000
.66000	-2880.00000	.22000	-1040.00000	-.10000	72.00000	-.52000	436.00000
.64000	-2800.00000	.20000	-950.00000	-.11000	76.00000	-.54000	516.00000
.62000	-2710.00000	.18000	-820.00000	-.12000	80.00000	-.56000	628.00000
.60000	-2630.00000	.16000	-780.00000	-.14000	88.00000	-.58000	780.00000
.58000	-2550.00000	.14000	-720.00000	-.16000	96.00000	-.60000	1000.00000

THE NONLINEAR DAMPING COEFFICIENT VALUES BETWEEN M1 AND BASE ARE AS FOLLOWS

RELATIVE DISPLACEMENT BETWEEN M1 AND BASE (IN)	DAMPING COEFFICIENT BETWEEN M1 AND BASE (LB-IN/SEC)	RELATIVE DISPLACEMENT BETWEEN M1 AND BASE (IN)	DAMPING COEFFICIENT BETWEEN M1 AND BASE (LB-IN/SEC)	RELATIVE DISPLACEMENT BETWEEN M1 AND BASE (IN)	DAMPING COEFFICIENT BETWEEN M1 AND BASE (LB-IN/SEC)	RELATIVE DISPLACEMENT BETWEEN M1 AND BASE (IN)	DAMPING COEFFICIENT BETWEEN M1 AND BASE (LB-IN/SEC)
1.00000	3.25000	.56000	3.25000	.12000	3.25000	-.18000	3.25000
.98000	3.25000	.54000	3.25000	.10000	3.25000	-.20000	3.25000
.96000	3.25000	.52000	3.25000	.08000	3.25000	-.22000	3.25000
.94000	3.25000	.50000	3.25000	.06000	3.25000	-.24000	3.25000
.92000	3.25000	.48000	3.25000	.04000	3.25000	-.26000	3.25000
.90000	3.25000	.46000	3.25000	.02000	3.25000	-.28000	3.25000
.88000	3.25000	.44000	3.25000	.01000	3.25000	-.30000	3.25000
.86000	3.25000	.42000	3.25000	0.00000	3.25000	-.32000	3.25000
.84000	3.25000	.40000	3.25000	-.01000	3.25000	-.34000	3.25000
.82000	3.25000	.38000	3.25000	-.02000	3.25000	-.36000	3.25000
.80000	3.25000	.36000	3.25000	-.03000	3.25000	-.38000	3.25000
.78000	3.25000	.34000	3.25000	-.04000	3.25000	-.40000	3.25000
.76000	3.25000	.32000	3.25000	-.05000	3.25000	-.42000	3.25000
.74000	3.25000	.30000	3.25000	-.06000	3.25000	-.44000	3.25000
.72000	3.25000	.28000	3.25000	-.07000	3.25000	-.46000	3.25000
.70000	3.25000	.26000	3.25000	-.08000	3.25000	-.48000	3.25000
.68000	3.25000	.24000	3.25000	-.09000	3.25000	-.50000	3.25000
.66000	3.25000	.22000	3.25000	-.10000	3.25000	-.52000	3.25000
.64000	3.25000	.20000	3.25000	-.11000	3.25000	-.54000	3.25000
.62000	3.25000	.18000	3.25000	-.12000	3.25000	-.56000	3.25000
.60000	3.25000	.16000	3.25000	-.14000	3.25000	-.58000	3.25000
.58000	3.25000	.14000	3.25000	-.16000	3.25000	-.60000	3.25000

INPUT MOTION IS A SHOCK PULSE DESCRIBED BY THE FOLLOWING TABLE

TIME (SEC)	ACCELERATION (G-S)
0.0000000	0.0000000
.0010000	-.0141500
.0020000	-.0283000
.0030000	-.0424500
.0040000	-.0565000
.0050000	-.0565600
.0060000	-.0848000
.0070000	-.1130600
.0080000	-.1415000
.0090000	-.1570000
.0100000	-.1600000
.0110000	-.1590000
.0120000	-.1560000
.0130000	-.1450000
.0140000	-.1272000
.0150000	-.1130000
.0160000	-.0990000
.0170000	-.1130000
.0180000	-.1272000
.0190000	-.1415000
.0200000	-.1700000

PULSE DURATION = 2.00000E-02 SEC

```
**********************************************************************************************************************

        PROGRAM CONTROL PARAMETERS

             DESIRED TERMINATION
                  TIME VALUE WILL NOT EXCEED      .0200 SECONDS
                  AS A SAFETY MEASURE WE WILL NOT PERMIT MORE THAN 3000 STEPS
                  CALCULATION WILL CONTINUE     1 CYCLES AFTER PULSE DURATION.
             STEP SIZE
                  INITIAL STEP SIZE FOR CALCULATION PURPOSES IS 1.000E-04 SECONDS
                  VALUES ARE PRINTED OUT EVERY 5.000E-04 SECONDS
                  EVERY     1TH POINT IS PLOTTED IF CALCOMP IS USED
                  ERROR CRITERION FOR INTEGRATION TECHNIQUE 2.000E-03
                  MINIMUM STEP-SIZE =, 1.00000E-06 SECONDS
                  NO. OF INTEGRATIONS BEFORE STEP-SIZE IS DOUBLED=     2
                  NORMALIZED ERROR LIMIT FOR INTEGRATION TECHNIQUE      .0100

        INITIAL OR RESTART CONDITIONS
                  INITIAL TIME            =-0.        SECONDS
                  DISPLACEMENT OF MASS 1  =-0.        INCHES
                  VELOCITY OF MASS 1      =-0.        IN/SEC
                  DISPLACEMENT OF MASS 2  =-0.        INCHES
                  VELOCITY OF MASS 2      =-0.        IN/SEC
                  DISPLACEMENT OF MASS 3  =-0.        INCHES
                  VELOCITY OF MASS 3      =-0.        IN/SEC
```

```
 000   U   U  TTTTT  PPPP   U   U  TTTTT
0   0  U   U    T    P   P  U   U    T
0   0  U   U    T    PPPP   U   U    T
0   0  U   U    T    P      U   U    T
 000    UUU     T    P       UUU     T
```

TIME (SEC)	FILM THICKNESS (INCHES)	DISPLACEMENT OF MASS 1 (INCHES)	DISPLACEMENT OF MASS 2 (INCHES)	DISPLACEMENT OF ROTOR (INCHES)	VELOCITY OF MASS 1 (IN/SEC)	VELOCITY OF MASS 2 (IN/SEC)	VELOCITY OF ROTOR (IN/SEC)	RELATIVE DISP. BET. MASS2 *MASS1	FORCING FUNCTION (INCHES)	REL. DISP. BET M1*BASE (INCHES)
.0005	9.0128E-04	-7.4055E-10	-1.2309E-10	-5.2229E-12	-4.6111E-06	-1.1125E-06	-5.9736E-08	-6.1746E-10	-3.4143E-07	3.4069E-07
.0010	9.0128E-04	-6.5854E-09	-2.4202E-09	-2.4723E-10	-2.1060E-05	-9.8175E-06	-1.3309E-06	-4.1652E-09	-1.3657E-06	1.3591E-06
.0015	9.0129E-04	-2.5879E-08	-1.2185E-08	-2.1033E-09	-6.2308E-05	-3.2788E-05	-7.3158E-06	-1.3694E-08	-3.7557E-06	3.7298E-06
.0020	9.0131E-04	-7.6023E-08	-4.0522E-08	-9.5477E-09	-1.4631E-04	-8.7142E-05	-2.5428E-05	-3.5501E-08	-8.1943E-06	8.1183E-06
.0025	9.0135E-04	-1.8260E-07	-1.0706E-07	-3.1741E-08	-2.9307E-04	-1.8874E-04	-6.8987E-05	-7.5537E-08	-1.5364E-05	1.5182E-05
.0030	9.0143E-04	-3.8366E-07	-2.4154E-07	-8.6009E-08	-5.2719E-04	-3.6350E-04	-1.5766E-04	-1.4212E-07	-2.5949E-05	2.5565E-05
.0035	9.0156E-04	-7.2868E-07	-4.8679E-07	-2.0137E-07	-8.7497E-04	-6.3644E-04	-3.1834E-04	-2.4189E-07	-4.0628E-05	3.9899E-05
.0040	9.0176E-04	-1.2827E-06	-9.0019E-07	-4.2196E-07	-1.3671E-03	-1.0421E-03	-5.8430E-04	-3.8251E-07	-6.0082E-05	5.8799E-05
.0045	9.0202E-04	-2.1244E-06	-1.5563E-06	-8.0975E-07	-2.0313E-03	-1.6124E-03	-9.9482E-04	-5.6817E-07	-8.4650E-05	8.2526E-05
.0050	9.0238E-04	-3.3476E-06	-2.5460E-06	-1.4478E-06	-2.8971E-03	-2.3825E-03	-1.5924E-03	-8.0165E-07	-1.1467E-04	1.1132E-04
.0055	9.0282E-04	-5.0609E-06	-3.9777E-06	-2.4406E-06	-3.9991E-03	-3.3870E-03	-2.4206E-03	-1.0831E-06	-1.5083E-04	1.4577E-04
.0060	9.0334E-04	-7.3926E-06	-5.9793E-06	-3.9142E-06	-5.3765E-03	-4.6687E-03	-3.5232E-03	-1.4133E-06	-1.9381E-04	1.8641E-04
.0065	9.0396E-04	-1.0491E-05	-8.6992E-06	-6.0168E-06	-7.0796E-03	-6.2685E-03	-4.9437E-03	-1.7923E-06	-2.4497E-04	2.3447E-04
.0070	9.0467E-04	-1.4536E-05	-1.2311E-05	-8.9184E-06	-9.1682E-03	-8.2458E-03	-6.7273E-03	-2.2255E-06	-3.0567E-04	2.9113E-04
.0075	9.0548E-04	-1.9734E-05	-1.7017E-05	-1.2813E-05	-1.1706E-02	-1.0655E-02	-8.9240E-03	-2.7178E-06	-3.7729E-04	3.5755E-04
.0080	9.0641E-04	-2.6329E-05	-2.3050E-05	-1.7921E-05	-1.4765E-02	-1.3567E-02	-1.1590E-02	-3.2796E-06	-4.6119E-04	4.3486E-04
.0085	9.0746E-04	-3.4598E-05	-3.0679E-05	-2.4493E-05	-1.8417E-02	-1.7051E-02	-1.4793E-02	-3.9196E-06	-5.5843E-04	5.2383E-04
.0090	9.0867E-04	-4.4858E-05	-4.0209E-05	-3.2815E-05	-2.2737E-02	-2.1186E-02	-1.8605E-02	-4.6486E-06	-6.7008E-04	6.2522E-04
.0095	9.1005E-04	-5.7459E-05	-5.1986E-05	-4.3213E-05	-2.7796E-02	-2.6048E-02	-2.3112E-02	-5.4731E-06	-7.9658E-04	7.3912E-04
.0100	9.1161E-04	-7.2788E-05	-6.6391E-05	-5.6057E-05	-3.3062E-02	-3.1716E-02	-2.8401E-02	-6.3969E-06	-9.3838E-04	8.6559E-04
.0105	9.1337E-04	-9.1266E-05	-8.3848E-05	-7.1760E-05	-4.0400E-02	-3.8262E-02	-3.4563E-02	-7.4185E-06	-1.0955E-03	1.0043E-03
.0110	9.1531E-04	-1.1334E-04	-1.0481E-04	-9.0780E-05	-4.8069E-02	-4.5757E-02	-4.1685E-02	-8.5319E-06	-1.2681E-03	1.1547E-03
.0115	9.1743E-04	-1.3950E-04	-1.2977E-04	-1.1362E-04	-5.6727E-02	-5.4263E-02	-4.9846E-02	-9.7269E-06	-1.4559E-03	1.3164E-03
.0120	9.1972E-04	-1.7024E-04	-1.5925E-04	-1.4081E-04	-6.6426E-02	-6.3837E-02	-5.9114E-02	-1.0991E-05	-1.6589E-03	1.4887E-03
.0125	9.2215E-04	-2.0611E-04	-1.9380E-04	-1.7293E-04	-7.7215E-02	-7.4530E-02	-6.9546E-02	-1.2311E-05	-1.8768E-03	1.6707E-03
.0130	9.2470E-04	-2.4765E-04	-2.3398E-04	-2.1056E-04	-8.9136E-02	-8.6381E-02	-8.1186E-02	-1.3672E-05	-2.1093E-03	1.8616E-03
.0135	9.2734E-04	-2.9544E-04	-2.8038E-04	-2.5432E-04	-1.0222E-01	-9.9424E-02	-9.4065E-02	-1.5061E-05	-2.3555E-03	2.0601E-03
.0140	9.3005E-04	-3.5007E-04	-3.3360E-04	-3.0483E-04	-1.1650E-01	-1.1368E-01	-1.0820E-01	-1.6467E-05	-2.6149E-03	2.2649E-03
.0145	9.3281E-04	-4.1214E-04	-3.9426E-04	-3.6273E-04	-1.3199E-01	-1.2916E-01	-1.2361E-01	-1.7880E-05	-2.8867E-03	2.4745E-03
.0150	9.3560E-04	-4.8226E-04	-4.6297E-04	-4.2865E-04	-1.4870E-01	-1.4588E-01	-1.4029E-01	-1.9290E-05	-3.1700E-03	2.6874E-03
.0155	9.3840E-04	-5.6104E-04	-5.4035E-04	-5.0323E-04	-1.6663E-01	-1.6384E-01	-1.5823E-01	-2.0692E-05	-3.4643E-03	2.9033E-03
.0160	9.4120E-04	-6.4909E-04	-6.2702E-04	-5.8709E-04	-1.8578E-01	-1.8302E-01	-1.7742E-01	-2.2078E-05	-3.7688E-03	3.1197E-03
.0165	9.4400E-04	-7.4702E-04	-7.2358E-04	-6.8086E-04	-2.0615E-01	-2.0343E-01	-1.9785E-01	-2.3447E-05	-4.0835E-03	3.3365E-03
.0170	9.4677E-04	-8.5544E-04	-8.3064E-04	-7.8515E-04	-2.2773E-01	-2.2504E-01	-2.1951E-01	-2.4797E-05	-4.4085E-03	3.5530E-03
.0175	9.4953E-04	-9.7495E-04	-9.4882E-04	-9.0056E-04	-2.5052E-01	-2.4787E-01	-2.4236E-01	-2.6131E-05	-4.7443E-03	3.7694E-03
.0180	9.5228E-04	-1.1062E-03	-1.0787E-03	-1.0277E-03	-2.7453E-01	-2.7189E-01	-2.6641E-01	-2.7453E-05	-5.0918E-03	3.9856E-03
.0185	9.5502E-04	-1.2497E-03	-1.2209E-03	-1.1672E-03	-2.9975E-01	-2.9712E-01	-2.9164E-01	-2.8768E-05	-5.4515E-03	4.2018E-03
.0190	9.5777E-04	-1.4061E-03	-1.3760E-03	-1.3195E-03	-3.2620E-01	-3.2356E-01	-3.1804E-01	-3.0084E-05	-5.8242E-03	4.4181E-03
.0195	9.6054E-04	-1.5761E-03	-1.5447E-03	-1.4854E-03	-3.5386E-01	-3.5120E-01	-3.4563E-01	-3.1407E-05	-6.2109E-03	4.6348E-03
.0200	9.6335E-04	-1.7602E-03	-1.7274E-03	-1.6654E-03	-3.8276E-01	-3.8007E-01	-3.7441E-01	-3.2743E-05	-6.6127E-03	4.8525E-03

SPECIFIED TIME HAS BEEN ATTAINED.

```
      PROGRAM PN457(INPUT,OUTPUT,TAPE5=INPUT,TAPE6=OUTPUT,TAPE22)
      COMMON TPRINT,TMAX,IPSTEP,NCYCLS,MOTION,TITLE(15),YBA,YBINT(200)
      COMMON NR,NW,NCASE,MODEL,LOADF,IDAMP,IFOFT,ICC,
     1              M1,M2,M3,K1,C1,K2,GL,FA,ALOAD,ADAMP,BLOAD,BDAMP,
     2CLOAD,CDAMP,DLOAD,DDAMP,HINIT,IFM7,AMPLD,FREQ,PEAKS,PDURS,PEAKH,
     3PDURH,NINCP,TINCP,TP(200),PUVAL(200),PULDOT(200),TINIT,Y1IN,Y2IN,
     4Y3IN,V1IN,V2IN,V3IN,TIME(6000),Y1,Y2,Y3,V1,V2,V3,N,VEC(6),DVEC(6),
     5MAXINC,H,HM,M,E,AKO,NE,T,              ELIM,INDX,     YB,YBDOT,
     6OMEGA,WHO,WY3Y2H,BY3Y2H
      COMMON FILMT(6000),Y2MY1(6000),VAPEAK(6000),YBPLOT(6000)
      COMMON IBUF(5000)
C MAINLINE PROGRAM PN 457. THIS PROGRAM CALCULATES THE RESPONSE OF A
C THRUST BEARING-ROTOR SYSTEM TO EXTERNALLY APPLIED SHOCK AND VIBRATION
C IT TREATS THE SYSTEM AS A THREE-DEGREE-OF-FREEDOM VIBRATION MODEL
C
      NR=5
      NW=6
      IFLAG=1
    5 READ(NR,1010) NCASE,(TITLE(I),I=1, 8)                              CDC
      IF(NCASE) 10,6,10
    6 IF(IFLAG.EQ.2)  CALL PLOT(18.,0.,999)
    9 CALL EXIT
   10 WRITE(NW,1000)
      WRITE(NW,1015)
      CALL SDATE(DATE)                                                   CDC
      WRITE(NW,1005) NCASE,(TITLE(I),I=1, 8),DATE                        CDC
      CALL INPUT
      IF(IFLAG.EQ.2)   GO TO 24
   20 IF(ICC.EQ.13)  GO TO 25
      IFLAG=2
      CALL PLOTS(IBUF,5000,22)
      GO TO 25
   24 CALL PLOT(18.,0.,-3)
   25 CALL SOLVE
      GO TO 5
 1000 FORMAT( 7H1PN457,10X,73HRESPONSE OF VERTICAL THRUST BEARING TO AXI
     1ALLY-APPLIED SHOCK OR VIBRATION/)
 1005 FORMAT(I5,7A10,A5,2X,A8)                                           CDC
 1010 FORMAT(I5,7A10,A5)
 1015 FORMAT(// 1X,119(1H*))
      END
```

```
      SUBROUTINE DIFEQ(N,T,VEC,DVEC)
      DIMENSION VEC(6),DVEC(6)
      DIMENSION A(2)
      COMMON TPRINT,TMAX,IPSTEP,NCYCLS,MOTION,TITLE(15),YBA,YBINT(200)
      COMMON NR,NW,NCASE,MODEL,LOADF,IDAMP,IFOFT,ICC,
     1             M1,M2,M3,K1,C1,K2,GL,FA,ALOAD,ADAMP,BLOAD,BDAMP,
     2CLOAD,CDAMP,DLOAD,DDAMP,HINIT,IFM7,AMPLD,FREQ,PEAKS,PDURS,PEAKH,
     3PDURH,NINCP,TINCP,TP(200),PUVAL(200),PULDOT(200),TINIT,Y1IN,Y2IN,
     4Y3IN,V1IN,V2IN,V3IN,TIME(6000),Y1,Y2,Y3,V1,V2,V3,
     5NDUM,DDUM(6),DVUM(6),
     5MAXINC,H,HM,M,E,AKO,NE,TTDUM,          ELIM,INDX,      YB,YBDOT,
     6OMEGA,WHO,WY3Y2H,BY3Y2H
      COMMON FILMT(6000),Y2MY1(6000),VAPEAK(6000),YBPLOT(6000)
      COMMON TZ,ITIME,YBPREV
      COMMON NONLIN,ITYP1,ITYP2,ITYP3,TAB1,TAB2,TAB3,C2,C3,K3,          EM
     1DISPW1(300),DISPW2(300),DISPW3(300),W1FTAB(300),W2FTAB(300),      EM
     2W3FTAB(300),DISPB1(300),DISPB2(300),DISPB3(300),B1FTAB(300),      EM
     3B2FTAB(300),B3FTAB(300),NOW1,NOW2,NOW3,NOB1,NOB2,NOB3             EM
      REAL M1,M2,M3,C1,K1,K2,K3                                         EM
      EXTERNAL FX
C THIS SUBROUTINE DEFINES THE DIFFERENTIAL EQUATIONS SOLVED BY RONKU
      DATA MAXIT,ERR/100,.01/
      WEX(X)=ALOAD*EXP(BLOAD*X)
      WPF(X)=CLOAD*X**DLOAD
      BEX(X)=ADAMP*EXP(BDAMP*X)
      BPF(X)=CDAMP*X**DDAMP
      PI=3.1415926535
      IFM7=IFOFT-7
      IF(MODEL.EQ.3) GO TO 20
      DVEC(4)=VEC(1)
      DVEC(5)=VEC(2)
      DVEC(6)=VEC(3)
   20 GO TO (30,60,90,120),IFM7
30    OMEGA=2.*PI*FREQ
      YB=AMPLD*SIN(OMEGA*T)
      YBDOT=OMEGA*AMPLD*COS(OMEGA*T)
      YBA=-YB*(2.*PI*FREQ)**2/386.069
      IF(MOTION.EQ.0)   GO TO 130
      YB=-386.069/OMEGA**2*AMPLD*SIN(OMEGA*T)
      YBDOT=-386.069/OMEGA*AMPLD*COS(OMEGA*T)
      GO TO 130
60    YB=0.
      IF(T.LT.PDURS) YB=PEAKS*SIN(PI*T/PDURS)
      YBDOT=0.
      YBA=YB
      IF(MOTION.EQ.1) GO TO 65
      IF(T.LT.PDURS) YBDOT=PI/PDURS*PEAKS*COS(PI*T/PDURS)
      GO TO 130
   65 IF(T.LT.PDURS) YB=386.069*PEAKS*PDURS/PI*(T-PDURS/PI*
     1 SIN(PI*T/PDURS))
      IF(T.LT.PDURS) YBDOT=386.069*PEAKS*PDURS/PI*(1.-COS(PI*T/PDURS))
      IF(.NOT.(T.LT.PDURS)) YBDOT=772.138*PEAKS*PDURS/PI
      IF(.NOT.(T.LT.PDURS)) YB=386.069*PEAKS*PDURS**2/PI+YBDOT*(T-PDURS)
      GO TO 130
90    YB=0.
      IF(T.LT.PDURH) YB=0.5*PEAKH*(1.-COS(2.*PI*T/PDURH))
      YBDOT=0.
      YBA=YB
      IF(MOTION.EQ.1)  GO TO 95
      IF(T.LT.PDURH) YBDOT=PI/PDURH*SIN(2.*PI*T/PDURH)*PEAKH
      GO TO 130
   95 IF(T.LT.PDURH) YB=386.069/4.*PEAKH*(T**2-PDURH**2/(2.*PI**2)*
     1 (1.-COS(2.*PI*T/PDURH)))
      IF(T.LT.PDURH) YBDOT=386.069/4.*PEAKH*(2.*T-PDURH/PI*
     1 SIN(2.*PI*T/PDURH))
      IF(.NOT.(T.LT.PDURH)) YBDOT=193.035*PEAKH*PDURH
      IF(.NOT.(T.LT.PDURH)) YB=386.069/4.*PEAKH*PDURH**2+YBDOT*(T-PDURH)
      GO TO 130
```

```
  120 ANINCP=NINCP
      PDURT=ANINCP*TINCP
      IF(T.GT.PDURT)  YB=0.0
      IF(T.GT.PDURT)  YBDOT=0.0
      IF(T.GT.PDURT.AND.MOTION.EQ.0) GO TO 130
       IF(T.GT.PDURT.AND.MOTION.EQ.1)  GO TO 125
      NP1=NINCP+1
      CALL TLU(T,YB,TP,PUVAL,NP1)
      IF(MOTION.EQ.1) GO TO 125
      CALL TLU(T,YBDOT,TP,PULDOT,NP1)
      GO TO 130
  125 YBA=YB
 1240 A(1)=TZ
      A(2)=T
      IOP=1
      IF(T.GT.PDURT)  GO TO 1270
      IF(ITIME.EQ.1)   GO TO 1260
 1250 MRET=126
      CALL SIMINI(YB,FX,A,ERR,0,MAXIT,1.,MRET)
      IF(MRET.EQ. 126) GO TO 126
      YB=386.069*YB+YBPREV
      GO TO (127,1280,1265),IOP
 1260 ITIME=2
      IGR=1
      YBPREV=0.0
      IF(TZ) 1261,1250,1261
 1261 A(1)=0.0
      A(2)=TZ
      IOP=3
      GO TO 1250
 1265 YBPREV=YB
      GO TO 1240
C  SAVE YB VALUE
C T GREATER THAN PDURT
 1270 IF(IGR.EQ.3)  GO TO 1275
      A(2)=PDURT
      IGR=2
      IOP=2
      GO TO 1250
 1275 YB=YBPDUR
      GO TO 2126
 1280 YBPDUR=YB
      GO TO 127
  126 WRITE(NW,102) MAXIT,ERR
      WRITE(NW,103)
  127 IF(T.LT.PDURT.OR.IGR.LE.2)   GO TO 2127
 2126 YBDOT=DOTDUR
      GO TO 2128
 2127 CALL TLU(T,YBDOT,TP,YBINT,NP1)
      YBDOT=YBDOT*386.069
      IF(IGR.NE.2)   GO TO 130
      IGR=3
      DOTDUR=YBDOT
 2128 YB=YB+YBDOT*(T-PDURT)
  130 IF(MODEL.NE.3) GO TO 150
      ARGU=VEC(2)-YB+HINIT
      IF(ARGU.LT..0002)  ARGU=ELIM
      IF(LOADF.EQ.4) WY3Y2H=WEX(ARGU)
      IF(LOADF.EQ.4) WHO=WEX(HINIT)
       IF(LOADF.EQ.5) WY3Y2H=WPF(ARGU)
      IF(LOADF.EQ.5) WHO=WPF(HINIT)
      IF(IDAMP.EQ.6) BY3Y2H=BEX(ARGU)
      IF(IDAMP.EQ.7) BY3Y2H=BPF(ARGU)
      GO TO 190
```

```
C SELECT FUNCTIONS
  150 ARGU=VEC(6)-VEC(5)+HINIT
      IF(ARGU.LT..0002) ARGU=ELIM
      IF(LOADF.EQ.4)  WY3Y2H=WEX(ARGU)
      IF(LOADF.EQ.4) WHO=WEX(HINIT)
      IF(LOADF.EQ.5)  WY3Y2H=WPF(ARGU)
      IF(LOADF.EQ.5) WHO=WPF(HINIT)
       IF(IDAMP.EQ.6)  BY3Y2H=BEX(ARGU)
      IF(IDAMP.EQ.7)  BY3Y2H=BPF(ARGU)
C NOW DEFINE DIFFERENTIAL EQUATIONS
C CORRECTIONS DIFEQ
  190 IF(NONLIN.EQ.0) GO TO 195                                          EM
      CALL DEQNL(VEC,DVEC)                                               EM
      GO TO 401                                                          EM
  195 IF(MODEL-2) 200,300,400                                            EM
200   DVEC(1)=(K2/M1)*(VEC(5)-VEC(4))-(K1/M1)*(VEC(4)-YB)-C1/M1*(DVEC
     1 (4)-YBDOT)
300   DVEC(2)=-(1./M2)*WY3Y2H+(1./M2)*WHO+(1./M2)*(DVEC(6)-DVEC(5))
     1 *BY3Y2H-(K2/M2)*(VEC(5)-VEC(4))
      DVEC(3)=-(1./M3)*WHO+(1./M3)*WY3Y2H-(1./M3)*(DVEC(6)-DVEC(5))*BY3Y
     12H
      IF(MODEL.EQ.2) DVEC(1)=(K2/M1)*(VEC(5)-VEC(4))-(K1/M1)*(VEC(4)-
     1 YB)
      GO TO 401
  400 DVEC(2)=VEC(1)
      DVEC(1)=-WHO+WY3Y2H-(DVEC(2)-YBDOT)*BY3Y2H
      DVEC(1)=DVEC(1)/M3
  401 RETURN
  100 FORMAT(/ 6(3X,3HVEC,I3),5X,1HT,6(3X,4HDVEC,I3))
  101 FORMAT(1X,6E9.3,F5.4,6E10.4)
  102 FORMAT(1H0,29HMAXIMUM NUMBER OF ITERATIONS,I3,25H WAS REACHED BEFO
     1RE EPS =,E11.4)
  103 FORMAT( 5X,6HFOR YB)
  104 FORMAT(5X,9HFOR YBDOT)
      END
```

```
FUNCTION FK1(Y1MYB,DY1MYB)
REAL K1
K1=58000.
FK1=K1*Y1MYB
RETURN
END
FUNCTION FC1(Y1MYB,DY1MYB)
FC1=.00001
RETURN
END
FUNCTION FK2(Y2MYB,DY2MYB)
REAL K2
K2=670000.
FK2=K2*Y2MYB
RETURN
END
FUNCTION FC2(Y2MYB,DY2MYB)
FC2=.00001
RETURN
END
FUNCTION FK3(H,E)
A=105.
B=-2554.8
FK3=A*EXP(B*H)
RETURN
END
FUNCTION FC3(H,E)
C=.31112E-3
D=-1.4984
FC3=C*H**D
RETURN
END
```

```
      SUBROUTINE CALCOM
      DIMENSION CLX(20),CLY(20)
      COMMON TPRINT,TMAX,IPSTEP,NCYCLS,MOTION,TITLE(15),YBA,YBINT(200)
      COMMON NR,NW,NCASE,MODEL,LOADF,IDAMP,IFOFT,ICC,
     1              M1,M2,M3,K1,C1,K2,GL,FA,ALOAD,ADAMP,BLOAD,BDAMP,
     2CLOAD,CDAMP,DLOAD,DDAMP,HINIT,IFM7,AMPLD,FREQ,PEAKS,PDURS,PEAKH,
     3PDURH,NINCP,TINCP,TP(200),PUVAL(200),PULDOT(200),TINIT,Y1IN,Y2IN,
     4Y3IN,V1IN,V2IN,V3IN,TIME(6000),Y1,Y2,Y3,V1,V2,V3,N,VEC(6),DVEC(6),
     5MAXINC,H,HM,M,E,AKO,NE,T,              ELIM,INDX,      YB,YBDOT,
     6OMEGA,WHO,WY3Y2H,BY3Y2H
      COMMON FILMT(6000),Y2MY1(6000),VAPEAK(6000),YBPLOT(6000)
      COMMON IBUF(5000)
      DATA XORIG,YORIG,AXLEN,AYLEN/2.,1.5,12.,6./
      WRITE(NW,202)
  202 FORMAT(1H1,30HROAD MARKERS FOR CALCOMP PLOTS)
      NVALS=INDX
      NPTS=NVALS/IPSTEP
      I=NPTS*IPSTEP+1
      J=I+IPSTEP
      WRITE(NW,200) NVALS,NPTS,I,J
      CALL FACTOR(.75)
C CHANGES IN CALCOM. INSERT AFTER CALL TO PLOTS
C STOMP OUT NEGATIVE FILM THICKNESSES. TAG FIRST VAL FOR ERROR MESSAGE.
      ITAG=0
      CALL PLOT(XORIG,YORIG,-3)
      DO 20 K=1,NPTS
      IF(ITAG) 15,15,16
15    IF(FILMT(K) .LT. 0.) ITAG=K
16    IF(FILMT(K) .LT. 0.)  FILMT(K)=0.
20    CONTINUE
      CALL SCALE(TIME,AXLEN,NPTS,IPSTEP)
      WRITE(NW,201) TIME(I),TIME(J)
      IF(ITAG) 22,22,21
   21 XPAGE=TIME(ITAG)/TIME(J)
      CALL SYMBOL(XPAGE,0.,.14,7HCONTACT,30.,7)
C SCALE THE AXIS ACCORDING TO THE DATA BUT FORCE THE MINIMUM FILMT TO 0.
C  DEFINE AN ADDITIONAL FILMT TO INSURE AT LEASE ONE ZERO
22    FILMT(I)=0.
C CALL SCALE USING I POINTS, IT WILL STORE 0. AS FILM(J) AND DELTAV IN
C   FILMT(J+IPSTEP)
      NP1=NPTS+1
      CALL SCALE(FILMT,AYLEN,NP1,IPSTEP)
      II=NP1*IPSTEP+1
      JJ= II+IPSTEP
      WRITE(NW,203) FILMT(II),FILMT(JJ)
C NOW MOVE FIRSTV AND DELTAV BACK WHERE THEY BELONG.
      FILMT(I)=FILMT(J)
      FILMT(J)=FILMT(J+IPSTEP)
C SCALE DATA FOR TIME AND INPUT MOTION
      CALL SCALE(TIME,AXLEN,NPTS,IPSTEP)
      CALL SCALE(YBPLOT,AYLEN,NPTS,IPSTEP)
      CALL PLOT(-XORIG,-YORIG,-3)
      WRITE(NW,204)  YBPLOT(I),YBPLOT(J)
C DRAW THE AXIS FOR THE APPROPRIATE INPUT MOTION
     0IF(MOTION .EQ. 0 .AND. IFOFT .EQ. 8)CALL AXIS(1.,1.5,24HINPUT VIBR
     1ATION - INCHES,24,AYLEN,90.,YBPLOT(I),YBPLOT(J))
     0IF(MOTION .EQ. 1 .AND. IFOFT .EQ. 8)CALL AXIS(1.,1.5,37HINPUT VIBR
     1ATION - ACCELERATION IN G*S,37,AYLEN,90.,YBPLOT(I),YBPLOT(J))
     0IF(MOTION .EQ. 0 .AND. IFOFT .GT. 8)CALL AXIS(1.,1.5,20HINPUT SHOC
     1K - INCHES,20,AYLEN,90.,YBPLOT(I),YBPLOT(J))
     0IF(MOTION .EQ. 1 .AND. IFOFT .GT. 8)CALL AXIS(1.,1.5,33HINPUT SHOC
     1K - ACCELERATION IN G*S,33,AYLEN,90.,YBPLOT(I),YBPLOT(J))
      WRITE(NW,205)
C DRAW THE AXIS FOR FILM THICKNESS
     0CALL AXIS(XORIG,YORIG,31HBEARING FILM THICKNESS - INCHES,
     131,AYLEN,90.,FILMT(I),FILMT(J))
      WRITE(NW,206)
```

```
C DRAW TIME AXIS
     0CALL AXIS(XORIG,YORIG,    14HTIME - SECONDS,-14,AXLEN,0.,
     1TIME(I),TIME(J))
      CALL PLOT(XORIG,YORIG,-3)
      WRITE(NW,207)
C PLOT THE GRAPHS
      IF(NPTS.LT.30) NOPON=1
      IF(NPTS.GE.30)  NOPON=NPTS/30
      CALL  LINE(TIME,YBPLOT, NPTS,IPSTEP,NOPON,3)
      CALL  LINE(TIME,FILMT, NPTS,IPSTEP,NOPON,1)
      WRITE(NW,208)
C DRAW A CENTERLINE TO REPRESENT EQUILIBRIUM FILM THICKNESS
   98 CALL PLOT(-XORIG,-YORIG,-3)
      WRITE(NW,209)
      DO 99 K=1,13
      CLY(K)=YORIG+HINIT/FILMT(J)
99    CLX(K)=XORIG+FLOAT(K-1)/12.*AXLEN
      CLX(14)=0.0
      CLX(15)=1.0
      CLY(14) =0.
      CLY(15)=1.
      CALL CNTRLN(CLX,CLY,13,1)
      WRITE(NW,210)
C
C RETURN REFERENCE TO LOWER LEFT HAND CORNER AND LETTER TITLE
C
  100 CALL SYMBOL(2.50,0.50,.14,TITLE,0.,75)
      FNCASE=NCASE
      CALL SYMBOL(11.5,.30,.100,11HCASE NO. = ,0.,11)
      CALL NUMBER(999.,0.30,.10,FNCASE,0.,-1)
      CALL SDATE(DATE)                                                    CDC
      CALL SYMBOL(11.5,0.15,.10,DATE,0.,8)                                CDC
C PERFORM ANNOTATION
     0IF(MODEL .EQ. 1) CALL SYMBOL(4.50,9.65,.14,
     1 53HSIMULATOR, VERTICAL ON ISOLATORS                      ,0.,53)
     0IF(MODEL .EQ. 2) CALL SYMBOL(4.50,9.65,.14,
     1 53HSIMULATOR VERTICAL ON RIGID MOUNTS                    ,0.,53)
     0IF(MODEL .EQ. 3) CALL SYMBOL(4.50,9.65,.14,
     1 55HSIMULATOR VERTICAL ON RIGID MOUNTS, CASING, AND FLEXURE,0.,55)
      CALL SYMBOL(4.50,9.25,.14,19HINPUT FUNCTION IS  ,0.,19)
     0IF(IFOFT .EQ. 8) CALL SYMBOL(999.,9.25,.14,
     1 40HSTEADY-STATE VIBRATION                    ,0.,40)
      IF(IFOFT.EQ. 9.AND.MOTION.EQ.0) CALL SYMBOL(999.,9.25,.14,
     140HHALF SINE DISPLACEMENT SHOCK               ,0.,40)
      IF(IFOFT.EQ. 9.AND.MOTION.EQ.1) CALL SYMBOL(999.,9.25,.14,
     140HHALF SINE ACCELERATION SHOCK               ,0.,40)
      IF(IFOFT.EQ.10.AND.MOTION.EQ.0) CALL SYMBOL(999.,9.25,.14,
     140HHAVERSINE DISPLACEMENT SHOCK               ,0.,40)
      IF(IFOFT.EQ.10.AND.MOTION.EQ.1) CALL SYMBOL(999.,9.25,.14,
     140HHAVERSINE ACCELERATION SHOCK               ,0.,40)
      IF(IFOFT.EQ.11.AND.MOTION.EQ.0) CALL SYMBOL(999.,9.25,.14,
     141HSHOCK DISPLACEMENT VALUES READ IN AS DATA,0.,41)
      IF(IFOFT.EQ.11.AND.MOTION.EQ.1) CALL SYMBOL(999.,9.25,.14,
     141HSHOCK ACCELERATION VALUES READ IN AS DATA,0.,41)
      GO TO (110,120,130,140),IFM7
  110 CALL SYMBOL(4.50,8.85,.14,13HAMPLITUDE IS ,0.,13)
      CALL NUMBER(999.,8.85,.14,AMPLD,0.,5)
  111 IF(MOTION.EQ.0) CALL SYMBOL(999.,8.85,.14,7H INCHES,0.,7)
      IF(MOTION.EQ.1) CALL SYMBOL(999.,8.85,.14,7H G#S   ,0.,7)
      GO TO (112,116,116,140),IFM7
  112 CALL SYMBOL(999.,8.85,.14,17H    FREQUENCY IS ,0.,17)
      CALL NUMBER(999.,8.85,.14,FREQ,0.,5)
      CALL SYMBOL(999.,8.85,.14,3H HZ,0.,3)
      GO TO 150
  115 CALL SYMBOL(4.50,8.85,.14,14HPEAK VALUE IS ,0.,14)
      CALL NUMBER(999.,8.85,.14,OPEAK,0.,5)
      GO TO 111
```

```
116 CALL SYMBOL(999.,8.85,.14,24H      PULSE DURATION IS ,0.,24)
    CALL NUMBER(999.,8.85,.14,ODOR,0.,5)
    CALL SYMBOL(999.,8.85,.14,8H SECONDS,0.,8)
    GO TO 150
120 OPEAK=PEAKS
    ODOR=PDURS
    GO TO 115
130 OPEAK=PEAKH
    ODOR=PDURH
    GO TO 115
140 ODOR=FLOAT(NINCP)*TINCP
    CALL SYMBOL(4.50,8.85,.14,25HPEAK VALUE IS SHOWN       ,0.,25)
    GO TO 116
150 CALL SYMBOL(4.57,8.32,.14,3,0.,-1)
    CALL SYMBOL(5.00,8.25,.14,17H = INPUT FUNCTION,0.,17)
    CALL SYMBOL(4.57,8.07,.14,1,0.,-1)
    CALL SYMBOL(5.00,8.00,.14,32H = THRUST BEARING FILM THICKNESS,0.,
   132)
    WRITE(NW,211)
    CLX(16)=4.50
    CLY(16)=7.82
    CLX(17)=5.25
    CLY(17)=7.82
    CLX(18)=0.
    CLY(18)=0.
    CLX(19)=1.
    CLY(19)=1.
    CALL CNTRLN(CLX(16),CLY(16),2,1)
    CALL SYMBOL(5.42,7.75,.14,26HEQUILIBRIUM FILM THICKNESS,0.,26)
    CALL PLOT(-.4,0.,-3)
    CALL DASHPT(0.,11.3,.113)
    CALL DASHPT(14.7,11.3,.147)
    CALL DASHPT(14.7,0.,.113)
    WRITE(NW,212)
200 FORMAT(/5X,6HNVALS=,I5,6H NPTS=,I5,3H I=,I5,3H J=,I5)
201 FORMAT(/5X,8HTIME(I)=,E12.5,8HTIME(J)=,E12.5)
203 FORMAT(/5X,10HFILMT(II)=,E12.5,10HFILMT(JJ)=,E12.5)
204 FORMAT(/5X,10HYBPLOT(I)=,E12.5,10HYBPLOT(J)=,E12.5)
205 FORMAT(/5X,25HDIAG VERT AXIS-1 DRAWN    )
206 FORMAT(/5X,25HDIAG VERT AXIS-2 DRAWN    )
207 FORMAT(/5X,25HDIAG HORIZ AXIS DRAWN     )
208 FORMAT(/5X,25HCURVES  PLOTTED           )
209 FORMAT(/5X,25HORIGIN SHIFTED            )
210 FORMAT(/5X,25HCENTERLINE DRAWN          )
211 FORMAT(/5X,25HANNOTATION  ALMOST DONE   )
212 FORMAT(/5X,25HANNOTATION DONE           )
    RETURN
    END
```

```
      SUBROUTINE INPUT
C THIS SUBROUTINE IS A PART OF PROGRAM #SHAKE#
C IT SERVES TO PREPARE THE INPUT FOR #SHAKE#
C IT CALLS A SUBROUTINE #FILM# WHICH FINDS EQUILIBRIUM FILM THICKNESS.
C PROGRAM WRITTEN FOR UNIVAC 1107
C
      COMMON TPRINT,TMAX,IPSTEP,NCYCLS,MOTION,TITLE(15),YBA,YBINT(200)
      COMMON NR,NW,NCASE,MODEL,LOADF,IDAMP,IFOFT,ICC,
     1            M1,M2,M3,K1,C1,K2,GL,FA,ALOAD,ADAMP,BLOAD,BDAMP,
     2CLOAD,CDAMP,DLOAD,DDAMP,HINIT,IFM7,AMPLD,FREQ,PEAKS,PDURS,PEAKH,
     3PDURH,NINCP,TINCP,TP(200),PUVAL(200),PULDOT(200),TINIT,Y1IN,Y2IN,
     4Y3IN,V1IN,V2IN,V3IN,TIME(6000),Y1,Y2,Y3,V1,V2,V3,N,VEC(6),DVEC(6),
     5MAXINC,H,HM,M,E,AKO,NE,T,              ELIM,INDX,     YB,YBDOT,
     6OMEGA,WHO,WY3Y2H,BY3Y2H
      COMMON FILMT(6000),Y2MY1(6000),VAPEAK(6000),YBPLOT(6000)
      COMMON TZ,ITIME,YBPREV                                              EM
      COMMON NONLIN,ITYP1,ITYP2,ITYP3,TAB1,TAB2,TAB3,C2,C3,K3,            EM
     1DISPW1(300),DISPW2(300),DISPW3(300),W1FTAB(300),W2FTAB(300),        EM
     2W3FTAB(300),DISPB1(300),DISPB2(300),DISPB3(300),B1FTAB(300),        EM
     3B2FTAB(300),B3FTAB(300),NOW1,NOW2,NOW3,NOB1,NOB2,NOB3               EM
      REAL M1,M2,M3,C1,K1,K2,K3                                           EM
      LOGICAL 01,02,03,04,05,06,07,08,09,010
C     NONLIN= 0   USE EXISTING VERSION OF PROGRAM                         EM
C     NONLIN= 1   USE NEW VERSION  3/70                                   EM
C             INDICATES ONLY NONLINEARITY IN THE SYSTEM IN THE THRUST     EM
C             BEARING.                                                    EM
      LOGICAL NEW                                                         EM
C     NEW INDICATES NONLIN = 1                                            EM
      WRITE(NW,1500)
C PRINT A ROW OF ASTERISKS
      WRITE(NW,1030)
      WRITE(NW,1020)
      WRITE(NW,1031)
C
C
C CHOOSE OPTIONS
C
C     READ NEW PARAMETERS                                                 EM
      READ(NR,30) MODEL,LOADF,IDAMP,IFOFT,ICC,MOTION,                     EM
     1 NONLIN,ITYP1,TAB1,ITYP2,TAB2,ITYP3,TAB3                            EM
   30 FORMAT(7I5,3(I5,E10.4))                                             EM
      NEW= NONLIN.EQ.1                                                    EM
      IF(TAB1.NE.0.0.AND.ITYP1.NE.3) WRITE(NW,1533)                       EM
      IF(TAB2.NE.0.0.AND.ITYP2.NE.3) WRITE(NW,1534)                       EM
      IF(TAB3.NE.0.0.AND.ITYP3.NE.3)  WRITE(NW,1535)
C
C
C SET LOGICAL VARIABLES AND TEST FOR CORRECTNESS OF INPUT
C
C
      01=MODEL.LT.1
      02=MODEL.GT.3
      03=LOADF.LT.4
      04=LOADF.GT.5
      05=IDAMP.LT.6
      06=IDAMP.GT.7
      07=IFOFT.LT.8
      08=IFOFT.GT.11
      09=ICC.LT.12
      010=ICC.GT.13
      IF(01.OR.02)WRITE(NW,40)
      IF(NEW)  GO TO 35                                                   EM
      IF(03.OR.04)WRITE(NW,50)
      IF(05.OR.06)WRITE(NW,60)
   35 IF(07.OR.08) WRITE(NW,70)                                           EM
      IF(09.OR.010)WRITE(NW,80)
```

```
C  ERROR MESSAGES
   40 FORMAT(    35H0     IMPROPER INPUT CARD 2,COL 5.  )
   50 FORMAT(    35H0     IMPROPER INPUT CARD 2,COL10.  )
   60 FORMAT(    35H0     IMPROPER INPUT CARD 2,COL15.  )
   70 FORMAT(    35H0     IMPROPER INPUT CARD 2,COL20.  )
   80 FORMAT(    35H0     IMPROPER INPUT CARD 2,COL25.  )
      IF(NEW) GO TO 36                                                    EM
      IF(03.OR.04.OR.05.OR.06) CALL EXIT                                  EM
   36 IF(01.OR.02.OR.07.OR.08.OR.09.OR.010)  CALL EXIT                    EM
      IF(MODEL.EQ.1) WRITE(NW,1040)
      IF(MODEL.EQ.1) WRITE(NW,1050)
      IF(MODEL.EQ.1) WRITE(NW,1040)
      IF(MODEL.EQ.1) WRITE(NW,1400)
      IF(MODEL.EQ.1) WRITE(NW,1060)
      IF(MODEL.EQ.1) WRITE(NW,1400)
      IF(MODEL.EQ.1) WRITE(NW,1070)
      IF(MODEL.EQ.2) WRITE(NW,1050)
      IF(MODEL.EQ.2) WRITE(NW,1400)
      IF(MODEL.EQ.2) WRITE(NW,1040)
      IF(MODEL.EQ.2) WRITE(NW,1060)
      IF(MODEL.EQ.2) WRITE(NW,1040)
      IF(MODEL.EQ.2) WRITE(NW,1400)
      IF(MODEL.EQ.2) WRITE(NW,1070)
      IF(MODEL.EQ.2) WRITE(NW,1400)
      IF(MODEL.EQ.3) WRITE(NW,1050)
      IF(MODEL.EQ.3) WRITE(NW,1400)
      IF(MODEL.EQ.3) WRITE(NW,1060)
      IF(MODEL.EQ.3) WRITE(NW,1400)
      IF(MODEL.EQ.3) WRITE(NW,1040)
      IF(MODEL.EQ.3) WRITE(NW,1070)
      IF(MODEL.EQ.3) WRITE(NW,1040)
C
C
C
C PHYSICAL PARAMETERS I/O
      IF(NEW) READ(NR,90) M1,M2,M3,K1,K2,K3,C1,C2,C3,HINIT
      IF(NEW) GO TO 109                                                   EM
      READ(NR,90) M1,M2,M3,K1,C1,K2
90    FORMAT(8E10.4)
C CORRECTION TO CHECK FOR M3=0
      IF (M3) 902,900,902
C  M3=0
  900 WRITE(NW,901) M3
      CALL EXIT
  901 FORMAT(24H0   IMPROPER INPUT M3 = ,E10.4)
  902 WRITE(NW,1020)
       WRITE(NW,1080)
      IF(LOADF.EQ.4) WRITE(NW,1040)
      IF(LOADF.EQ.4) WRITE(NW,1090)
      IF(LOADF.EQ.4) WRITE(NW,1040)
      IF(LOADF.EQ.4) WRITE(NW,1400)
      IF(LOADF.EQ.4) WRITE(NW,1100)
      IF(LOADF.EQ.4) WRITE(NW,1400)
      IF(LOADF.EQ.5) WRITE(NW,1090)
      IF(LOADF.EQ.5) WRITE(NW,1400)
      IF(LOADF.EQ.5) WRITE(NW,1040)
      IF(LOADF.EQ.5) WRITE(NW,1100)
      IF(LOADF.EQ.5) WRITE(NW,1040)
      WRITE(NW,1110)
      IF(IDAMP.EQ.6) WRITE(NW,1040)
      IF(IDAMP.EQ.6) WRITE(NW,1120)
      IF(IDAMP.EQ.6) WRITE(NW,1040)
      IF(IDAMP.EQ.6) WRITE(NW,1400)
      IF(IDAMP.EQ.6) WRITE(NW,1130)
      IF(IDAMP.EQ.6) WRITE(NW,1400)
      IF(IDAMP.EQ.7) WRITE(NW,1120)
```

```
      IF(IDAMP.EQ.7) WRITE(NW,1400)
      IF(IDAMP.EQ.7) WRITE(NW,1040)
      IF(IDAMP.EQ.7) WRITE(NW,1130)
      IF(IDAMP.EQ.7) WRITE(NW,1040)
      WRITE(NW,1531)
      WRITE(NW,1020)
      WRITE(NW,1400)
C READ LOAD AND DAMPING PARAMETERS
      READ(NR,90) ALOAD,BLOAD,CLOAD,DLOAD,ADAMP,BDAMP,CDAMP,DDAMP
      IF(LOADF.EQ.4) WRITE(NW,1230)ALOAD,BLOAD
      IF(LOADF.EQ.5)  WRITE(NW,1235) CLOAD,DLOAD
      IF(IDAMP.EQ.6) WRITE(NW,1245) ADAMP,BDAMP
      IF(IDAMP.EQ.7) WRITE(NW,1240) CDAMP,DDAMP
C READ THE LOCAL GRAVITATIONAL ACCELERATION UNITS) AND AERODYNAMIC
C  FORCES
  109 READ(NR,90) GL,FA,ELIM                                          EM
C CALCULATE THE EQUILIBRIUM GAS FILM THICKNESS VIA A SUBPROGRAM #FILM#
      IF(NEW) CALL FILMT2                                             EM
      IF(NONLIN.EQ.0)  CALL FILM
C PRINT FILM THICKNESS AND STEADY STATE ROTOR FORCES
      IF(ELIM.GT.0.0)  GO TO 110
      ELIM=.0002
  110 WRITE(NW,1251)  ELIM
      WRITE(NW,1500)
      WRITE(NW,1020)
C CONVERT HINIT TO MILS FOR PRINTOUT PURPOSES
      HINIT=HINIT*1000.
      WRITE(NW,1250)HINIT,FA,GL
C RECONVERT TO INCHES FOR CALCULATION PURPOSES
      HINIT=HINIT/1000.
      WRITE(NW,1020)
      IF(NEW) CALL NLINP(1)                                           EM
      IF(NEW) GO TO 112                                               EM
      IF(MODEL.EQ.1)WRITE(NW,1220)M1,M2,M3,K1,C1,K2
      IF(MODEL.EQ.2)WRITE(NW,1340)M1,M2,M3,K1,K2
      IF(MODEL.EQ.3) WRITE(NW,1330)M3
C CHANGE UNITS
  112 M1=M1/386.069                                                   EM
      M2=M2/ 386.069
      M3=M3/ 386.069
      WRITE(NW,1020)
      WRITE(NW,1531)
      WRITE(NW,1020)
      WRITE(NW,1140)
      IF(IFOFT.EQ.8) WRITE(NW,1040)
      IF(IFOFT.EQ.8) WRITE(NW,1150)
      IF(IFOFT.EQ.8) WRITE(NW,1040)
      IF(IFOFT.EQ.8) WRITE(NW,1400)
      IF(IFOFT.EQ.8) WRITE(NW,1160)
      IF(IFOFT.EQ.8) WRITE(NW,1400)
      IF(IFOFT.EQ.8) WRITE(NW,1170)
      IF(IFOFT.EQ.8) WRITE(NW,1400)
      IF(IFOFT.EQ.8) WRITE(NW,1180)
      IF(IFOFT.EQ.9) WRITE(NW,1400)
      IF(IFOFT.EQ.9) WRITE(NW,1150)
      IF(IFOFT.EQ.9) WRITE(NW,1400)
      IF(IFOFT.EQ.9) WRITE(NW,1040)
      IF(IFOFT.EQ.9) WRITE(NW,1160)
      IF(IFOFT.EQ.9) WRITE(NW,1040)
      IF(IFOFT.EQ.9) WRITE(NW,1400)
      IF(IFOFT.EQ.9) WRITE(NW,1170)
      IF(IFOFT.EQ.9) WRITE(NW,1400)
      IF(IFOFT.EQ.9) WRITE(NW,1180)
      IF(IFOFT.EQ.10) WRITE(NW,1400)
      IF(IFOFT.EQ.10) WRITE(NW,1150)
      IF(IFOFT.EQ.10) WRITE(NW,1400)
```

```
      IF(IFOFT.EQ.10) WRITE(NW,1160)
      IF(IFOFT.EQ.10) WRITE(NW,1400)
      IF(IFOFT.EQ.10)WRITE(NW,1040)
      IF(IFOFT.EQ.10)WRITE(NW,1170)
      IF(IFOFT.EQ.10)WRITE(NW,1040)
      IF(IFOFT.EQ.10) WRITE(NW,1400)
      IF(IFOFT.EQ.10) WRITE(NW,1180)
      IF(IFOFT.EQ.10) WRITE(NW,1400)
      IF(IFOFT.EQ.11) WRITE(NW,1400)
      IF(IFOFT.EQ.11) WRITE(NW,1150)
      IF(IFOFT.EQ.11) WRITE(NW,1400)
      IF(IFOFT.EQ.11) WRITE(NW,1160)
      IF(IFOFT.EQ.11) WRITE(NW,1400)
      IF(IFOFT.EQ.11) WRITE(NW,1170)
      IF(IFOFT.EQ.11) WRITE(NW,1400)
      IF(IFOFT.EQ.11)WRITE(NW,1040)
      IF(IFOFT.EQ.11)WRITE(NW,1180)
      IF(IFOFT.EQ.11)WRITE(NW,1040)
      WRITE(NW,1531)
      WRITE(NW,1020)
      WRITE(NW,1190)
      IF(ICC.EQ.12) WRITE(NW,1040)
      IF(ICC.EQ.12) WRITE(NW,1200)
      IF(ICC.EQ.12) WRITE(NW,1040)
      IF(ICC.EQ.12) WRITE(NW,1400)
      IF(ICC.EQ.12) WRITE(NW,1210)
      IF(ICC.EQ.13) WRITE(NW,1200)
      IF(ICC.EQ.13) WRITE(NW,1400)
      IF(ICC.EQ.13) WRITE(NW,1040)
      IF(ICC.EQ.13) WRITE(NW,1210)
      IF(ICC.EQ.13) WRITE(NW,1040)
      WRITE(NW,1400)
      WRITE(NW,1020)
      IF(NEW) CALL NLINP(2)
C PRINT PARAMETERS ASSOCIATED WITH FORCING FUNCTION
      IFM7=IFOFT-7
      GO TO (120,130,140,150),IFM7
C STEADY STATE SINE FORCE
120   READ(NR,90) AMPLD,FREQ
      WRITE(NW,1320) FREQ
      IF(MOTION.EQ.0) WRITE(NW,1520) AMPLD
      IF(MOTION.EQ.1) WRITE(NW,1530) AMPLD
      GO TO 160
130   READ(NR,90) PEAKS,PDURS
      WRITE(NW,1310) PDURS
      IF(MOTION.EQ.0) WRITE(NW,1520) PEAKS
      IF(MOTION.EQ.1) WRITE(NW,1530) PEAKS
      GO TO 160
140   READ(NR,90)PEAKH,PDURH
      WRITE(NW,1300) PDURH
      IF(MOTION.EQ.0) WRITE(NW,1520) PEAKH
      IF(MOTION.EQ.1) WRITE(NW,1530) PEAKH
      GO TO 160
150   WRITE(NW,1260)
      IF(MOTION.EQ.0)  WRITE(NW,1261)
      IF(MOTION.EQ.1)   WRITE(NW,1262)
C ABOVE IS HEADING FOR SHOCK PULSE TABLE
C NOW READ THE NUMBER OF INCREMENTS IN THE PULSE AND THE INCREMENTAL
C TIME INTO WHICH PULSE IS DIVIDED
      READ(NR,154) NINCP,TINCP
  154 FORMAT(I5,F10.4)
C INITIALIZE FIRST YB VALUE
      INCP0=NINCP+1
      READ(NR,90) (PUVAL(I),I=2, INCP0)
  151 PUVAL(1) =0.0
      TP(1)=0.0
```

```
  153 DO 159 I=2,INCPO
      EYE=I-1
      TP(I)=EYE*TINCP
      IM1=I-1
      IP1=I+1
  159 IF(.NOT.(I.EQ.1.OR.I.EQ.INCPO)) PULDOT(I)=(PUVAL(IP1)-
     1PUVAL(IM1))/(2.*TINCP)
      DO 158 I=1,INCPO
      MAPGE=(I/45)*45-I
      IF(MAPGE.EQ.0)  WRITE(NW,1531)
  158 WRITE(NW,1265) TP(I),PUVAL(I)
      WRITE(NW,1500)
      ANINCP=NINCP
      PDURT=ANINCP*TINCP
      WRITE(NW,1510) PDURT
 1265 FORMAT(13X,2F12.7)
      PULDOT(1)=(PUVAL(2)-PUVAL(1))/TINCP
      PULDOT(INCPO)=(PUVAL(INCPO)-PUVAL(NINCP))/TINCP
C FORM A NEW TABLE FOR THE INTEGRAL OF YB
      IF (MOTION.EQ.1)  CALL FORMT
      WRITE(NW,1531)
C READ PROGRAM CONTROL CARDS
  160 WRITE(NW,1531)
      READ(NR,91) IPSTEP,M,MAXINC,NCYCLS,TPRINT,TMAX,H,E,HM,BOGUS
   91 FORMAT(4I5,6E10.4)
      WRITE (NW,1500)
      WRITE(NW,1020)
      NCONE=NCYCLS
      IF(NCYCLS.EQ.0)  NCONE= NCYCLS+1
      WRITE(NW,1280) TMAX,MAXINC,NCONE,H,TPRINT,IPSTEP,E,HM,M,BOGUS
C READ AND WRITE INITIAL CONDITIONS
      READ(NR,90)TINIT,Y1IN,Y2IN,Y3IN,V1IN,V2IN,V3IN
      WRITE(NW,1270) TINIT,Y1IN,V1IN,Y2IN,V2IN,Y3IN,V3IN
      WRITE(NW,1531)
 1010 FORMAT(I5,75H
     1                    )
 1020  FORMAT(1H ,119(1H*))
 1030 FORMAT(40X,15HPROGRAM OPTIONS/20X,58HOPTIONS SELECTED FOR THIS PAR
     1TICULAR RUN ARE DESIGNATED BY/70X,8H--------/71X,6HOPTION/70X,
     28H--------)
 1031 FORMAT(10X,25HCHOICE OF VIBRATION MODEL/)
 1040 FORMAT(20X,50H--------------------------------------------------)
 1050 FORMAT(20X,50H1 = THREE-DEGREE OF FREEDOM SYSTEM USING ISOLATORS)
 1060 FORMAT(20X,53H2 = THREE-DEGREE OF FREEDOM SYSTEM USING RIGID MOUNT
     1S)
 1070 FORMAT(20X,52H3 = SIMPLE MODEL, ENTIRELY RIGID EXCEPT FOR GAS FILM
     1)
 1080 FORMAT(/10X,34HGAS FILM FUNCTIONAL REPRESENTATION/15X,19HLOAD CHAR
     1ACTERISTIC/)
 1090 FORMAT(20X,35H4 = EXPONENTIAL LOAD CHARACTERISTIC)
 1100 FORMAT(20X,38H5 = POWER FUNCTION LOAD CHARACTERISTIC)
 1110 FORMAT(10X,22HDAMPING CHARACTERISTIC/)
 1120 FORMAT(20X,35H6 = EXPONENTIAL DAMPING COEFFICIENT)
 1130 FORMAT(20X,38H7 = POWER FUNCTION DAMPING COEFFICIENT)
 1140 FORMAT(1H0,9X,27HTYPE OF EXCITATION FUNCTION/)
 1150 FORMAT(20X,      27H8 = STEADY SINUSOIDAL INPUT)
 1160 FORMAT(20X,      19H9 = HALF SINE SHOCK)
 1170 FORMAT(20X,     44H10 = HAVERSINE SHOCK                          )
 1180 FORMAT(20X,     44H11 = ARBITRARY SHOCK (TABLE)                  )
 1190 FORMAT(1H0, 9X,26HIS CALCOMP OUTPUT DESIRED-)
 1200 FORMAT(20X, 8H12 = YES)
 1210 FORMAT(20X, 7H13 = NO)
```

```
1220 FORMAT(1H0,20X,53HPARAMETERS OF THE THREE-DEGREE SYSTEM USING ISOL
    1ATORS//12X, 7HMASS OF,       5X,14HEFFECTIVE MASS, 4X,7HMASS OF,
    2 6X,9HSTIFFNESS, 6X,7HDAMPING, 7X, 7HFLEXURE/13X,6HCASING,9X
    3   , 8HOF PLATE, 7X,6HROTOR ,10X,2HOF,12X,2HOF, 9X, 9HSTIFFNESS/
    426X,11HAND FLEXURE,18X, 9HISOLATORS, 5X, 9HISOLATORS/
    514X,4H(LB),10X,4H(LB),10X,4H(LB), 9X, 7H(LB/IN), 5X,11H(LB-SEC/IN)
    6, 4X, 7H(LB/IN)//10X,5(G10.3,4X),E12.4)
1230 FORMAT(1H0, 9X,23HDESCRIPTION OF GAS FILM//
    120X,50HTHE EXPONENTIAL LOAD CHARACTERISTIC IS OF THE FORM/
    225X,22HLOAD (LB) = A*EXP(B*H)/20X,5HWHERE/
    325X,27HH = FILM THICKNESS (INCHES)/25X, 4HA = ,E12.4,5H (LB)/
    425X, 4HB = ,E12.4, 7H( 1/IN))
1240 FORMAT(1H0,9X,53HTHE POWER FUNCTION DAMPING COEFFICIENT IS OF THE
    1FORM/20X,21HB (LB*SEC/IN) = C*H**D/10X,5HWHERE/
    220X,28HH = FILM THICKNESSS (INCHES)/
    320X, 3HC= ,E12.4,10H LB-SEC/IN/                                    EM
    420X, 3HD= ,E12.4, 7H (1/IN)    )                                   EM
1250 FORMAT(10X,29HEQUILIBRIUM FILM THICKNESS IS,G12.5, 5H MILS//
    115X,56HASSUMING STEADY-STATE AERODYNAMIC FORCES ON THE ROTOR OF,
    2G12.5, 3H LB/ 15X,34HAND A LOCAL GRAVITATIONAL FIELD OF,G12.5,
    315H TIMES STANDARD)
1251 FORMAT(/10X,85HNON-LINEAR LOAD AND DAMPING FUNCTIONS ARE HELD CONS
    1TANT AT FILM THICKNESSES LESS THAN,G10.3,8H INCHES.)
1260 FORMAT(10X,62HINPUT MOTION IS A SHOCK PULSE DESCRIBED BY THE FOLLO
    1WING TABLE)
1261 FORMAT(/20X,4HTIME,2X,12HDISPLACEMENT/19X,5H(SEC),4X,
    1 8H(INCHES))
1262 FORMAT(/20X,4HTIME,2X,12HACCELERATION/19X,5H(SEC),4X,5H(G#S))
1270 FORMAT(1H0,9X,29HINITIAL OR RESTART CONDITIONS/
    120X,12HINITIAL TIME,11X,1H=,G10.3,8H SECONDS/
    220X,24HDISPLACEMENT OF MASS 1 =,G10.3, 7H INCHES/
    320X,18HVELOCITY OF MASS 1,5X,1H=,G10.3, 7H IN/SEC/
    420X,24HDISPLACEMENT OF MASS 2 =, G10.3, 7H INCHES/
    520X,18HVELOCITY OF MASS 2,5X,1H=,G10.3, 7H IN/SEC/
    620X,24HDISPLACEMENT OF MASS 3 =,G10.3, 7H INCHES/
    720X,18HVELOCITY OF MASS 3,5X,1H=,G10.3,7H IN/SEC/)
1280 FORMAT(/ 10X,26HPROGRAM CONTROL PARAMETERS//15X,19HDESIRED TERMINA
    1TION/20X,26HTIME VALUE WILL NOT EXCEED,F10.4,8H SECONDS/20X,
    248HAS A SAFETY MEASURE WE WILL NOT PERMIT MORE THAN,I5,6H STEPS/
    320X,25HCALCULATION WILL CONTINUE,I5,28H CYCLES AFTER PULSE DURATIO
    4N/15X,9HSTEP SIZE/20X,45HINITIAL STEP SIZE FOR CALCULATION PURPOSE
    5S IS,G10.3,8H SECONDS/20X,28HVALUES ARE PRINTED OUT EVERY ,G10.3,
    68H SECONDS/20X,5HEVERY,I5,38HTH POINT IS PLOTTED IF CALCOMP IS USE
    7D/20X,41HERROR CRITERION FOR INTEGRATION TECHNIQUE,G10.3/ 20X,20HM
    8INIMUM STEP-SIZE =,G12.5,8H SECONDS/20X,48HNO. OF INTEGRATIONS BEF
    9ORE STEP-SIZE IS DOUBLED=,I5/20X,48HNORMALIZED ERROR LIMIT FOR INT
    1EGRATION TECHNIQUE,F10.4)
1300 FORMAT(10X,37HINPUT MOTION IS HAVERSINE SHOCK PULSE/
    215X,17HPULSE DURATION IS,F10.4, 8H SECONDS/ )
1310 FORMAT(10X,37HINPUT MOTION IS HALF-SINE SHOCK PULSE/
    215X,17HPULSE DURATION IS,F10.4,8H SECONDS/)
1320 FORMAT(10X,59HDESCRIPTION OF INPUT MOTION IS STEADY-STATE SINE EXC
    1ITATION/
    315X,12HFREQUENCY IS,F10.4, 3H HZ/ )
1330 FORMAT(10X,58HTHRUST BEARING ON RIGID FLEXURE (SINGLE DEGREE OF FR
    1EEDOM)/10X,13HMASS OF ROTOR/13X,4H(LB)/10X,G10.3/)
1340 FORMAT(10X,55HPARAMETERS OF THE SYSTEM ON RIGID MOUNTS ARE AS FOLL
    10WS//13X,50HEFFECTIVE MASS    EFFECTIVE MASS     MASS OF ROTOR,
    26X,9HSTIFFNESS,9X,8HFLEXURE /12X,16HOF LOWER HOUSING,2X,19HOF STAT
    30R + FLEXURE,16X,16HOF LOWER HOUSING,6X,9HSTIFFNESS/
    416X,12H(MASS1),(LB),4X,12H(MASS2),(LB),7X,12H(MASS3),(LB),6X,
    5 7H(LB/IN),11X,7H(LB/IN)/ 16X,G10.3,6X,G10.3,9X,G10.3,2(5X,E12.4))
1350 FORMAT(30X,14HPROGRAM OUTPUT)
```

```
 1360 FORMAT(14X,4HTIME, 6X, 8HGAS FILM, 4X, 8HPEDESTAL, 7X,2HY1,10X,
     12HY2,10X,2HY3,10X,2HV1,10X,2HV2,10X,2HV3/
     224X, 9HTHICKNESS, 2X,10HDEFLECTIVE/25X, 7H(Y3-Y2), 5X, 7H(Y2-Y1)/
     3    12X, 9H(SECONDS), 4X,6H(MILS), 6X,6H(MILS), 6X,6H(MILS), 6X,
     46H(MILS), 6X,6H(MILS), 4X,10H(MILS/SEC), 2X,10H(MILS/SEC), 2X,
     510H(MILS/SEC))
 1370 FORMAT(10X,9(F10.4,2X))
 1380 FORMAT(25X,50HRESTART CONDITIONS (FINAL) AND IDENTIFICATION CODE/
     114X,4HTIME, 9X,2HY1,10X,2HY2,10X,2HY3,10X,2HV1,10X,2HV2,10X,2HV3,
     2 6X,5HNCASE/ 14X,5H(SEC), 6X,6H(MILS), 6X,6H(MILS), 6X,6H(MILS),
     3 4X,10H(MILS/SEC), 2X,10H(MILS/SEC), 2X,10H(MILS/SEC)/
     411X,7(F10.4,2X),I5)
 1235 FORMAT(1H0,9X,27HCHARACTERISTICS OF GAS FILM//
     120X,53HTHE POWER FUNCTION LOAD CHARACTERISTIC IS OF THE FORM//
     225X,18HLOAD (LB) = C*H**D     /20X,5HWHERE/
     325X,27HH = FILM THICKNESS (INCHES)/25X, 4HC = ,E12.4,
     418H LB-SEC/IN.**(1+D)/
     525X, 4HD = ,E12.4            )
1245  FORMAT(1H0,9X,53HTHE EXPONENTIAL DAMPING COEFFICIENT IS OF THE FOR
     1M   /20X,25HB(LB*SEC/IN) = C*EXP(D*H)/10X,5HWHERE/
     220X,28HH = FILM THICKNESSS (INCHES)/
     320X, 4HC = ,E12.4,15H LB-SEC/(IN**2)/
     420X, 4HD = ,E12.4,21H(DIMENSIONLESS UNITS))
 1400 FORMAT(/)
 1500 FORMAT(//)
 1510 FORMAT(// 10X,16HPULSE DURATION =, G12.5,4H SEC)
 1520 FORMAT(15X,17HPEAK AMPLITUDE IS,F10.4,20H INCHES DISPLACEMENT)
 1530 FORMAT(15X,17HPEAK AMPLITUDE IS,F10.4,17H G#S ACCELERATION)
 1531 FORMAT(/1H1)
 1533 FORMAT(/ 5X,30HIMPROPER INPUT CARD 2 COL. 40 )                    EM
 1534 FORMAT(/ 5X,30HIMPROPER INPUT CARD 2 COL. 55 )                    EM
 1535 FORMAT(/ 5X,30HIMPROPER INPUT CARD 2 COL. 70 )                    EM
  999 RETURN
      END
```

```
      SUBROUTINE FILMT2
      COMMON TPRINT,TMAX,IPSTEP,NCYCLS,MOTION,TITLE(15),YBA,YBINT(200)
      COMMON NR,NW,NCASE,MODEL,LOADF,IDAMP,IFOFT,ICC,
     1               M1,M2,M3,K1,C1,K2,GL,FA,ALOAD,ADAMP,BLOAD,BDAMP,
     2CLOAD,CDAMP,DLOAD,DDAMP,HINIT,IFM7,AMPLD,FREQ,PEAKS,PDURS,PEAKH,
     3PDURH,NINCP,TINCP,TP(200),PUVAL(200),PULDOT(200),TINIT,Y1IN,Y2IN,
     4Y3IN,V1IN,V2IN,V3IN,TIME(6000),Y1,Y2,Y3,V1,V2,V3,N,VEC(6),DVEC(6),
     5MAXINC,H,HM,M,E,AKO,NE,T,                ELIM,INDX,      YB,YBDOT,
     60MEGA,WHO,WY3Y2H,BY3Y2H
      COMMON FILMT(6000),Y2MY1(6000),VAPEAK(6000),YBPLOT(6000)
      COMMON TZ,ITIME,YBPREV                                                EM
      COMMON NONLIN,ITYP1,ITYP2,ITYP3,TAB1,TAB2,TAB3,C2,C3,K3,              EM
     1DISPW1(300),DISPW2(300),DISPW3(300),W1FTAB(300),W2FTAB(300),          EM
     2W3FTAB(300),DISPB1(300),DISPB2(300),DISPB3(300),B1FTAB(300),          EM
     3B2FTAB(300),B3FTAB(300),NOW1,NOW2,NOW3,NOB1,NOB2,NOB3                 EM
      REAL M1,M2,M3,C1,K1,K2,K3                                             EM
      CALL NLINP(3)
      W3F=M3*GL-FA
      WHO=W3F
      GO TO (40,20,30),ITYP3
   20 DEXI=1.E-8
      EX=1.E-10
      DO 25 K=1,50
      FXX=FK3(EX)
      FDX=FK3(EX+DEXI)
      R=FXX-W3F
      DRDX=(FDX-FXX)/DEXI
      DEXI=-R/DRDX
      IF(ABS(R).LT.1.E-6)  GO TO 28
   25 EX=EX+DEXI
      WRITE(NW,101)
      WRITE(NW,100) EX,DEXI,R,FXX,FDX
      CALL EXIT
   28 HINIT=EX
      GO TO 40
   30 CALL TLU(W3F,HINIT,W3FTAB,DISPW3,NOW3)
   40 RETURN
  101 FORMAT(/5X,20HITERATIONS EXCEEDED      )
  100 FORMAT(/5X,15HX,DX,R,FXX,FDX      / 5E12.4)
      END
```

```
      SUBROUTINE NLINP(JOP)
      COMMON TPRINT,TMAX,IPSTEP,NCYCLS,MOTION,TITLE(15),YBA,YBINT(200)
      COMMON NR,NW,NCASE,MODEL,LOADF,IDAMP,IFOFT,ICC,
     1              M1,M2,M3,K1,C1,K2,GL,FA,ALOAD,ADAMP,BLOAD,BDAMP,
     2CLOAD,CDAMP,DLOAD,DDAMP,HINIT,IFM7,AMPLD,FREQ,PEAKS,PDURS,PEAKH,
     3PDURH,NINCP,TINCP,TP(200),PUVAL(200),PULDOT(200),TINIT,Y1IN,Y2IN,
     4Y3IN,V1IN,V2IN,V3IN,TIME(6000),Y1,Y2,Y3,V1,V2,V3,
     5NDUM,DDUM(6),DVUM(6),
     5MAXINC,H,HM,M,E,AKO,NE,TTDUM,          ELIM,INDX,      YB,YBDOT,
     60MEGA,WHO,WY3Y2H,BY3Y2H
      COMMON FILMT(6000),Y2MY1(6000),VAPEAK(6000),YBPLOT(6000)
      COMMON TZ,ITIME,YBPREV
      COMMON NONLIN,ITYP1,ITYP2,ITYP3,TAB1,TAB2,TAB3,C2,C3,K3,          EM
     1DISPW1(300),DISPW2(300),DISPW3(300),W1FTAB(300),W2FTAB(300),      EM
     2W3FTAB(300),DISPB1(300),DISPB2(300),DISPB3(300),B1FTAB(300),      EM
     3B2FTAB(300),B3FTAB(300),NOW1,NOW2,NOW3,NOB1,NOB2,NOB3             EM
      REAL M1,M2,M3,C1,K1,K2,K3                                         EM
C     ITYP1  =          1                    2                   3
C     W1 AND B1  = CONSTANTS(INPUT) USER FUNC. SUBPROGRAMS  INPUT TABLES
C     ITYP2  =          1                    2                   3
C     W2 AND B2  = CONSTANTS(INPUT) USER FUNC. SUBPROGRAMS  INPUT TABLES
C     ITYP3  =          1                    2                   3
C     W3 AND B3  = CONSTANTS(INPUT) USER FUNC. SUBPROGRAMS  INPUT TABLES
C     TAB1,TAB2,TAB3 INPUT REQUIRED IF ITYP1,ITYP2,ITYP3 = 3, RESPECT.
C     TAB1,TAB2,TAB3 =  0.0  IF TABLE INCREMENT IRREGULAR
C     TAB1,TAB2,TAB3 =  DINC, SPECIFIES TABLE INCREMENT
C      DISPW1,DISPW2,DISPW3 DISPLACE. ARRAYS FOR W1,W2,W3 TABLE INPUT
C     W1FTAB,W2FTAB,W3FTAB = W1,W2,W3  VALUE ARRAYS       TABLE INPUT
C      DISPB1,DISPB2,DISPB3 DISPLACE. ARRAYS FOR B1,B2,B3 TABLE INPUT
C     B1FTAB,B2FTAB,B3FTAB = W1,W2,W3  VALUE ARRAYS       TABLE INPUT
C     NOW1,NOW2,NOW3   = NUMBER OF W1,W2,W3 VALUES        TABLE INPUT
C     NOB1,NOB2,NOB3   = NUMBER OF B1,B2,B3 VALUES        TABLE INPUT
      GO TO (10,20,200),JOP
   10 WRITE(NW,1536)
      WRITE(NW,1540) M1,M2,M3
      IF(ITYP1.EQ.1) WRITE(NW,1537) K1,C1
      IF(ITYP2.EQ.1) WRITE(NW,1538) K2,C2
      IF(ITYP3.EQ.1) WRITE(NW,1539) K3,C3
      RETURN
   20 WRITE(NW,1531)
      WRITE(NW,1547)
      WRITE(NW,1541)
      IF(ITYP1.EQ.1) WRITE(NW,1544)
      IF(ITYP1.EQ.2) WRITE(NW,1545)
      IF(ITYP1.EQ.3) WRITE(NW,1546)
      WRITE(NW,1542)
      IF(ITYP2.EQ.1) WRITE(NW,1544)
      IF(ITYP2.EQ.2) WRITE(NW,1545)
      IF(ITYP2.EQ.3) WRITE(NW,1546)
      WRITE(NW,1543)
      IF(ITYP3.EQ.1) WRITE(NW,1544)
      IF(ITYP3.EQ.2) WRITE(NW,1545)
      IF(ITYP3.EQ.3) WRITE(NW,1546)
C FUNCTION INPUT- SUBROUTINE MUST BE COMPILED BY USER AS
C     FK1 AND FC1   OF (Y1-YB) AND (Y1DOT-YBDOT)
C     FK2 AND FC2   OF (Y2-Y1) AND (Y2DOT-Y1DOT)
C     FK3 AND FC3   OF (Y3-Y2) AND (Y3DOT-Y2DOT)
C
C TABLE INPUT- FOLLOWS FUNCTION INPUT TEXT CARDS (ALL FORMATS  8E10.4)
C     FIRST CARD CONTAINS INITIAL VALUE OF DISPLACEMENT FOR W1F,W2F,W3F
C               IF INITIAL VALUE =0.0, INCREMENT IN DISP. TABLE VARIES
C               IF INITIAL VALUE =NON-ZERO, INCREMENT SPECIFIED BY TAB1,
C                  TAB2 OR TAB3 CORRESPONDING TO W1F,W2F, OR W3F
C     1ST SET OF CARDS GIVES DISPLACEMENT VALUES, SUPPLY THIS SET
C       ONLY IF INCREMENT  IS 0.0, BLANK CARD ENDS THIS SET.
C       LAST VALUE OF A SET MUST NOT BE ZERO
C     2ND SET OF CARDS CONTAINS W-VALUES -  END ON BLANK CARD
```

```
C     NEXT CARD CONTAINS INITIAL DISPLACEMENT FOR B1F,B2F OR B3F
C               (SAME RESTRICTIONS AS FIRST CARD)
C     3RD SET OF CARDS CONTAINS B-VALUES -  END ON BLANK CARD
  114 IF(ITYP1.NE.3) GO TO 115
      WRITE(NW,1557)
      WRITE(NW,1558)
      WRITE(NW,1548)
      WRITE(NW,1549)
      WRITE(NW,1553)
      CALL TABIN(DISPW1,W1FTAB,NOW1,TAB1,3)
      IF(NOW1.GT.100) WRITE(NW,1531)
      WRITE(NW,1561)
      WRITE(NW,1558)
      WRITE(NW,1552)
      WRITE(NW,1549)
      WRITE(NW,1554)
      CALL TABIN(DISPB1,B1FTAB,NOB1,TAB1,3)
  115 IF(ITYP2.NE.3) GO TO 116
      WRITE(NW,1557)
      WRITE(NW,1559)
      WRITE(NW,1548)
      WRITE(NW,1550)
      WRITE(NW,1553)
      CALL TABIN(DISPW2,W2FTAB,NOW2,TAB2,3)
      IF(NOW2.GT.100) WRITE(NW,1531)
      WRITE(NW,1561)
      WRITE(NW,1559)
      WRITE(NW,1552)
      WRITE(NW,1550)
      WRITE(NW,1554)
      CALL TABIN(DISPB2,B2FTAB,NOB2,TAB2,3)
  116 IF(ITYP3.NE.3) GO TO 117
      WRITE(NW,1557)
      WRITE(NW,1560)
      WRITE(NW,1548)
      WRITE(NW,1551)
      WRITE(NW,1553)
      CALL TABIN(DISPW3,W3FTAB,NOW3,TAB3,3)
      IF(NOW3.GT.100) WRITE(NW,1531)
      WRITE(NW,1561)
      WRITE(NW,1560)
      WRITE(NW,1552)
      WRITE(NW,1551)
      WRITE(NW,1554)
      CALL TABIN(DISPB3,B3FTAB,NOB3,TAB3,3)
  117 RETURN
  200 IF(ITYP1.NE.3)  GO TO 210
      CALL TABIN(DISPW1,W1FTAB,NOW1,TAB1,1)
      CALL TABIN(DISPB1,B1FTAB,NOB1,TAB1,2)
  210 IF(ITYP2.NE.3)  GO TO 220
      CALL TABIN(DISPW2,W2FTAB,NOW2,TAB2,1)
      CALL TABIN(DISPB2,B2FTAB,NOB2,TAB2,2)
  220 IF(ITYP3.NE.3)  GO TO 117
      CALL TABIN(DISPW3,W3FTAB,NOW3,TAB3,1)
      CALL TABIN(DISPB3,B3FTAB,NOB3,TAB3,2)
      GO TO 117
 1531 FORMAT(/ 1H1)
 1536 FORMAT(10X,55HPARAMETERS OF THE SYSTEM ON RIGID MOUNTS ARE AS FOLL
     10WS//10X, 110H      M1            M2            M3            K1
     2 K2           K3           C1           C2           C3              /
     36X, 3(8X,4H(LB)), 2X,3(5X,7H(LB/IN)),2X,3(12H (LB-SEC/IN))       )
 1537 FORMAT(1H+,44X,G12.4,24X,G12.4)
 1538 FORMAT(1H+,56X,G12.4,24X,G12.4)
 1539 FORMAT(1H+,68X,G12.4,24X,G12.4)
 1540 FORMAT(1H ,10X,3G12.4)
```

```
1541 FORMAT(/10X,65HTHE STIFFNESS AND DAMPING PROPERTIES ARE S
    1AS FOLLOWS                    /
    1 20X, 10HK1 AND C1   )
1542 FORMAT(20X,10HK2 AND C2 )
1543 FORMAT(20X,10HK3 AND C3 )
1544 FORMAT(1H+,34X, 25HCONSTANT                    )
1545 FORMAT(1H+,34X, 25HUSER SUPPLIED FUNCTION     )
1546 FORMAT(1H+,34X, 25HTABLES                      )
1547 FORMAT(1H 119(1H*))
1548 FORMAT(10X,4(28H     RELATIVE         FORCE     )/
    2 10X,4(28H  DISPLACEMENT     BETWEEN     ) /
    3 10X,4(28H     BETWEEN                  ) )
1549 FORMAT(10X,8(14H  M1 AND BASE )  )
1550 FORMAT(10X,8(14H   M2 AND M1    ) )
1551 FORMAT(10X,8(14H   M3 AND M2    ) )
1552 FORMAT( 10X,4(28H  RELATIVE         DAMPING       )/
    2         10X,4(28H DISPLACEMENT    COEFFICIENT     )/
    3         10X,4(28H   BETWEEN         BETWEEN       ))
1553 FORMAT(10X,4(28H      (IN)            (LB)      )/)
1554 FORMAT(10X,4(28H      (IN)         (LB-IN/SEC) )/)
1555 FORMAT(/1H1)
1556 FORMAT(//)
1557 FORMAT(/1H1,23X,70HTHE NONLINEAR LOAD VALUES BETWEEN
    1ARE AS FOLLOWS                  )
1558 FORMAT(1H+,58X, 11HM1 AND BASE//)
1559 FORMAT(1H+,58X, 11H M2 AND M1 //)
1560 FORMAT(1H+,58X, 11H M3 AND M2 //)
1561 FORMAT(//10X,   80HTHE NONLINEAR DAMPING COEFFICIENT VALUES BETWEE
    1N               ARE AS FOLLOWS           )
     END
```

```
      SUBROUTINE TABIN(DK,AK,NOVAL,DINC,JB)
C PURPOSE - READ IN TABLE VALUES - ARRAYS DK  VS. AK - EACH FOLLOWED BY
C           A BLANK CARD  (ALL FORMATS 8E10.4)
C        FIRST CARD OF DK SET CONTAINS INITIAL VALUE, ONLY IF INTERVAL
C           (SPECIFIED BY DINC) IS NOT ZERO. AK VALUES SET FOLLOWS.
C        FIRST AND SUCCEEDING CARDS CONTAIN DK VALUES, ONLY IF INTERVAL
C           (SPECIFIED BY DINC) IS ZERO. BLANK CARD,  AK VALUES SET,
C           AND BLANK CARD FOLLOW.
C      JB=1 SPECIFIES W VALUES
C      JB=2 SPECIFIES B VALUES
      DIMENSION DK(1),AK(1)
      DATA NR,NW/5,6/
      LOGICAL IOP
      IOP=DINC.NE.0.0
      GO TO (1,1,200),JB
    1 IF(IOP) GO TO 20
C  INTERVAL = 0.0, READ DK VALUES SET
    2 DO 10 J=1,280,8
      MK=J+7
      READ(NR,100) (DK(K), K=J,MK)
      DO 5 K=J,MK
      IF(DK(K)) 10,5,10
    5 CONTINUE
      GO TO 25
   10 CONTINUE
   15 WRITE(NW,101) DK(MK),AK(MK)
      CALL EXIT
   20 GO TO (21,25,200),JB
   21 READ(NR,100) DINT
   25 DO 50 J=1,280,8
      ICNT=0
      MK=J+7
      READ(NR,100) (AK(K),K=J,MK)
      DO 40 K=J,MK
      IF(IOP) DK(K)=DINT+FLOAT(K-1)*DINC
      IF(AK(K).EQ.0.0) GO TO 30
      LAST=K
      GO TO 40
   30 ICNT=ICNT+1
   40 CONTINUE
      IF(ICNT.EQ.8) GO TO 60
   50 CONTINUE
      GO TO 15
   60 NOVAL=LAST
      IF(DK(NOVAL).NE.0.0) GO TO 350
   70 WRITE(NW,102)
C WRITE TABLE VALUES - FIND MAX. NO. PER COLUMN
  200 NOCOL=FLOAT(NOVAL)/4.+.5
      DO 300 J1=1,NOCOL
      J2=J1+NOCOL
      IF(J2.GT.NOVAL) GO TO 210
      J3=J2+NOCOL
      IF(J3.GT.NOVAL) GO TO 220
      J4=J3+NOCOL
      IF(J4.GT.NOVAL) GO TO 230
      WRITE(NW,103) DK(J1),AK(J1),DK(J2),AK(J2),DK(J3),AK(J3),
     1 DK(J4),AK(J4)
      GO TO 300
  210 WRITE(NW,103) DK(J1),AK(J1)
      GO TO 300
  220 WRITE(NW,103) DK(J1),AK(J1),DK(J2),AK(J2)
      GO TO 300
  230 WRITE(NW,103) DK(J1),AK(J1),DK(J2),AK(J2),DK(J3),AK(J3)
  300 CONTINUE
      WRITE(NW,104)
  350 RETURN
  100 FORMAT(8E10.4)
  101 FORMAT(/5X,37HNUMBER OF VALUES IN TABLE EXCEEDS 280/
     1 15H      DISP =     ,E12.4,15H    W OR B  =     , E12.4)
  102 FORMAT(/5X,75HNUMBER OF VALUES IN DISPLACEMENT TABLE IS LESS THAN
     1 NO. OF W OR B VALUES          /
     2 5X,  35HOR LAST DISPLACEMENT VALUE IS ZERO )
  103 FORMAT(8X,8F14.5)
  104 FORMAT(//)
      END
```

```
      SUBROUTINE SOLVE
      REAL M1,M2,M3,C1,K1,K2
      COMMON TPRINT,TMAX,IPSTEP,NCYCLS,MOTION,TITLE(15),YBA,YBINT(200)
      COMMON NR,NW,NCASE,MODEL,LOADF,IDAMP,IFOFT,ICC,
     1              M1,M2,M3,K1,C1,K2,GL,FA,ALOAD,ADAMP,BLOAD,BDAMP,
     2CLOAD,CDAMP,DLOAD,DDAMP,HINIT,IFM7,AMPLD,FREQ,PEAKS,PDURS,PEAKH,
     3PDURH,NINCP,TINCP,TP(200),PUVAL(200),PULDOT(200),TINIT,Y1IN,Y2IN,
     4Y3IN,V1IN,V2IN,V3IN,TIME(6000),Y1,Y2,Y3,V1,V2,V3,N,VEC(6),DVEC(6),
     5MAXINC,H,HM,M,E,AKO,NE,T,              ELIM,INDX,     YB,YBDOT,
     6OMEGA,WHO,WY3Y2H,BY3Y2H
      COMMON FILMT(6000),Y2MY1(6000),VAPEAK(6000),YBPLOT(6000)
      COMMON TZ,ITIME,YBPREV
C THIS SUBROUTINE SOLVES THE EQUATIONS OF MOTION,WHICH WILL BE DEFINED
C   IN SUBROUTINE DIFFEQ
C
C INITIALIZE THE VECTORS
C INITIALIZE STORAGE FOR MAX AND MIN VALUES
      ITIME=1
      IVAL=1
      IMAXIM=0
      IFM7= IFOFT-7
      ISTEAD=1
      WRITE(NW,1111)
      IF(MODEL.EQ.3)  GO TO 10
      WRITE(NW,1112)
      N=6
      VEC(1)=V1IN
      VEC(2)=V2IN
      VEC(3)=V3IN
      VEC(4)=Y1IN
      VEC(5)=Y2IN
      VEC(6)=Y3IN
      GO TO 20
   10 WRITE(NW,1113)
      N=2
      VEC(1)=V3IN
      VEC(2)=Y3IN
   20 T=TINIT
C SAVE VALUE OF M= NO. OF INTEGRATIONS BEFORE STEP SIZE IS DOUBLED
      MOLD =M
C INITIALIZE STORAGE FOR T- PRINT VALUES
      TPRVAL=T+TPRINT
      KELP=1
      DO  200 KOUNT=1,MAXINC
C SET FLAG OFF FOR PRINT
      IPRINT=2
C INITIALIZE M AND NE
      M=MOLD
      IF(KOUNT.EQ. 1) NE=0
      IF(KOUNT.NE.1 ) NE=1
      TADINC=T+2.*H
      IF(TADINC.LT.TPRVAL)  GO TO 1200
      TOINC=T+H
      IF(TOINC.LT.TPRVAL)  GO TO 1190
C T+  DT WILL EXCEED PRINT VALUE
C SAVE OLD DT VALUE, I.E.  SAVE H
      HOLD=H
      H=TPRVAL -T
C SAVE NEW DT VALUE
      HNEW=H
C TURN PRINT FLAG ON
      IPRINT=1
C SET M=10,000  , SO THAT DT WILL NOT BE DOUBLED
 1190 M=10000
```

```
C RONKU INTEGRATION
 1200 TZ=T
      CALL RONKU(T,VEC,DVEC,H,HM,N,NE,M,E,AKO)
      YBPREV=YB
C TEST PRINT FLAG ON, 1=ON,  2=OFF
      IF(IPRINT.EQ.2)  GO TO 1536
C TEST DT =NEW DT
      IF(H-HNEW)  1536,1210,1536
C RESET DT TO OLD DT
 1210 H=HOLD
C INCREASE FOR NEXT PRINT VALUE
      TPRVAL=T+TPRINT
C FORM AN INDEX TO TAG NO. OF ITERATIONS
      INDX=KELP
      IF(MOTION.EQ.0)    YBPLOT(KELP)=YB
      IF(MOTION.EQ.1)  YBPLOT(KELP) =YBA
      TIME(KELP)=T
      MAPGE=(KELP/45)*45-KELP
      IF(MAPGE.EQ.0)  WRITE(NW,1118)
      IF(MODEL.EQ.3) GO TO 1490
      Y2MY1(KELP)=VEC(4)-VEC(5)
      FILMT(KELP)=HINIT+VEC(6)-VEC(5)
      Y1MYB=VEC(4)-YB                                                    PAUL457
      WRITE(NW,2222) T,FILMT(KELP),(VEC(IO),IO=4,6),(VEC(IO),IO=1,3),
     1Y2MY1(KELP),YB,Y1MYB                                               PAUL457
      GO TO 1530
1490  FILMT(KELP)=HINIT+VEC(2)-YB
      WRITE(NW,2222) T,FILMT(KELP),VEC(2),VEC(1),YB,YBA
 1530 IF(FILMT(KELP).LT.0.0)  GO TO 1531
      GO TO (400,500,600,700),IFM7
 1531 IF(IFOFT.EQ.8)  GO TO 400
      WRITE(NW,1115)
 1115 FORMAT(/5X,47HRUN COMPLETE AT THIS POINT. ROTOR HAS BOTTOMED.)
      GO TO 666
  400 IF(KELP.LT.3)  GO TO 1535
      D1=FILMT(KELP)
      D2=FILMT(KELP-1)
      D3=FILMT(KELP-2)
      IF(D1.LT.D2.AND.D2.GT.D3)  GO TO 410
      IF(D1.GT.D2.AND.D2.LT.D3)  GO TO 420
      GO TO 1535
  410 IMAXIM = 1
      GO TO 425
  420 IMAXIM=2
  425 VAPEAK(IVAL)=D2
      IVAL=IVAL+1
C TEST FOR MIN OR MAX
      GO TO (1535,430),IMAXIM
C TEST FOR STEADY-STATE
  430 IF(ISTEAD.NE.1)  GO TO 661
      IF(IVAL.LE.5) GO TO 1535
      ERRC=(VAPEAK(IVAL-3)-VAPEAK(IVAL-5))/VAPEAK(IVAL-3)
      IF(ABS(ERRC).GT..01) GO TO 1535
      ISTEAD= 2
      GO TO 1535
C IFOFT = 9
  500 IF (T.LT.PDURS)  GO TO 1535
  510 IF(KELP.LT.3)  GO TO 1535
      D1=FILMT(KELP)
      D2=FILMT(KELP-1)
      D3=FILMT(KELP-2)
      IF(D1.LT.D2.AND.D2.GT.D3)  GO TO 515
      IF(D1.GT.D2.AND.D2.LT.D3)  GO TO 515
      GO TO 1535
  515 IMAXIM=IMAXIM+1
      IF(NCYCLS.EQ.0) GO TO 520
      IF(IMAXIM.GT.(2*NCYCLS))  GO TO 666
      GO TO 1535
```

```
  520 IF(IMAXIM.GE.2) GO TO 666
      GO TO 1535
C IFOFT = 10
  600 IF(T.LT.PDURH)  GO TO 1535
      GO TO 510
  700 ANINCP=NINCP
      IF(T.LT.ANINCP*TINCP)    GO TO 1535
      GO TO 510
 1535 KELP=KELP+1
 1536 IF(T.GT.TMAX)  GO TO 660
  200 CONTINUE
      WRITE(NW,1114)  MAXINC
      GO TO 666
C MAKE A HEADING AND PRINT RESULTS
 1111  FORMAT(1H1,19X,43H  000   U   U  TTTTT  PPPP   U   U  TTTTT  /
     1         20X, 43H 0   0  U   U    T    P   P  U   U    T    /
     2         20X, 43H 0   0  U   U    T    PPPP   U   U    T    /
     3         20X, 43H 0   0  U   U    T    P      U   U    T    /
     4         20X, 43H  000    UUU     T    P       UUU     T    ////
     5)
 1112 FORMAT(132H   TIME      FILM      DISPLACEMENT DISPLACEMENT DISPLACPAUL457
     1EMENT  VELOCITY    VELOCITY    VELOCITY    RELATIVE    FORCING    PAUL457
     1REL. DISP.              /                                         PAUL457
     2       132H           THICKNESS   OF MASS 1    OF MASS 2    OF ROTPAUL457
     3OR    OF MASS 1   OF MASS 2    OF ROTOR   DISP. BET.   FUNCTION   PAUL457
     3BET M1+BASE             /                                         PAUL457
     4       132H    (SEC)    (INCHES)     (INCHES)      (INCHES)      (INCHEPAUL457
     5S)    (IN/SEC)     (IN/SEC)      (IN/SEC)  MASS2 +MASS1 (INCHES)    PAUL457
     5 (INCHES)               /)                                        PAUL457
 1113 FORMAT(95H0   TIME     FILM     DISPLACEMENT   VELOCITY       FORCING
     1    FORCING                                                      /
     2       75H          THICKNESS   OF ROTOR      OF ROTOR     FUNCTION
     3    FUNCTION        /
     4       75H    (SEC) (INCHES)     (INCHES)      (IN/SEC)     (INCHES)
     5    (G*S)           /)
 1114 FORMAT( /5X,38HMAXIMUM NO. OF TIME STEPS HAS EXCEEDED,I5)
 2222 FORMAT(1X,F7.4,E11.4,3E13.4,6E12.4)                              PAUL457
 1116 FORMAT(/5X,42HSTEADY-STATE CRITERION HAS BEEN SATISFIED.)
 1117 FORMAT(/5X,33HSPECIFIED TIME HAS BEEN ATTAINED.)
 1118 FORMAT(1H1)
  660 WRITE(NW,1117)
      GO TO 666
  661 WRITE(NW,1116)
  666 IF(ICC.EQ.12) CALL CALCOM
      RETURN
      END
```

```
      SUBROUTINE SIMINI(SI,FX,A,E,REL,MAXIT,FK,MRET)
      EXTERNAL FX
      LOGICAL REL
      DIMENSION A(2)
      AA=A(1)
      BB=A(2)
      H = (BB-AA) / 6.0
      XMID = (AA+BB) * .5
      Q = 2. * FX(XMID,FK)
      S1 = FX(AA,FK) + Q + FX(BB,FK)
      PR = H*(S1+Q)
      IF(MAXIT.EQ.1) GO TO 150
      DO 100 IT=2,MAXIT
      ISTOP = 2**IT - 1
      H= .5*H
      S=0.
      DO 80 M=1,ISTOP,2
      X=AA+3.0*M*H
   80 S=S+FX(X,FK)
      SI=H*(4.*S +S1)
      DIFF=ABS(SI-PR)
      IF(REL) DIFF=DIFF/ABS(SI)
      IF(DIFF.LE.E) GO TO 160
      PR=SI
      S1=S1+S+S
  100 CONTINUE
      RETURN
  150 SI=PR
  160 MRET=0
      RETURN
      END
```

```
      SUBROUTINE TLU(A,B,C,D,N)                                          TLU     1
            LINEAR INTERPOLATION ROUTINE                                 TLU     2
      A= INDEPENDENT VARIABLE                                            TLU  0003
      B= DEPENDENT VARIABLE  (ANSWER)                                    TLU  0004
      C= INDEPENDENT TABLE                                               TLU  0005
      D= DEPENDENT TABLE                                                 TLU  0006
      N= NUMBER OF POINTS IN TABLE                                       TLU  0007
      INDEPENDENT TABLE MUST BE SORTED, EITHER ASCENDING OR DESCENDING   TLU  0008
      DIMENSION C(1),D(1)                                                TLU  0009
      IF(N-1)1,2,3                                                       TLU  0010
    1 B=0.                                                               TLU  0011
      GO TO 100                                                          TLU  0012
    2 B=D(1)                                                             TLU  0013
      GO TO 100                                                          TLU  0014
    3 ML=1                                                               TLU  0015
      MU=N                                                               TLU  0016
    8 IF(MU-ML-1) 15,15,9                                                TLU  0017
    9 M=(MU+ML)/2                                                        TLU  0018
      IF(C(1)-C(2))11,2,10                                               TLU  0019
   10 IF(C(M)-A)13,12,14                                                 TLU  0020
   11 IF(A-C(M))13,12,14                                                 TLU  0021
   12 B=D(M)                                                             TLU  0022
      GO TO 100                                                          TLU  0023
   13 MU=M                                                               TLU  0024
      GO TO 8                                                            TLU  0025
   14 ML=M                                                               TLU  0026
      GO TO 8                                                            TLU  0027
   15 B=D(ML)+(D(MU)-D(ML))*((A-C(ML))/(C(MU)-C(ML)))                    TLU  0028
  100 RETURN                                                             TLU  0029
      END                                                                TLU  0030
```

```
      FUNCTION FX(X,FK)
      COMMON TPRINT,TMAX,IPSTEP,NCYCLS,MOTION,TITLE(15),YBA,YBINT(200)
      COMMON NR,NW,NCASE,MODEL,LOADF,IDAMP,IFOFT,ICC,
     1              M1,M2,M3,K1,C1,K2,GL,FA,ALOAD,ADAMP,BLOAD,BDAMP,
     2CLOAD,CDAMP,DLOAD,DDAMP,HINIT,IFM7,AMPLD,FREQ,PEAKS,PDURS,PEAKH,
     3PDURH,NINCP,TINCP,TP(200),PUVAL(200),PULDOT(200),TINIT,Y1IN,Y2IN,
     4Y3IN,V1IN,V2IN,V3IN,TIME(6000),Y1,Y2,Y3,V1,V2,V3,N,VEC(6),DVEC(6),
     5MAXINC,H,HM,M,E,AKO,NE,T,              ELIM,INDX,     YB,YBDOT,
     6OMEGA,WHO,WY3Y2H,BY3Y2H
      COMMON FILMT(6000),Y2MY1(6000),VAPEAK(6000),YBPLOT(6000)
      REAL M1,M2,M3,C1,K1,K2
      K=FK
      NP1=NINCP+1
      GO TO (1,2) ,K
    1 CALL TLU(X,F1,TP,YBINT ,NP1)
      FX=F1
      RETURN
    2 CALL TLU(X,F2,TP,PUVAL,NP1)
      FX=F2
      RETURN
      END
```

```
      SUBROUTINE FORMT
      DIMENSION A(2)
      COMMON TPRINT,TMAX,IPSTEP,NCYCLS,MOTION,TITLE(15),YBA,YBINT(200)
      COMMON NR,NW,NCASE,MODEL,LOADF,IDAMP,IFOFT,ICC,
     1              M1,M2,M3,K1,C1,K2,GL,FA,ALOAD,ADAMP,BLOAD,BDAMP,
     2CLOAD,CDAMP,DLOAD,DDAMP,HINIT,IFM7,AMPLD,FREQ,PEAKS,PDURS,PEAKH,
     3PDURH,NINCP,TINCP,TP(200),PUVAL(200),PULDOT(200),TINIT,Y1IN,Y2IN,
     4Y3IN,V1IN,V2IN,V3IN,TIME(6000),Y1,Y2,Y3,V1,V2,V3,N,VEC(6),DVEC(6),
     5MAXINC,H,HM,M,E,AKO,NE,T,              ELIM,INDX,     YB,YBDOT,
     6OMEGA,WHO,WY3Y2H,BY3Y2H
      COMMON FILMT(6000),Y2MY1(6000),VAPEAK(6000),YBPLOT(6000)
      DATA MAXIT,ERR/100,.01/
      EXTERNAL FX
      REAL M1,M2,M3,C1,K1,K2
      NP1=NINCP +1
      YBINT(1)=0.0
      DO 10 I=2,NP1
      A(1)=TP(I-1)
      A(2)=TP(I)
      MRET=5
      CALL SIM1NI(TEMP,FX,A,ERR,0,MAXIT,2.,MRET)
      IF(MRET.EQ.5) GO TO 5
      GO TO 10
    5 WRITE(NW,102) MAXIT,ERR
      WRITE(NW,101)
   10 YBINT(I)=YBINT(I-1)+TEMP
      RETURN
  101 FORMAT(5X,49HFOR FORMATION OF NEW TABLE FOR THE INTEGRAL OF YB)
  102 FORMAT(1H0,29HMAXIMUM NUMBER OF ITERATIONS,I3,25H WAS REACHED BEFO
     1RE EPS =,E11.4)
      END
```

```
      SUBROUTINE FILM
C THIS SUBR. IS CALLED BY SUBR. #INPUT# WHICH IS PART OF #SHAKE#
C  IT CALCULATES THE EQUILIBRIUM GAS FILM THICKNESS
      COMMON TPRINT,TMAX,IPSTEP,NCYCLS,MOTION,TITLE(15),YBA,YBINT(200)
      COMMON NR,NW,NCASE,MODEL,LOADF,IDAMP,IFOFT,ICC,
     1              M1,M2,M3,K1,C1,K2,GL,FA,ALOAD,ADAMP,BLOAD,BDAMP,
     2CLOAD,CDAMP,DLOAD,DDAMP,HINIT,IFM7,AMPLD,FREQ,PEAKS,PDURS,PEAKH,
     3PDURH,NINCP,TINCP,TP(200),PUVAL(200),PULDOT(200),TINIT,Y1IN,Y2IN,
     4Y3IN,V1IN,V2IN,V3IN,TIME(6000),Y1,Y2,Y3,V1,V2,V3,N,VEC(6),DVEC(6),
     5MAXINC,H,HM,M,E,AKO,NE,T,              ELIM,INDX,     YB,YBDOT,
     6OMEGA,WHO,WY3Y2H,BY3Y2H
      COMMON FILMT(6000),Y2MY1(6000),VAPEAK(6000),YBPLOT(6000)
      REAL M1,M2,M3,C1,K1,K2
      W=-FA+M3*GL
      IF(LOADF-4)11,11,21
11    BH=ALOG(W)-ALOG(ALOAD)
      B=BLOAD
      IF(ABS(BLOAD).LT..00001.AND.BLOAD.LT.0.0) B=-.00001
      IF(ABS(BLOAD).LT..00001.AND.BLOAD.GT.0.0)     B=.00001
      HINIT=BH/B
      RETURN
   21 CABIN =W/CLOAD
      D=DLOAD
      IF(ABS(DLOAD).LT..00001.AND.DLOAD.GT.0.0)     D=.00001
      IF(ABS(DLOAD).LT..00001.AND.DLOAD.LT.0.0) D=-.00001
      ONENT=ALOG(CABIN)/D
      IF(ABS(ONENT).GT.88.0) GO TO 30
      HINIT=EXP(ONENT)
      RETURN
   30 WRITE(NW,100) DLOAD
      CALL EXIT
  100 FORMAT(25H0DLOAD IS TOO BIG. DLOAD=,E15.5)
      END
```

```
      SUBROUTINE RONKU    (X,Y,DY,H,HH,N,NE,M,E,AKO)
C     REVISED 3/30/64 FOR NORMALIZED ERROR
      DIMENSION Y(6),DY(6),Y1(6),YD(6),YP(6,5),QP(6,5),A(4),B(4),C(4)
   30 IF(NE) 1,1,2
    1 A(1)=0.5
      A(2)= .2928932
      A(3)=      1.7071068
      A(4)=1.0/6.0
      B(1)=2.0
      B(2)=1.0
      B(3)=1.0
      B(4)=2.0
      C(1)=0.5
      C(2)=A(2)
      C(3)=A(3)
      C(4)=0.5
      IF (NE) 32,11,2
   11 DO 3 I=1,N
      YP(I,1)=Y(I)
    3 QP(I,1)=0.0
   32 K1=0
    2 X1=X
      HH=H
      K=1
   12 X50 = X1
      DO 4 J=2,5
      DO 17 I=1,N
   17 YD(I)=YP(I,J-1)
      CALL DIFEQ(N,X1,YD,DY)
      IF (J-3) 151,153,152
  151 X1=X1+0.5*HH
      GO TO 153
  152 X1=X1+0.5*HH
  153 CONTINUE
      DO 5 I=1,N
      TERM=A(J-1)*(DY(I)-B(J-1)*QP(I,J-1))
      YP(I,J)=YP(I,J-1)+HH*TERM
    5 QP(I,J)=QP(I,J-1)+3.0*TERM-C(J-1)*DY(I
    4 CONTINUE
      X1 =X50
      IF (K-2) 6,7,8
    6 DO 61 J=1,N
      Y1(J)=YP(J,5)
      YP(J,1)=Y(J)
   61 QP(J,1)=0.0
      K=K+1
      HH=H/2.0
      GO TO 12
    7 K=K+1
      X1=X1+HH
      DO 71 J=1,N
      QP(J,1)=QP(J,5)
   71 YP(J,1)=YP(J,5)
      GO TO 12
    8 DO 81 J=1,N
      T1=SQRT(Y1(J)**2+YP(J,5)**2)
      IF(T1) 18,81,18                                          0060
   18 TEST=ABS (Y1(J)-YP(J,5))/T1
      IF (TEST-E) 81,81,9
   81 CONTINUE
      K1=K1+1
      AKO=TEST
      IF (K1-M) 10,13,13
    9 K1=0
      IF (ABS (H/2.0)-ABS (HH))14,15,15
   14 AKO=TEST
      GO TO 10
   15 H=H/2.0
      DO 16 J=1,N
   16 YP(J,1)=Y(J)
      GO TO 2
   13 K1=0
      H=H+H
   10 X=X1    +HH
      DO 82 J=1,N
      QP(J,1)=QP(J,5)
      YP(J,1)=YP(J,5)+(YP(J,5)-Y1(J))/15.0
   82 Y(J)=YP(J,1)
      CALL DIFEQ(N,X,Y,DY)
      RETURN
      END
```

```
      SUBROUTINE DEQNL(VEC,DVEC)
      DIMENSION VEC(6),DVEC(6)
      COMMON TPRINT,TMAX,IPSTEP,NCYCLS,MOTION,TITLE(15),YBA,YBINT(200)
      COMMON NR,NW,NCASE,MODEL,LOADF,IDAMP,IFOFT,ICC,
     1              M1,M2,M3,K1,C1,K2,GL,FA,ALOAD,ADAMP,BLOAD,BDAMP,
     2CLOAD,CDAMP,DLOAD,DDAMP,HINIT,IFM7,AMPLD,FREQ,PEAKS,PDURS,PEAKH,
     3PDURH,NINCP,TINCP,TP(200),PUVAL(200),PULDOT(200),TINIT,Y1IN,Y2IN,
     4Y3IN,V1IN,V2IN,V3IN,TIME(6000),Y1,Y2,Y3,V1,V2,V3,
     5NDUM,DDUM(6),DVUM(6),
     5MAXINC,H,HM,M,E,AKO,NE,TTDUM,          ELIM,INDX,      YB,YBDOT,
     6OMEGA,WHO,WY3Y2H,BY3Y2H
      COMMON FILMT(6000),Y2MY1(6000),VAPEAK(6000),YBPLOT(6000)
      COMMON TZ,ITIME,YBPREV
      COMMON NONLIN,ITYP1,ITYP2,ITYP3,TAB1,TAB2,TAB3,C2,C3,K3,          EM
     1DISPW1(300),DISPW2(300),DISPW3(300),W1FTAB(300),W2FTAB(300),      EM
     2W3FTAB(300),DISPB1(300),DISPB2(300),DISPB3(300),B1FTAB(300),      EM
     3B2FTAB(300),B3FTAB(300),NOW1,NOW2,NOW3,NOB1,NOB2,NOB3             EM
      REAL M1,M2,M3,C1,K1,K2,K3                                         EM
C INSERT COMMON CARDS +  REAL CARD
      IF(MODEL.EQ.3) GO TO 200
      Y1MYB= VEC(4)-YB
      DY1MYB= VEC(1)-YBDOT
C     Y2  -Y1   DEFINED AS X2MY1  SINCE Y2MY1  DIMENSIONED IN COMMON
      X2MY1 = VEC(5)-VEC(4)
      DY2MY1= VEC(2)-VEC(1)
      Y3MY2= VEC(6)-VEC(5)
      HIPPY=Y3MY2+HINIT
      DY3MY2= VEC(3)-VEC(2)
      GO TO (10,20,30),ITYP1
   10 W1F=K1*Y1MYB
      B1F=C1
      GO TO 40
   20 W1F=FK1(Y1MYB,DY1MYB)
      B1F=FC1(Y1MYB,DY1MYB)
      GO TO 40
   30 CALL TLU(Y1MYB,W1F,DISPW1,W1FTAB,NOW1)
      CALL TLU( Y1MYB,B1F,DISPB1,B1FTAB,NOB1)
      W1F=-W1F
      GO TO 40
   40 GO TO (50,60,70),ITYP2
   50 W2F=K2*X2MY1
      B2F=C2
      GO TO 80
   60 W2F=FK2(X2MY1,DY2MY1)
      B2F=FC2(X2MY1,DY2MY1)
      GO TO 80
   70 CALL TLU(X2MY1,W2F,DISPW2,W2FTAB,NOW2)
      CALL TLU( Y2MY1,B2F,DISPB2,B2FTAB,NOB2)
      W2F=-W2F
   80 IF(HIPPY.LT..0002) HIPPY=ELIM
      GO TO (90,100,110),ITYP3
   90 W3F=K3*Y3MY2
      B3F=C3
      GO TO 120
  100 W3F=FK3(HINIT,DY3MY2)-FK3(HIPPY,DY3MY2)
      B3F=FC3(HIPPY,DY3MY2)
      GO TO 120
  110 CALL TLU(HIPPY,WHY,DISPW3,W3FTAB,NOW3)
      CALL TLU(HIPPY,B3F,DISPB3,B3FTAB,NOB3)
      W3F=WHO-WHY
  120 IF(MODEL.EQ.3)  GO TO 250
      SUM1=W1F+B1F*DY1MYB
      SUM2=W2F+B2F*DY2MY1
      SUM3=W3F+B3F*DY3MY2
      DVEC(1)=(1./M1)*(SUM2-SUM1)
      DVEC(2)=(1./M2)*(SUM3-SUM2)
      DVEC(3)=(1./M3)*(-SUM3)
      GO TO 300
  200 Y3MY2= VEC(2)-YB
      HIPPY=HINIT+Y3MY2
      DY3MY2=VEC(1)-YBDOT
      GO TO 80
  250 DVEC(2)=VEC(1)
      DVEC(1)=(-1./M3)*(W3F+B3F*(DVEC(2)-YBDOT))
  300 RETURN
      END
```

APPENDIX C

ANALYSIS OF DYNAMIC RESPONSE OF BRAYTON ROTATING UNIT TO AXIAL RANDOM EXCITATIONS

The Brayton rotating unit was modeled as a three-mass system, as shown in Figure 13. A sketch of the BRU is shown in Figure 7, in which the various masses and springs are identified with the model shown in Figure 13. The base of the three-mass system is the shake table where random excitations are transmitted to the BRU. k_1 and c_1 are respectively the stiffness and damping of the connector which provides the joint between the BRU and the shake table. m_1 is the mass of the BRU housing structure. k_2 and c_2 are respectively the stiffness and damping of the gimbal support. k_3 and c_3 are the thrust bearing gas-film stiffness and damping respectively. Finally, m_3 is the rotor mass. The equations of motion of the three-mass system shown in Figure 13 are:

$$m_1\ddot{x}_1 + c_1(\dot{x}_1-\dot{x}_b) + c_2(\dot{x}_1-\dot{x}_2) + k_1(x_1-x_b) + k_2(x_1-x_2) = 0 \tag{C.1}$$

$$m_2\ddot{x}_2 + c_2(\dot{x}_2-\dot{x}_1) + c_3(\dot{x}_2-\dot{x}_3) + k_2(x_2-x_1) + k_3(x_2-x_3) = 0 \tag{C.2}$$

$$m_3\ddot{x}_3 + c_3(\dot{x}_3-\dot{x}_2) + k_3(x_3-x_2) = 0 \tag{C.3}$$

Introducing relative coordinates between mass points,

$$\begin{aligned} y_1 &= x_1 - x_b \\ y_2 &= x_2 - x_1 \\ y_3 &= x_3 - x_2 \end{aligned} \tag{C.4}$$

Equations (C.1) and (C.3) become

$$m_1\ddot{y}_1 + c_1\dot{y}_1 - c_2\dot{y}_2 + k_1y_1 - k_2y_2 = -m_1\ddot{x}_b \tag{C.5}$$

$$m_2(\ddot{y}_1+\ddot{y}_2) + c_2\dot{y}_2 - c_3\dot{y}_3 + k_2y_2 - k_3y_3 = -m_2\ddot{x}_b \tag{C.6}$$

$$m_3(\ddot{y}_1+\ddot{y}_2+\ddot{y}_3) + c_3\dot{y}_3 + k_3y_3 = -m_3\ddot{x}_b \tag{C.7}$$

Dividing Equations (C.5), (C.6) and (C.7) by m_1, m_2 and m_3 respectively,

$$\ddot{y}_1 + \frac{c_1}{m_1}\dot{y}_1 - \frac{c_2}{m_1}\dot{y}_2 + \frac{k_1}{m_1}y_1 - \frac{k_2}{m_1}y_2 = -\ddot{x}_b \tag{C.8}$$

$$\ddot{y}_1 + \ddot{y}_2 + \frac{c_2}{m_2}\dot{y}_2 - \frac{c_3}{m_2}\dot{y}_3 + \frac{k_2}{m_2}y_2 - \frac{k_3}{m_2}y_3 = -\ddot{x}_b \tag{C.9}$$

$$\ddot{y}_1 + \ddot{y}_2 + \ddot{y}_3 + \frac{c_3}{m_3}\dot{y}_3 + \frac{k_3}{m_3}y_3 = -\ddot{x}_b \tag{C.10}$$

Subtracting Equation (C.8) from Equation (C.9),

$$\ddot{y}_2 - \frac{c_1}{m_1}\dot{y}_1 + \left[\frac{c_2}{m_1} + \frac{c_2}{m_2}\right]\dot{y}_2 - \frac{c_3}{m_2}\dot{y}_3 - \frac{k_1}{m_1}y_1 + \left[\frac{k_2}{m_1} + \frac{k_2}{m_2}\right]y_2 - \frac{k_3}{m_2}y_3 = 0 \tag{C.11}$$

Subtracting Equation (C.9) from Equation (C.10),

$$\ddot{y}_3 - \frac{c_2}{m_2}\dot{y}_2 + \left[\frac{c_3}{m_2} + \frac{c_3}{m_3}\right]\dot{y}_3 - \frac{k_2}{m_2}y_2 + \left[\frac{k_3}{m_2} + \frac{k_3}{m_3}\right]y_3 = 0 \tag{C.12}$$

Equations (C.8), (C.11) and (C.12) can be written in the matrix form as follows:

$$\begin{bmatrix} 1 & 0 & 0 \\ 0 & 1 & 0 \\ 0 & 0 & 1 \end{bmatrix} \cdot \begin{bmatrix} \ddot{y}_1 \\ \ddot{y}_2 \\ y_3 \end{bmatrix} + \begin{bmatrix} \frac{c_1}{m_1} & -\frac{c_2}{m_1} & 0 \\ -\frac{c_1}{m_1} & \frac{c_2}{m_1}+\frac{c_2}{m_2} & -\frac{c_3}{m_2} \\ 0 & -\frac{c_2}{m_2} & \frac{c_3}{m_2}+\frac{c_3}{m_3} \end{bmatrix} \cdot \begin{bmatrix} \dot{y}_1 \\ \dot{y}_2 \\ \dot{y}_3 \end{bmatrix} + \begin{bmatrix} \frac{k_1}{m_1} & -\frac{k_2}{m_1} & 0 \\ -\frac{k_1}{m_1} & \frac{k_2}{m_1}+\frac{k_2}{m_2} & -\frac{k_2}{m_2} \\ 0 & -\frac{k_2}{m_2} & \frac{k_3}{m_2}+\frac{k_3}{m_3} \end{bmatrix} \cdot \begin{bmatrix} y_1 \\ y_2 \\ y_3 \end{bmatrix} = \begin{bmatrix} -\ddot{x}_b \end{bmatrix} \cdot \begin{bmatrix} 1 \\ 0 \\ 0 \end{bmatrix} \tag{C.13}$$

To obtain the complex frequency response, assume

$$x_b = e^{i\omega t} \tag{C.14}$$

$$\begin{bmatrix} y_1 \\ y_2 \\ y_3 \end{bmatrix} = \begin{bmatrix} H_{y_1}(\omega) \\ H_{y_2}(\omega) \\ H_{y_3}(\omega) \end{bmatrix} \cdot e^{i\omega t} \tag{C.15}$$

and substitute into Equation (C.13):

$$-\omega^2 [I] \begin{bmatrix} H_{y_1}(\omega) \\ H_{y_2}(\omega) \\ H_{y_3}(\omega) \end{bmatrix} + i\omega[C] \begin{bmatrix} H_{y_1}(\omega) \\ H_{y_2}(\omega) \\ H_{y_3}(\omega) \end{bmatrix} + [K] \begin{bmatrix} H_{y_1}(\omega) \\ H_{y_2}(\omega) \\ H_{y_3}(\omega) \end{bmatrix} = \omega^2 \begin{bmatrix} 1 \\ 0 \\ 0 \end{bmatrix} \tag{C.16}$$

where

$$[I] = \begin{bmatrix} 1 & 0 & 0 \\ 0 & 1 & 0 \\ 0 & 0 & 1 \end{bmatrix} \tag{C.17}$$

$$[C] = \begin{bmatrix} \frac{c_1}{m_1} & -\frac{c_2}{m_1} & 0 \\ -\frac{c_1}{m_1} & \frac{c_2}{m_1} + \frac{c_2}{m_2} & -\frac{c_3}{m_2} \\ 0 & -\frac{c_2}{m_2} & \frac{c_3}{m_2} + \frac{c_3}{m_3} \end{bmatrix} \tag{C.18}$$

$$[K] = \begin{bmatrix} \frac{k_1}{m_1} & -\frac{k_2}{m_1} & 0 \\ -\frac{k_1}{m_1} & \frac{k_2}{m_1}+\frac{k_2}{m_2} & -\frac{k_3}{m_2} \\ 0 & -\frac{k_2}{m_2} & \frac{k_3}{m_2}+\frac{k_3}{m_3} \end{bmatrix} \tag{C.19}$$

Define a matrix Z:

$$[Z] \equiv -[I] + i\frac{1}{\omega}[C] + \frac{1}{\omega^2}[K] \tag{C.20}$$

Equation (C.16) can be written as

$$[Z] \begin{bmatrix} H_{y_1}(\omega) \\ H_{y_2}(\omega) \\ H_{y_3}(\omega) \end{bmatrix} = \begin{bmatrix} 1 \\ 0 \\ 0 \end{bmatrix}$$

Thus,

$$\begin{bmatrix} H_{y_1}(\omega) \\ H_{y_2}(\omega) \\ H_{y_3}(\omega) \end{bmatrix} = [Z]^{-1} \begin{bmatrix} 1 \\ 0 \\ 0 \end{bmatrix} \tag{C.21}$$

The complex frequency responses, $H_{y_1}(\omega)$, $H_{y_2}(\omega)$ and $H_{y_3}(\omega)$ can be readily calculated from Equation (C.21). The complex frequency response functions are sometimes called transfer functions. They give the response at one point due to a unit input excitation at some other point.

It was shown, for example, in References 4 and 9 that the input and output power spectral densities of a random process are also related by the transfer functions in the following manner.

$$S_{y_i}(\omega) = |H_{y_i}(\omega)|^2 \quad S_0(\omega) \qquad (i=1, 2, 3) \tag{C.22}$$

where

$S_{y_i}(\omega)$ = PSD of the system output y_i (i=1, 2, 3).

$S_0(\omega)$ = PSD of the system input.

$H_{y_i}(\omega)$ = magnitude of transfer function as calculated from (C.21).

APPENDIX D

COMPUTER PROGRAM FOR PREDICTING THE DYNAMIC RESPONSE OF THE BRAYTON ROTATING UNIT TO AXIAL RANDOM EXCITATIONS

This appendix presents a complete listing of the computer program (MTI PN-492) which calculates the axial response of the Brayton Rotating Unit under random excitation. Also included in this appendix are instructions for preparing input data cards, sample input and sample computer output.

PROGRAM INPUT CARDS

Card 1 FORMAT (I5)

This card reads in NCASE which is the number of cases.

Card 2 FORMAT (80H)

This card contains the descriptive identification for the case being computed.

Card 3 FORMAT (8E10.3)

This card reads in FAC.

FAC = numerical factor to be multiplied with the power spectral density specifications to permit calculations at various levels without requiring the entire specification to be modified and resubmitted as input.

Card 4 FORMAT (8E10.3)

This card contains ENGM(1), ENGC(1) and ENGK(1).

ENGM(1) = m_1 in pounds
ENGC(1) = c_1 in lb sec/in.
ENGK(1) = k_1 in lb/in.

The quantities m_1, c_1 and k_1 are shown in Figure 13.

Card 5 FORMAT (8E10.3)

This card contains ENGM(2), ENGC(2) and ENGK(2).

ENGM(2) = m_2 in pounds
ENGC(2) = c_2 in lb sec/in.
ENGK(2) = k_2 in lb/in.

The quantities m_2, c_2 and k_2 are shown in Figure 13.

Card 6 FORMAT (8E10.3)

This card contains ENGM(3), ENGC(3) and ENGK(3).

ENGM(3) = m_3 in pounds
ENGC(3) = c_3 in lb sec/in.

ENGK(3) = k_3 in lb/in.

The quantities m_3, c_3 and k_3 are shown in Figure 13.

Card 7 FORMAT (5I5)

This card contains NRANG, SPEC.

NRANG = number of frequency ranges. Each frequency range will be defined in Card 8 by an initial frequency, a final frequency and an incremental frequency.

SPEC = 1: PSD of Figure 10 will be read in.
2: a white noise displacement PSD of 1 in^2/Hz will be read in.
3: a white noise acceleration PSD of 0.01 g^2/Hz will be read in.

NOTE: The PSD values read in will be multiplied by FAC specified in Card 3.

Card 8 FORMAT (8E10.3)

This set of cards specifies the frequencies at which the response PSD will be calculated. The number of cards in this set is equal to NRANG of Card 7. Each card containing, WINIT, WFIN and WDELT represents a frequency range.

WINIT = initial frequency in Hz.
WFIN = final frequency in Hz.
WDELT = incremental frequency in Hz.

NOTE: Card 2 through Card 8 represent one case. The whole sequence can be repeated as many times as the number of cases specified in Card 1.

MATHEMATICAL SYMBOLS

A = arbitrary constant used to obtain curve fit; acceleration amplitude, g's.

B = coefficient of viscous damping of thrust-bearing gas film, a nonlinear function of arguments indicated in suffixed parentheses, lb-sec/in.; arbitrary constant used to obtain curve fit.

C = arbitrary constant used to obtain curve fit.

c = coefficient of viscous damping, lb-sec/in.

D = arbitrary constant used to obtain curve fit.

e = base of natural logarithms.

F_a = net aerodynamic force acting on rotor, lb.

f = frequency, Hz.

G = net force exerted by thrust-bearing gas film, a nonlinear function of arguments usually indicated in suffixed parentheses, lb.

g = local gravitational acceleration, in/sec^2.

H = transfer function

h = thrust-bearing gas-film thickness, in.

k = spring stiffness, lb/in.

m = mass, $lb\text{-}sec^2/in.$

S = power spectral density level

T = averaging time parameter, sec.

t = time, sec.

W = static component of thrust-bearing gas-film force, a nonlinear function of arguments usually listed in suffixed parentheses, lb.

x = displacement with respect to inertial reference frame, in.

y = displacement relative to position of static equilibrium, in.

ω = angular velocity, radians/sec.

```
    1
AXIAL RANDOM VIBRATION RESPONSE - NOMINAL CASE
0.01
96.          0.02       300000.
 7.          0.02       250000.
21.         84.         113500.
    3    1
  20.        200.          2.
 200.        400.          5.
 400.       2000.         20.
000000000000000000000000
```

AXIAL RANDOM VIBRATION RESPONSE - NOMINAL CASE

MULTIPLIER FOR INPUT PSD = 1.000E-02

INPUT VIBRATION POWER SPECTRAL DENSITY SPECIFICATION CODE IS 1.

ROTOR BEARING SYSTEM PROPERTIES ARE SPECIFIED BY THE FOLLOWING SETS OF VALUES

MASS SPRING NO	WEIGHT OF MASS (LBS)	DAMPING (LBS*SEC PER INCH)	SPRING STIFFNESS (LBS/INCH)
1	96.000	.020	3.000E+05
2	7.000	.020	2.500E+05
3	21.000	84.000	1.135E+05

THE FOLLOWING 3 FREQUENCY RANGES WILL BE RUN

RANGE NO	INITIAL FREQUENCY	FINAL FREQUENCY	FREQUENCY INCREMENT
1	20.00	200.00	2.000
2	200.00	400.00	5.000
3	400.00	2000.00	20.000

MATRIX M

1.000E+00	0.	0.
0.	1.000E+00	0.
0.	0.	1.000E+00

MATRIX C

4.021E-02	-4.021E-02	0.
-4.021E-02	5.916E-01	-2.316E+03
0.	-5.514E-01	3.088E+03

MATRIX K

1.206E+06	-1.005E+06	0.
-1.206E+06	1.479E+07	-6.259E+06
0.	-1.379E+07	8.345E+06

FREQUENCY RANGE NUMBER 1
COVERS THE RANGE FROM 20.00 TO 200.00
IN INCREMENTS OF 2.00

FREQUENCY (HZ)	PSD OF Y1 (IN*IN/HZ)	PSD OF Y2 (IN*IN/HZ)	PSD OF Y3 (IN*IN/HZ)	PSD INPUT (IN*IN/HZ)	PSD INPUT (G*G/HZ)
20.000	5.328E-12	3.975E-13	1.087E-12	1.792E-08	3.000E-05
22.000	5.910E-12	4.424E-13	1.210E-12	1.347E-08	3.300E-05
24.000	6.506E-12	4.888E-13	1.337E-12	1.037E-08	3.600E-05
26.000	7.119E-12	5.370E-13	1.470E-12	8.159E-09	3.900E-05
28.000	7.750E-12	5.871E-13	1.607E-12	6.532E-09	4.200E-05
30.000	8.401E-12	6.394E-13	1.751E-12	5.311E-09	4.500E-05
32.000	9.074E-12	6.962E-13	1.902E-12	4.376E-09	4.800E-05
34.000	9.772E-12	7.516E-13	2.061E-12	3.648E-09	5.100E-05
36.000	1.050E-11	8.119E-13	2.227E-12	3.074E-09	5.400E-05
38.000	1.125E-11	8.755E-13	2.403E-12	2.613E-09	5.700E-05
40.000	1.204E-11	9.427E-13	2.589E-12	2.241E-09	6.000E-05
42.000	1.286E-11	1.014E-12	2.787E-12	1.936E-09	6.300E-05
44.000	1.372E-11	1.090E-12	2.997E-12	1.683E-09	6.600E-05
46.000	1.463E-11	1.170E-12	3.220E-12	1.473E-09	6.900E-05
48.000	1.558E-11	1.256E-12	3.459E-12	1.297E-09	7.200E-05
50.000	1.658E-11	1.348E-12	3.715E-12	1.147E-09	7.500E-05
52.000	1.764E-11	1.446E-12	3.990E-12	1.020E-09	7.800E-05
54.000	1.876E-11	1.552E-12	4.285E-12	9.107E-10	8.100E-05
56.000	1.995E-11	1.666E-12	4.603E-12	8.166E-10	8.400E-05
58.000	2.122E-11	1.789E-12	4.947E-12	7.350E-10	8.700E-05
60.000	2.257E-11	1.921E-12	5.320E-12	6.639E-10	9.000E-05
62.000	2.401E-11	2.066E-12	5.725E-12	6.017E-10	9.300E-05
64.000	2.556E-11	2.223E-12	6.166E-12	5.470E-10	9.600E-05
66.000	2.722E-11	2.394E-12	6.647E-12	4.988E-10	9.900E-05
68.000	2.900E-11	2.581E-12	7.174E-12	4.561E-10	1.020E-04
70.000	3.093E-11	2.786E-12	7.752E-12	4.181E-10	1.050E-04
72.000	3.302E-11	3.011E-12	8.388E-12	3.842E-10	1.080E-04
74.000	3.529E-11	3.259E-12	9.090E-12	3.539E-10	1.110E-04
76.000	3.776E-11	3.534E-12	9.868E-12	3.267E-10	1.140E-04
78.000	4.045E-11	3.839E-12	1.073E-11	3.022E-10	1.170E-04
80.000	4.341E-11	4.178E-12	1.170E-11	2.801E-10	1.200E-04
82.000	4.666E-11	4.557E-12	1.277E-11	2.601E-10	1.230E-04
84.000	5.025E-11	4.983E-12	1.398E-11	2.419E-10	1.260E-04
86.000	5.423E-11	5.461E-12	1.535E-11	2.255E-10	1.290E-04
88.000	5.865E-11	6.003E-12	1.689E-11	2.104E-10	1.320E-04
90.000	6.360E-11	6.618E-12	1.865E-11	1.967E-10	1.350E-04
92.000	6.916E-11	7.320E-12	2.065E-11	1.842E-10	1.380E-04
94.000	7.544E-11	8.126E-12	2.296E-11	1.726E-10	1.410E-04
96.000	8.257E-11	9.056E-12	2.562E-11	1.621E-10	1.440E-04
98.000	9.072E-11	1.014E-11	2.872E-11	1.524E-10	1.470E-04
100.000	1.001E-10	1.140E-11	3.235E-11	1.434E-10	1.500E-04
102.000	1.088E-10	1.263E-11	3.591E-11	1.325E-10	1.500E-04
104.000	1.189E-10	1.409E-11	4.010E-11	1.226E-10	1.500E-04
106.000	1.307E-10	1.582E-11	4.510E-11	1.136E-10	1.500E-04
108.000	1.447E-10	1.790E-11	5.110E-11	1.054E-10	1.500E-04
110.000	1.615E-10	2.042E-11	5.840E-11	9.794E-11	1.500E-04
112.000	1.819E-10	2.352E-11	6.737E-11	9.113E-11	1.500E-04
114.000	2.069E-10	2.738E-11	7.857E-11	8.490E-11	1.500E-04
116.000	2.382E-10	3.228E-11	9.278E-11	7.920E-11	1.500E-04
118.000	2.780E-10	3.860E-11	1.111E-10	7.396E-11	1.500E-04
120.000	3.297E-10	4.695E-11	1.354E-10	6.915E-11	1.500E-04
122.000	3.986E-10	5.826E-11	1.683E-10	6.473E-11	1.500E-04
124.000	4.935E-10	7.407E-11	2.144E-10	6.065E-11	1.500E-04
126.000	6.289E-10	9.701E-11	2.813E-10	5.689E-11	1.500E-04
128.000	8.313E-10	1.319E-10	3.830E-10	5.342E-11	1.500E-04
130.000	1.151E-09	1.879E-10	5.469E-10	5.021E-11	1.500E-04
132.000	1.692E-09	2.845E-10	8.293E-10	4.723E-11	1.500E-04
134.000	2.674E-09	4.634E-10	1.353E-09	4.448E-11	1.500E-04
136.000	4.513E-09	8.068E-10	2.361E-09	4.192E-11	1.500E-04
138.000	7.241E-09	1.336E-09	3.918E-09	3.954E-11	1.500E-04
140.000	7.807E-09	1.489E-09	4.373E-09	3.733E-11	1.500E-04
142.000	5.096E-09	1.005E-09	2.957E-09	3.527E-11	1.500E-04
144.000	2.477E-09	5.873E-10	1.732E-09	3.335E-11	1.500E-04
146.000	1.703E-09	3.601E-10	1.064E-09	3.156E-11	1.500E-04
148.000	1.086E-09	2.382E-10	7.050E-10	2.989E-11	1.500E-04
150.000	7.391E-10	1.681E-10	4.986E-10	2.833E-11	1.500E-04
152.000	5.289E-10	1.249E-10	3.713E-10	2.686E-11	1.500E-04
154.000	3.937E-10	9.669E-11	2.879E-10	2.550E-11	1.500E-04
156.000	3.024E-10	7.727E-11	2.306E-10	2.421E-11	1.500E-04
158.000	2.383E-10	6.339E-11	1.896E-10	2.301E-11	1.500E-04
160.000	1.916E-10	5.314E-11	1.592E-10	2.188E-11	1.500E-04
162.000	1.568E-10	4.537E-11	1.362E-10	2.082E-11	1.500E-04
164.000	1.302E-10	3.933E-11	1.183E-10	1.982E-11	1.500E-04
166.000	1.095E-10	3.456E-11	1.042E-10	1.888E-11	1.500E-04
168.000	9.311E-11	3.073E-11	9.282E-11	1.800E-11	1.500E-04
170.000	7.994E-11	2.760E-11	8.355E-11	1.717E-11	1.500E-04
172.000	6.922E-11	2.502E-11	7.591E-11	1.638E-11	1.500E-04
174.000	6.041E-11	2.288E-11	6.954E-11	1.564E-11	1.500E-04
176.000	5.309E-11	2.107E-11	6.419E-11	1.495E-11	1.500E-04
178.000	4.698E-11	1.954E-11	5.966E-11	1.428E-11	1.500E-04
180.000	4.182E-11	1.824E-11	5.580E-11	1.366E-11	1.500E-04
182.000	3.746E-11	1.713E-11	5.250E-11	1.307E-11	1.500E-04
184.000	3.374E-11	1.617E-11	4.966E-11	1.251E-11	1.500E-04
186.000	3.056E-11	1.534E-11	4.721E-11	1.198E-11	1.500E-04
188.000	2.784E-11	1.462E-11	4.510E-11	1.148E-11	1.500E-04
190.000	2.551E-11	1.400E-11	4.327E-11	1.100E-11	1.500E-04
192.000	2.350E-11	1.345E-11	4.168E-11	1.055E-11	1.500E-04
194.000	2.178E-11	1.298E-11	4.030E-11	1.012E-11	1.500E-04
196.000	2.031E-11	1.257E-11	3.911E-11	9.717E-12	1.500E-04
198.000	1.906E-11	1.221E-11	3.808E-11	9.330E-12	1.500E-04
200.000	1.801E-11	1.190E-11	3.719E-11	8.962E-12	1.500E-04
INTEGRATED Y	8.972E-08	1.699E-08	4.993E-08	1.772E-07	2.220E-02
TOTAL INT Y	8.972E-08	1.699E-08	4.993E-08	1.772E-07	2.220E-02

****

FREQUENCY RANGE NUMBER 2
COVERS THE RANGE FROM 200.00 TO 400.00
IN INCREMENTS OF 5.00

FREQUENCY (HZ)	PSD OF Y1 (IN*IN/HZ)	PSD OF Y2 (IN*IN/HZ)	PSD OF Y3 (IN*IN/HZ)	PSD INPUT (IN*IN/HZ)	PSD INPUT (G*G/HZ)
200.000	1.801E-11	1.190E-11	3.719E-11	8.962E-12	1.500E-04
205.000	1.611E-11	1.128E-11	3.543E-11	8.120E-12	1.500E-04
210.000	1.507E-11	1.082E-11	3.416E-11	7.373E-12	1.500E-04
215.000	1.473E-11	1.043E-11	3.309E-11	6.711E-12	1.500E-04
220.000	1.493E-11	1.002E-11	3.194E-11	6.121E-12	1.500E-04
225.000	1.547E-11	9.493E-12	3.041E-11	5.595E-12	1.500E-04
230.000	1.608E-11	8.768E-12	2.821E-11	5.124E-12	1.500E-04
235.000	1.646E-11	7.816E-12	2.527E-11	4.702E-12	1.500E-04
240.000	1.639E-11	6.689E-12	2.172E-11	4.322E-12	1.500E-04
245.000	1.579E-11	5.501E-12	1.793E-11	3.980E-12	1.500E-04
250.000	1.473E-11	4.375E-12	1.432E-11	3.671E-12	1.500E-04
255.000	1.340E-11	3.398E-12	1.116E-11	3.391E-12	1.500E-04
260.000	1.199E-11	2.604E-12	8.582E-12	3.138E-12	1.500E-04
265.000	1.062E-11	1.985E-12	6.562E-12	2.908E-12	1.500E-04
270.000	9.357E-12	1.514E-12	5.020E-12	2.698E-12	1.500E-04
275.000	8.240E-12	1.161E-12	3.857E-12	2.507E-12	1.500E-04
280.000	7.265E-12	8.960E-13	2.983E-12	2.333E-12	1.500E-04
285.000	6.423E-12	6.975E-13	2.327E-12	2.174E-12	1.500E-04
290.000	5.698E-12	5.480E-13	1.830E-12	2.027E-12	1.500E-04
295.000	5.075E-12	4.345E-13	1.452E-12	1.893E-12	1.500E-04
300.000	4.537E-12	3.477E-13	1.163E-12	1.770E-12	1.500E-04
305.000	4.072E-12	2.807E-13	9.384E-13	1.657E-12	1.500E-04
310.000	3.668E-12	2.286E-13	7.635E-13	1.553E-12	1.500E-04
315.000	3.317E-12	1.876E-13	6.260E-13	1.456E-12	1.500E-04
320.000	3.009E-12	1.552E-13	5.169E-13	1.368E-12	1.500E-04
325.000	2.738E-12	1.293E-13	4.297E-13	1.285E-12	1.500E-04
330.000	2.499E-12	1.085E-13	3.595E-13	1.209E-12	1.500E-04
335.000	2.288E-12	9.164E-14	3.025E-13	1.139E-12	1.500E-04
340.000	2.099E-12	7.789E-14	2.560E-13	1.073E-12	1.500E-04
345.000	1.931E-12	6.659E-14	2.178E-13	1.012E-12	1.500E-04
350.000	1.781E-12	5.726E-14	1.863E-13	9.556E-13	1.500E-04
355.000	1.646E-12	4.951E-14	1.600E-13	9.029E-13	1.500E-04
360.000	1.524E-12	4.302E-14	1.381E-13	8.538E-13	1.500E-04
365.000	1.414E-12	3.757E-14	1.197E-13	8.079E-13	1.500E-04
370.000	1.314E-12	3.297E-14	1.041E-13	7.651E-13	1.500E-04
375.000	1.224E-12	2.906E-14	9.093E-14	7.251E-13	1.500E-04
380.000	1.141E-12	2.573E-14	7.970E-14	6.877E-13	1.500E-04
385.000	1.066E-12	2.288E-14	7.010E-14	6.527E-13	1.500E-04
390.000	9.972E-13	2.042E-14	6.186E-14	6.199E-13	1.500E-04
395.000	9.341E-13	1.830E-14	5.476E-14	5.891E-13	1.500E-04
400.000	8.762E-13	1.646E-14	4.862E-14	5.602E-13	1.500E-04
INTEGRATED Y	1.432E-09	5.320E-10	1.708E-09	5.232E-10	3.000E-02
TOTAL INT Y	9.115E-08	1.752E-08	5.164E-08	1.777E-07	5.220E-02

FREQUENCY RANGE NUMBER 3
COVERS THE RANGE FROM 400.00 TO 2000.00
IN INCREMENTS OF 20.00

FREQUENCY (HZ)	PSD OF Y1 (IN**2/HZ)	PSD OF Y2 (IN**2/HZ)	PSD OF Y3 (IN**2/HZ)	PSD INPUT (IN**2/HZ)	PSD INPUT (G**2/HZ)
400.000	8.762E-13	1.646E-14	4.862E-14	5.602E-13	1.500E-04
420.000	6.866E-13	1.116E-14	3.104E-14	4.608E-13	1.500E-04
440.000	5.474E-13	7.954E-15	2.060E-14	3.826E-13	1.500E-04
460.000	4.428E-13	5.920E-15	1.412E-14	3.203E-13	1.500E-04
480.000	3.627E-13	4.573E-15	9.956E-15	2.701E-13	1.500E-04
500.000	3.004E-13	3.646E-15	7.185E-15	2.294E-13	1.500E-04
520.000	2.513E-13	2.984E-15	5.289E-15	1.961E-13	1.500E-04
540.000	2.120E-13	2.493E-15	3.955E-15	1.686E-13	1.500E-04
560.000	1.803E-13	2.117E-15	2.995E-15	1.458E-13	1.500E-04
580.000	1.544E-13	1.817E-15	2.287E-15	1.267E-13	1.500E-04
600.000	1.331E-13	1.570E-15	1.755E-15	1.106E-13	1.500E-04
620.000	1.154E-13	1.358E-15	1.349E-15	9.705E-14	1.500E-04
640.000	1.005E-13	1.172E-15	1.034E-15	8.547E-14	1.500E-04
660.000	8.806E-14	1.006E-15	7.887E-16	7.557E-14	1.500E-04
680.000	7.747E-14	8.554E-16	5.971E-16	6.707E-14	1.500E-04
700.000	6.844E-14	7.201E-16	4.480E-16	5.972E-14	1.500E-04
720.000	6.069E-14	5.997E-16	3.332E-16	5.336E-14	1.500E-04
740.000	5.402E-14	4.943E-16	2.457E-16	4.782E-14	1.500E-04
760.000	4.824E-14	4.038E-16	1.800E-16	4.298E-14	1.500E-04
780.000	4.322E-14	3.276E-16	1.311E-16	3.874E-14	1.500E-04
800.000	3.884E-14	2.644E-16	9.529E-17	3.501E-14	1.500E-04
820.000	3.500E-14	2.127E-16	6.918E-17	3.172E-14	1.500E-04
840.000	3.163E-14	1.709E-16	5.026E-17	2.880E-14	1.500E-04
860.000	2.865E-14	1.374E-16	3.661E-17	2.622E-14	1.500E-04
880.000	2.602E-14	1.106E-16	2.676E-17	2.391E-14	1.500E-04
900.000	2.369E-14	8.927E-17	1.965E-17	2.186E-14	1.500E-04
920.000	2.162E-14	7.227E-17	1.450E-17	2.002E-14	1.500E-04
940.000	1.977E-14	5.872E-17	1.076E-17	1.837E-14	1.500E-04
960.000	1.811E-14	4.790E-17	8.035E-18	1.688E-14	1.500E-04
980.000	1.663E-14	3.924E-17	6.034E-18	1.555E-14	1.500E-04
1000.000	1.529E-14	3.229E-17	4.559E-18	1.434E-14	1.500E-04
1020.000	1.409E-14	2.668E-17	3.466E-18	1.325E-14	1.500E-04
1040.000	1.301E-14	2.214E-17	2.650E-18	1.226E-14	1.500E-04
1060.000	1.202E-14	1.845E-17	2.038E-18	1.136E-14	1.500E-04
1080.000	1.113E-14	1.543E-17	1.576E-18	1.054E-14	1.500E-04
1100.000	1.032E-14	1.297E-17	1.226E-18	9.794E-15	1.500E-04
1120.000	9.587E-15	1.094E-17	9.587E-19	9.113E-15	1.500E-04
1140.000	8.916E-15	9.257E-18	7.535E-19	8.490E-15	1.500E-04
1160.000	8.302E-15	7.865E-18	5.951E-19	7.920E-15	1.500E-04
1180.000	7.740E-15	6.706E-18	4.723E-19	7.396E-15	1.500E-04
1200.000	7.226E-15	5.736E-18	3.766E-19	6.915E-15	1.500E-04
1220.000	6.754E-15	4.923E-18	3.016E-19	6.473E-15	1.500E-04
1240.000	6.319E-15	4.238E-18	2.426E-19	6.065E-15	1.500E-04
1260.000	5.920E-15	3.660E-18	1.960E-19	5.689E-15	1.500E-04
1280.000	5.551E-15	3.169E-18	1.589E-19	5.342E-15	1.500E-04
1300.000	5.211E-15	2.752E-18	1.294E-19	5.021E-15	1.500E-04
1320.000	4.897E-15	2.396E-18	1.057E-19	4.723E-15	1.500E-04
1340.000	4.606E-15	2.092E-18	8.667E-20	4.448E-15	1.500E-04
1360.000	4.336E-15	1.831E-18	7.131E-20	4.192E-15	1.500E-04
1380.000	4.086E-15	1.606E-18	5.888E-20	3.954E-15	1.500E-04
1400.000	3.854E-15	1.412E-18	4.876E-20	3.733E-15	1.500E-04
1420.000	3.638E-15	1.244E-18	4.052E-20	3.527E-15	1.500E-04
1440.000	3.437E-15	1.099E-18	3.376E-20	3.335E-15	1.500E-04
1460.000	3.250E-15	9.724E-19	2.822E-20	3.156E-15	1.500E-04
1480.000	3.075E-15	8.623E-19	2.365E-20	2.989E-15	1.500E-04
1500.000	2.912E-15	7.660E-19	1.988E-20	2.833E-15	1.500E-04
1520.000	2.760E-15	6.818E-19	1.675E-20	2.686E-15	1.500E-04
1540.000	2.617E-15	6.080E-19	1.415E-20	2.550E-15	1.500E-04
1560.000	2.484E-15	5.431E-19	1.198E-20	2.421E-15	1.500E-04
1580.000	2.359E-15	4.859E-19	1.017E-20	2.301E-15	1.500E-04
1600.000	2.242E-15	4.355E-19	8.657E-21	2.188E-15	1.500E-04
1620.000	2.132E-15	3.909E-19	7.383E-21	2.082E-15	1.500E-04
1640.000	2.029E-15	3.515E-19	6.311E-21	1.982E-15	1.500E-04
1660.000	1.932E-15	3.165E-19	5.406E-21	1.888E-15	1.500E-04
1680.000	1.840E-15	2.854E-19	4.640E-21	1.800E-15	1.500E-04
1700.000	1.754E-15	2.577E-19	3.991E-21	1.717E-15	1.500E-04
1720.000	1.673E-15	2.330E-19	3.439E-21	1.638E-15	1.500E-04
1740.000	1.597E-15	2.110E-19	2.970E-21	1.564E-15	1.500E-04
1760.000	1.525E-15	1.913E-19	2.569E-21	1.495E-15	1.500E-04
1780.000	1.457E-15	1.736E-19	2.226E-21	1.428E-15	1.500E-04
1800.000	1.392E-15	1.578E-19	1.933E-21	1.366E-15	1.500E-04
1820.000	1.332E-15	1.436E-19	1.681E-21	1.307E-15	1.500E-04
1840.000	1.274E-15	1.308E-19	1.464E-21	1.251E-15	1.500E-04
1860.000	1.220E-15	1.193E-19	1.278E-21	1.198E-15	1.500E-04
1880.000	1.168E-15	1.089E-19	1.117E-21	1.148E-15	1.500E-04
1900.000	1.119E-15	9.959E-20	9.775E-22	1.100E-15	1.500E-04
1920.000	1.073E-15	9.113E-20	8.570E-22	1.055E-15	1.500E-04
1940.000	1.029E-15	8.347E-20	7.524E-22	1.012E-15	1.500E-04
1960.000	9.874E-16	7.653E-20	6.616E-22	9.717E-16	1.500E-04
1980.000	9.478E-16	7.024E-20	5.825E-22	9.330E-16	1.500E-04
2000.000	9.102E-16	6.453E-20	5.136E-22	8.962E-16	1.500E-04
INTEGRATED Y	9.702E-11	1.216E-12	2.579E-12	7.428E-11	2.400E-01
TOTAL INT Y	9.125E-08	1.753E-08	5.164E-08	1.778E-07	2.922E-01

```
      PROGRAM VIBRAN(INPUT,OUTPUT,TAPE5=INPUT,TAPE6=OUTPUT)
      DIMENSION TITLE(10),M(3,3),C(3,3),K(3,3)
      DIMENSION WNAT(3),ZETA(3),MU(3),ENGM(3),ENGC(3),ENGK(3)
      DIMENSION WINIT(5),WDELT(5),WFIN(5),FINIT(5),FDELT(5),FFIN(5)
      DIMENSION PSD(3),PSDY(3)
      DIMENSION YINT(3),TOTY(3)
      REAL M,K,MU
      INTEGER SPEC
      READ(5,115)NCASE
      KCASE=0
    5 CALL READIT(TITLE,ENGM,ENGC,ENGK,NRANG,SPEC,WINIT,WFIN,WDELT,FAC)
      CALL WRITIT(TITLE,ENGM,ENGC,ENGK,NRANG,SPEC,WINIT,WFIN,WDELT,FAC)
      CALL MATRX2(M,C,K,ENGM,ENGC,ENGK)
      WRITE(6,195)
      DO 2 I=1,3
      TOTY(I)=0.
    2 WRITE(6,190)(M(I,J),J=1,3),(C(I,J),J=1,3),(K(I,J),J=1,3)
      TOTS=0.
      TOTP=0.
      DO 420 III=1,NRANG
      WRITE(6,90)
      WRITE(6,100)III,WINIT(III),WFIN(III),WDELT(III)
      WRITE(6,110)
      W=WINIT(III)
      DEL=WDELT(III)
      W=W-DEL
      DO 650 J=1,3
  650 YINT(J)=0.
      PSINT=0.
      SCALIN=0.
      DO 400 II=1,1000
      W=W+DEL
      XW=W
      IF(W.GT.WFIN(III)) GO TO 400
C     ALL CALCULATIONS ARE DONE IN RADIANS/SEC
      W=W*2.*3.14159
      CALL CALC(M,C,K,W,PSD)
C     CONVERT ALL FREQUENCIES IN TO HZ BEFORE CALLING FOR SPECS
      F=W/(2.*3.14159)
      GO TO (585,600,610,600,600 ),SPEC
  585 CALL SPEC1(F,SCALE)
      GO TO 645
  600 CALL SPEC2(F,SCALE)
      GO TO 645
  610 CALL SPEC3(F,SCALE)
  645 CONTINUE
      SCALE=SCALE*FAC
      IF(W.NE.0.) PSINCH=SCALE*(386.**2/W**4)
      IF(W.EQ.0.) PSINCH=SCALE*(386.**2/(1.E-15)**4)
      IF(II.EQ.1.OR.XW.GE.(WFIN(III)-.01)) GO TO 200
      PSINT=PSINT+PSINCH
      SCALIN=SCALIN+SCALE
      GO TO 220
  200 PSINT=PSINT+.5*PSINCH
      SCALIN=SCALIN+.5*SCALE
      IF(XW.LT.(WFIN(III)-.01)) GO TO 220
      PSINT=PSINT*WDELT(III)
      SCALIN=SCALIN*WDELT(III)
  220 CONTINUE
      DO 330 J=1,3
      PSDY(J)=SCALE*PSD(J)*386.**2
      IF(II.EQ.1.OR.XW.GE.(WFIN(III)-.01))GO TO 350
      YINT(J)=YINT(J)+PSDY(J)
      GO TO 330
  350 YINT(J)=YINT(J)+.5*PSDY(J)
      IF(XW.GE.(WFIN(III)-.01)) YINT(J)=YINT(J)*WDELT(III)
  330 CONTINUE
C     CONVERT ENGINEERING FREQUENCIES BACK INTO HZ
      W=W/(2.*3.14159)
      WRITE(6,120)W,(PSDY(J),J=1,3),PSINCH,SCALE
  400 IF(II.EQ.1000) WRITE(6,160)(YINT(J),J=1,3),PSINT,SCALIN
      DO 30 J=1,3
   30 TOTY(J)=TOTY(J)+YINT(J)
      TOTP=TOTP+PSINT
      TOTS=TOTS+SCALIN
      WRITE(6,170)(TOTY(J),J=1,3),TOTP,TOTS
  420 CONTINUE
      KCASE=KCASE+1
      IF(KCASE-NCASE)5,425,425
  425 CALL EXIT
   90 FORMAT(1H1,//25X,80(1H*)//)
  100 FORMAT(25X,22HFREQUENCY RANGE NUMBER,I5/
     1       25X,21HCOVERS THE RANGE FROM,F9.2,3X,2HTO,F9.2/
     2       25X,19HIN INCREMENTS OF   ,F7.2/)
  110 FORMAT(25X,80H  FREQUENCY      PSD OF Y1     PSD OF Y2     PSD OF Y3
     1    PSD INPUT    PSD INPUT   /
     2       25X,80H     (HZ)          (IN*IN/HZ)    (IN*IN/HZ)    (IN*IN/HZ)
     3   (IN*IN/HZ)      (G*G/HZ)     /)
  115 FORMAT(I5)
  120 FORMAT(25X,F12.3,4X,5(E10.3,3X))
  160 FORMAT(/25X,12HINTEGRATED Y,4X,5(E10.3,3X))
  170 FORMAT(25X,12HTOTAL INT Y ,4X,5(E10.3,3X))
  195 FORMAT(///5X,10HMATRIX M  ,36X,10HMATRIX C  ,36X,10HMATRIX K   )
  190 FORMAT(5X,3(E10.3,3X),7X,3(E10.3,3X),7X,3(E10.3,3X))
      END
```

```
      SUBROUTINE READIT(TITLE,ENGM,ENGC,ENGK,NRANG,SPEC,WINIT,WFIN,WDELT
     1,FAC               )
      INTEGER SPEC
      DIMENSION ENGM(3),ENGC(3),ENGK(3),WINIT(5),WFIN(5),WDELT(5)
      DIMENSION TITLE(8)
      READ(5,115)(TITLE(I),I=1,8)
      READ(5,100)FAC
      DO 10 I=1,3
   10 READ(5,100)ENGM(I),ENGC(I),ENGK(I)
      READ(5,110)NRANG,SPEC
      DO 20 I=1,NRANG
   20 READ(5,100)WINIT(I),WFIN(I),WDELT(I)
  100 FORMAT(8E10.3)
  110 FORMAT(5I5)
  115 FORMAT(8A10)
      RETURN
      END
      SUBROUTINE WRITIT(TITLE,ENGM,ENGC,ENGK,NRANG,SPEC,WINIT,WFIN,WDELT
     1,FAC               )
      INTEGER SPEC
      DIMENSION ENGM(3),ENGC(3),ENGK(3),WINIT(5),WFIN(5),WDELT(5)
      DIMENSION TITLE(8)
      I=3
      WRITE(6,100)(TITLE(I),I=1,8)
      WRITE(6,105)FAC
      WRITE(6,110)SPEC
      WRITE(6,120)
      WRITE(6,130)
      DO 10 J=1,I
   10 WRITE(6,140)J,ENGM(J),ENGC(J),ENGK(J)
      WRITE(6,150)NRANG
      WRITE(6,160)
      DO 20 I=1,NRANG
   20 WRITE(6,170)I,WINIT(I),WFIN(I),WDELT(I)
      RETURN
  100 FORMAT(1H1//30X,8A10//)
  105 FORMAT(40X,27HMULTIPLIER FOR INPUT PSD = ,E10.3 /)
  110 FORMAT(40X,60HINPUT VIBRATION POWER SPECTRAL DENSITY SPECIFICATION
     1 CODE IS,I5,1H./)
  120 FORMAT(40X,65HROTOR BEARING SYSTEM PROPERTIES ARE SPECIFIED BY THE
     1 FOLLOWING   /40X,   15HSETS OF VALUES /)
  130 FORMAT(45X,50H MASS          WEIGHT          DAMPING          SPRING  /
     1       45X,50HSPRING       OF MASS        (LBS*SEC       STIFFNESS /
     2       45X,50H  NO          (LBS)          PER INCH)      (LBS/INCH))
  140 FORMAT(45X,I5,2(5X,F10.3),5X,E10.3)
  150 FORMAT(//40X,   13HTHE FOLLOWING,I5,30H FREQUENCY RANGES WILL BE R
     1UN /)
  160 FORMAT(45X,50HRANGE         INITIAL          FINAL          FREQUENCY/
     1       45X,50H  NO        FREQUENCY       FREQUENCY       INCREMENT)
  170 FORMAT(45X,I5,2(5X,F10.2),5X,F10.3)
      END
      SUBROUTINE SPEC1(F,SCALE)
C
C     SNAP8 SPEC
C     NASA LEWIS SPEC 417-2,REV C, 1JUNE69
C     PARAGRAPH 3.5.1.2.2
C     EGS SYSTEM (OPERATING)
C
      IF(F .GT. 100. .AND. F .LT. 2000.) GO TO 5090
      IF(F .GT.2000. .OR. F.LT. 19.) GO TO 5110
      FX=F
      F2=100.
      PSD2=.015
      R=3.
      SCALE=PSD2*(FX/F2)**(R/3.)
      RETURN
 5090 SCALE=.015
      RETURN
 5110 SCALE=0.
      RETURN
      END
      SUBROUTINE SPEC2(F,SCALE)
      SCALE=(2.*3.14159*F)**4/386.**2
      RETURN
      END
      SUBROUTINE SPEC3(F,SCALE)
      SCALE=.01
      RETURN
      END
```

```
      SUBROUTINE MINV(A,N,D,L,M)
C     INVERT A MATRIX
C
C     USAGE
C     CALL MINV(A,N,D,L,M)
C
C     DESCRIPTION OF PARAMETERS
C     A - INPUT MATRIX, DISTROYED IN COMPUTATION AND REPLACED BY
C     RESULTANT INVERSE.
C     N - ORDER OF MATRIX A
C     D - RESULTANT DETERMINANT
C     L - WORK VECTOR OF LENGTH N
C     M - WORK VECTOR OF LENGTH N
C
C     REMARKS
C     MATRIX A MUST BE A GENERAL MATRIX
C
C     METHOD
C     THE STANDARD GAUSS-JORDAN METHOD IS USED. THE DETERMINANT
C     IS ALSO CALCULATED. A DETERMINANT OF ZERO INDICATES THAT
C     THE MATRIX IS SINGULAR.
C
      DIMENSION A(3,1),L(1),M(1)
      COMPLEX A,BIGA,HOLD,D
C     SEARCH FOR LARGEST ELEMENT
      D=1.0
      NK=-N
      DO 80 K=1,N
      NK=NK+N
      L(K)=K
      M(K)=K
      KK=NK+K
      BIGA=A(KK)
      DO 20 J=K,N
      IZ=N*(J-1)
      DO 20 I=K,N
      IJ=IZ+I
   10 IF(CABS(BIGA)-CABS(A(IJ))) 15,20,20
   15 BIGA=A(IJ)
      L(K)=I
      M(K)=J
   20 CONTINUE
C     INTERCHANGE ROWS
      J=L(K)
      IF(J-K) 35,35,25
   25 KI=K-N
      DO 30 I=1,N
      KI=KI+N
      HOLD=-A(KI)
      JI=KI-K+J
      A(KI)=A(JI)
   30 A(JI) =HOLD
```

```
C       INTERCHANGE COLUMNS
   35   I=M(K)
        IF(I-K) 45,45,38
   38   JP=N*(I-1)
        DO 40 J=1,N
        JK=NK+J
        JI=JP+J
        HOLD=-A(JK)
        A(JK)=A(JI)
   40   A(JI) =HOLD
C       DIVIDE COLUMN BY MINUS PIVOT (VALUE OF PIVOT ELEMENT IS
C       CONTAINED IN BIGA)
   45   IF(CABS(BIGA)) 48,46,48
   46   D=0.0
        RETURN
   48   DO 55 I=1,N
        IF(I-K) 50,55,50
   50   IK=NK+I
        A(IK)=A(IK)/(-BIGA)
   55   CONTINUE
C       REDUCE MATRIX
        DO 65 I=1,N
        IK=NK+I
        HOLD=A(IK)
        IJ=I-N
        DO 65 J=1,N
        IJ=IJ+N
        IF(I-K) 60,65,60
   60   IF(J-K) 62,65,62
   62   KJ=IJ-I+K
        A(IJ)=HOLD*A(KJ)+A(IJ)
   65   CONTINUE
C       DIVIDE ROW BY PIVOT
        KJ=K-N
        DO 75 J=1,N
        KJ=KJ+N
        IF(J-K) 70,75,70
   70   A(KJ)=A(KJ)/BIGA
   75   CONTINUE
C       PRODUCT OF PIVOJS
        D=D*BIGA
C       REPLACE PIVOT BY RECIPROCAL
        A(KK)=1.0/BIGA
   80   CONTINUE
C       FINAL ROW AND COLUMN INTERCHANGE
        K=N
  100   K=(K-1)
        IF(K) 150,150,105
  105   I=L(K)
        IF(I-K) 120,120,108
  108   JQ=N*(K-1)
        JR=N*(I-1)
        DO 110 J=1,N
        JK=JQ+J
        HOLD=A(JK)
        JI=JR+J
        A(JK)=-A(JI)
  110   A(JI) =HOLD
  120   J=M(K)
        IF(J-K) 100,100,125
  125   KI=K-N
        DO 130 I=1,N
        KI=KI+N
        HOLD=A(KI)
        JI=KI-K+J
        A(KI)=-A(JI)
  130   A(JI) =HOLD
        GO TO 100
  150   RETURN
        END
```

```
      SUBROUTINE MATRX2(M,C,K,ENGM,ENGC,ENGK)
      DIMENSION M(3,3),C(3,3),K(3,3),D(3),W(3),ZETA(3),MU(3)
      DIMENSION ENGM(3),ENGC(3),ENGK(3)
      REAL M,K,MU
      DATA N/3/
      DO 1090 I=1,N
      W(I)=SQRT(ENGK(I)/(ENGM(I)/386.))
      ZETA(I)=.5*(ENGC(I)/(SQRT(ENGK(I)*ENGM(I)/386.)))
 1090 CONTINUE
      DO 1135 I=1,N
      DO 1135 J=1,N
      M(I,J)=0.
      IF(I.EQ.J) M(I,J)=1.
 1135 CONTINUE
      MU(1)=1.
      MU(2)=ENGM(2)/ENGM(1)
      MU(3)=ENGM(3)/ENGM(2)
      C(1,1)=ZETA(1)*W(1)
      C(1,2)=-ZETA(2)*W(2)*MU(2)
      C(1,3)=0.
      C(2,1)=-ZETA(1)*W(1)
      C(2,2)=(1.+MU(2))*ZETA(2)*W(2)
      C(2,3)=-ZETA(3)*W(3)*MU(3)
      C(3,1)=0.0
      C(3,2)=-ZETA(2)*W(2)
      C(3,3)=(1.+MU(3))*ZETA(3)*W(3)
      K(1,1)=W(1)**2
      K(1,2)=-W(2)**2*MU(2)
      K(1,3)=0.
      K(2,1)=-W(1)**2
      K(2,2)=W(2)**2*(1.+MU(2))
      K(2,3)=-W(3)**2*MU(3)
      K(3,1)=0.0
      K(3,2)=-W(2)**2
      K(3,3)=W(3)**2*(1.+MU(3))
      RETURN
      END
      SUBROUTINE CALC(M,C,K,W,PSD)
      DIMENSION M(3,3),C(3,3),K(3,3),PSD(3),Z(3,3),H(3,3),DUMY1(3),
     1          DUMY2(3)
      COMPLEX EYE,Z,DUMY1,DUMY2,H,DETZ
      REAL M,K
      DATA N/3/
      EYE=CMPLX(0.,1.)
      DO 60 J=1,N
      DO 60 I=1,N
   60 Z(I,J)=(-W*W*M(I,J)+K(I,J))+EYE*W*C(I,J)
      CALL MINV(Z,N,DETZ,DUMY1,DUMY2)
      DO 110 I=1,N
      DO 110 J=1,N
      H(I,J)=Z(I,J)
      PSD(I)=(CABS(H(I,1)))**2
  110 CONTINUE
      RETURN
      END
```

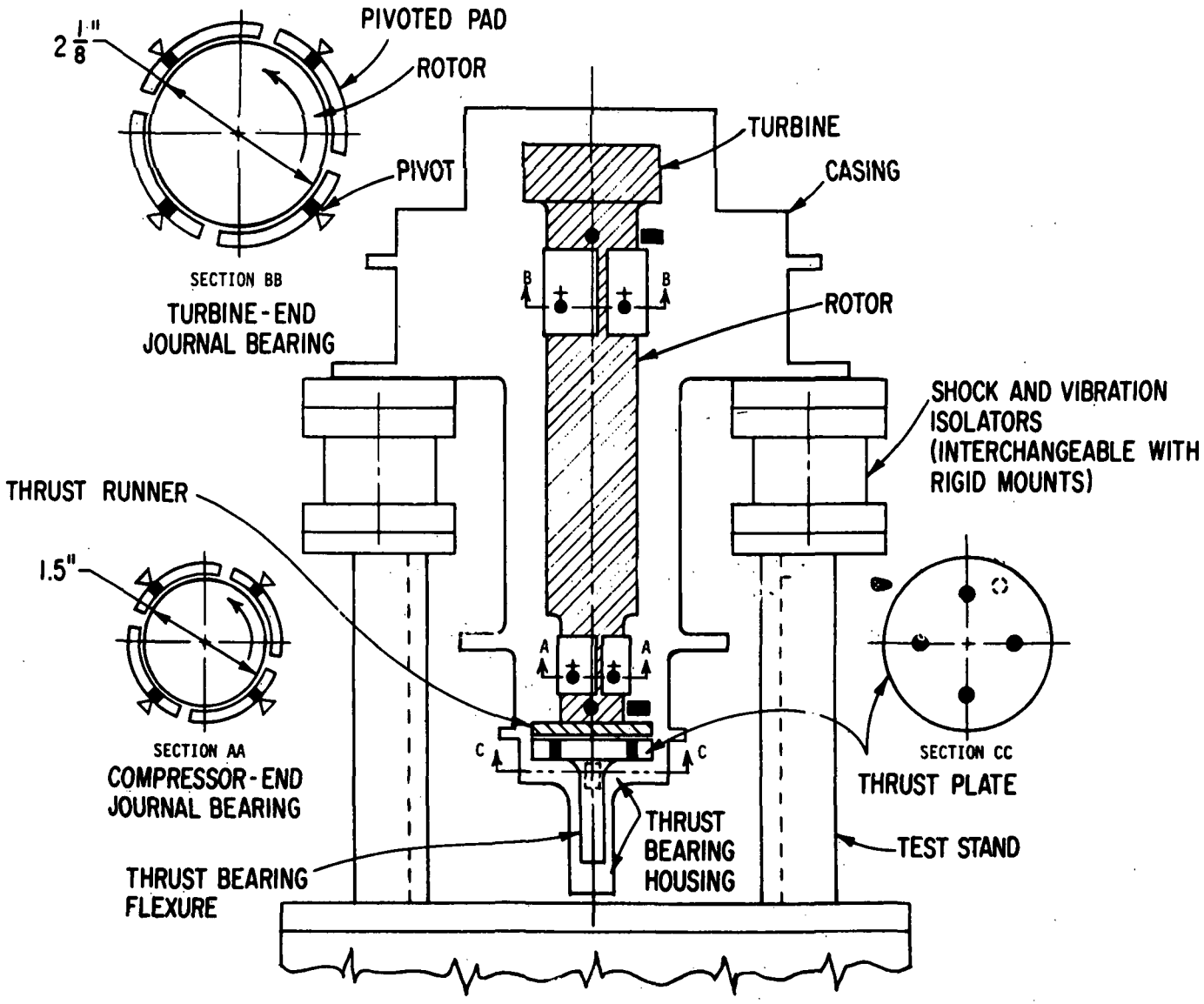

Fig. 1 Schematic of Turbocompressor Simulator Mounted On Test Stand (Vertical Orientation)

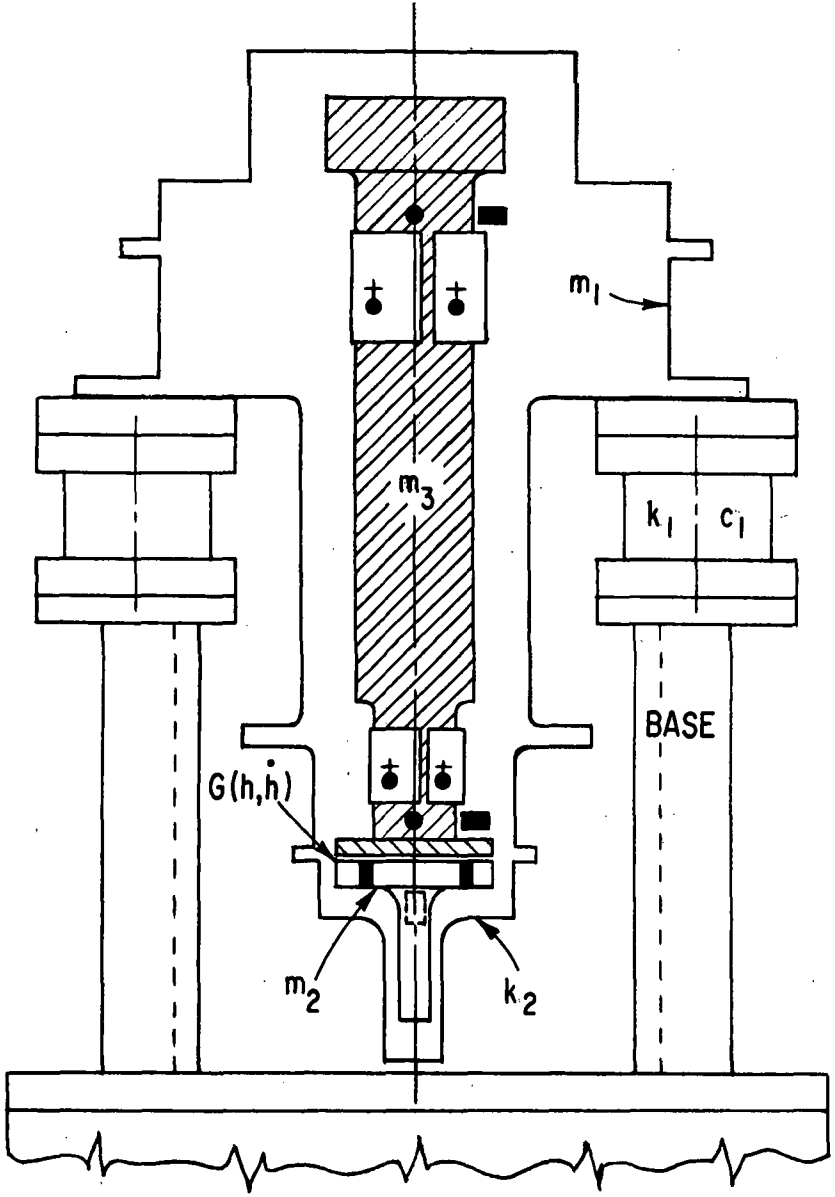

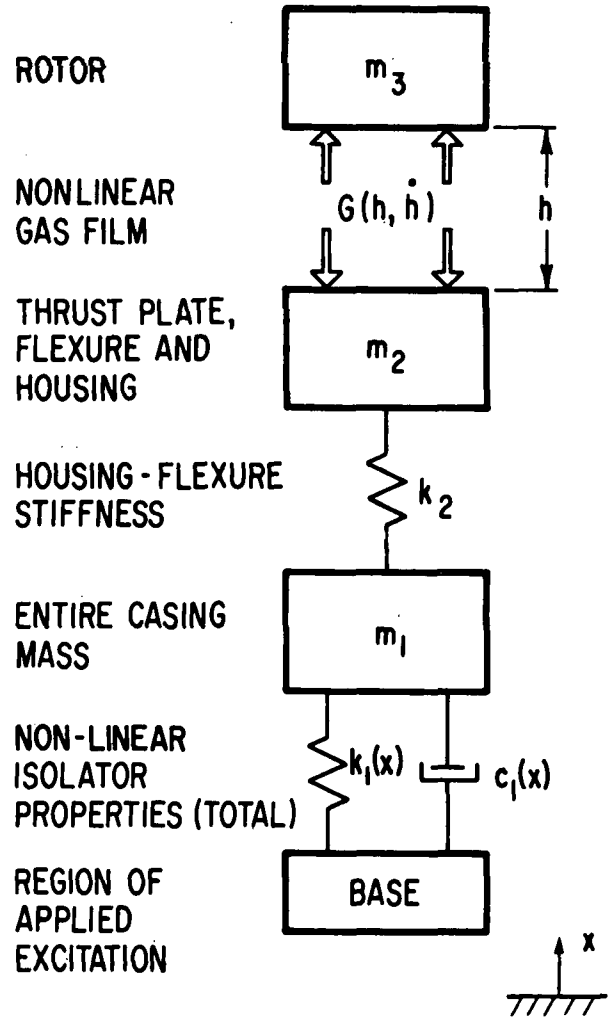

Fig. 2 Three-Degree-of-Freedom Nonlinear Axial Response Model of Simulator On Shock and Vibration Isolators

MPI-12281

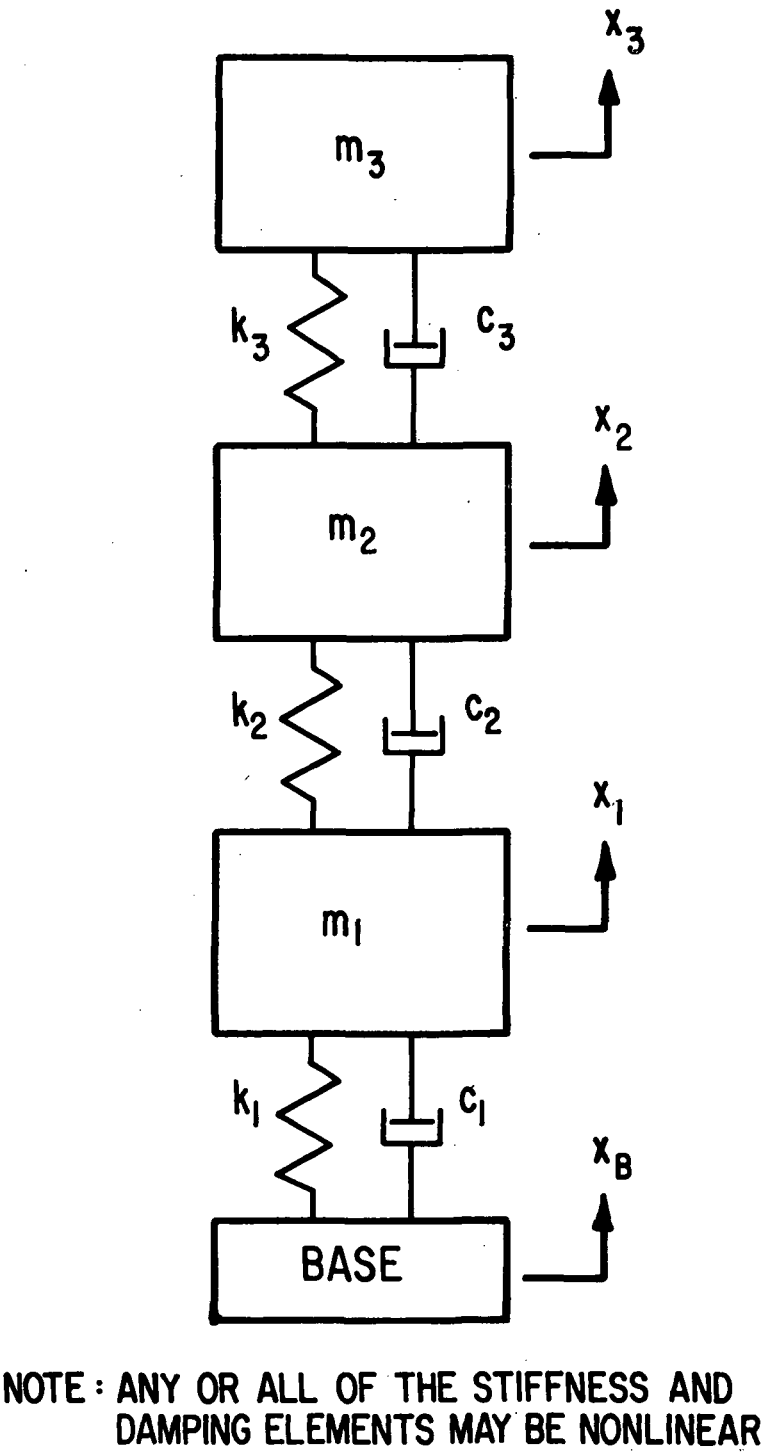

Fig. 3 Lumped-Mass Model Used for Nonlinear-Element Computer Program

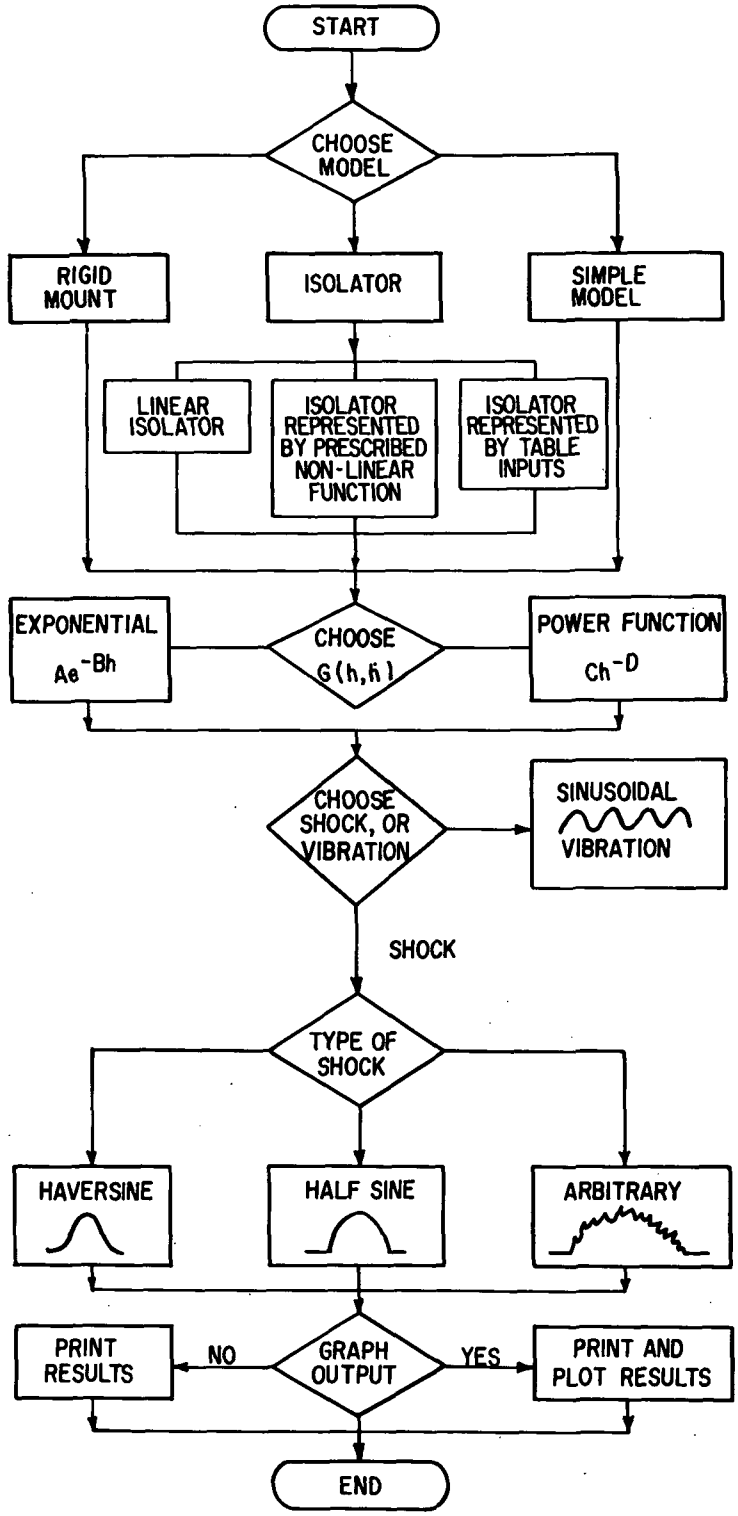

Fig. 4 General Flowchart of Axial Shock and Vibration Response Computer Program

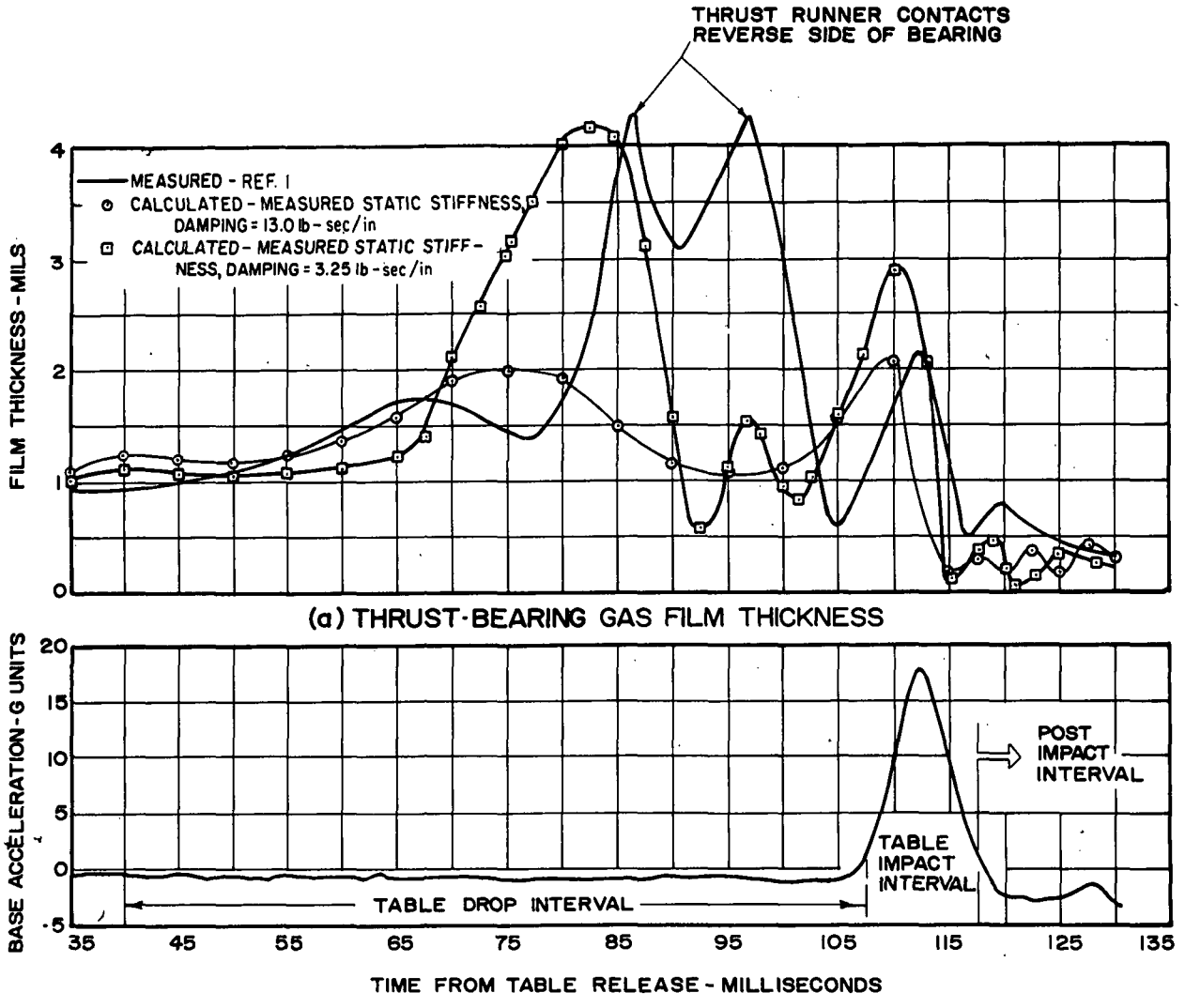

Fig. 5 Measured and Calculated Axial Shock Response For Turbocompressor Simulator

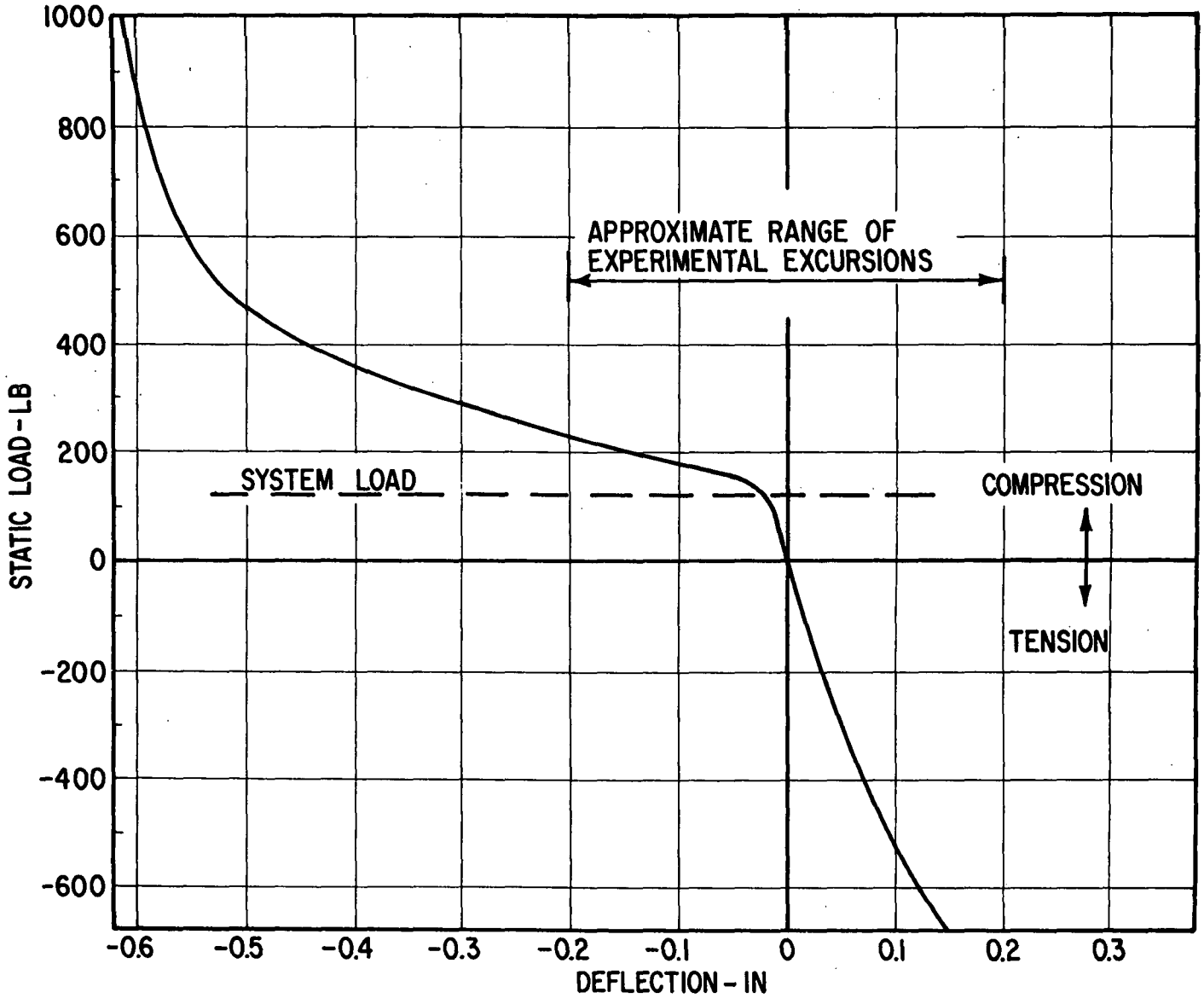

Fig. 6 Static Load-Deflection Curve Of The Nonlinear Isolator

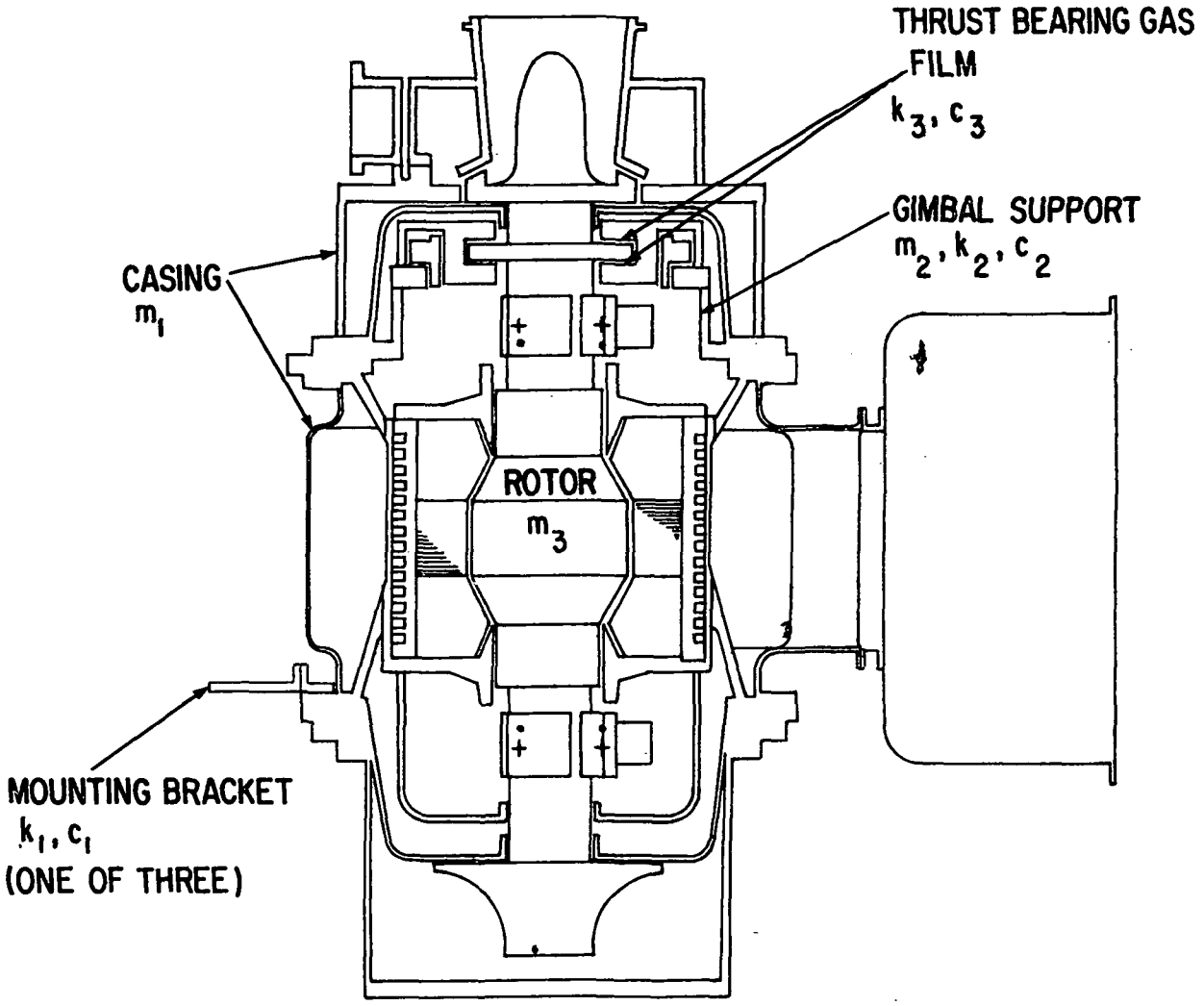

Fig. 7 Schematic of Brayton Rotating Unit With Mass, Spring And Damper Designations

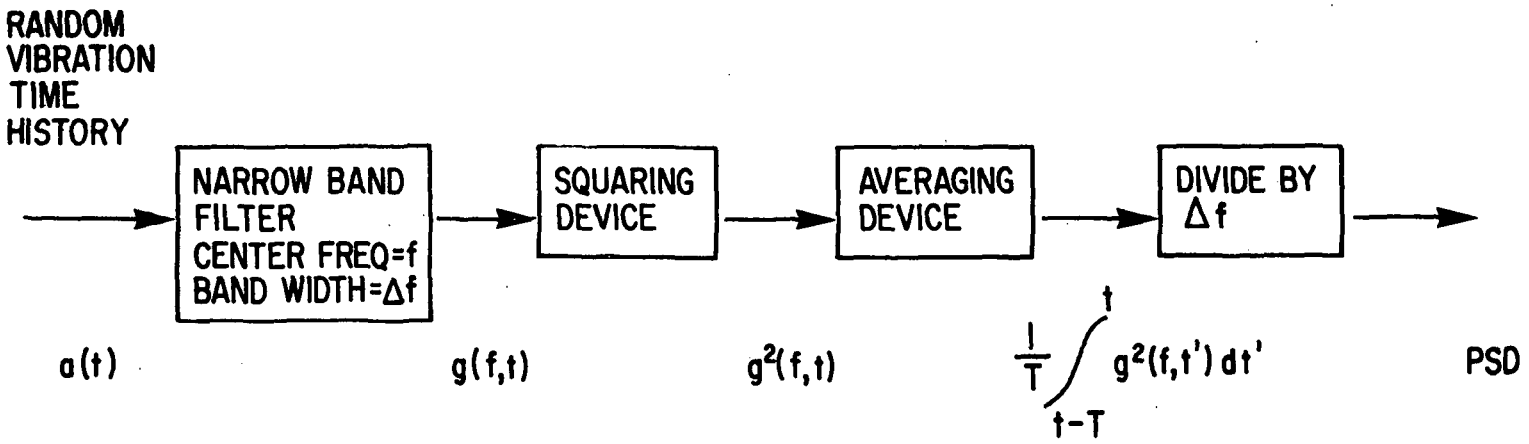

Fig. 8 Schematic Concept of Power Spectral Density (PSD)

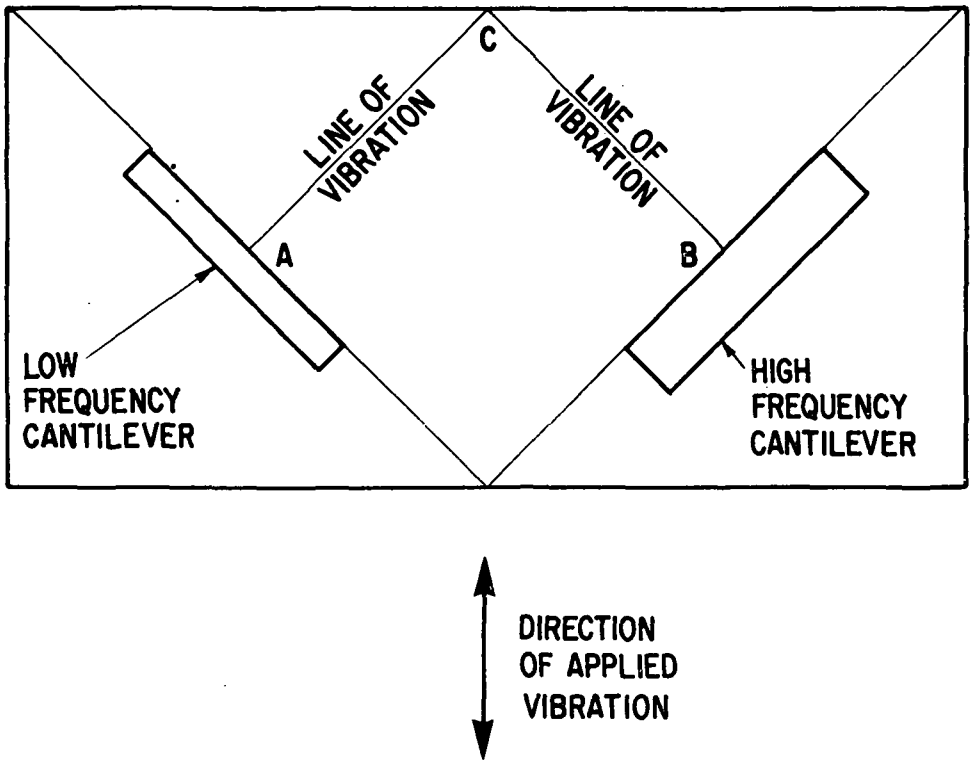

Fig. 9 Model for Demonstration Of Potentially Different Responses Due to Sinusoidal and Random Vibration

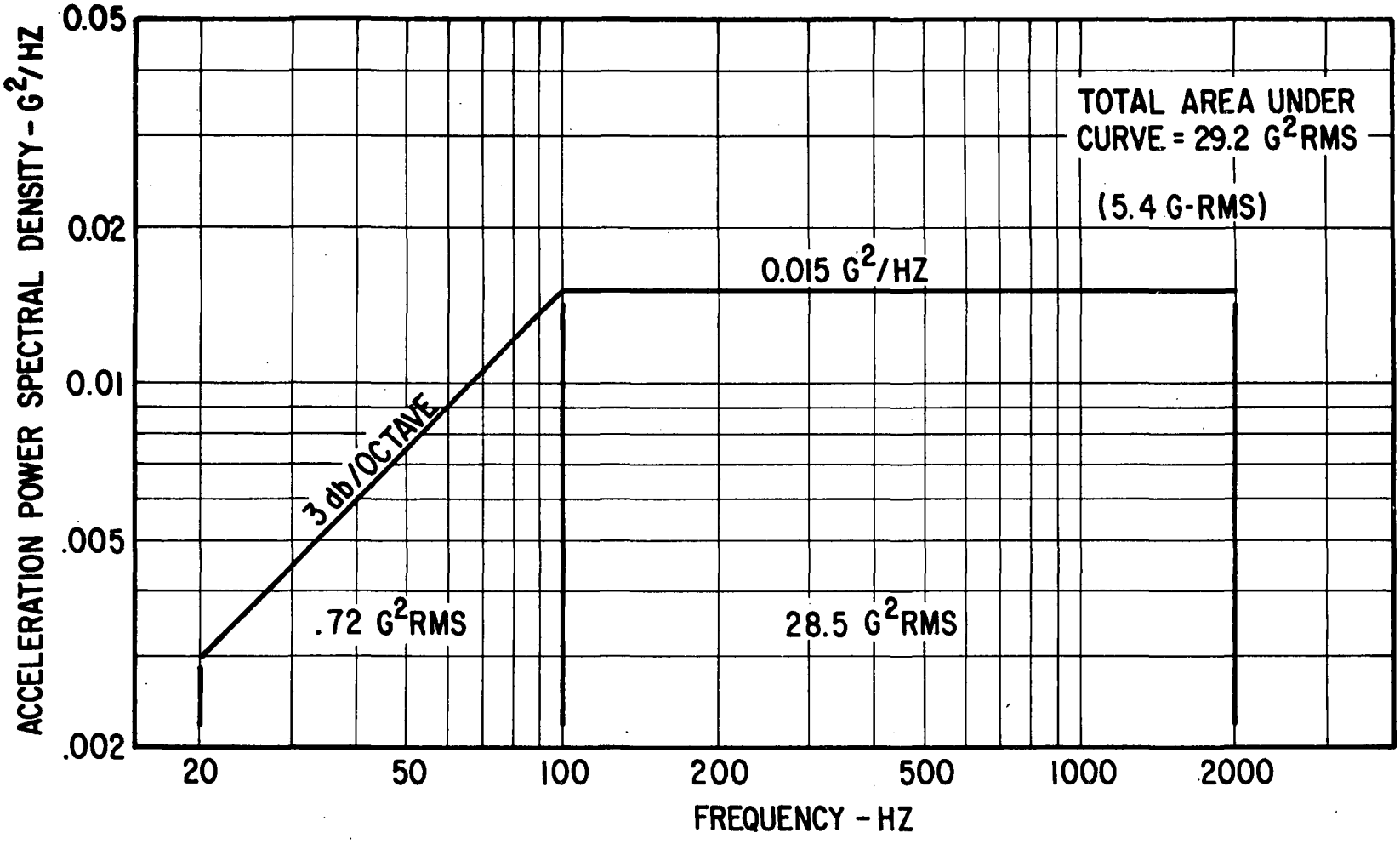

Fig. 10 Random Vibration Power Spectral Density Test Specification 417-2 (Rev. C) For Electrical Generating System Components (Operating) During Space Flight Operation

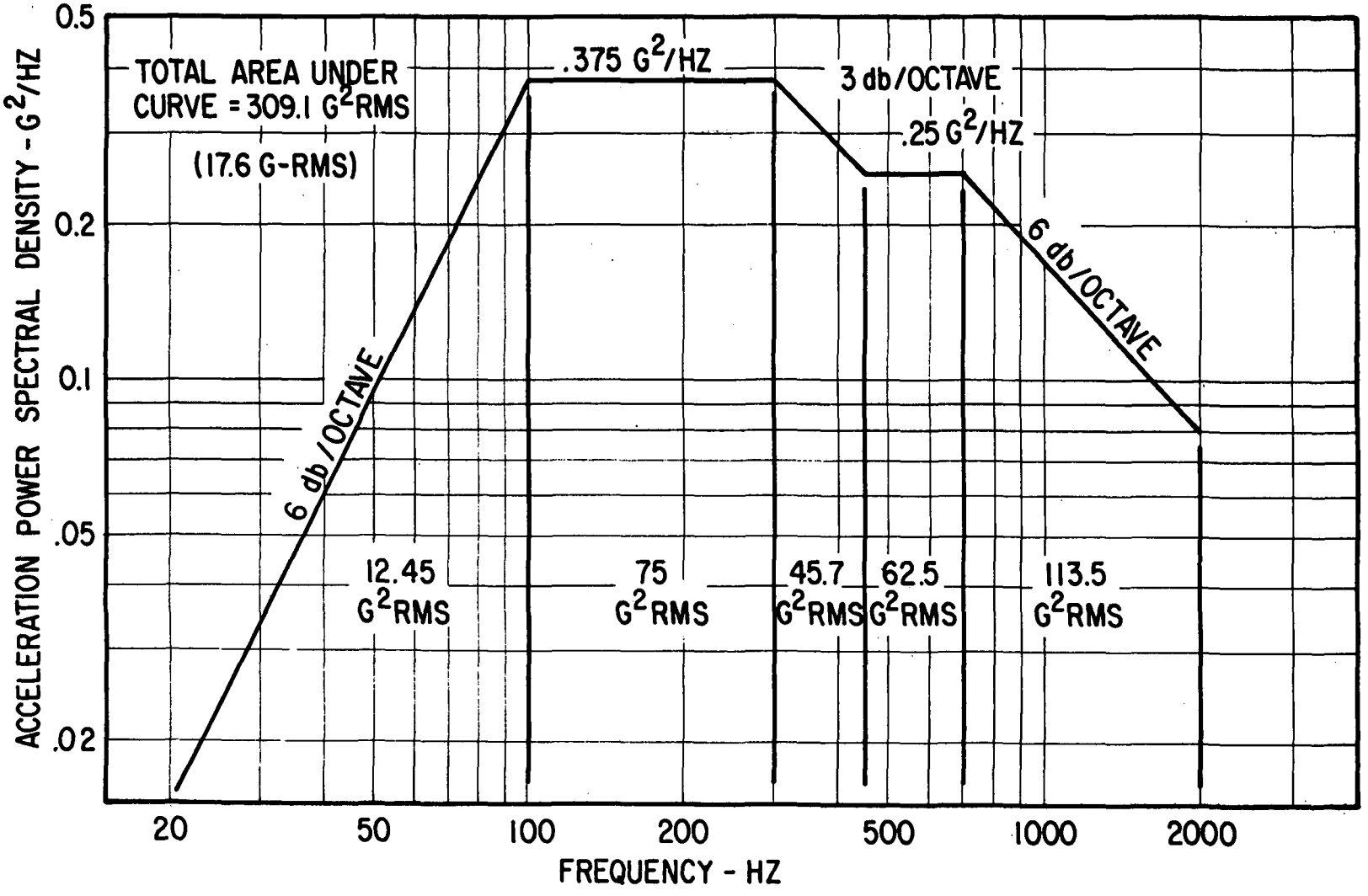

Fig. 11 Random Vibration Power Spectral Density Test Specification 417-2 (Rev. C) For Electrical Generating Systems (Nonoperating) During Launch

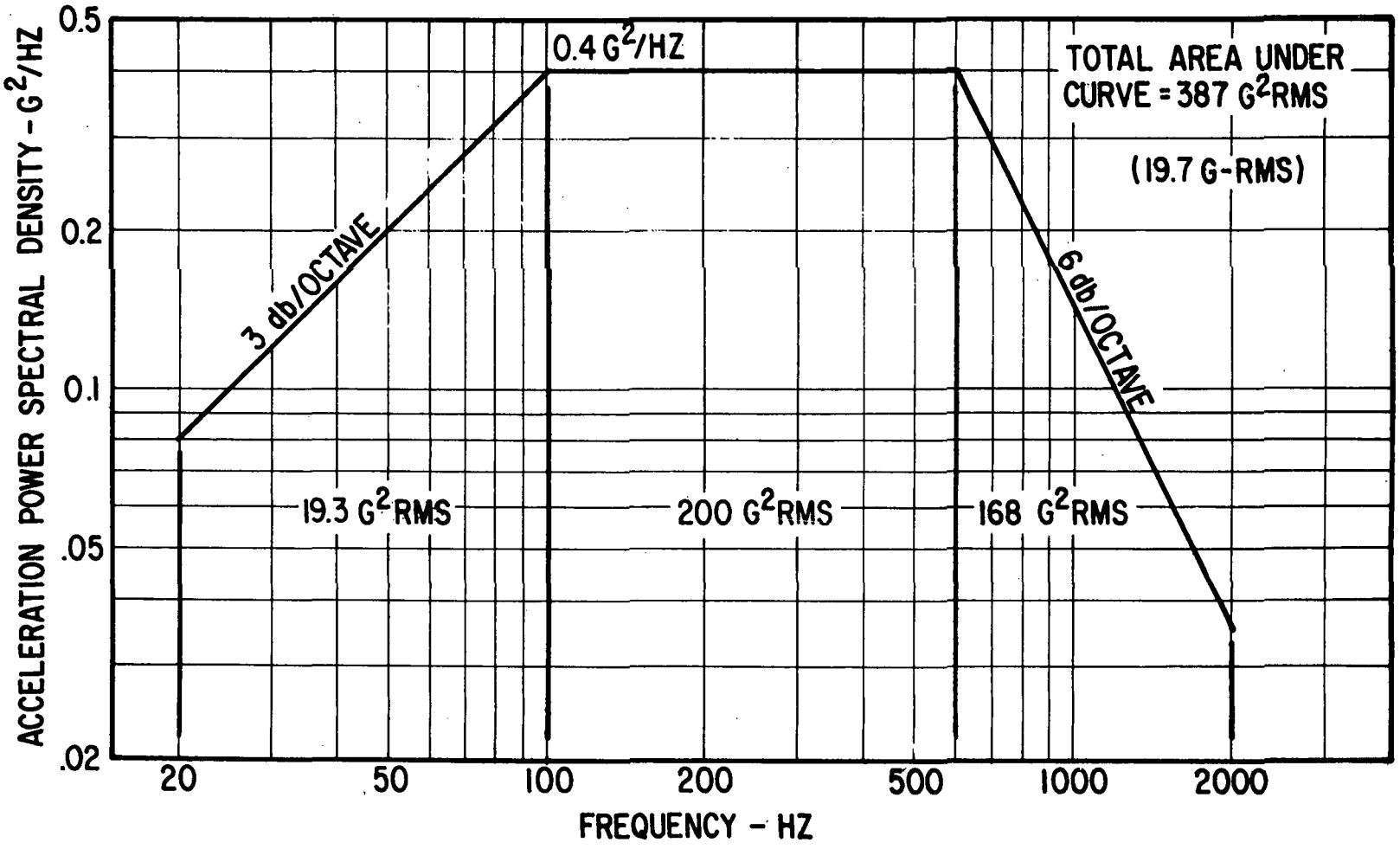

Fig. 12 Random Vibration Power Spectral Density Test Specification 417-2 (Rev. C) For Electrical Generating System Components (Nonoperating) During Launch

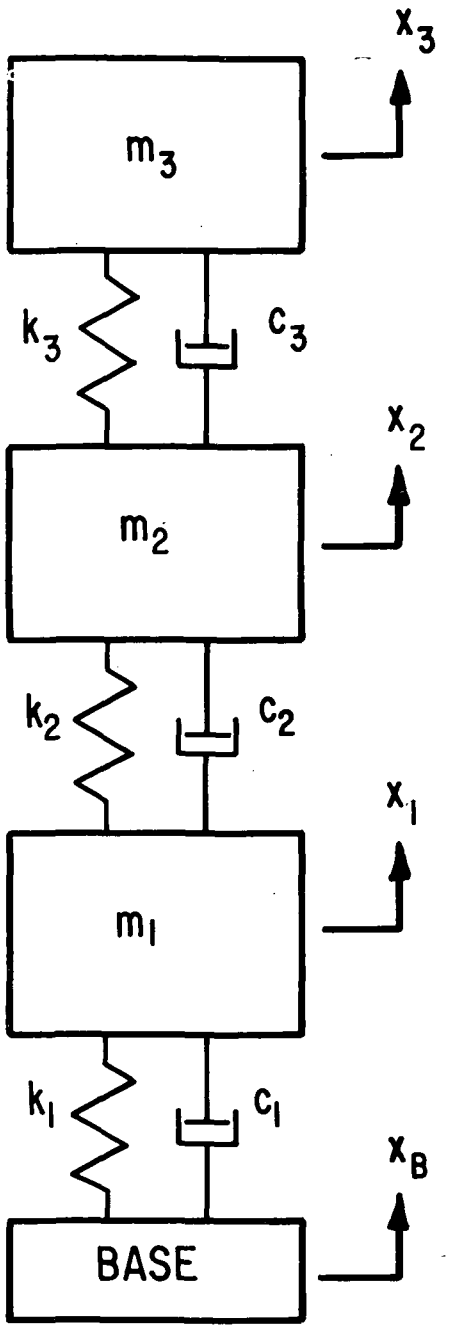

Fig. 13 Lumped-Mass Model Used For Calculation of Axial Vibration Response of BRU Rotor Bearing System to Specified Random Base Excitation

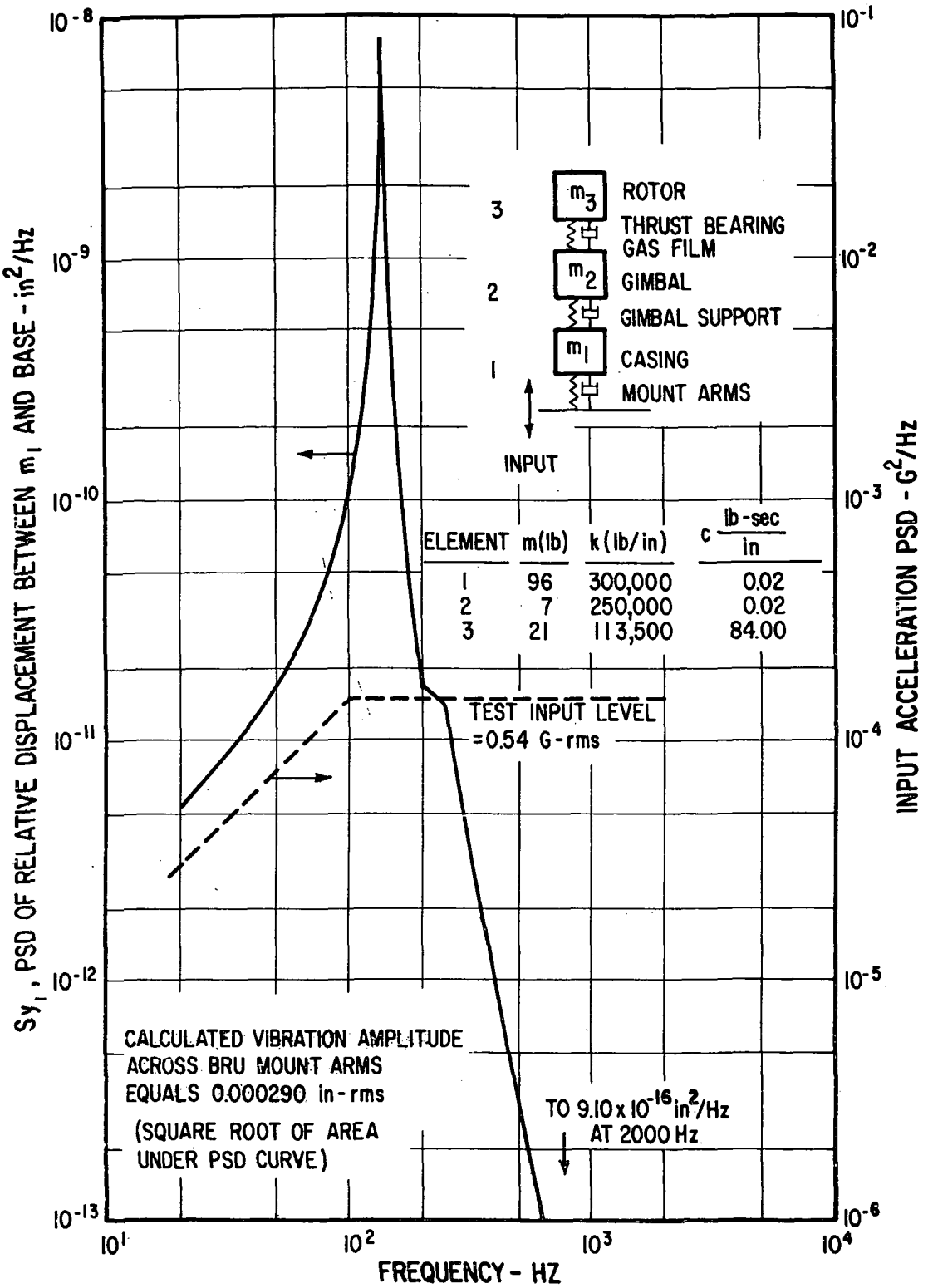

Fig. 14 Calculated Power Spectral Density of the Relative Displacement Between m_1 and Base

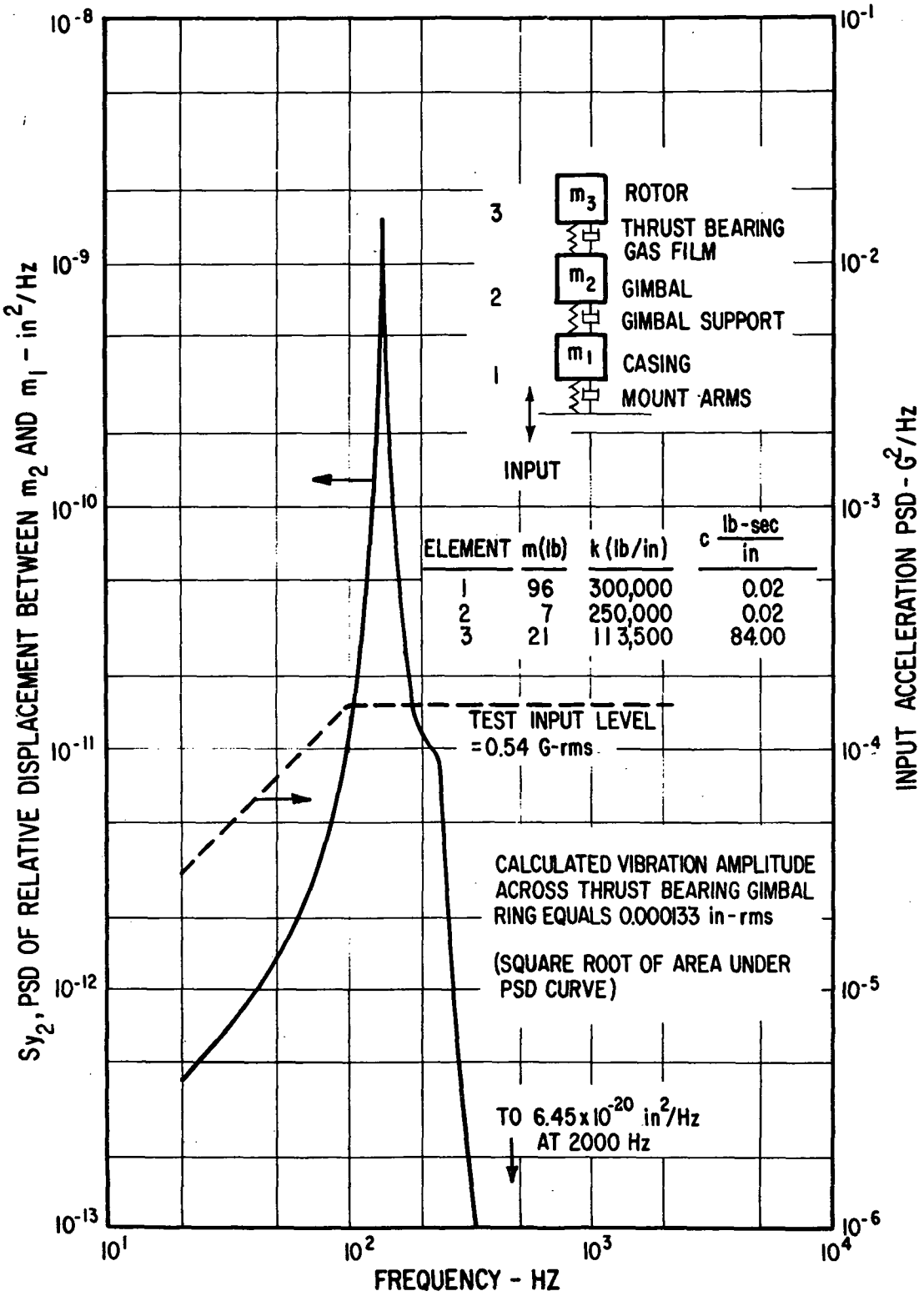

Fig. 15 Calculated Power Spectral Density of the Relative Displacement Between m_2 and m_1

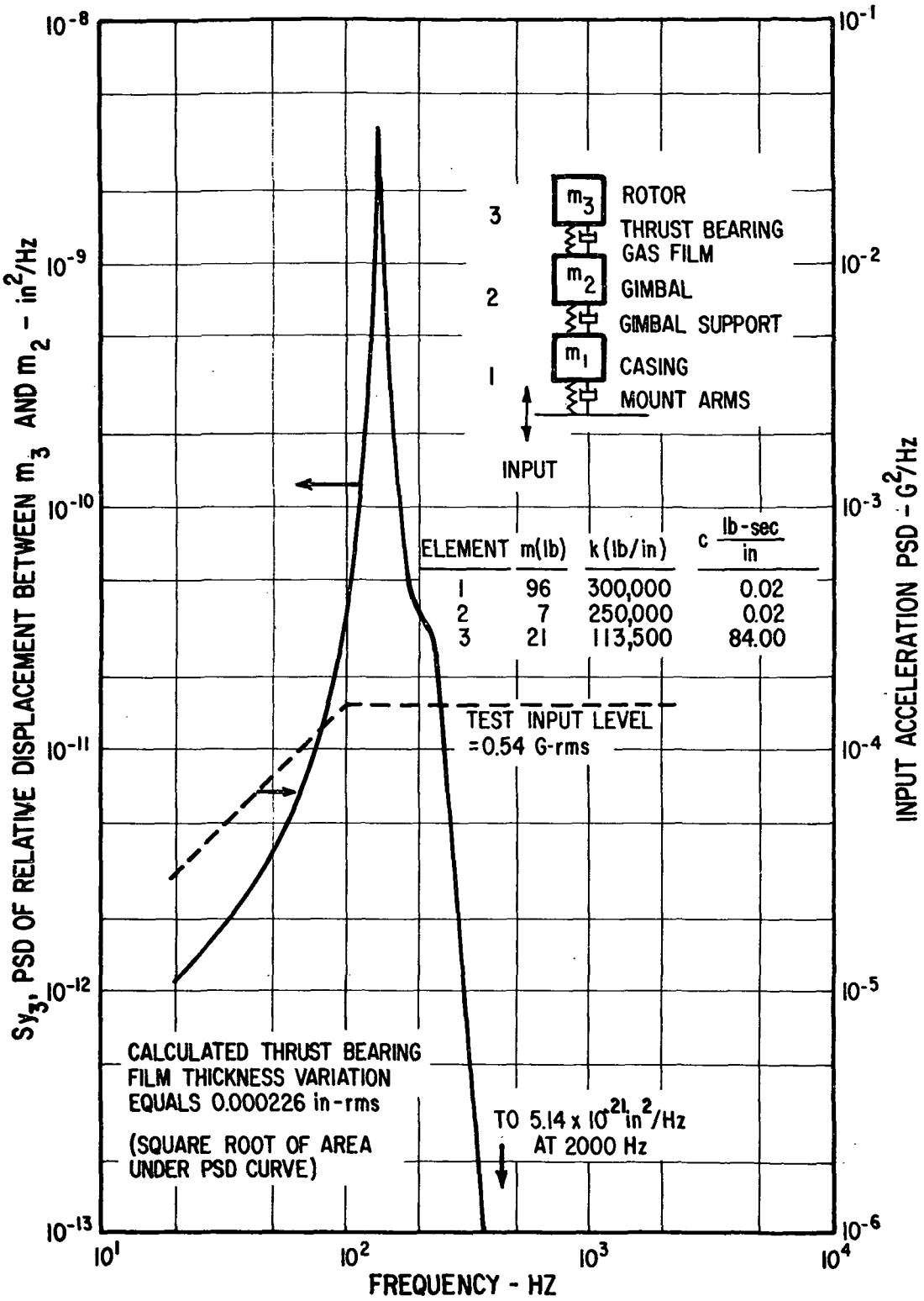

Fig. 16 Calculated Power Spectral Density of the Relative Displacement Between m_3 and m_2

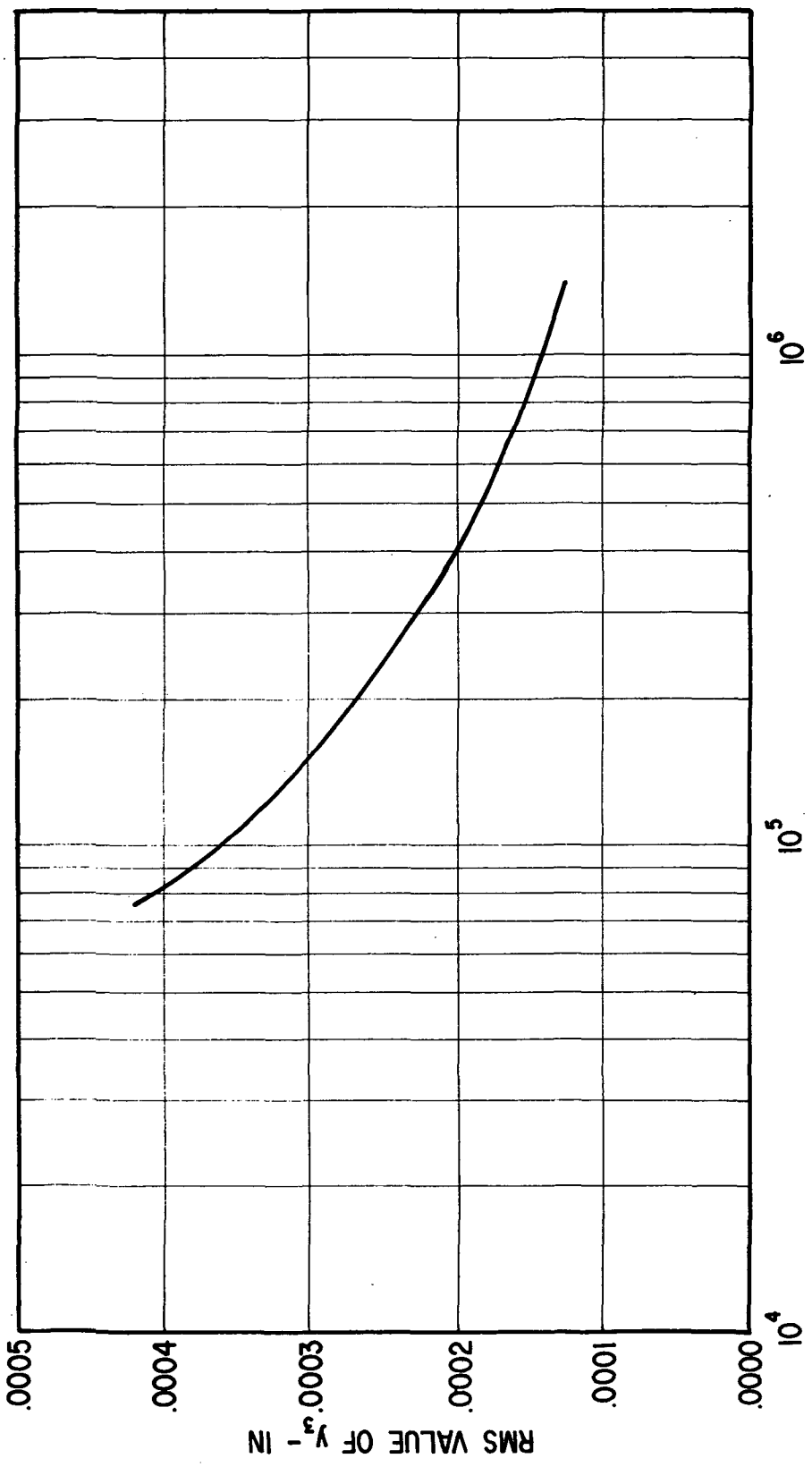

Fig. 17 Variation of RMS Value of y_3 With Mounting Bracket Stiffness k_1 For Nominal Values of System Properties Given in Table I

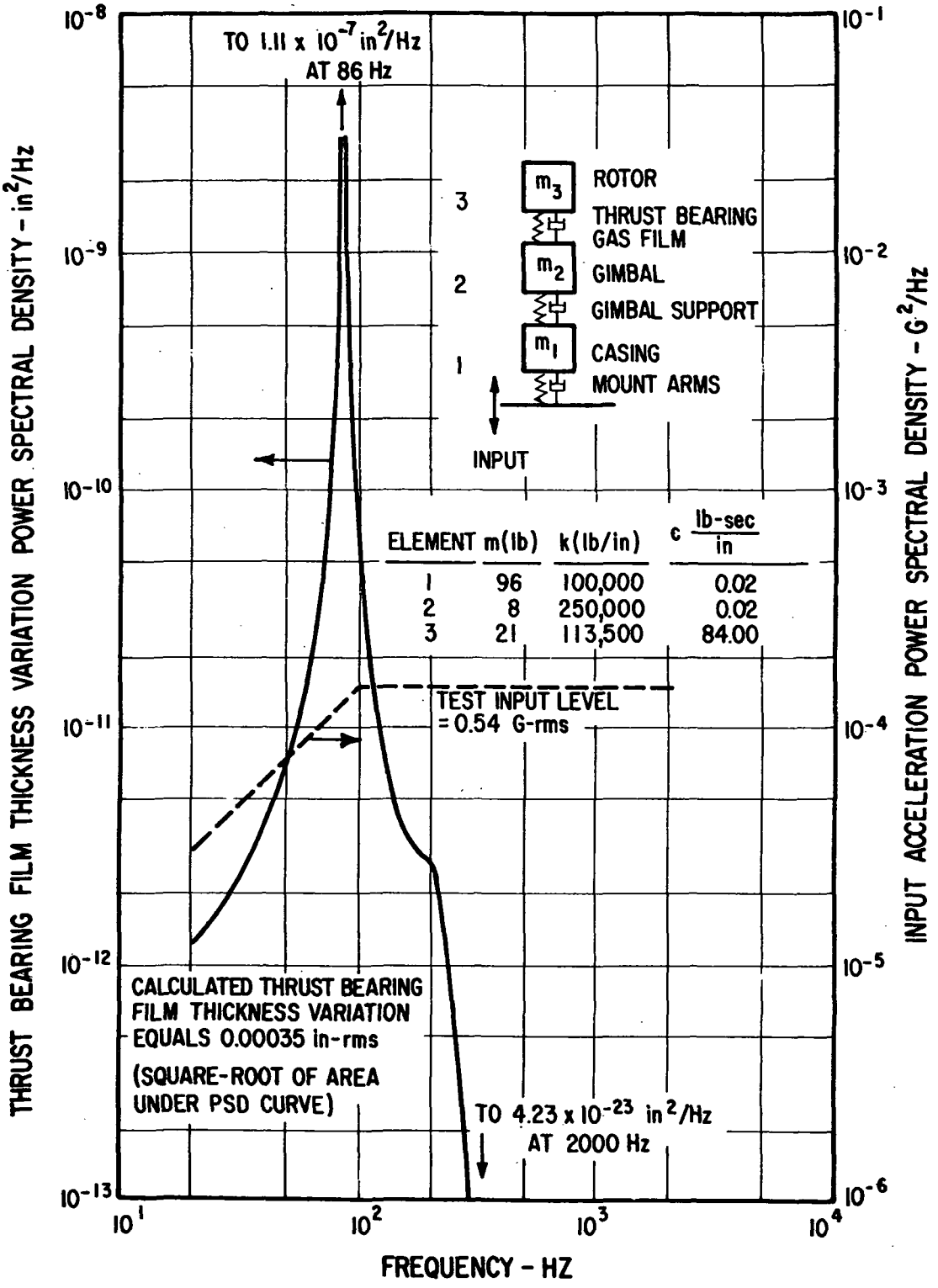

Fig. 18 Calculated Brayton Rotating Unit Thrust Bearing Film Thickness Variation Power Spectral Density and Equivalent RMS Value for One Axial Random Vibration BRU Test Condition

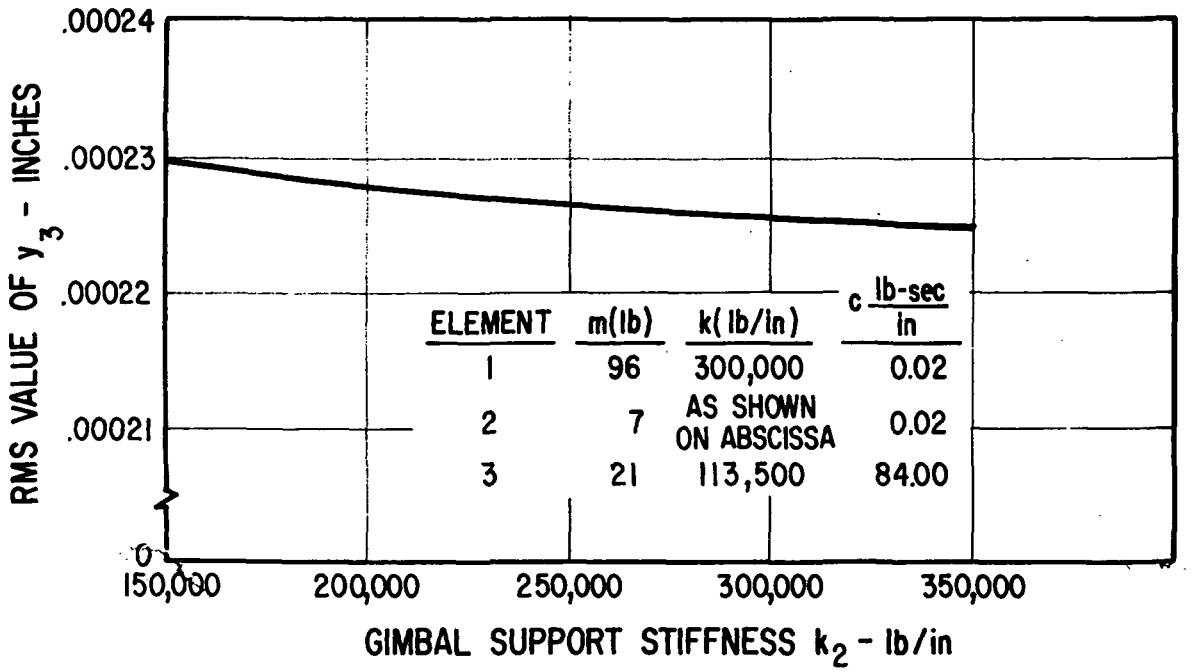

Fig. 19 RMS Value Of The Thrust Bearing Gas Film Thickness Variation Versus Gimbal Support Stiffness

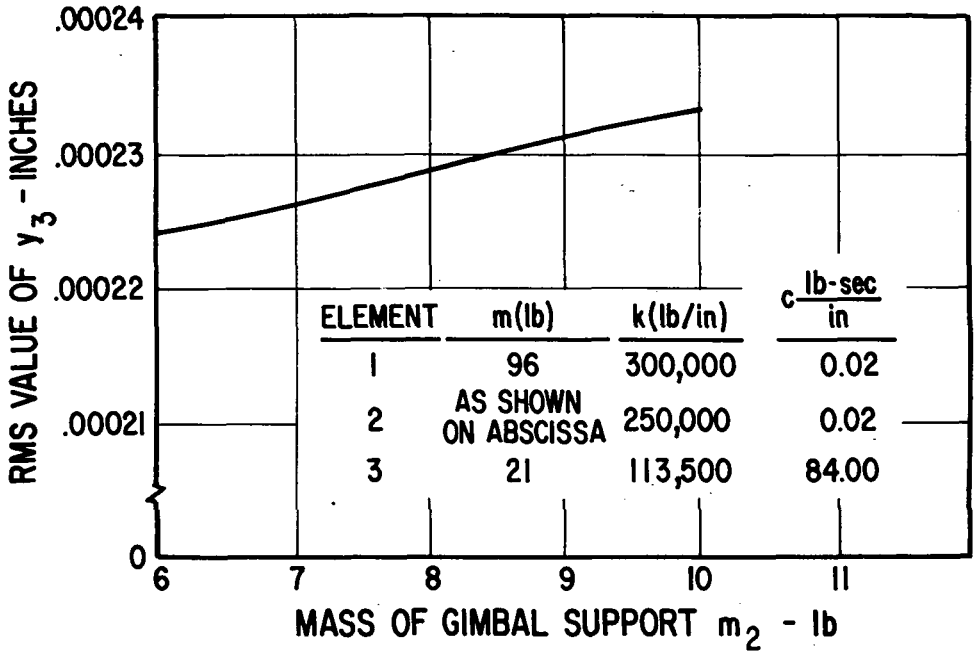

Fig. 20 RMS Value Of The Thrust Bearing Gas Film Thickness Variation Versus Mass of Gimbal Support

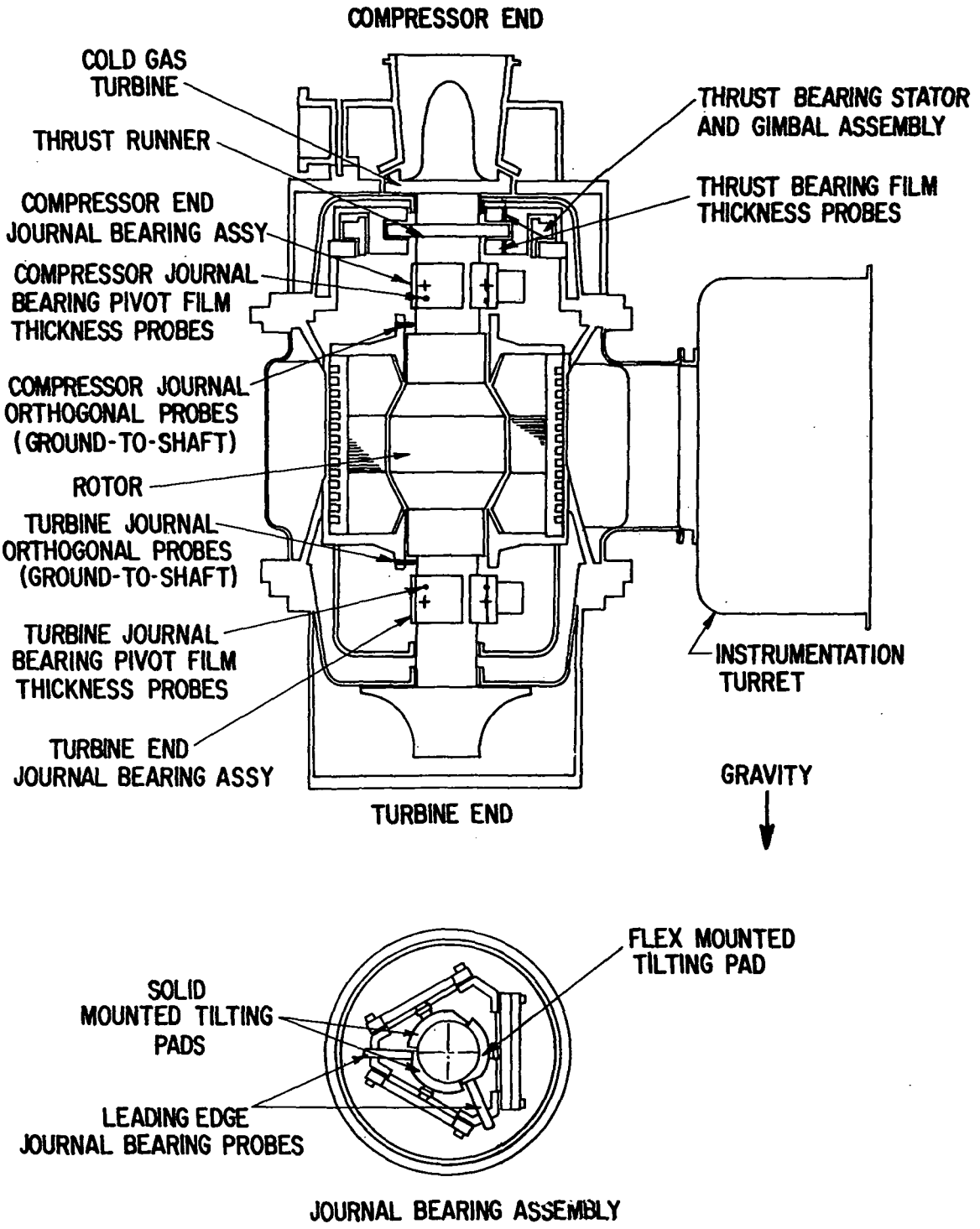

Fig. 21 Schematic of BRU Simulator

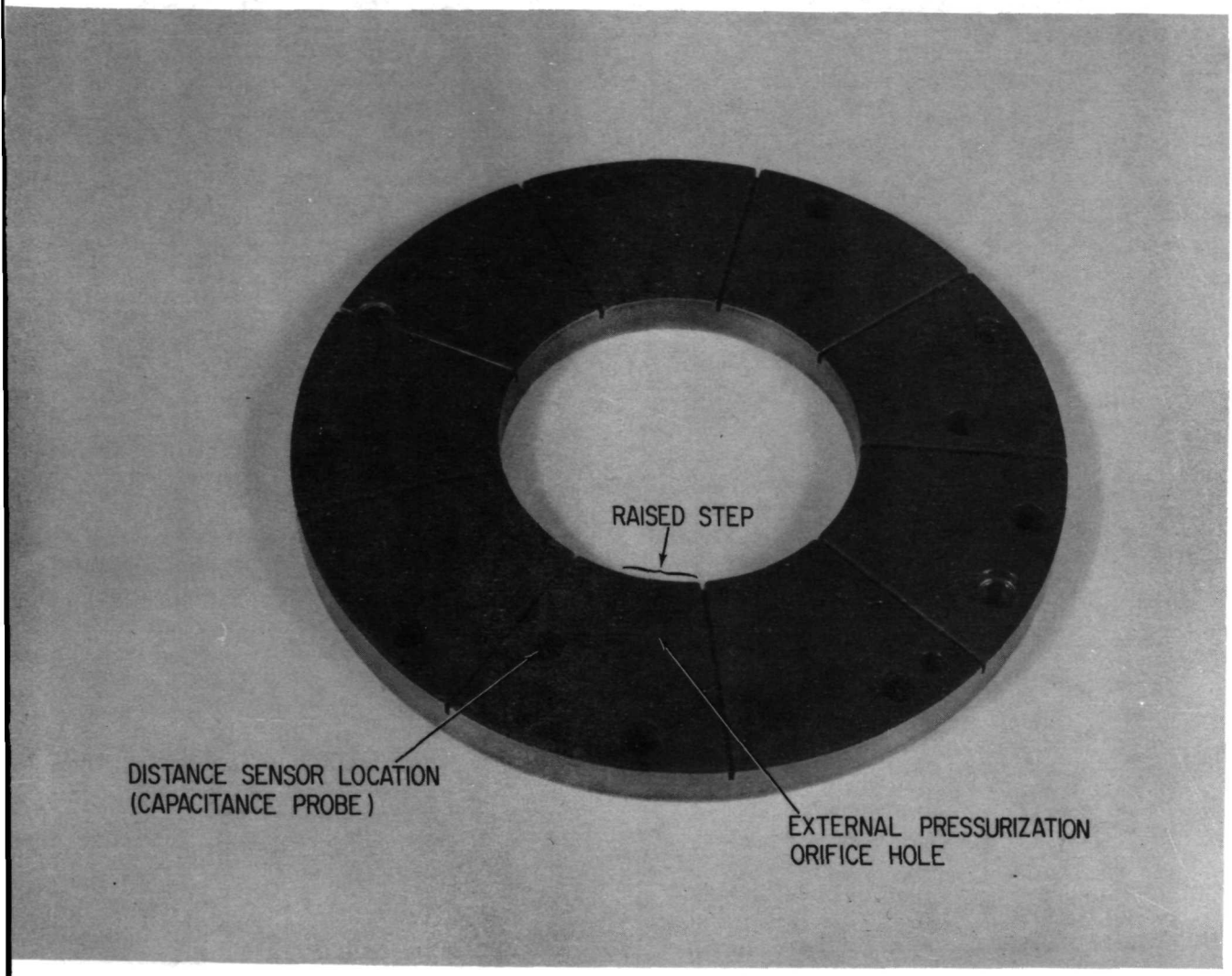

Fig. 22 BRU Thrust Bearing Stator

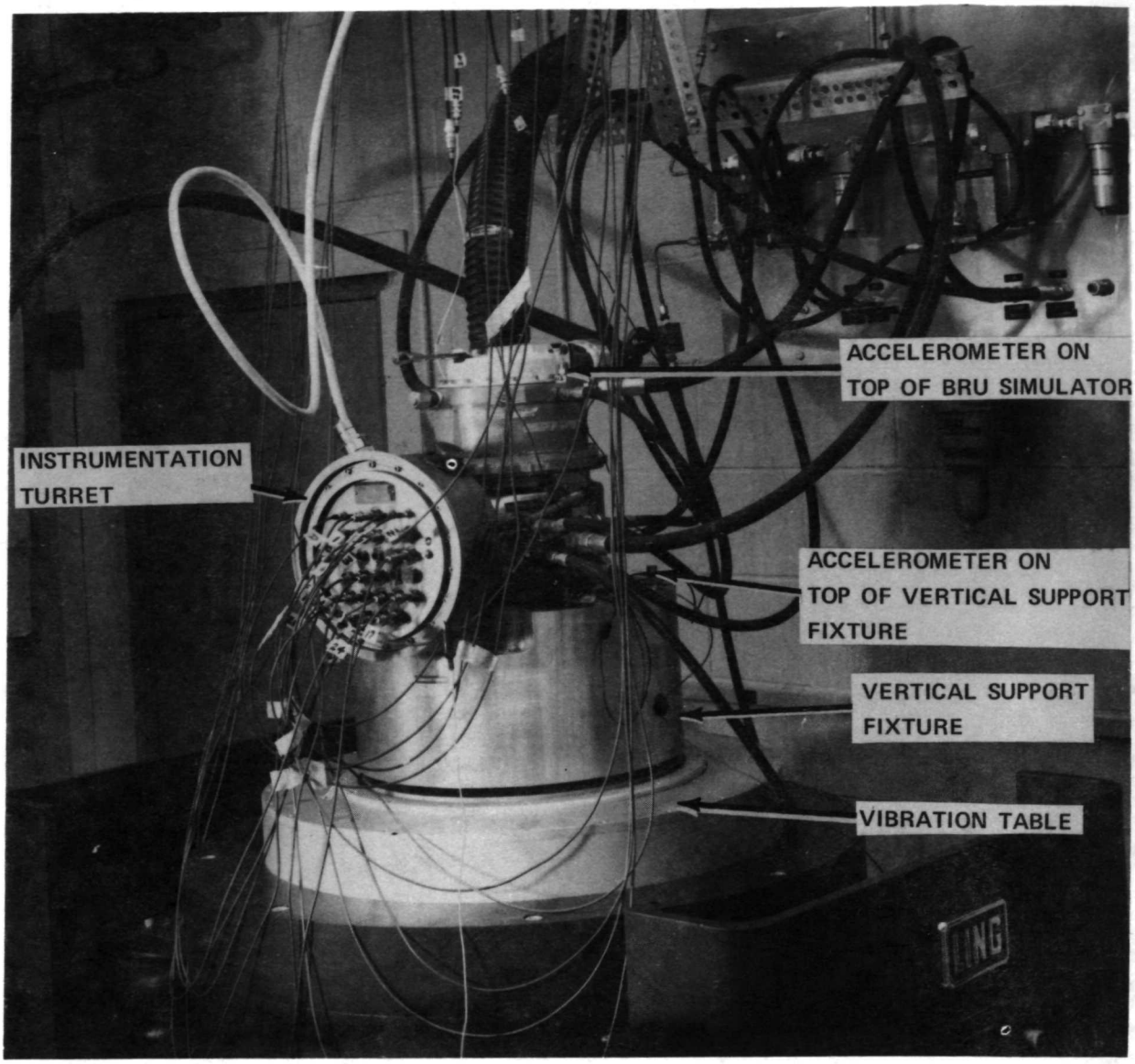

Fig. 23 BRU Simulator In Vertical Support Fixture For Vibration Testing

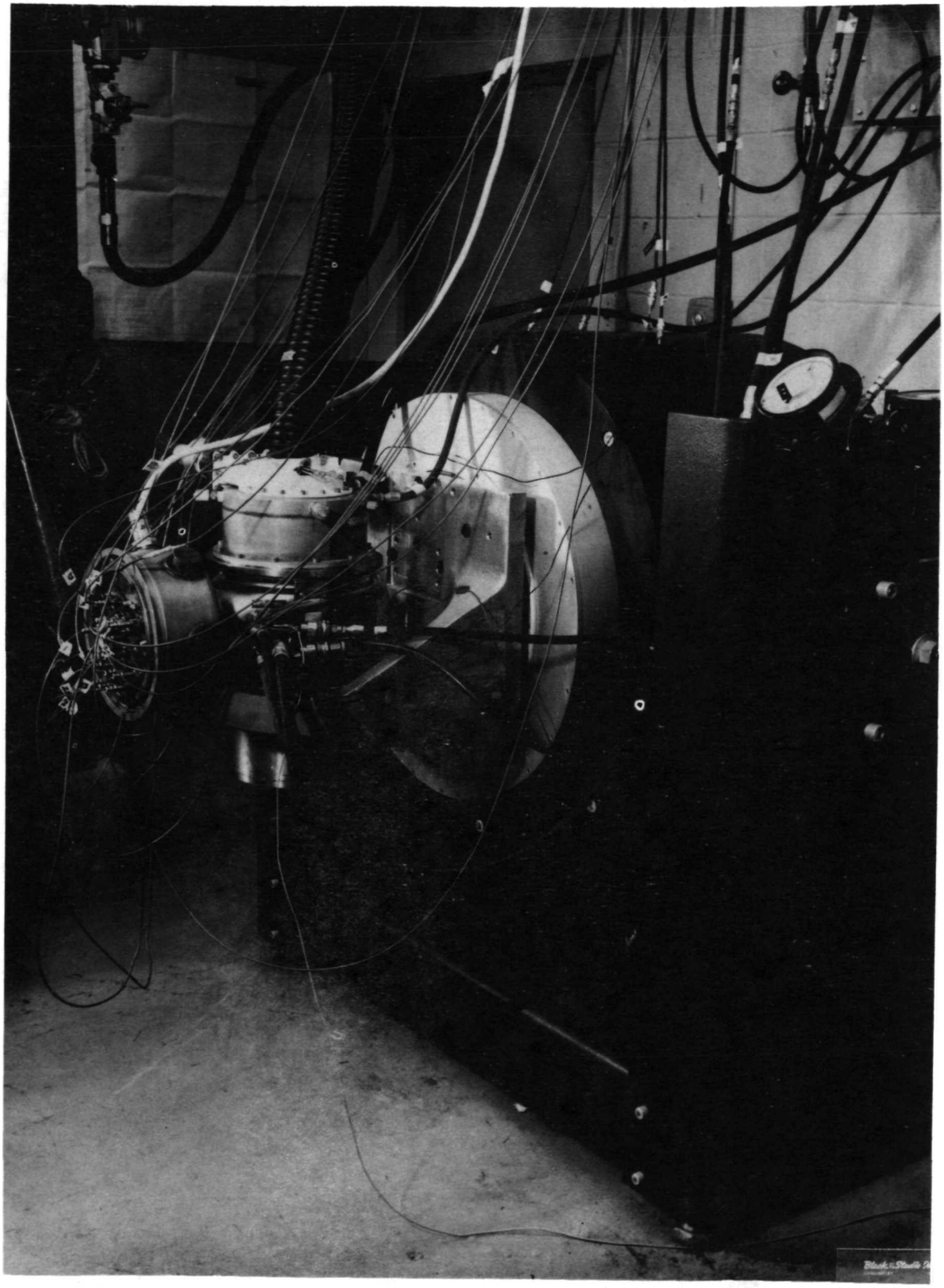

Fig. 24 BRU Simulator In Support Fixture For Transverse Vibration Testing

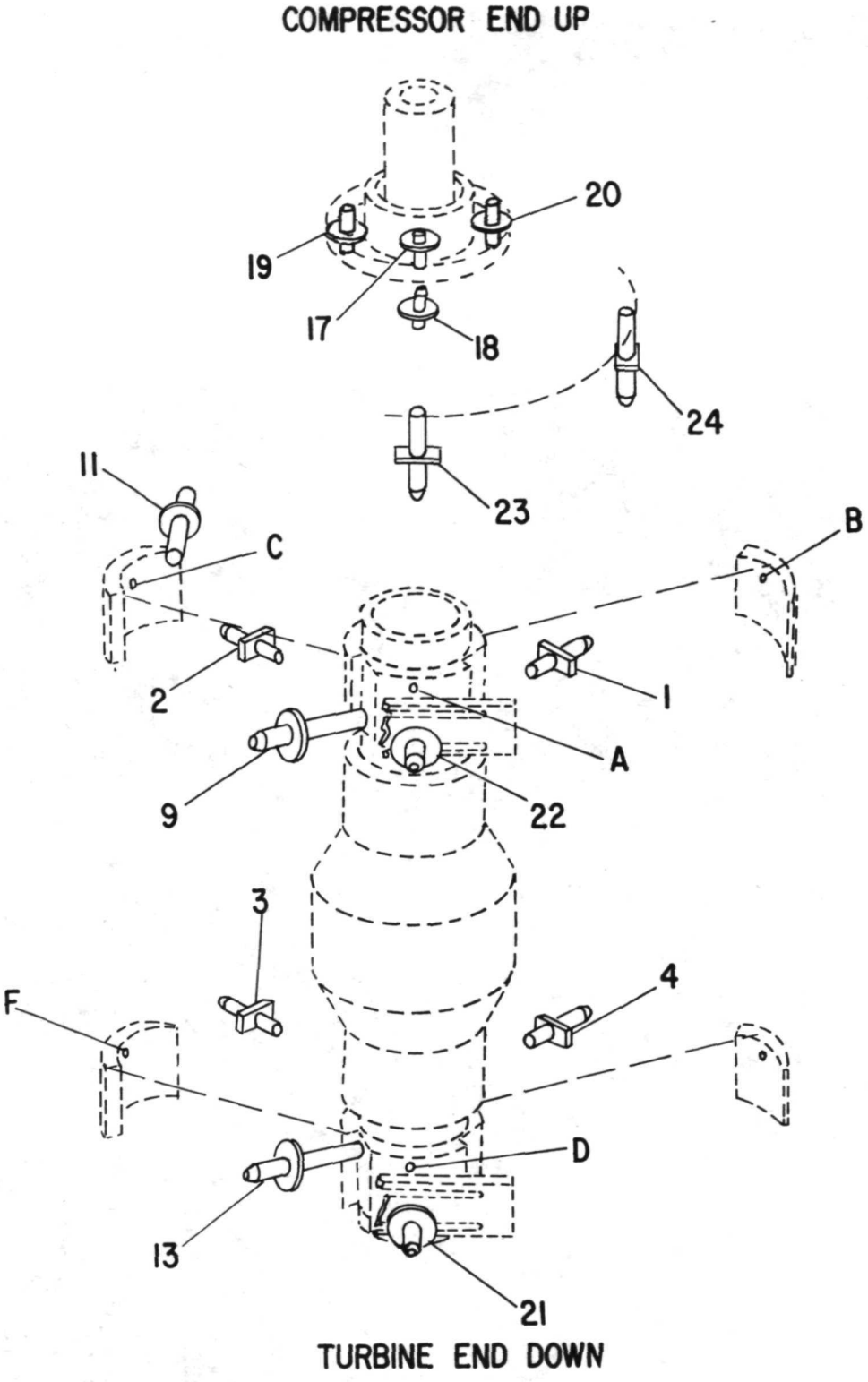

Fig. 25 Proximity Probe Locations on BRU Simulator Rotor and Bearings

PROXIMITY PROBE DESIGNATION ON BRU SIMULATOR	
Probe Identification	Proximity Probe Designation
A	Pivot film thickness probe, flex mounted pad, compressor end
B	Pivot film thickness probe, solid mounted pad, compressor end
C	Pivot film thickness probe, solid mounted pad, compressor end
D	Pivot film thickness probe, flex mounted pad, turbine end
F	Pivot film thickness probe, solid mounted pad, turbine end
1	Compressor journal orthogonal probe
2	Compressor journal orthogonal probe
3	Turbine journal orthogonal probe
4	Turbine journal orthogonal probe
9	Flex mounted pad leading edge probe, compressor end
11	Solid mounted pad leading edge probe, compressor end
13	Flex mounted pad leading edge probe, turbine end
17	Compressor thrust plate film thickness probe
18	Turbine thrust plate film thickness probe
20	Turbine thrust plate film thickness probe
21	Turbine journal flex mount pad load probe
22	Compressor journal flex mount pad load probe
23	Thrust bearing gimbal probe to ground
24	Thrust bearing gimbal probe to ground

Fig. 26 Capacitance Probes Used On BRU Simulator For Vibration Testing

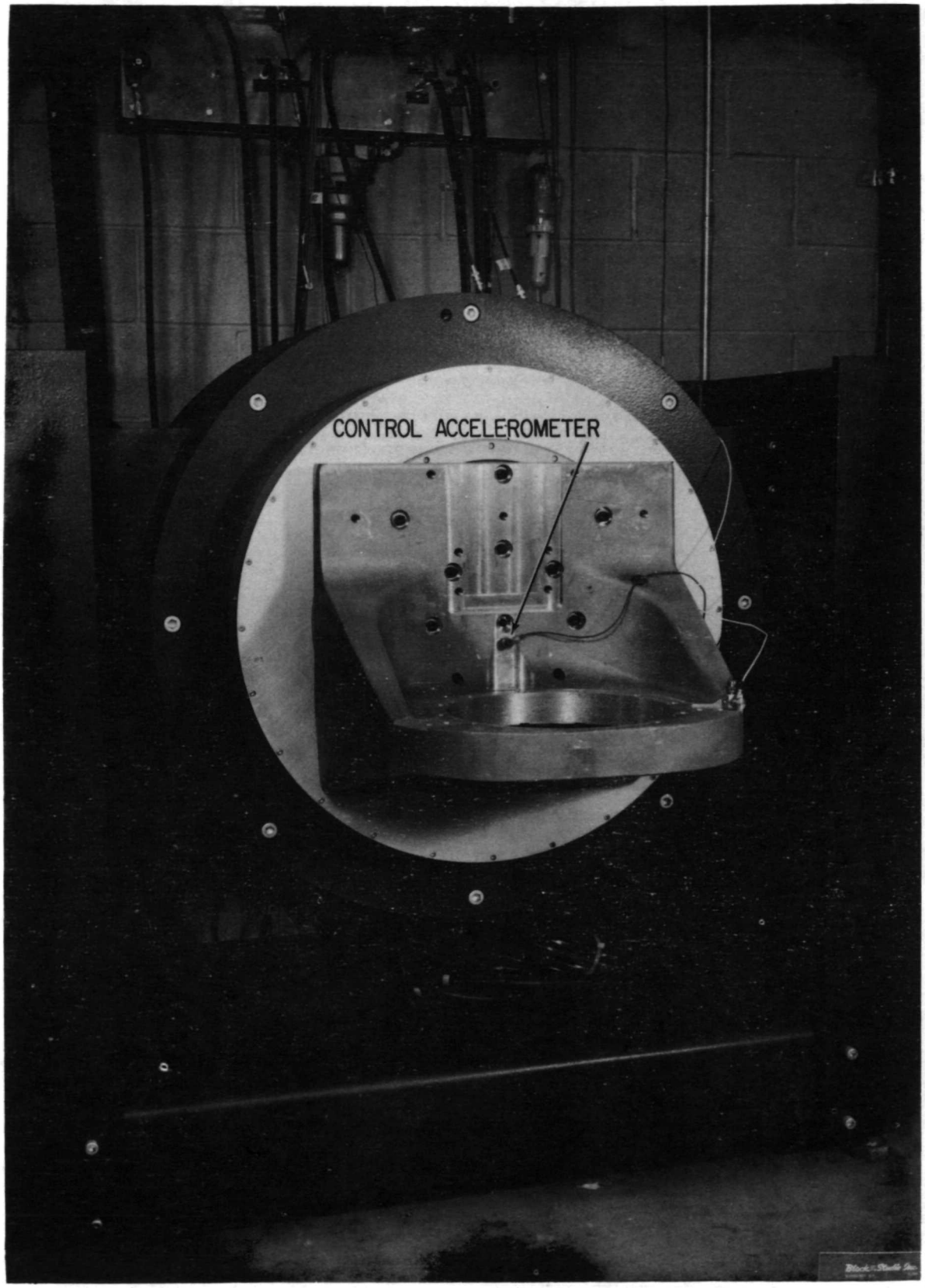

Fig. 27 Location Of Control Accelerometer on Transverse Vibration Test Support Fixture

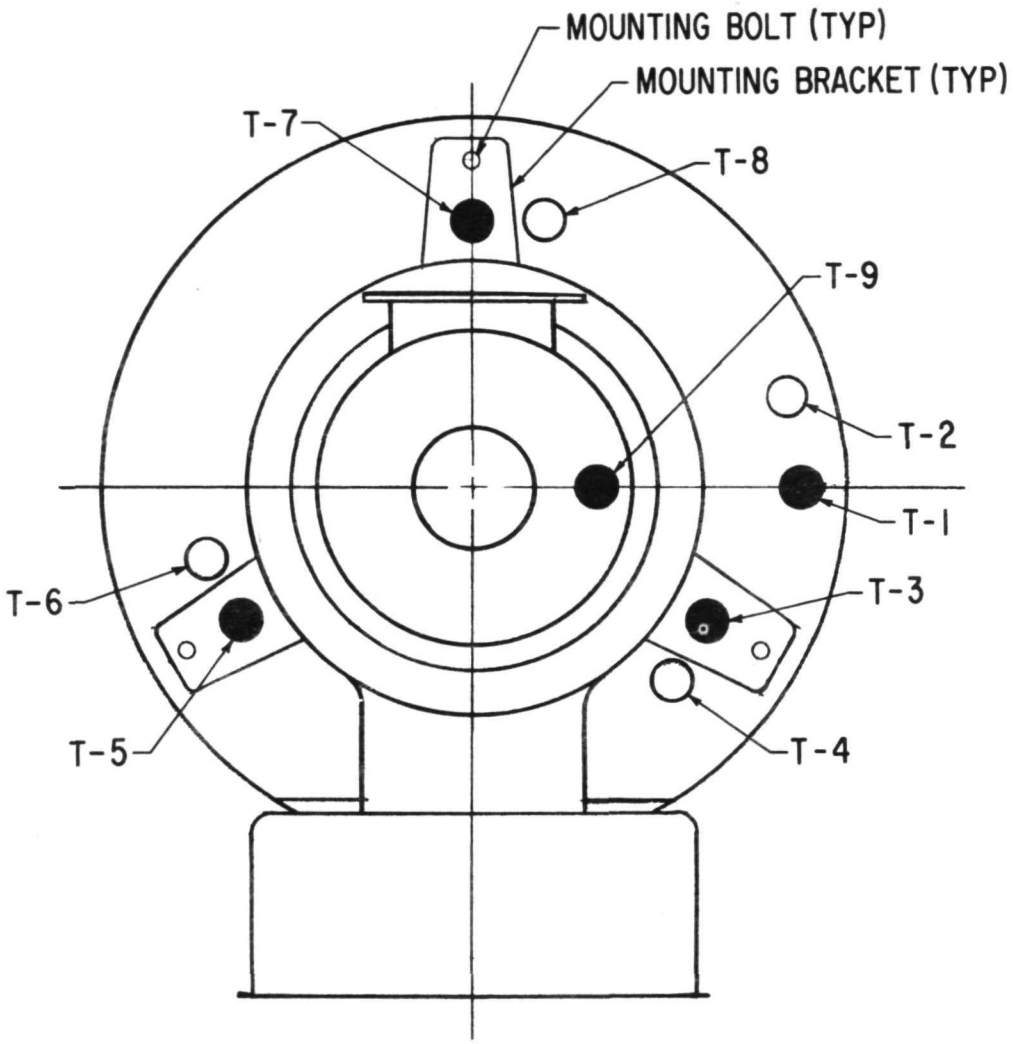

Fig. 28 Accelerometer Locations on BRU Simulator and Vertical Support Fixture

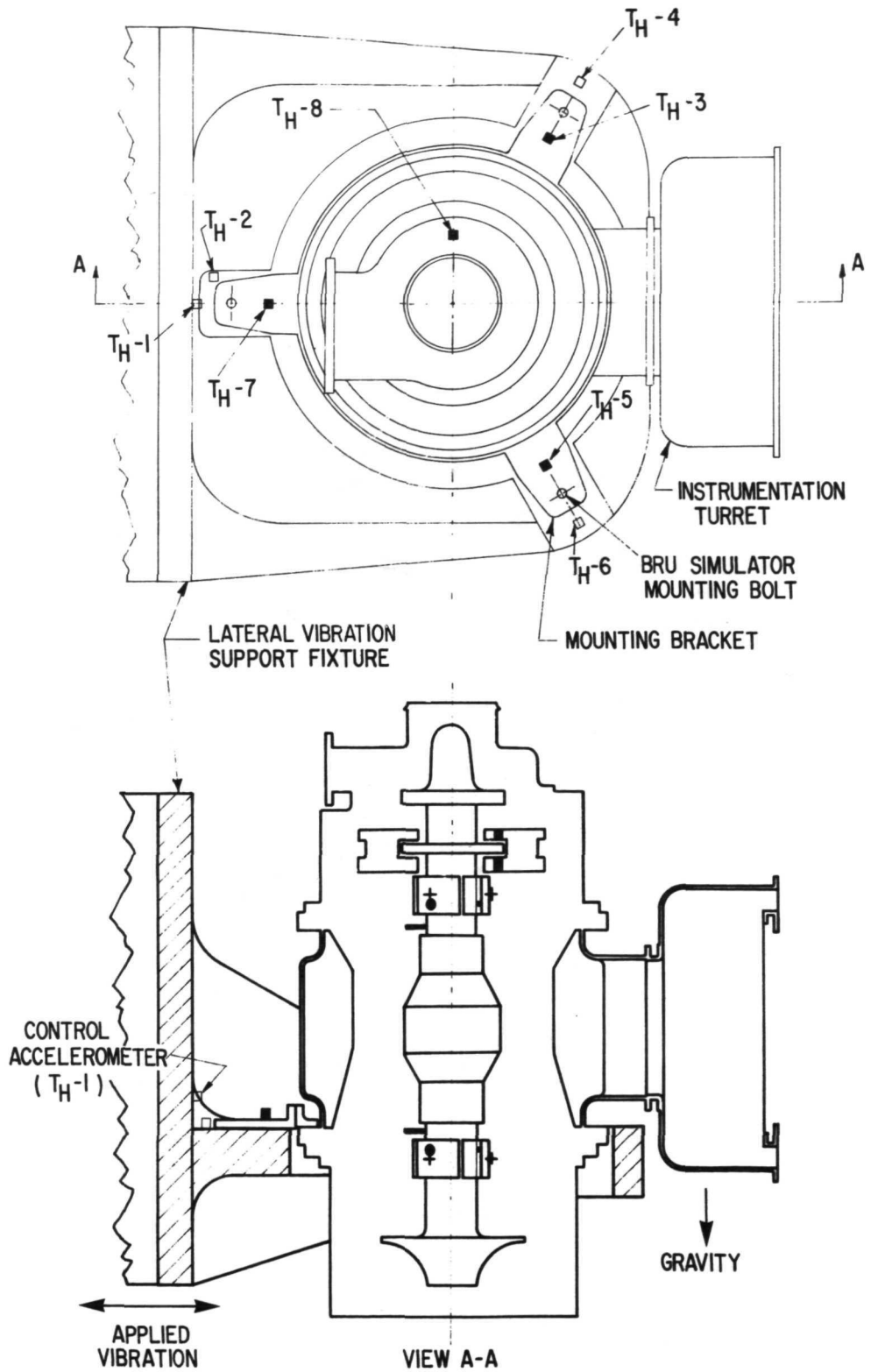

Fig. 29 Accelerometer Locations on Transverse Vibration Test Support Fixture and BRU Simulator Casing

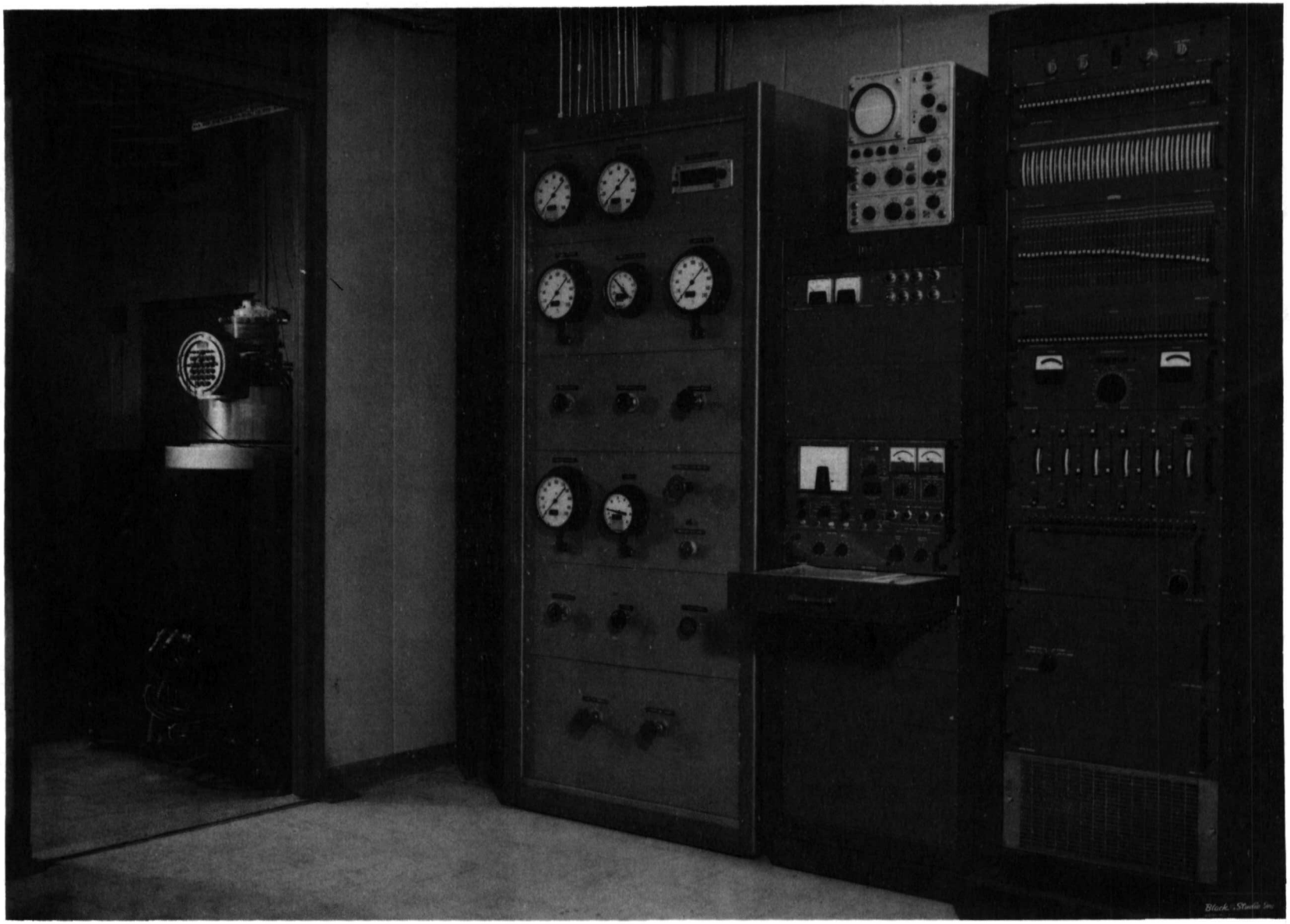

Fig. 30 Brayton Rotating Unit (BRU) Simulator Vibration Test Setup In MTI Latham Facility

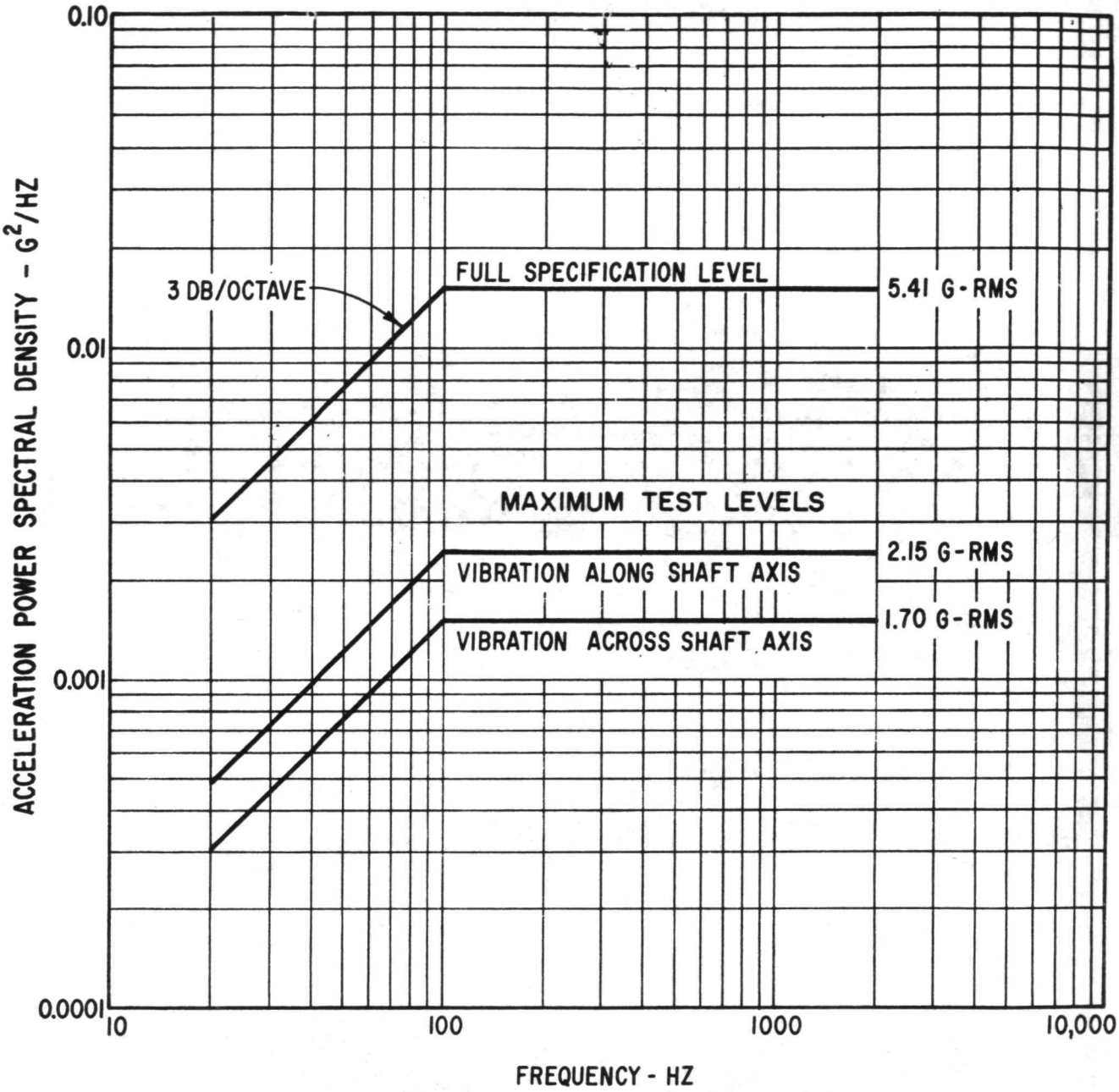

Fig. 31 Random Vibration Power Spectral Density Test Specification 417-2 (Rev. C) For Electrical Generating System Components (Operating) And Actual BRU Test Levels

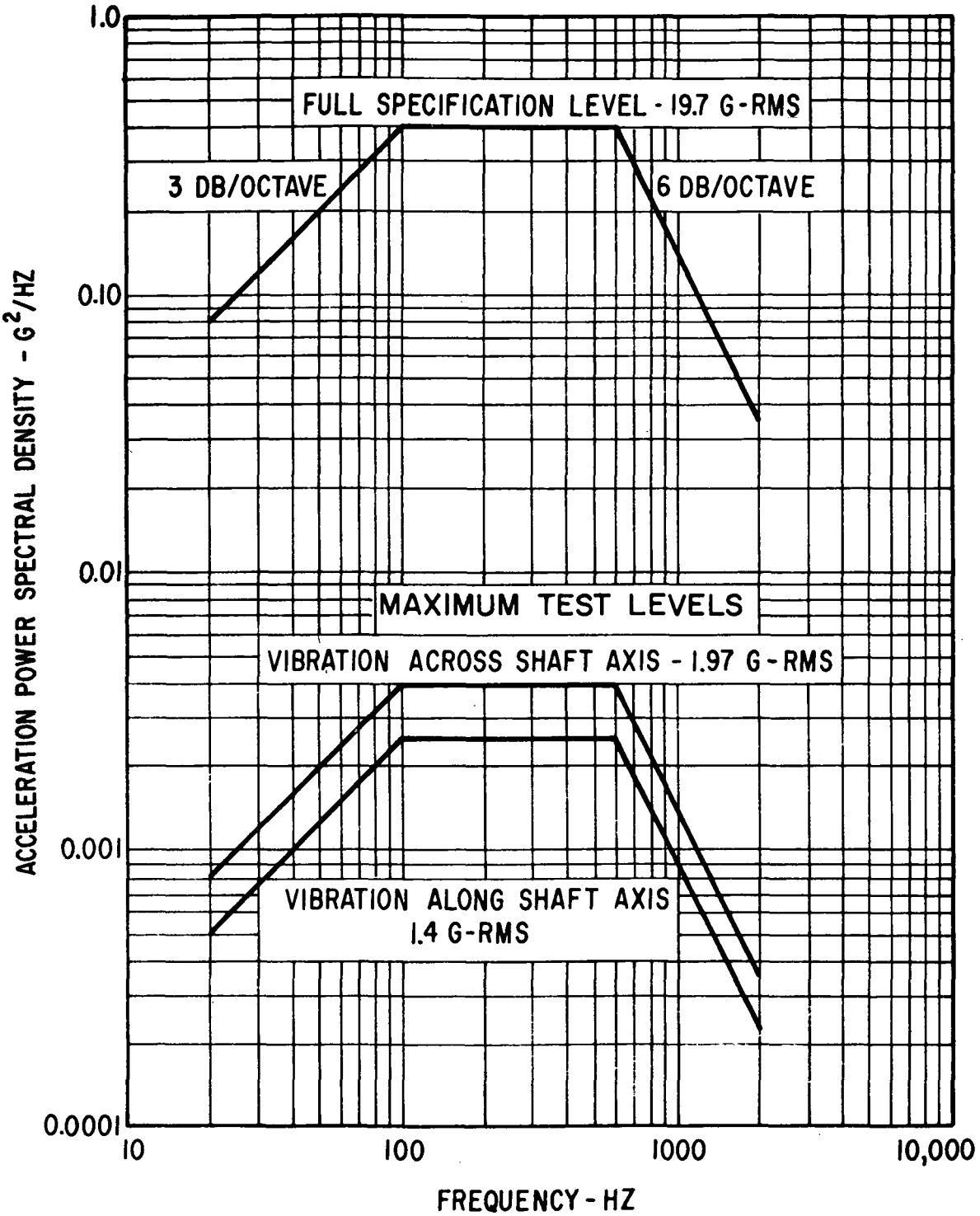

Fig. 32 Random Vibration Power Spectral Density Test Specification 417-2 (Rev. C) For Electrical Generating System Components (Nonoperating) And Actual BRU Test Levels

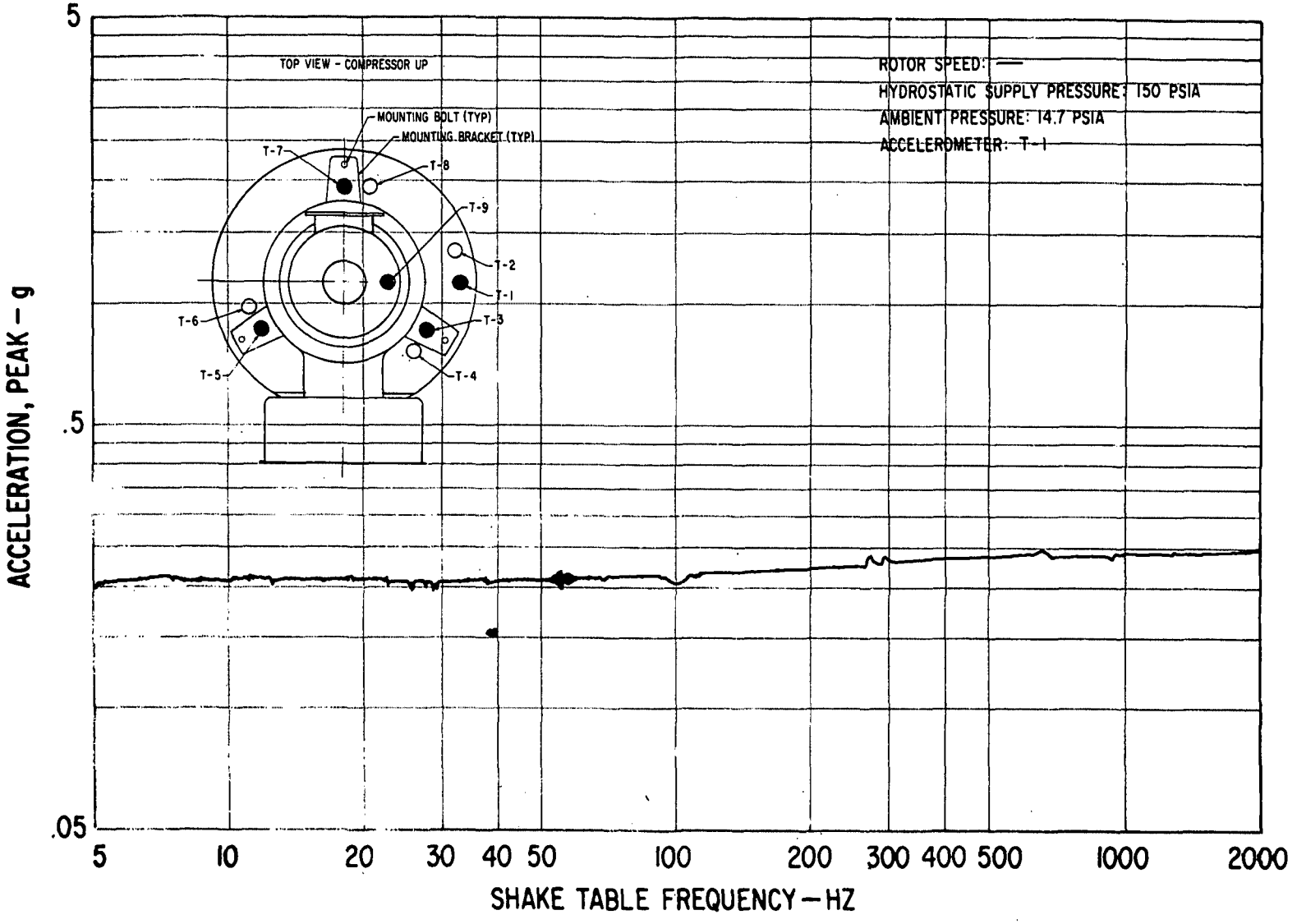

Fig. 33 Sinusoidal Acceleration At The Top of the Vertical Support Fixture (Input Control Accelerometer) (Direction of Applied Vibration In-Line With BRU Rotor Axis)

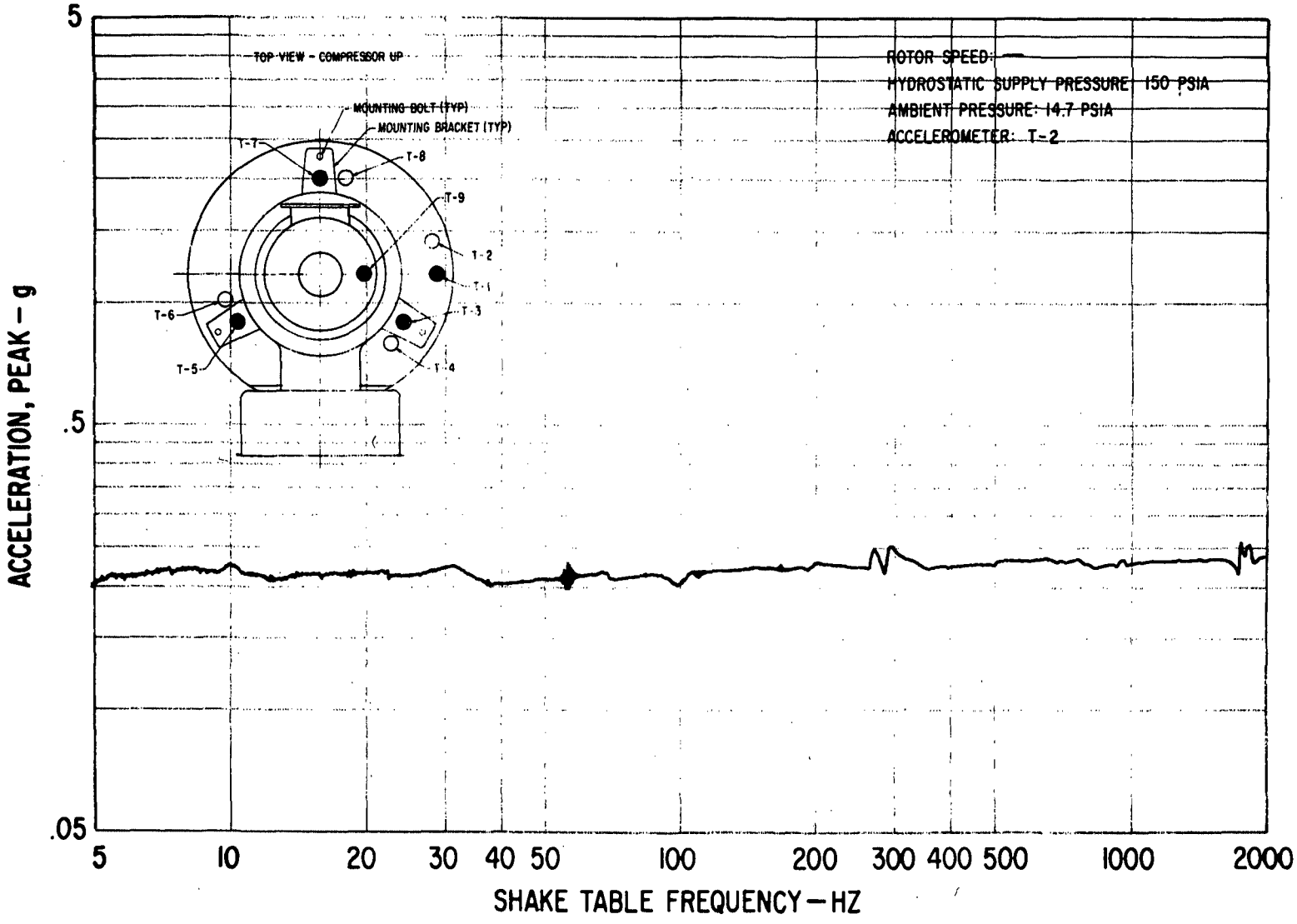

Fig. 34 Sinusoidal Acceleration At The Top of the Vertical Support Fixture At A Location Next to The Control Accelerometer (Direction of Applied Vibration In-Line With BRU Rotor Axis)

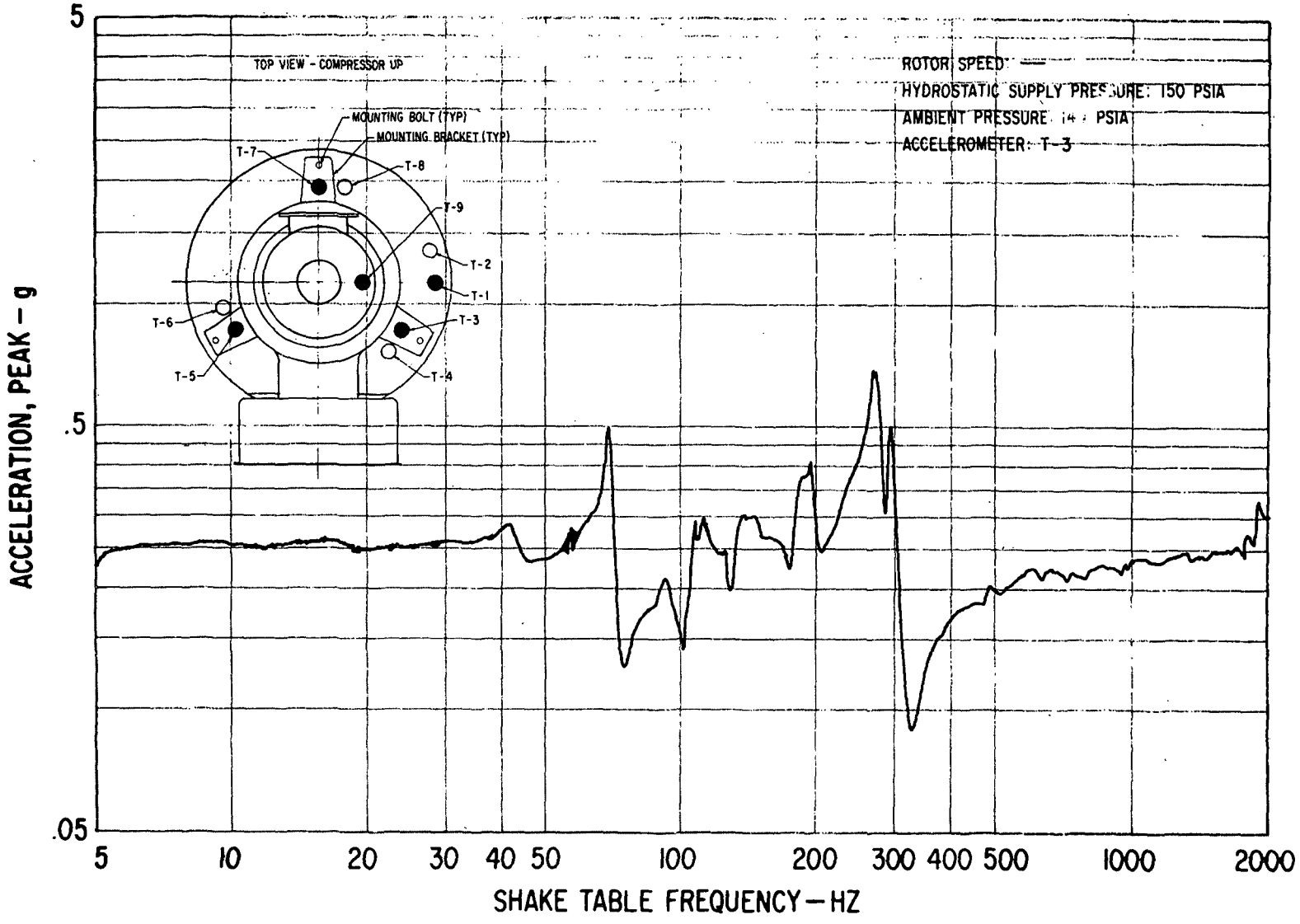

Fig. 35 Sinusoidal Acceleration on BRU Simulator Mounting Bracket, Counterclockwise From Turret (Direction Of Applied Vibration In-Line With BRU Rotor Axis)

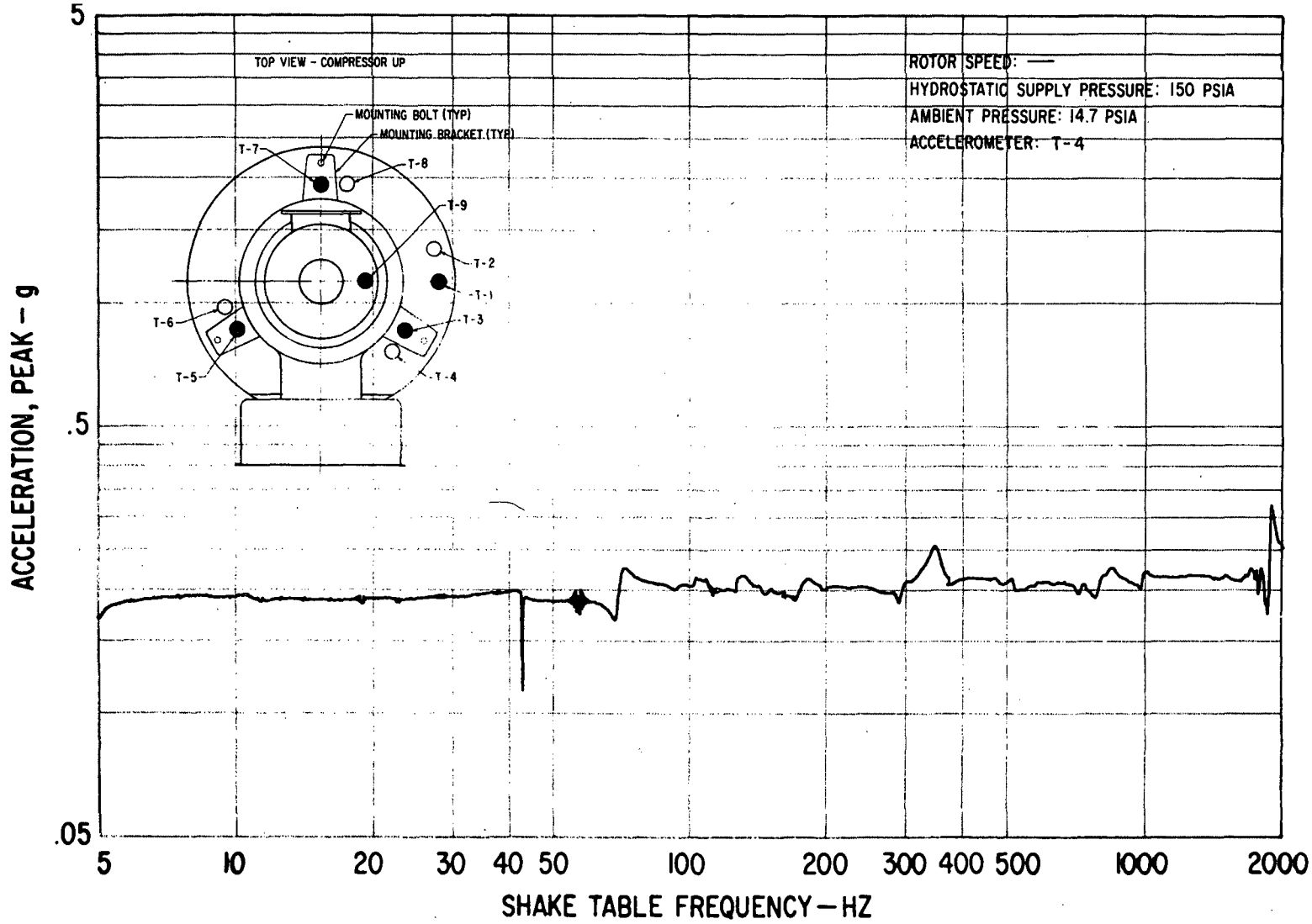

Fig. 36 Sinusoidal Acceleration At The Top of The Vertical Support Fixture, Counterclockwise From Turret (Direction Of Applied Vibration In-Line With BRU Rotor Axis)

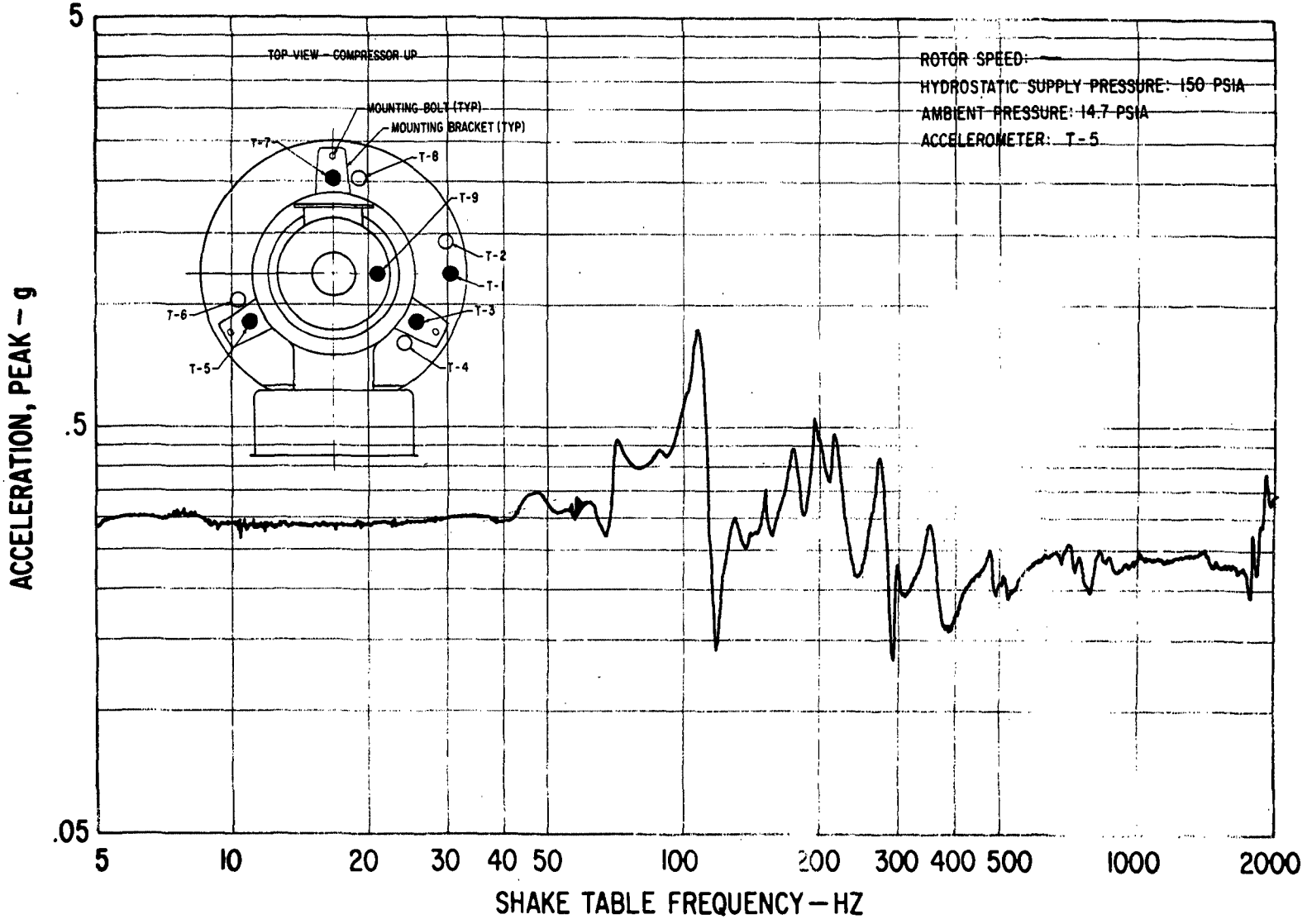

Fig. 37 Sinusoidal Acceleration on BRU Simulator Mounting Bracket, Clockwise From Turret (Direction Of Applied Vibration In-Line With BRU Rotor Axis)

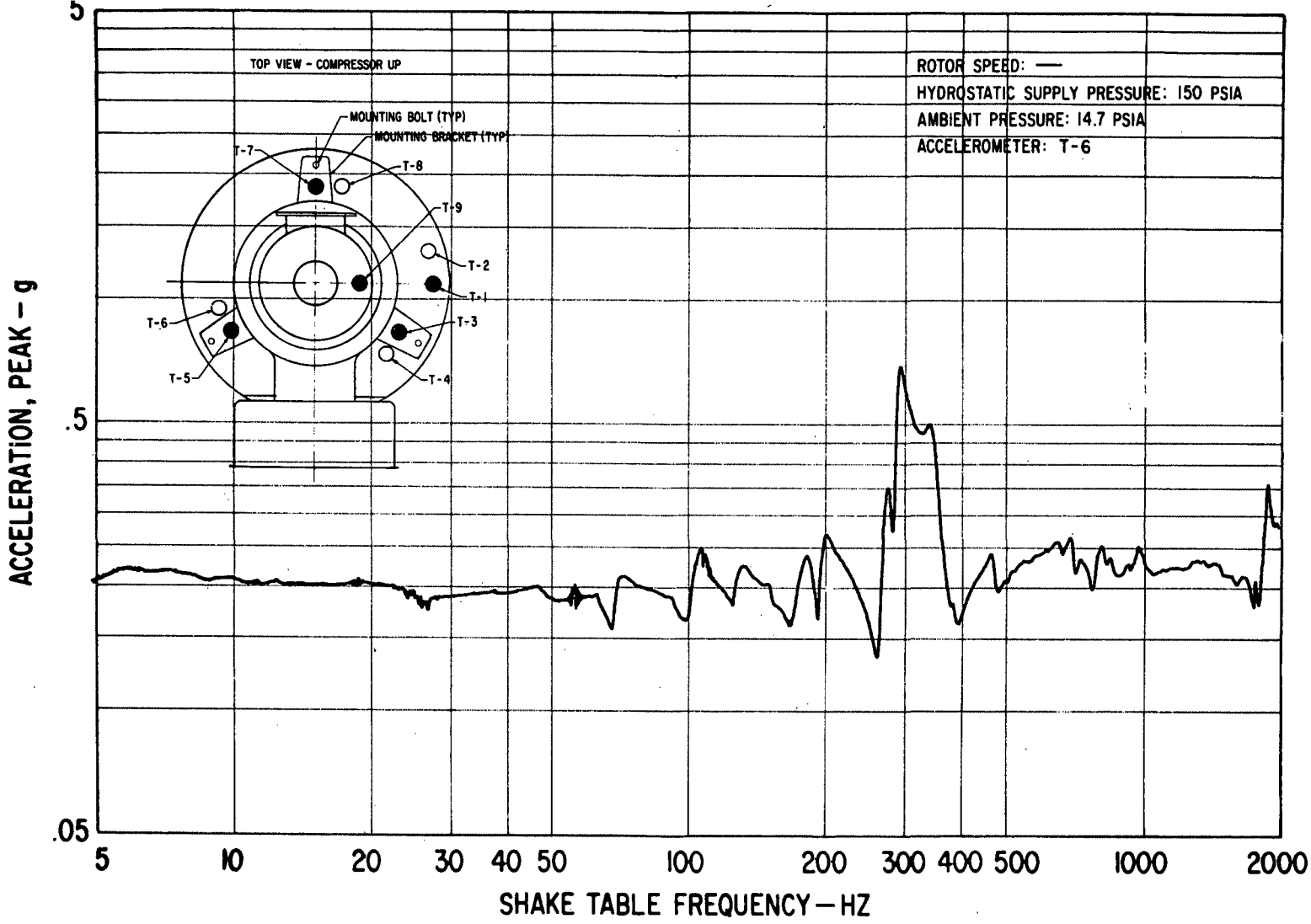

Fig. 38 Sinusoidal Acceleration at the Top of the Vertical Support Fixture, Clockwise from Turret (Direction of Applied Vibration In-Line With BRU Rotor Axis)

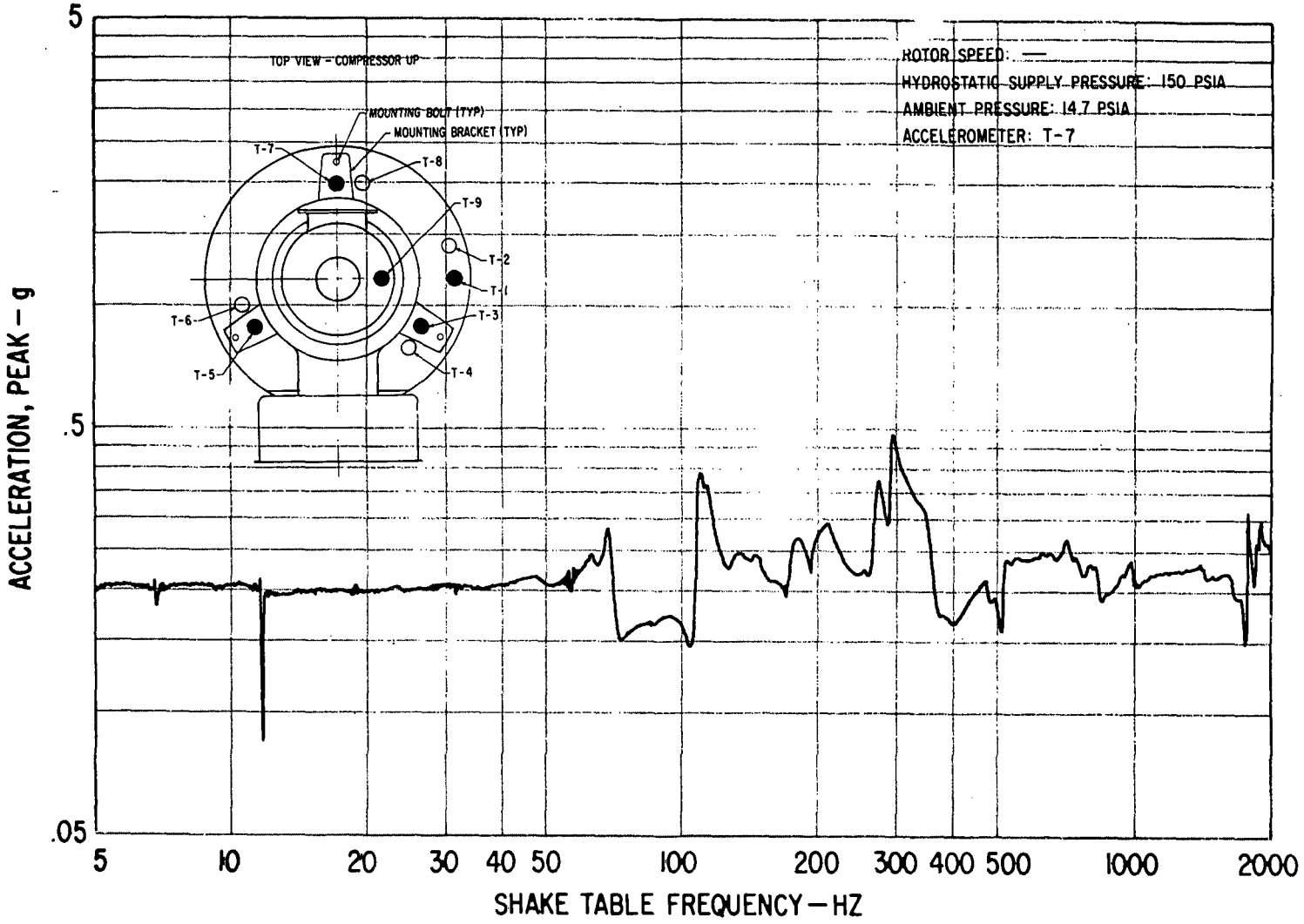

Fig. 39 Sinusoidal Acceleration on BRU Simulator Mounting Bracket Opposite From Turret (Direction of Applied Vibration

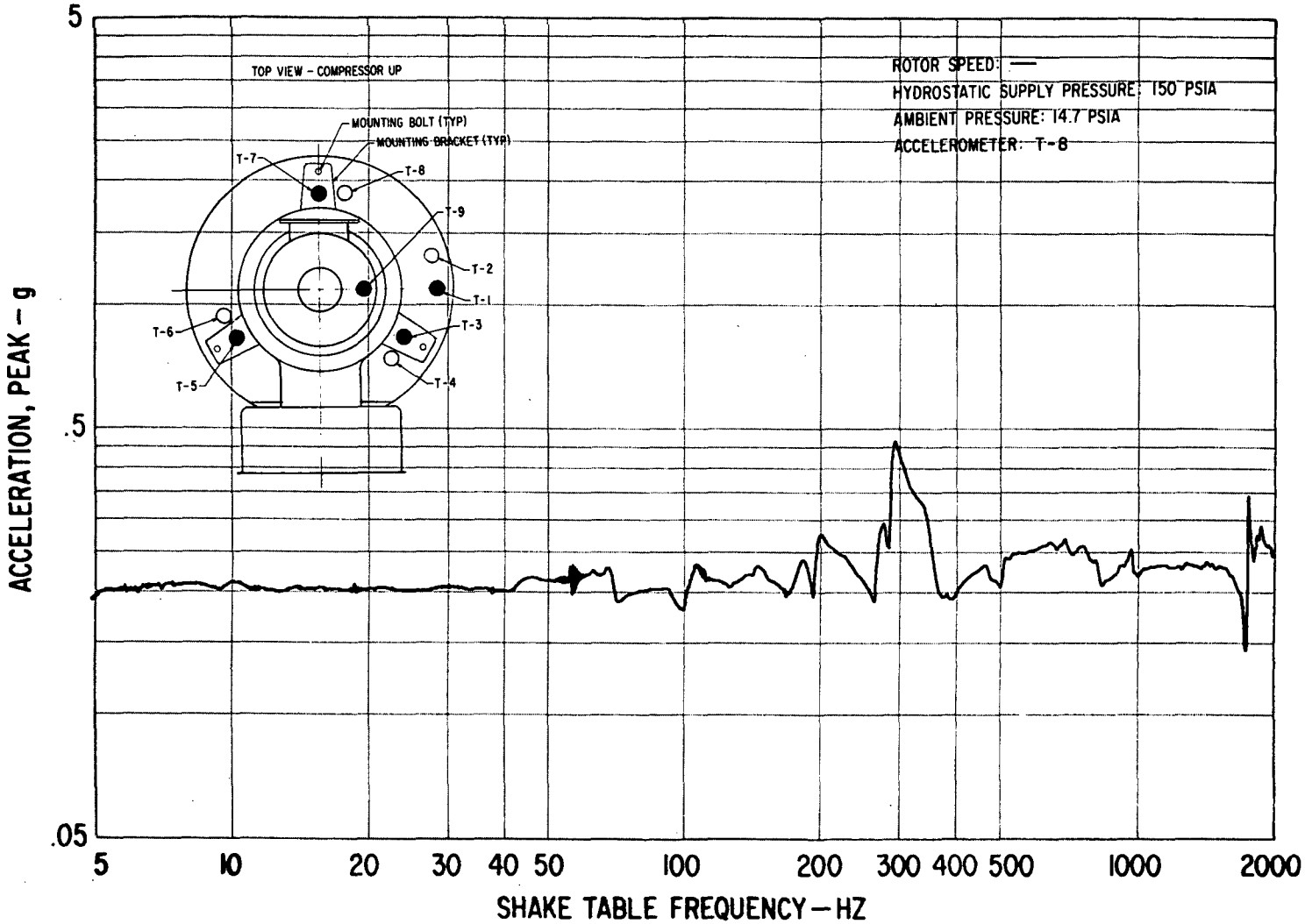

Fig. 40 Sinusoidal Acceleration at the Top of the Vertical Support Fixture Opposite From Turret (Direction of Applied Vibration In-Line With BRU Rotor Axis)

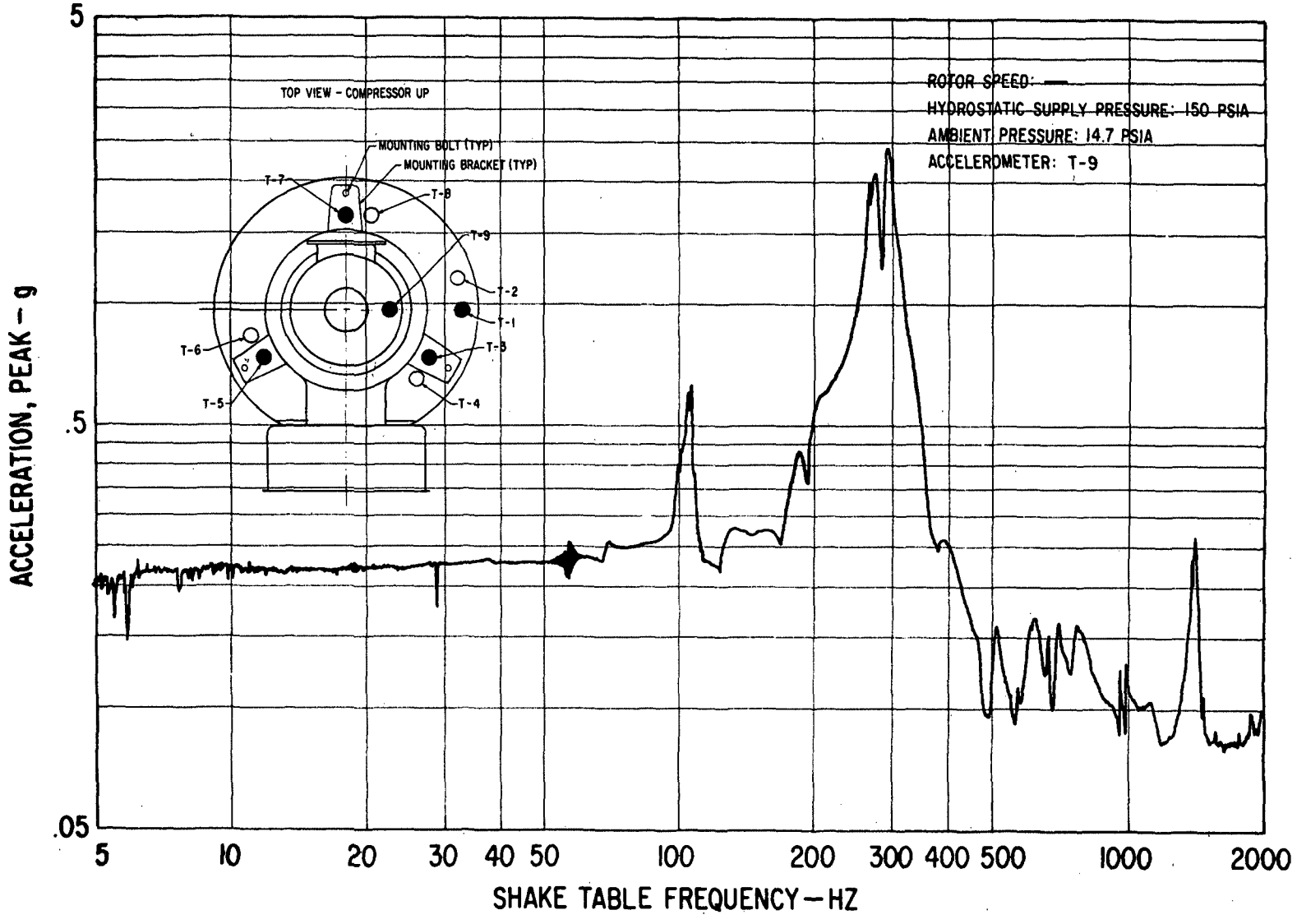

Fig. 41 Sinusoidal Acceleration on Top of BRU Simulator (Direction of Applied Vibration In-Line With BRU Rotor Axis)

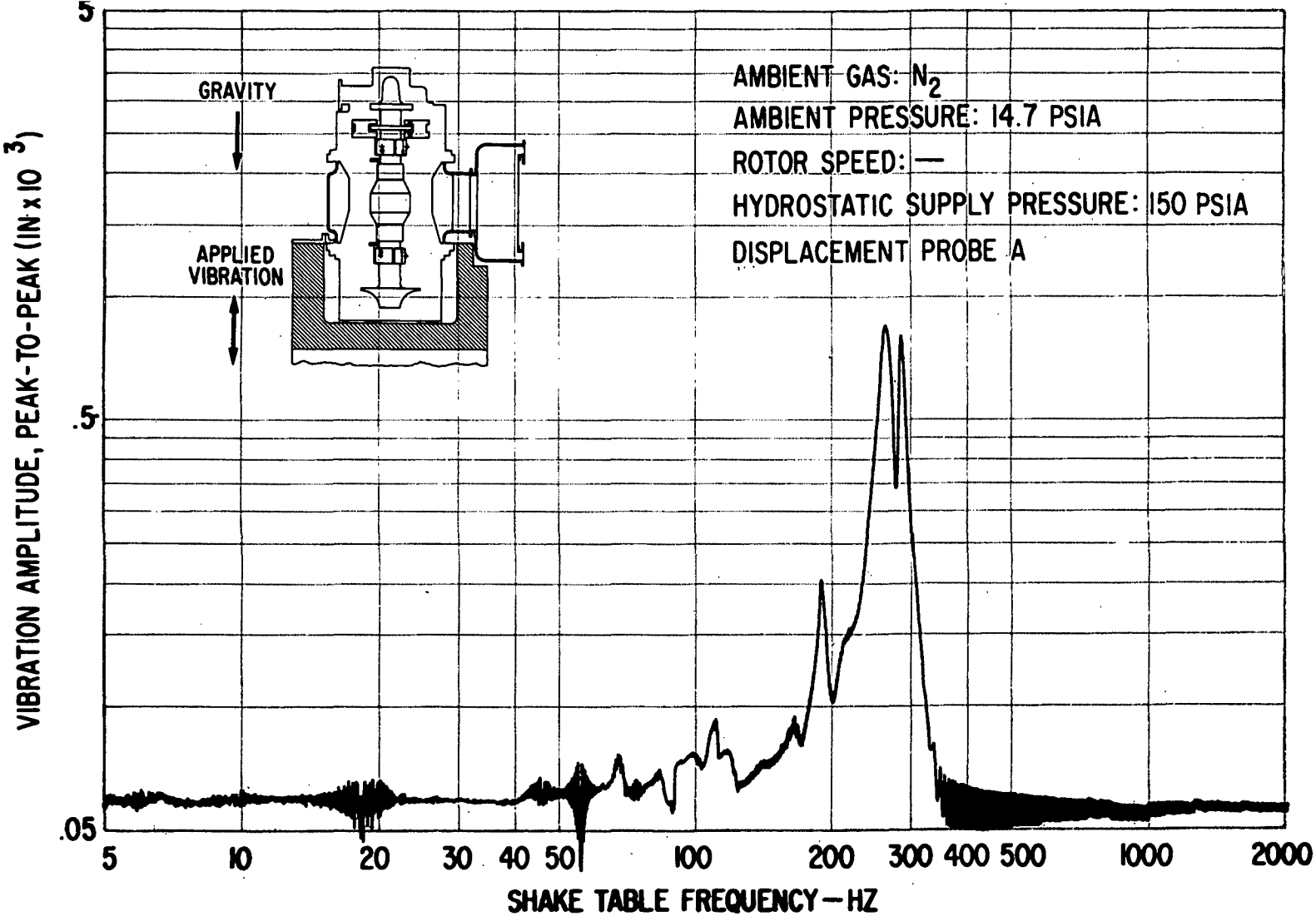

Fig. 42 Pad-To-Shaft Pivot Film Thickness Variation For Flex-Mounted Compressor Journal Bearing Pad Under Externally-Imposed Sinusoidal Vibration of 0.25 g peak

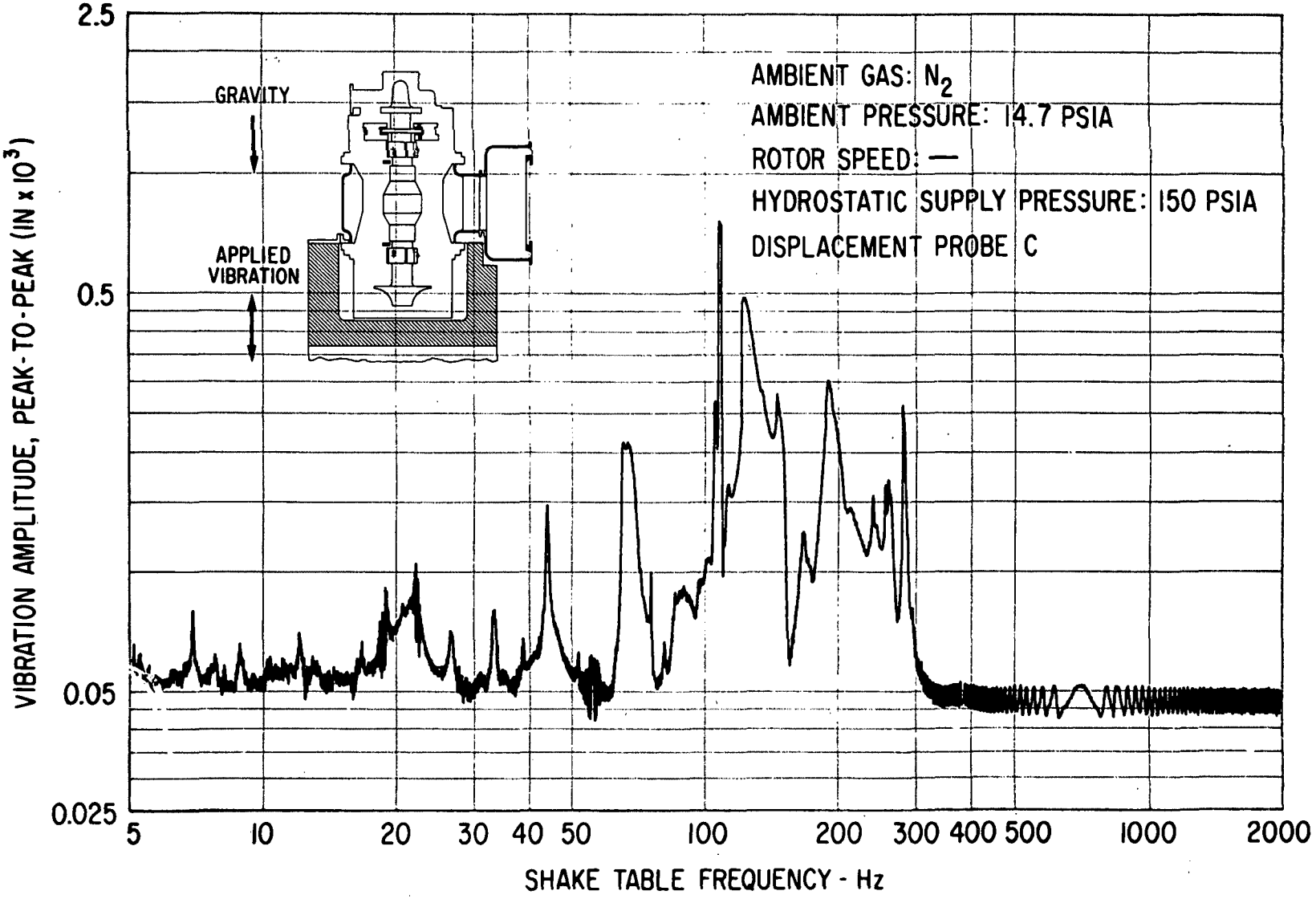

Fig. 43 Pad-To-Shaft Pivot Film Thickness Variation For Solid-Mounted Compressor Journal Bearing Pad Under Externally-Imposed Sinusoidal Vibration of 0.25 g peak

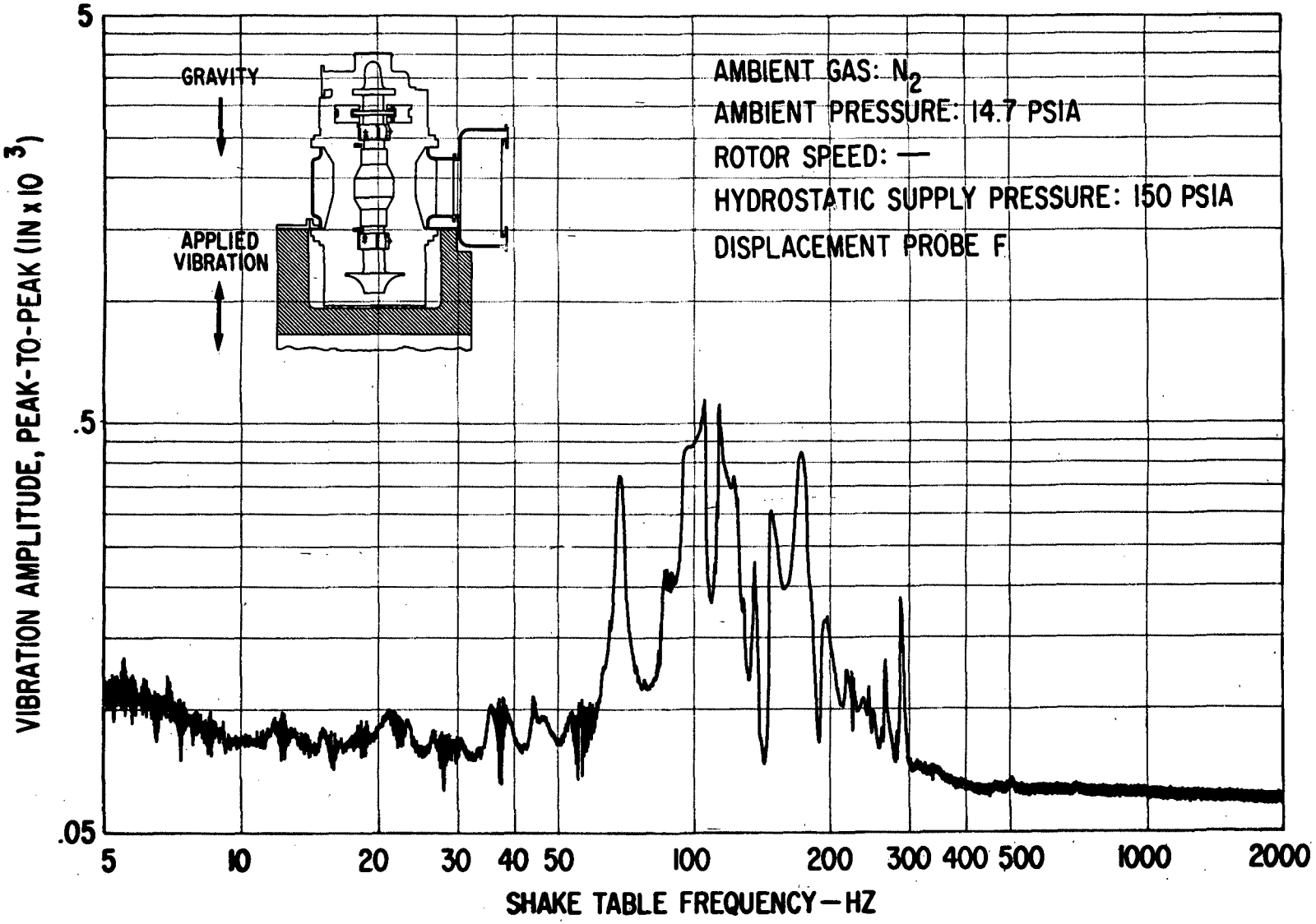

Fig. 44 Pad-To-Shaft Pivot Film Thickness Variation for Solid-Mounted Turbine Journal Bearing Pad Under Externally-Imposed Sinusoidal Vibration of 0.25 g peak

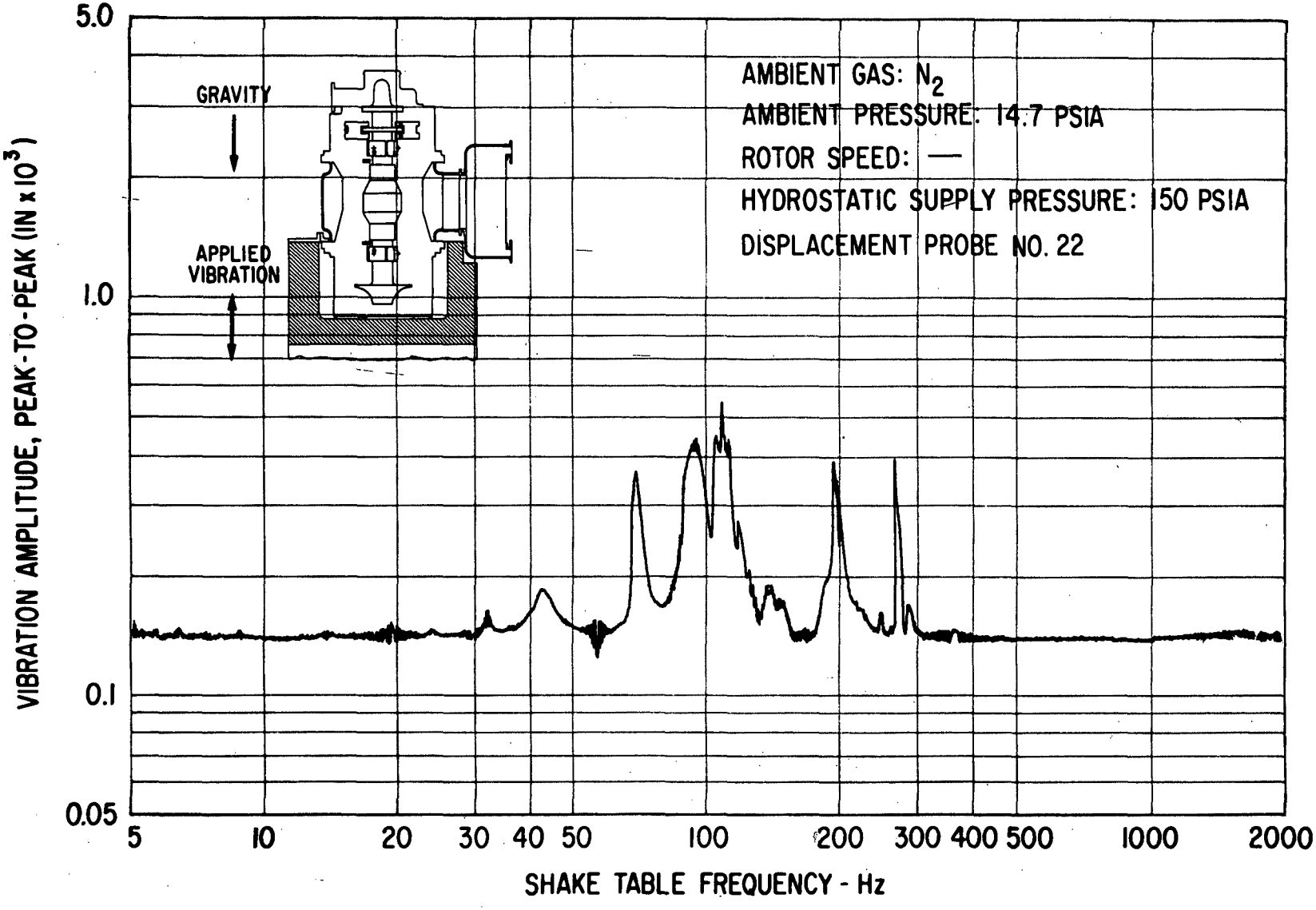

Fig. 45 Compressor Journal Flexure Amplitudes Under Externally-Imposed Sinusoidal Vibration of 0.25 g Peak

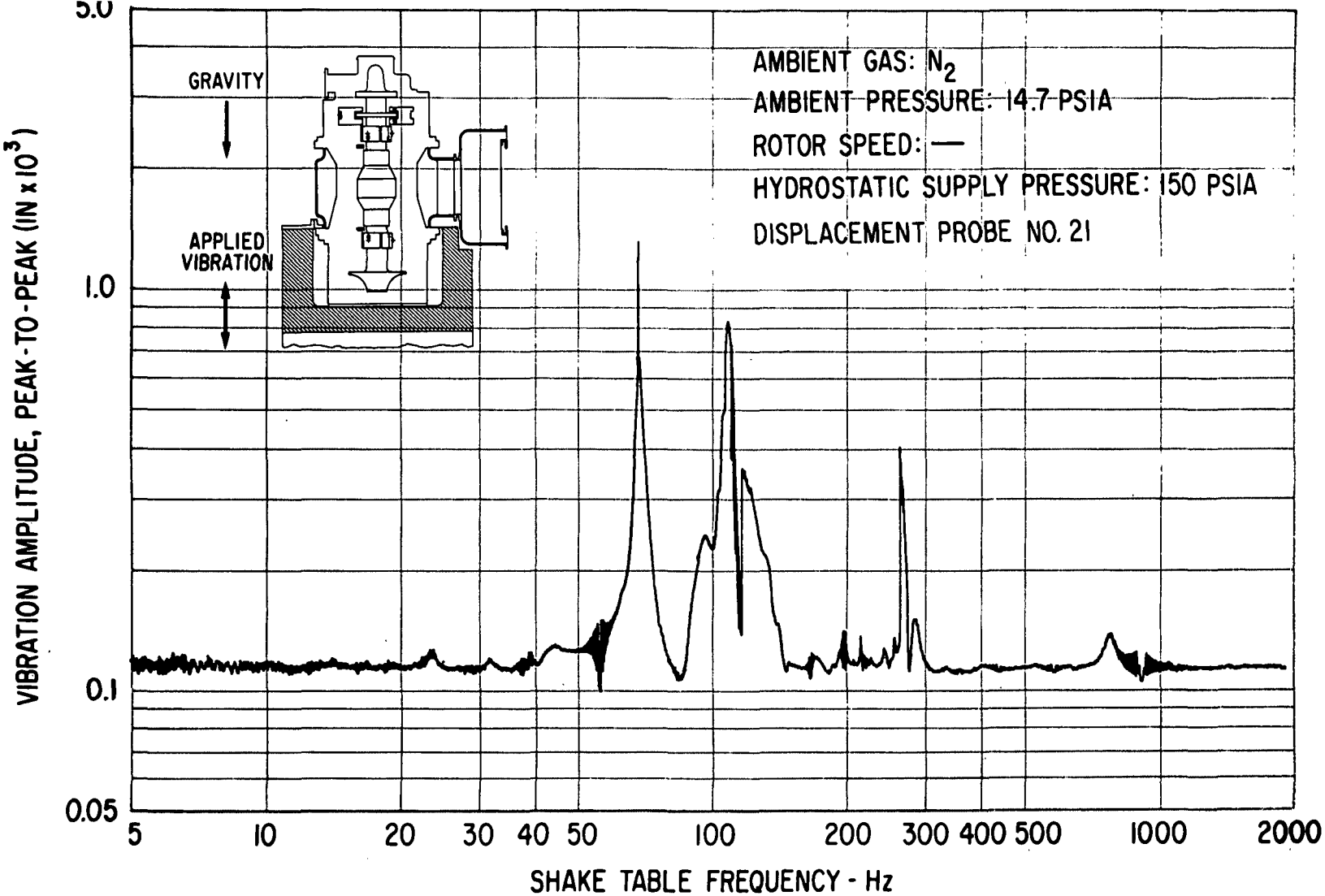

Fig. 46 Turbine Journal Flexure Amplitudes Under Externally-Imposed Sinusoidal Vibration of 0.25 g Peak

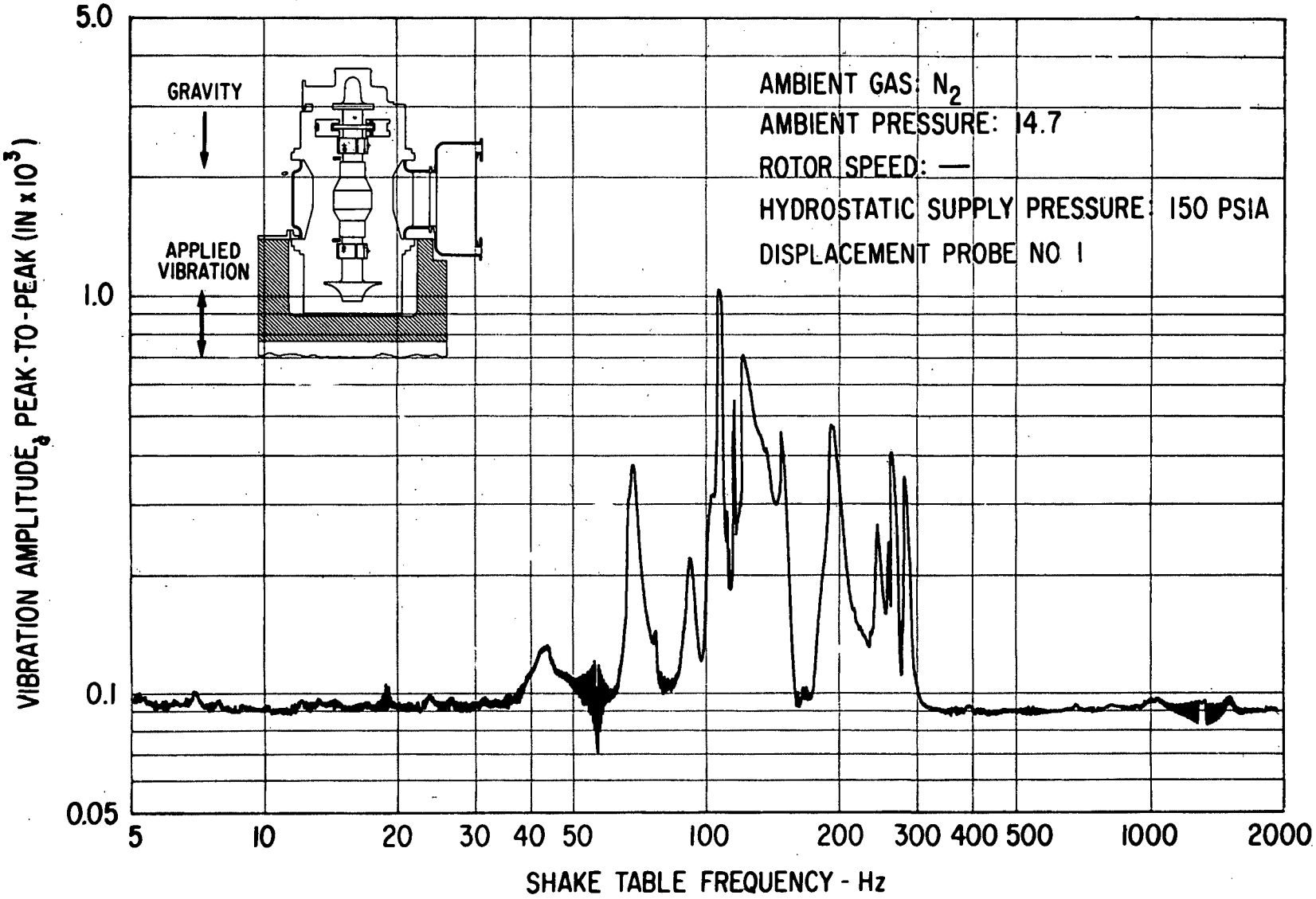

Fig. 47 Compressor Journal Rotor Amplitudes (Casing-to-Shaft) Under Externally-Imposed Sinusoidal Vibration of 0.25 g Peak

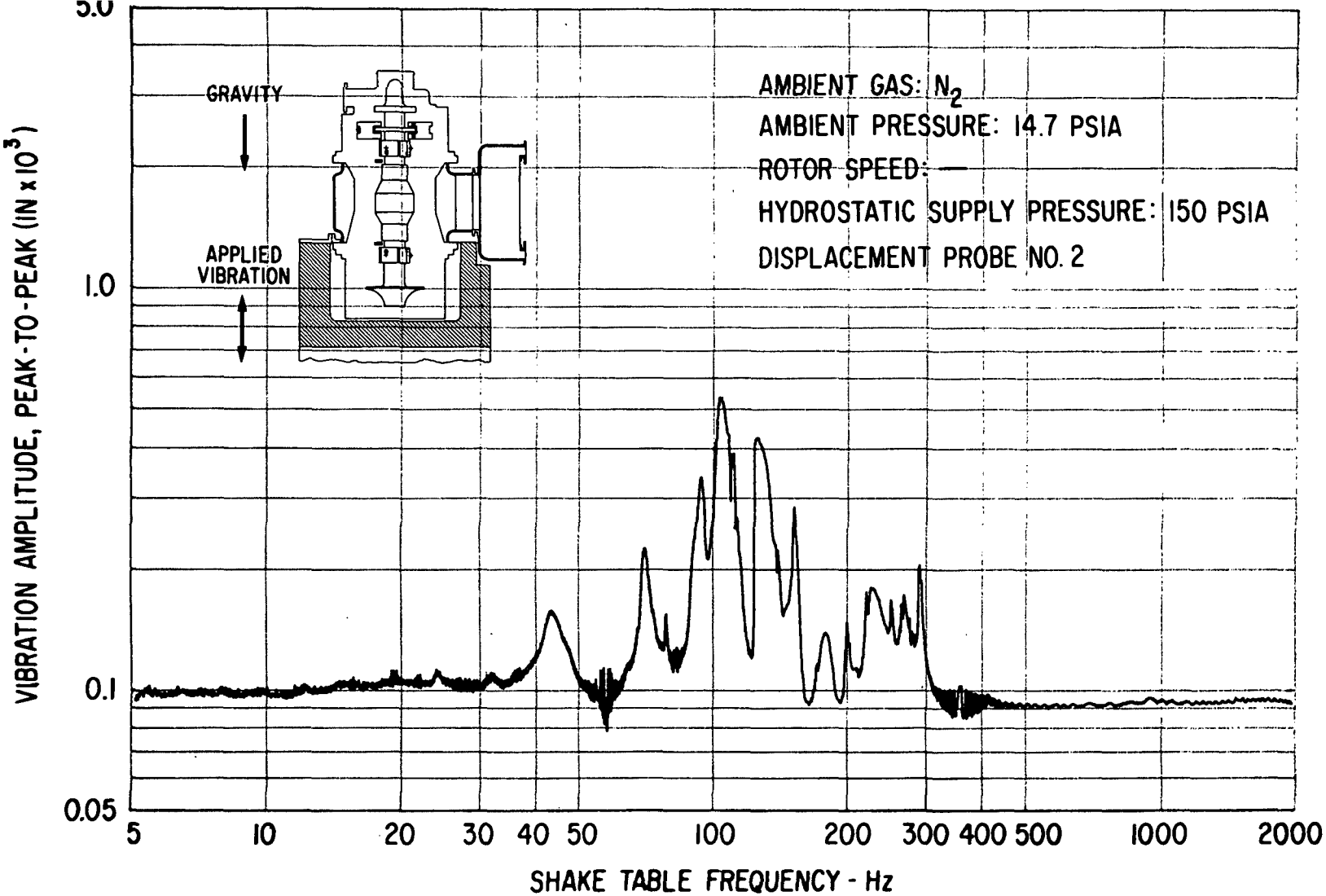

Fig. 48 Compressor Journal Rotor Amplitudes (Casing-to-Shaft) Under Externally-Imposed Sinusoidal Vibration of 0.25 g Peak

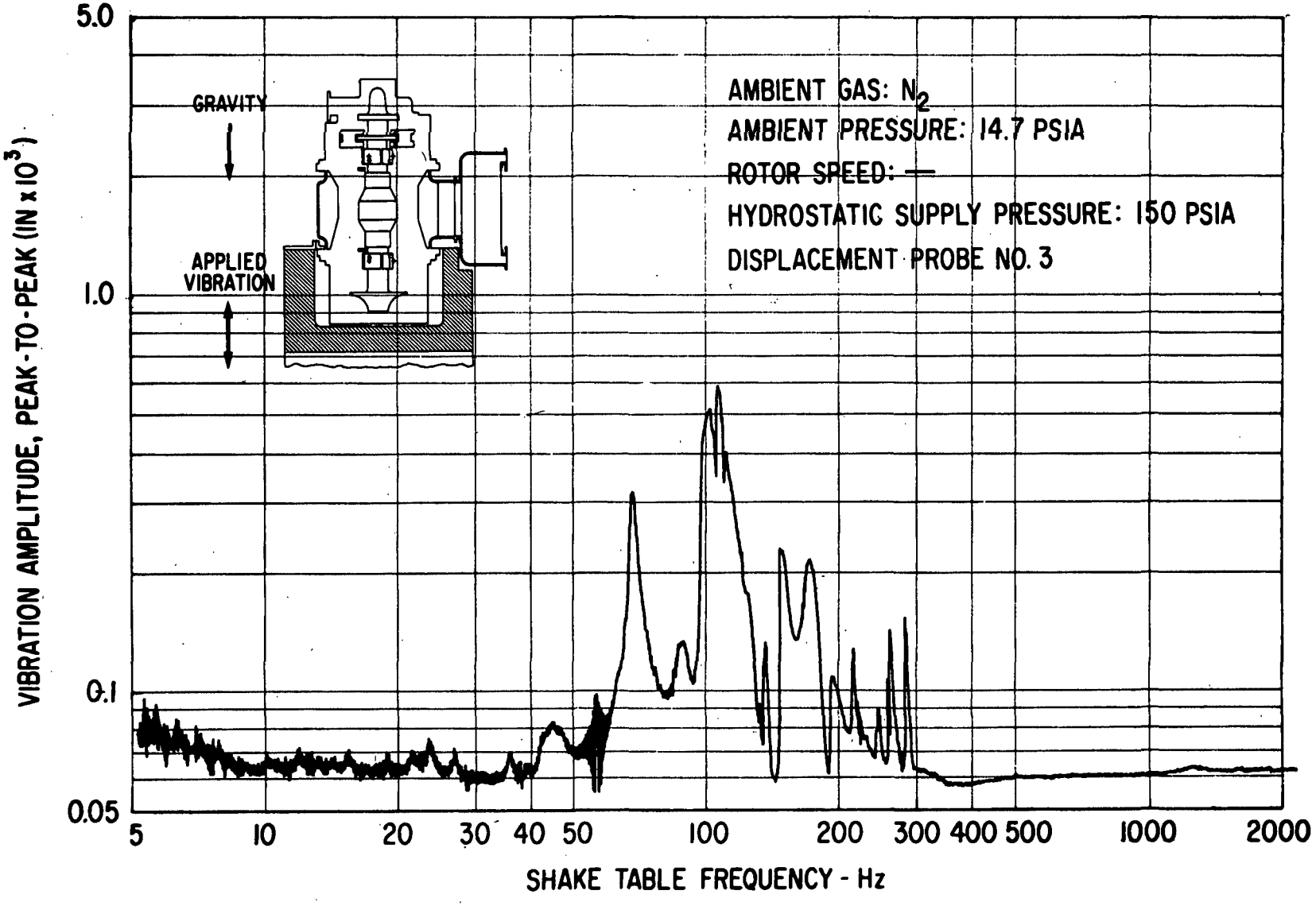

Fig. 49 Turbine Journal Rotor Amplitudes (Casing-to-Shaft) Under Externally-Imposed Sinusoidal Vibration of 0.25 g Peak

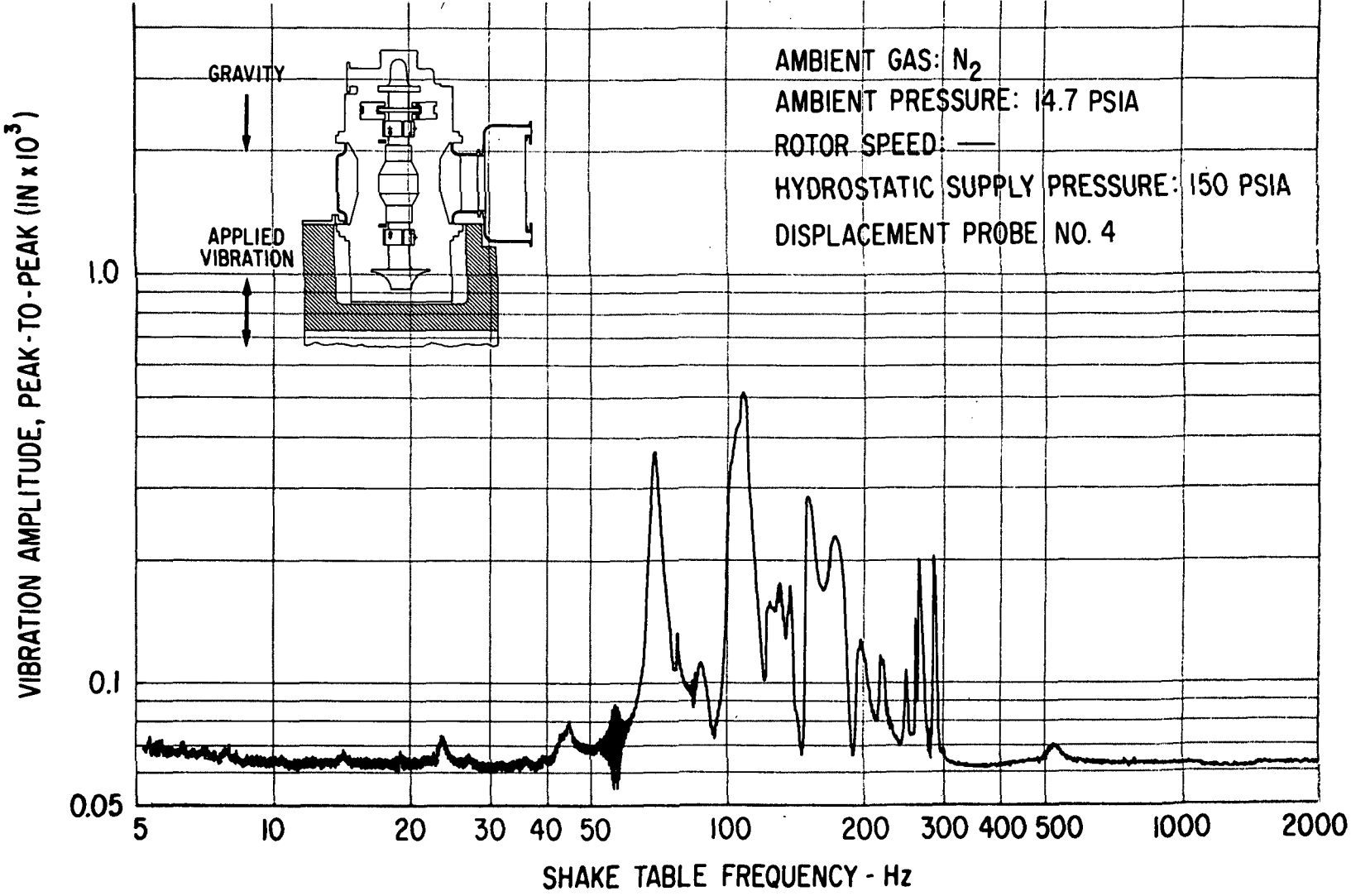

Fig. 50 Turbine Journal Rotor Amplitudes (Casing-to-Shaft) Under Externally-Imposed Sinusoidal Vibration of 0.25 g Peak

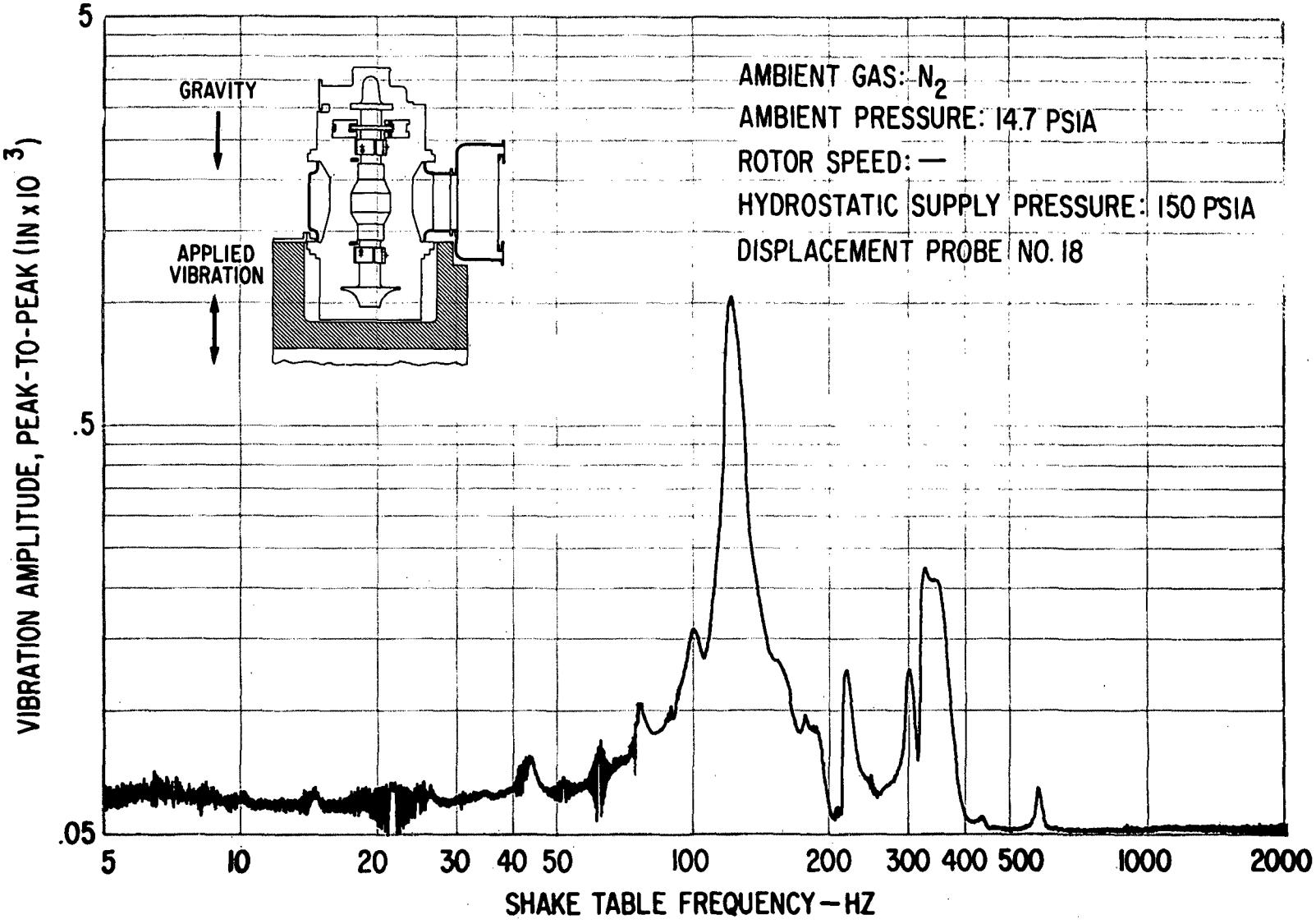

Fig. 51 Thrust Bearing Film Thickness Variation Under Externally-Imposed Sinusoidal Vibrations of 0.25 g Peak

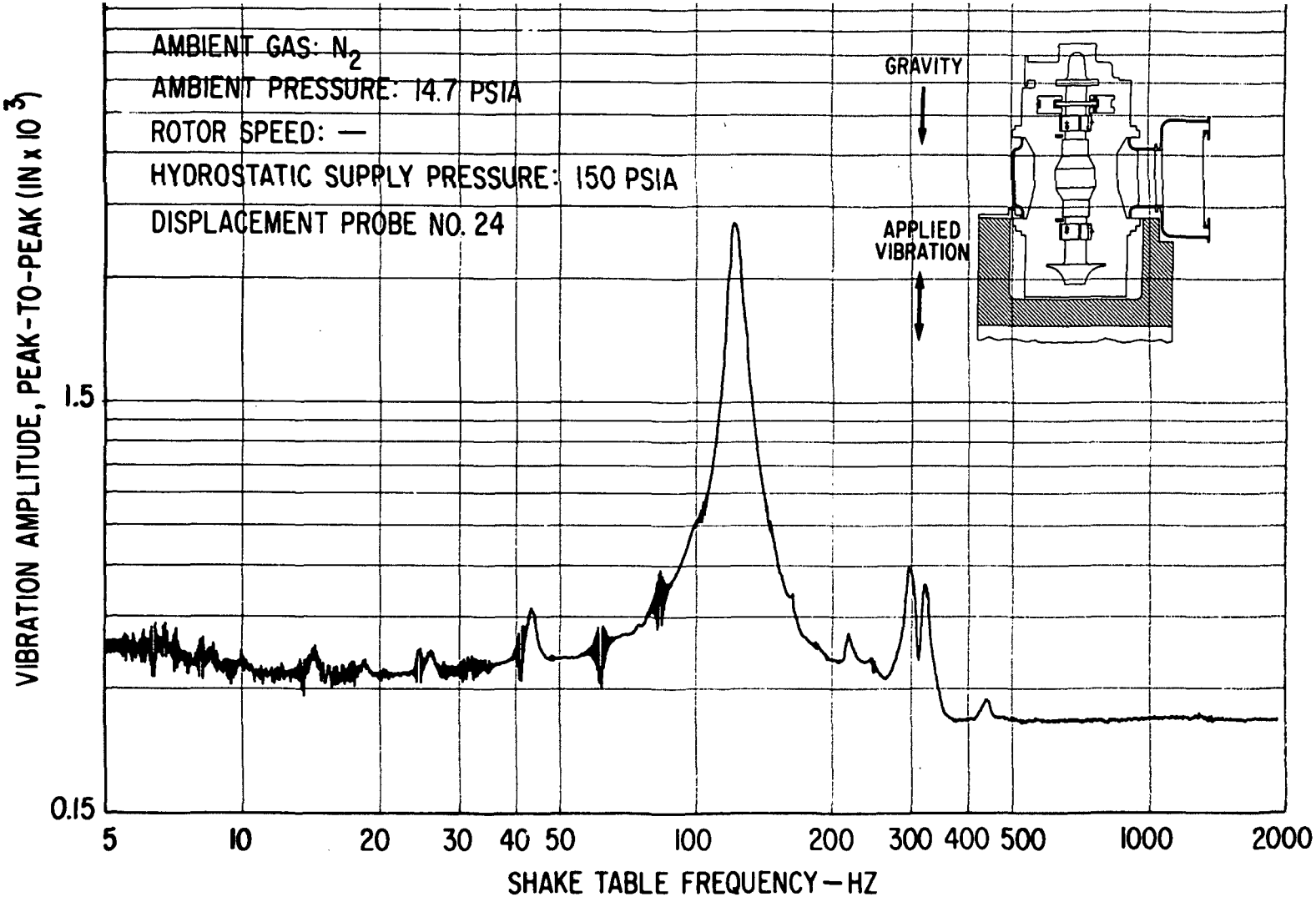

Fig. 52 Thrust Bearing Gimbal Amplitudes Under Externally-Imposed Sinusoidal Vibration of 0.25 g Peak

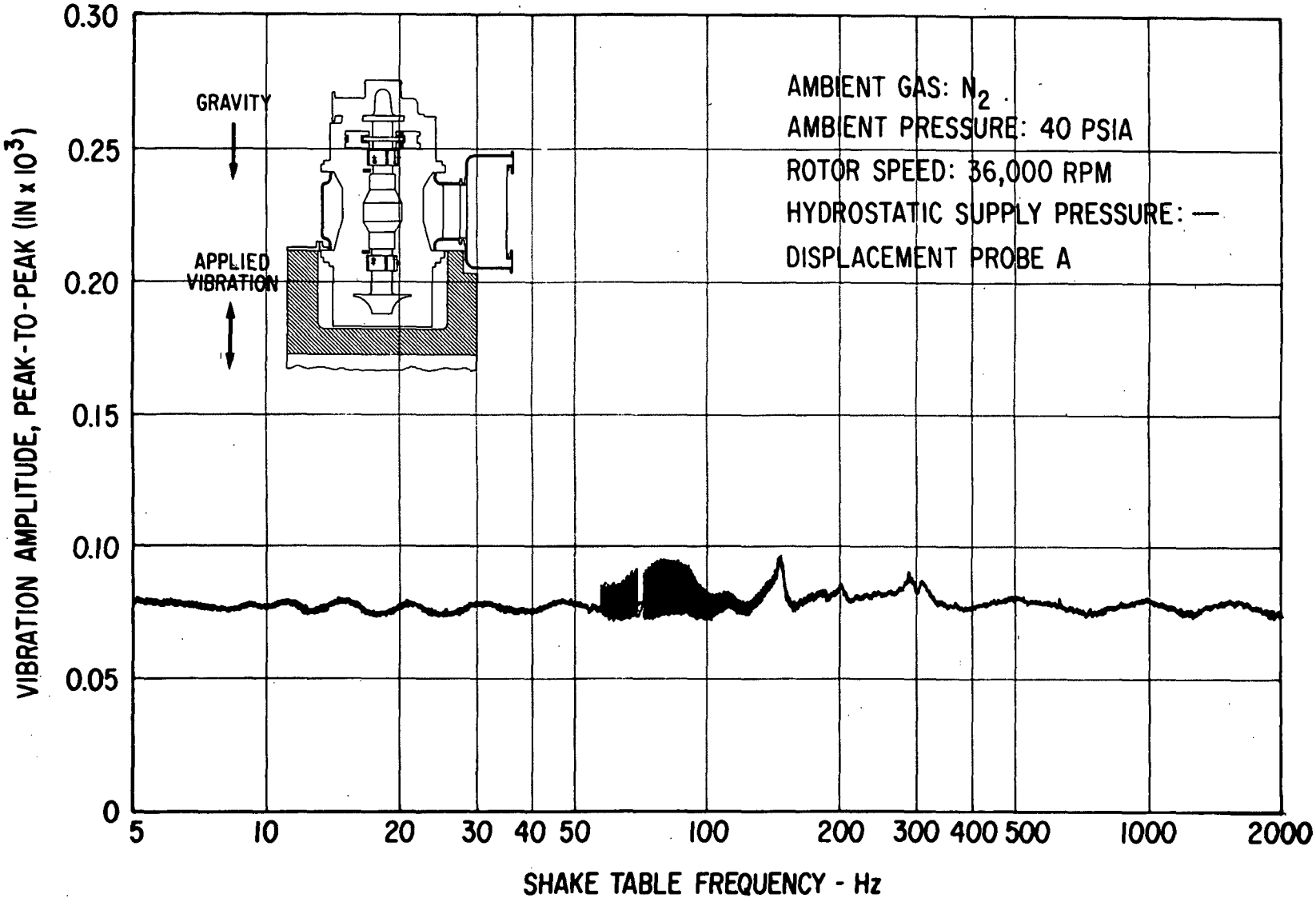

Fig. 53 Pad-To-Shaft Pivot Film Thickness Variation for Flex-Mounted Compressor Journal Bearing Pad Under Externally-Imposed Sinusoidal Vibration of 0.12 g Peak

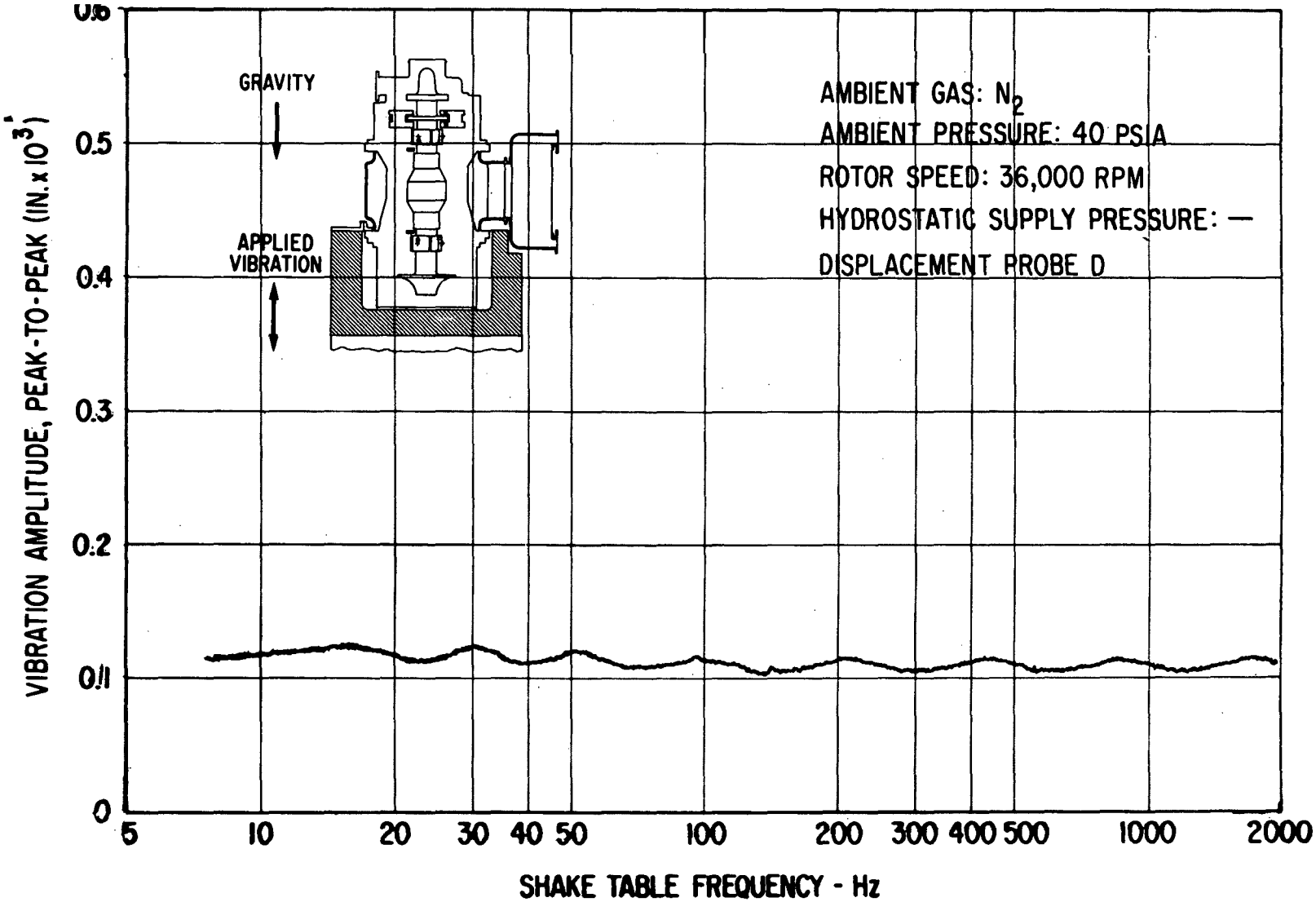

Fig. 54 Pad-To-Shaft Pivot Film Thickness Variation for Flex-Mounted Turbine Journal Bearing Pad Under Externally-Imposed Sinusoidal Vibration of 0.12 g Peak

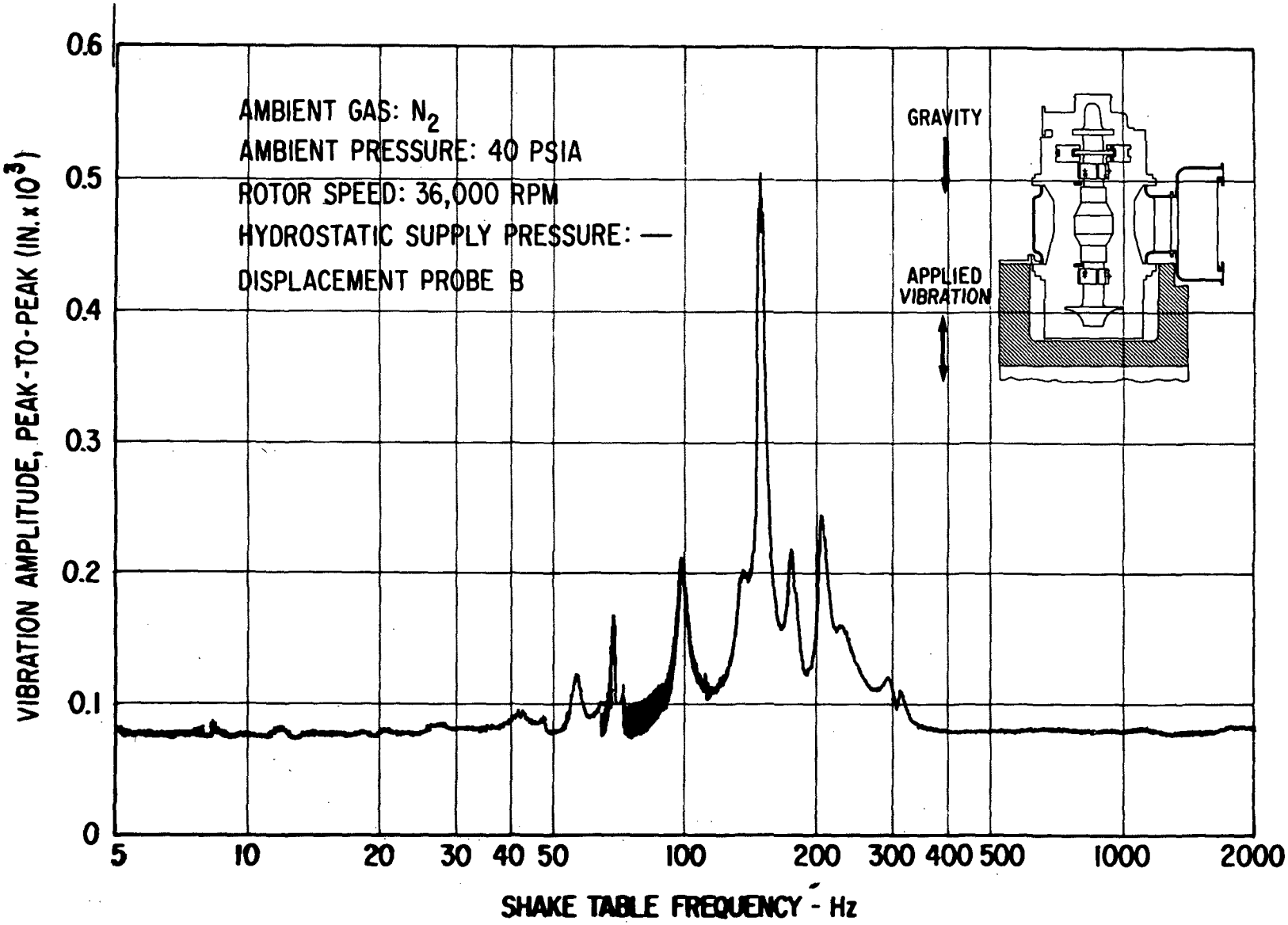

Fig. 55 Pad-To-Shaft Pivot Film Thickness Variation for Solid-Mounted Compressor Journal Bearing Pad Under Externally-Imposed Sinusoidal Vibration of 0.12 g Peak

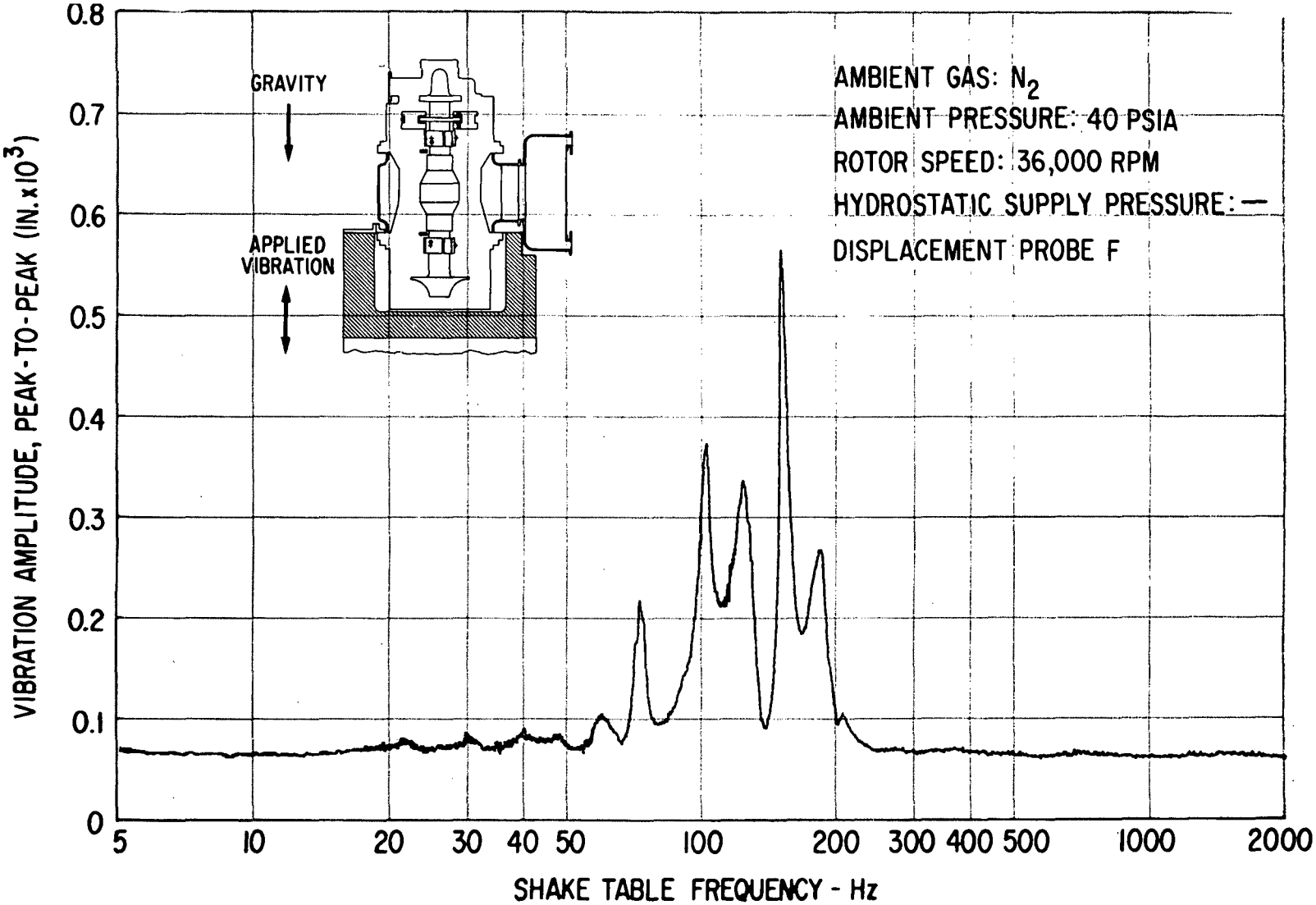

Fig. 56 Pad-To-Shaft Pivot Film Thickness Variation for Solid-Mounted Turbine Journal Bearing Under Externally-Imposed Sinusoidal Vibration of 0.12 g Peak

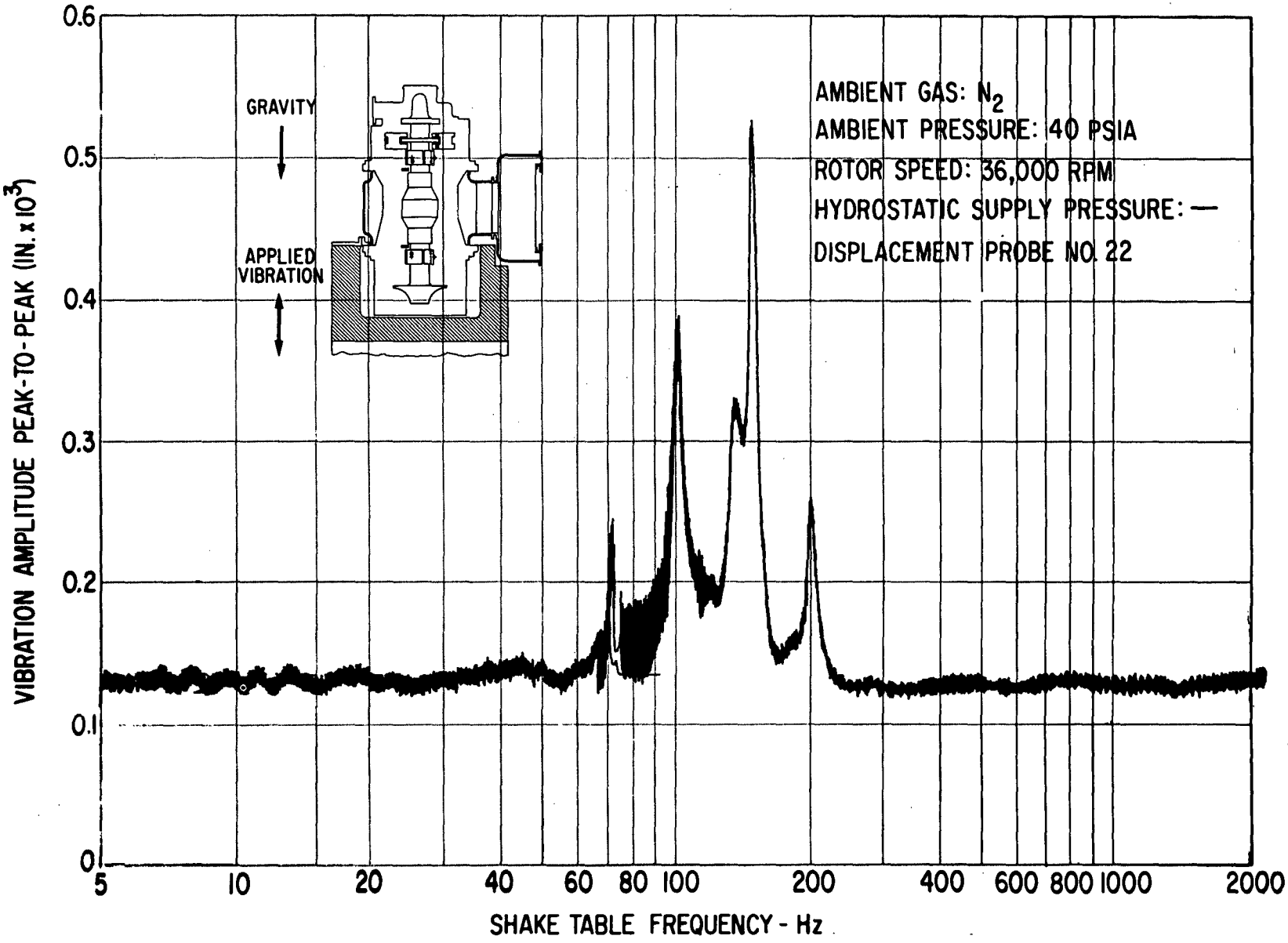

Fig. 57 Compressor Journal Flexure Amplitudes Under Externally-Imposed Sinusoidal Vibration of 0.12 g Peak

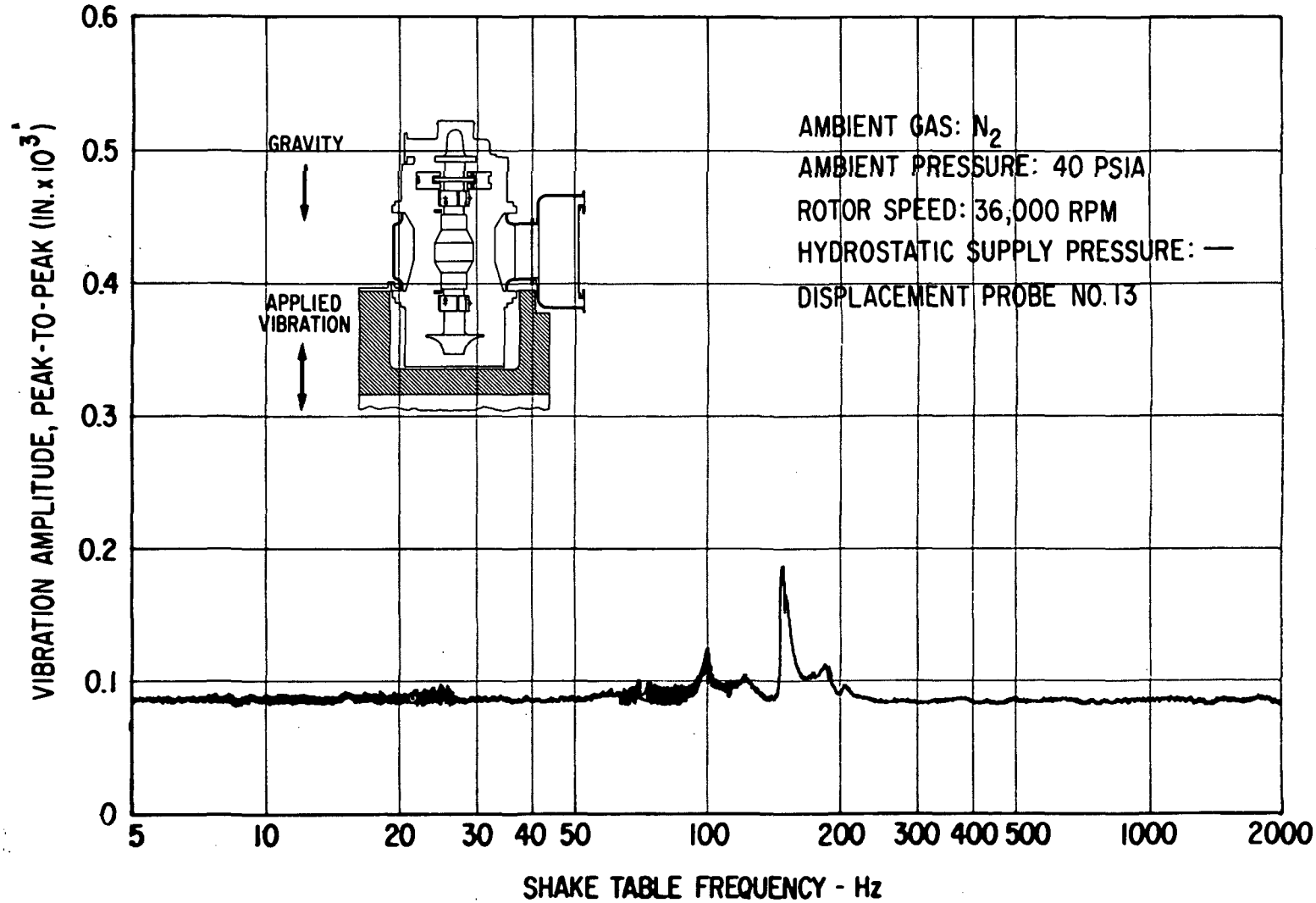

Fig. 58 Casing-To-Pad Leading Edge Amplitudes for Flex-Mounted Turbine Journal Bearing Pad Under Externally-Imposed Vibration of 0.12 g Peak

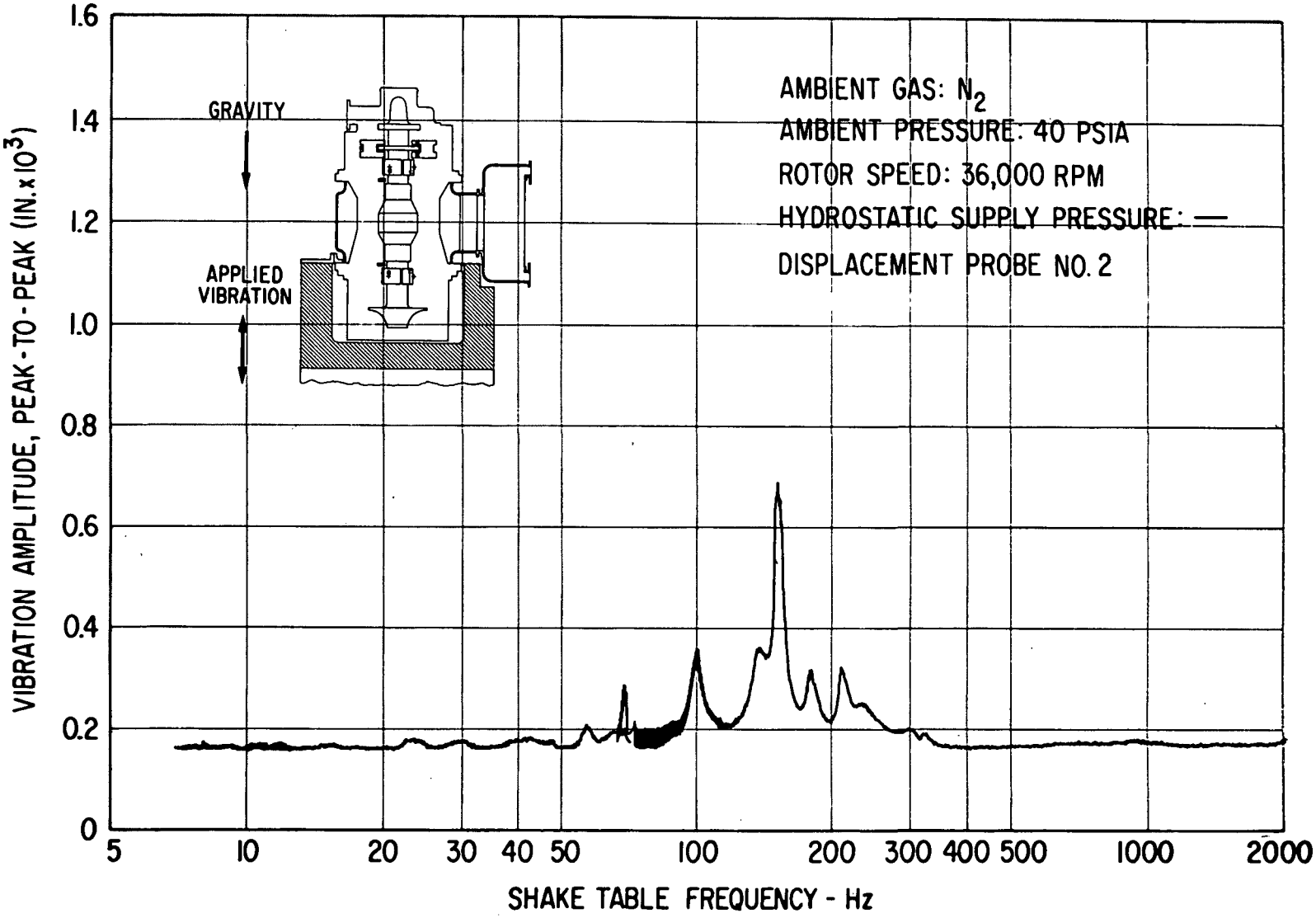

Fig. 59 Compressor Journal Rotor Amplitudes (Casing-To-Shaft) Under Externally-Imposed Sinusoidal Vibration of 0.12 g Peak

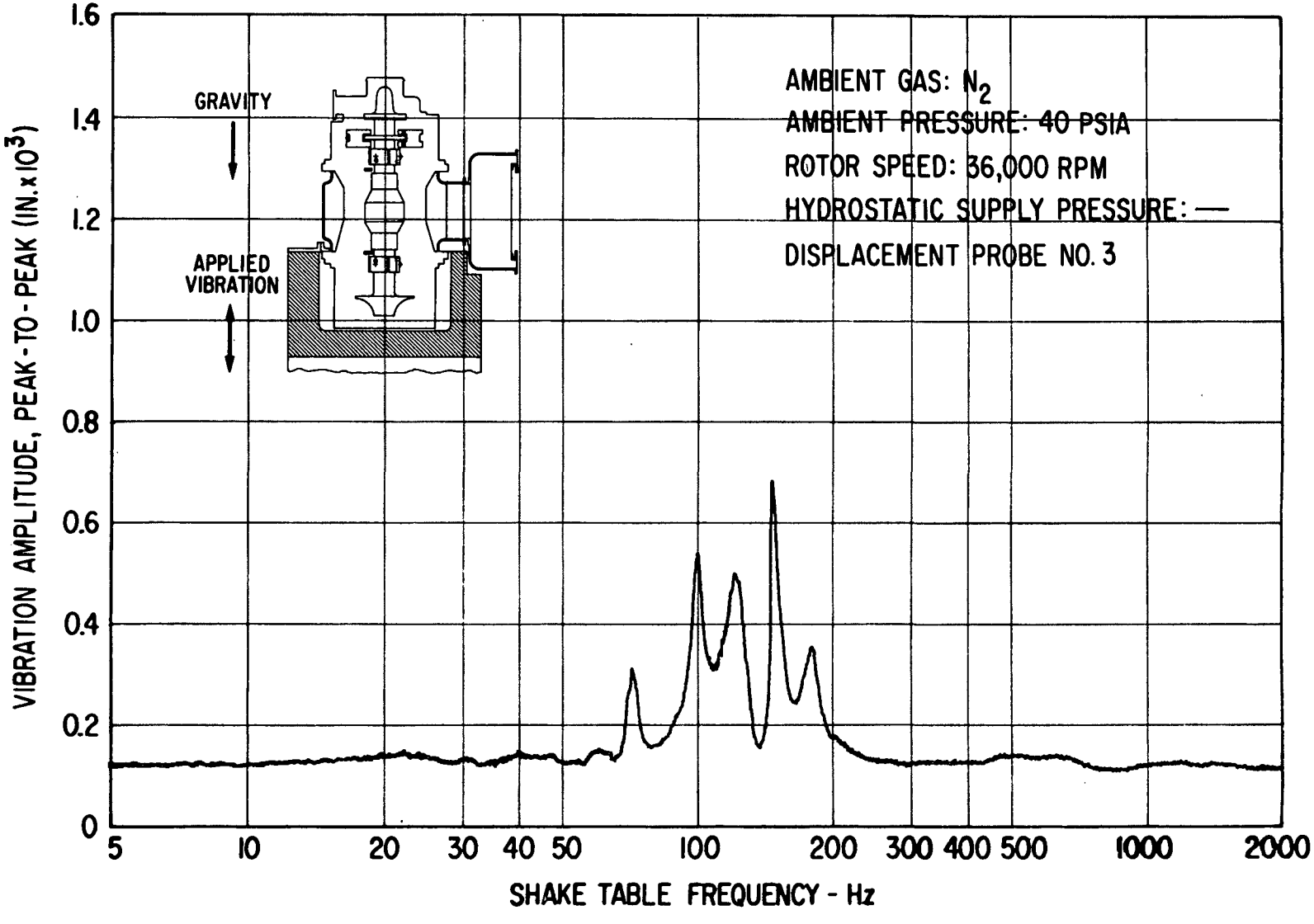

Fig. 60 Turbine Journal Rotor Amplitudes (Casing-To-Shaft) Under Externally-Imposed Sinusoidal Vibration of 0.12 g Peak

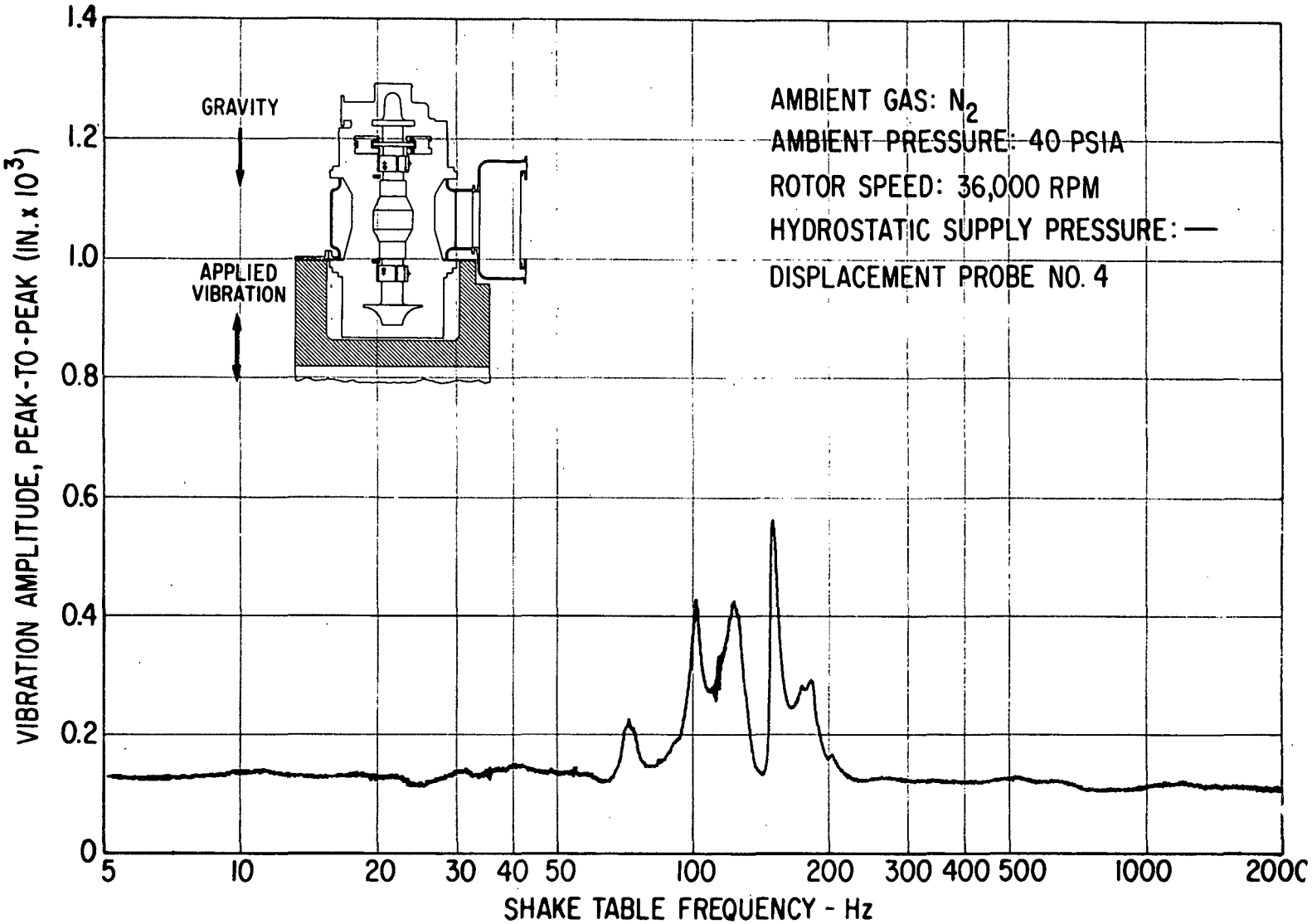

Fig. 61 Turbine Journal Rotor Amplitudes (Casing-To-Shaft) Under Externally-Imposed Sinusoidal Vibration of 0.12 g Peak

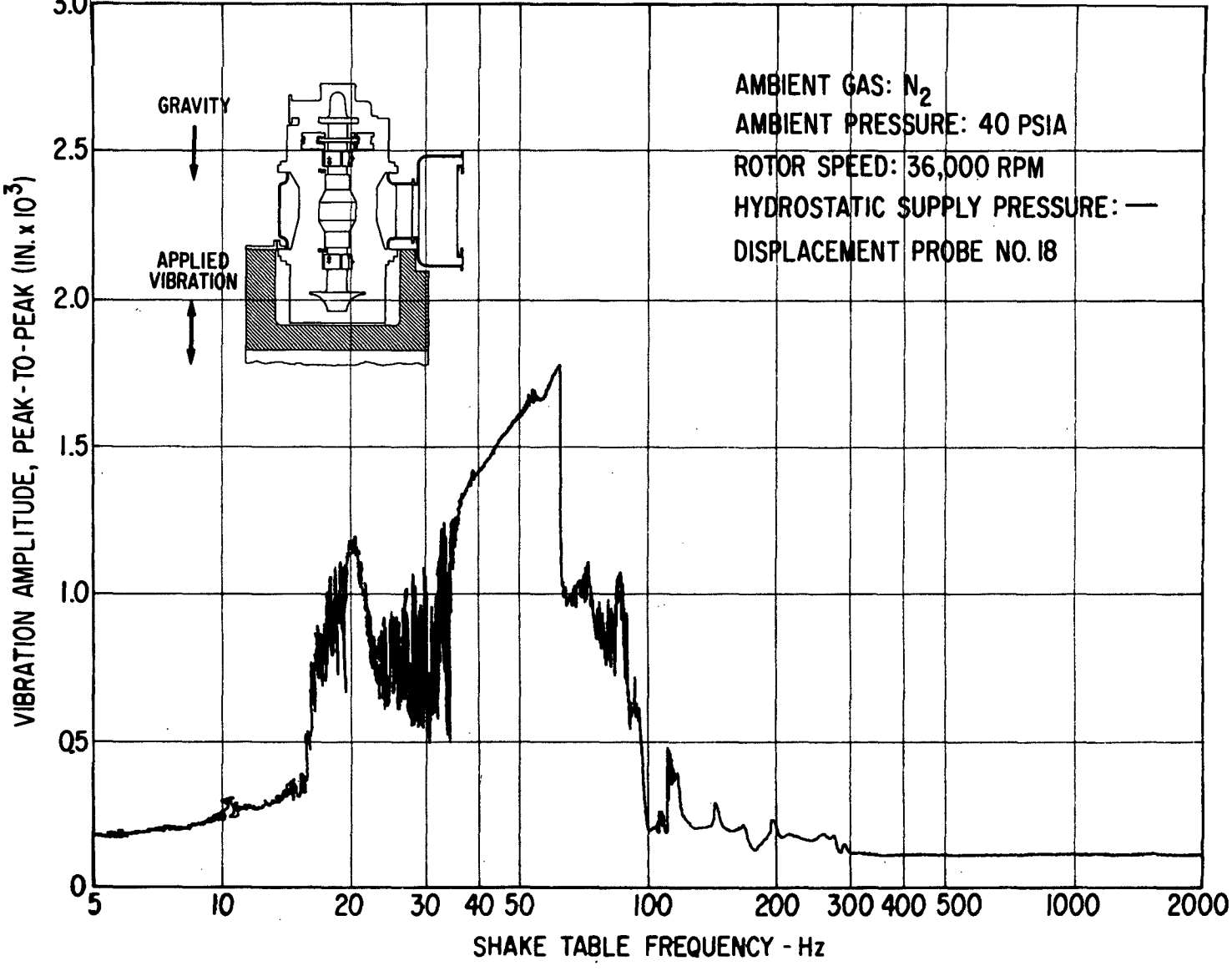

Fig. 62 Thrust Bearing Film Thickness Variation Under Externally-Imposed Sinusoidal Vibrations of 0.12 g Peak

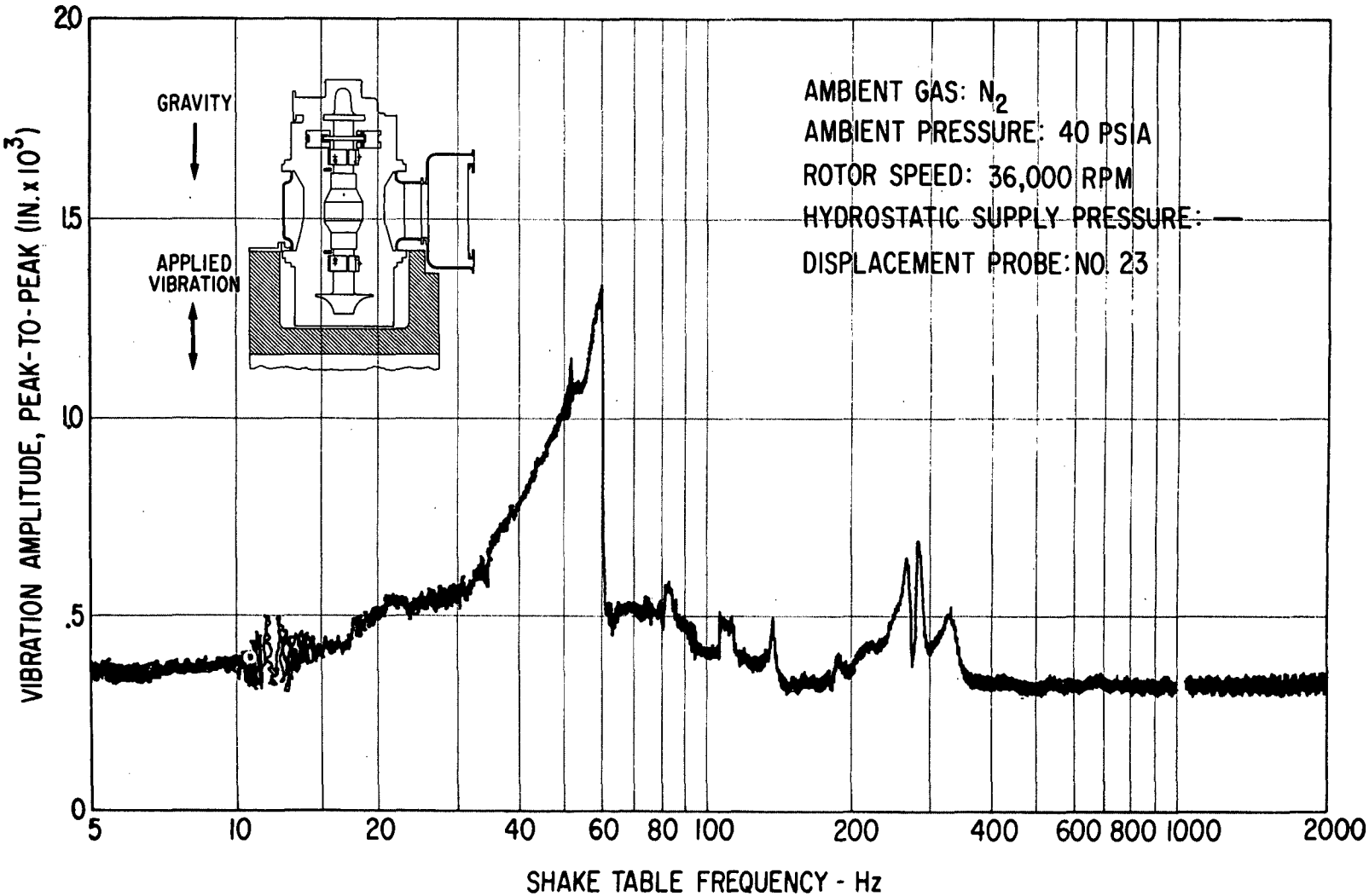

Fig. 63 Thrust Bearing Gimbal Amplitudes Under Externally-Imposed Sinusoidal Vibration of 0.12 g Peak

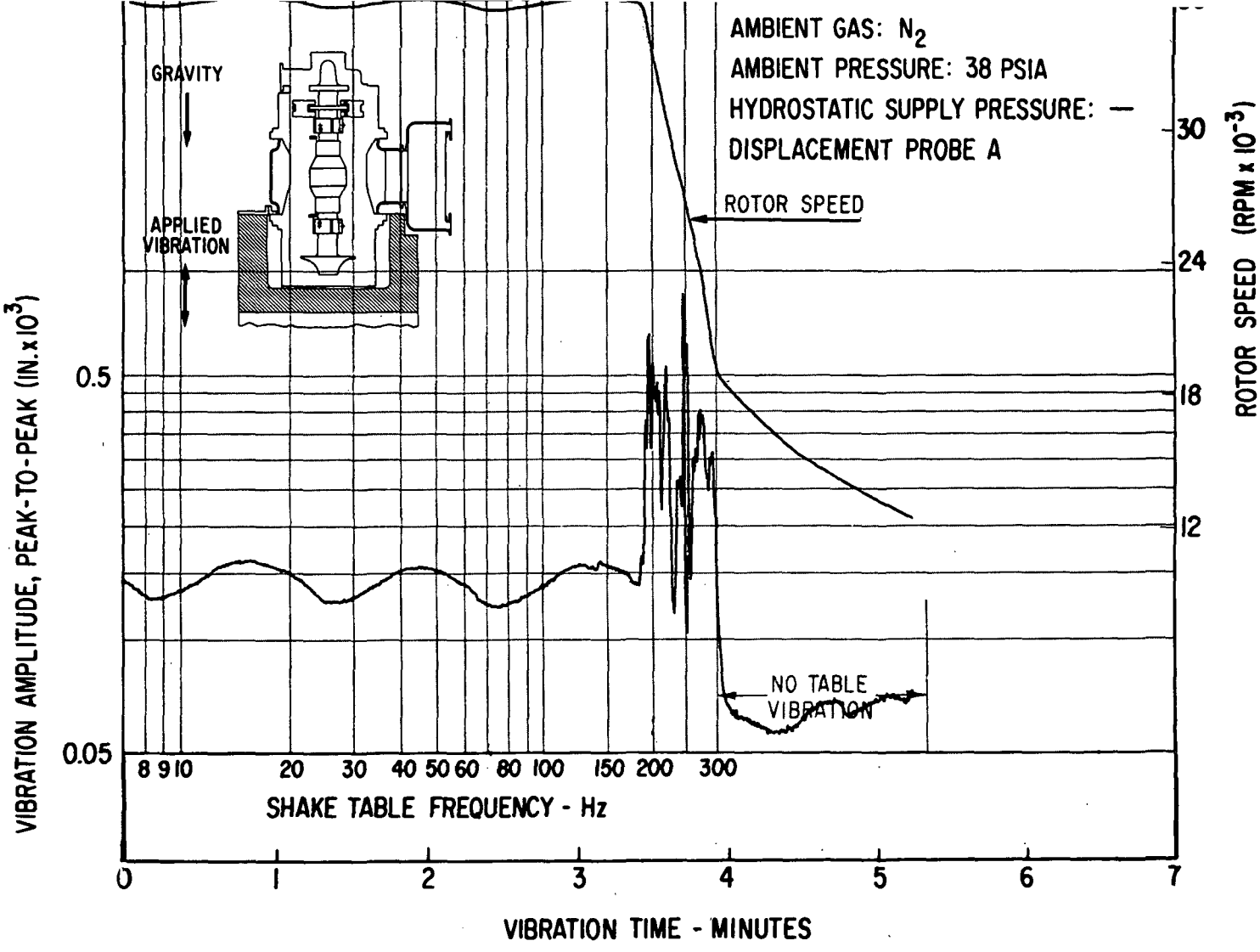

Fig. 64 Pad-To-Shaft Pivot Film Thickness Variation for Flex-Mounted Compressor Journal Bearing Pad (With Rub Occurring at 190 Hz) Under Externally-Imposed Sinusoidal Vibration of 0.12 g Peak

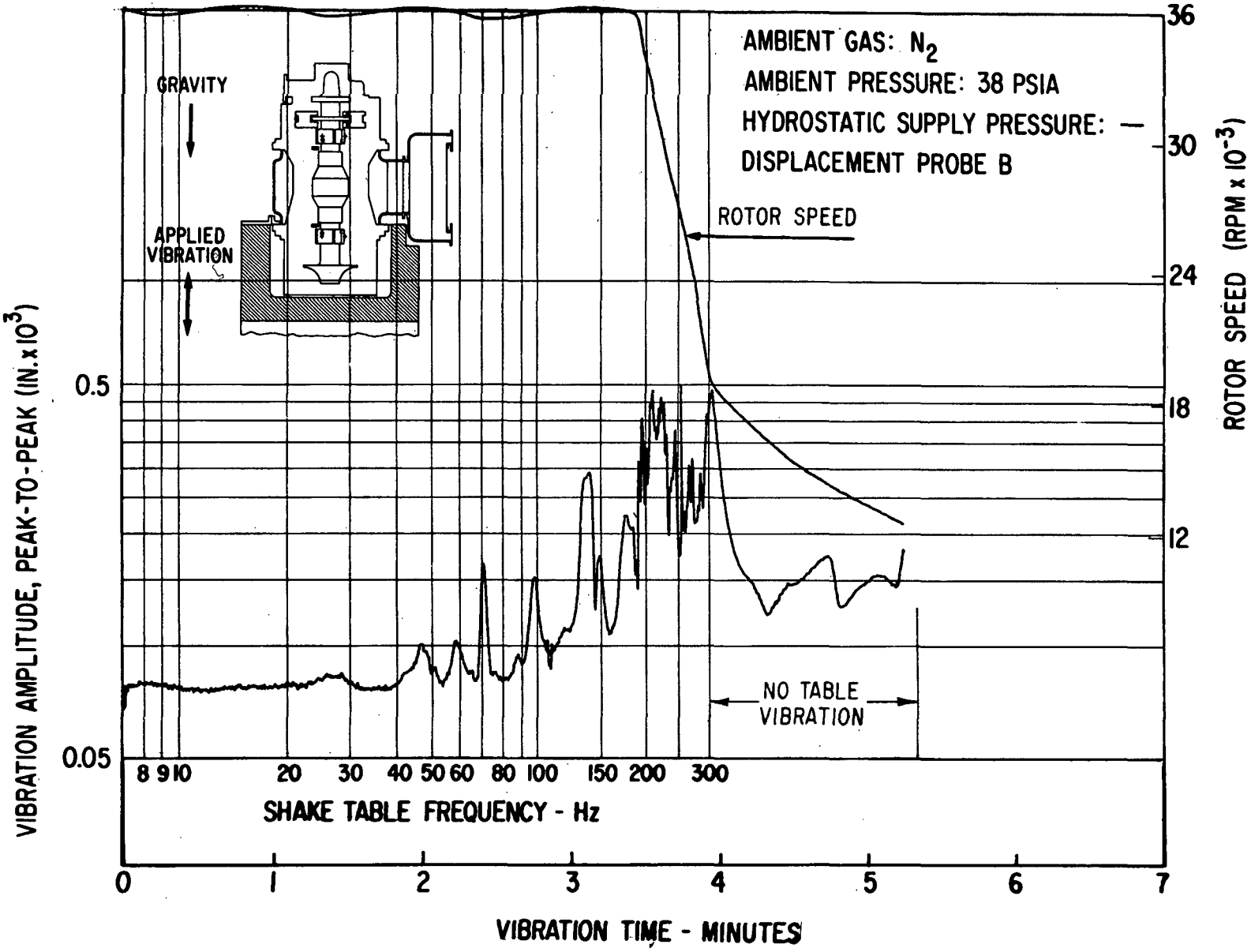

Fig. 65 Pad-To-Shaft Pivot Film Thickness Variation for Solid-Mounted Compressor Journal Bearing Pad (With Rub Occurring at 190 Hz) Under Externally-

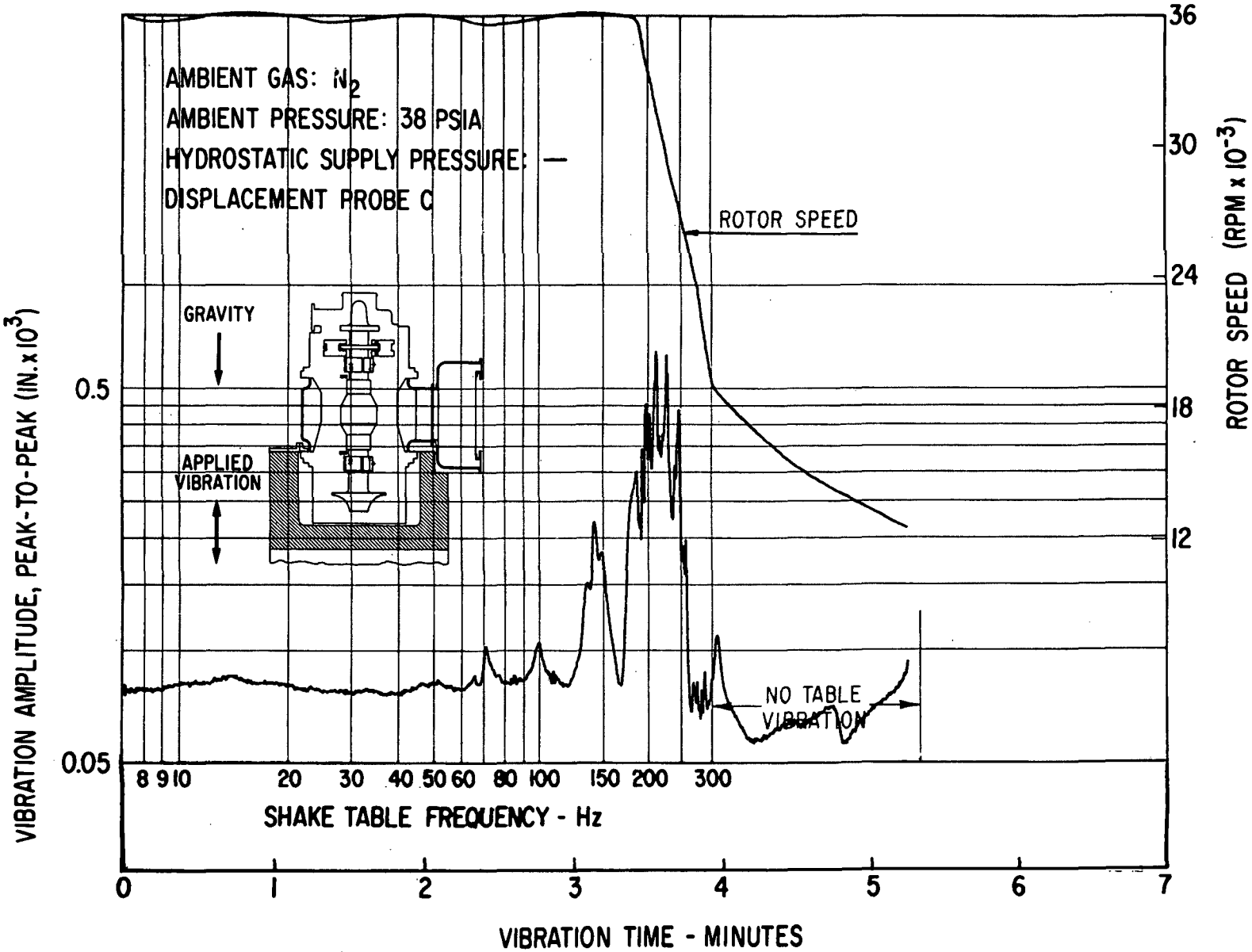

Fig. 66 Pad-To-Shaft Pivot Film Thickness Variation for Solid-Mounted Compressor Journal Bearing Pad (With Rub Occurring at 190 Hz) Under Externally-Imposed Sinusoidal Vibration of 0.12 g Peak

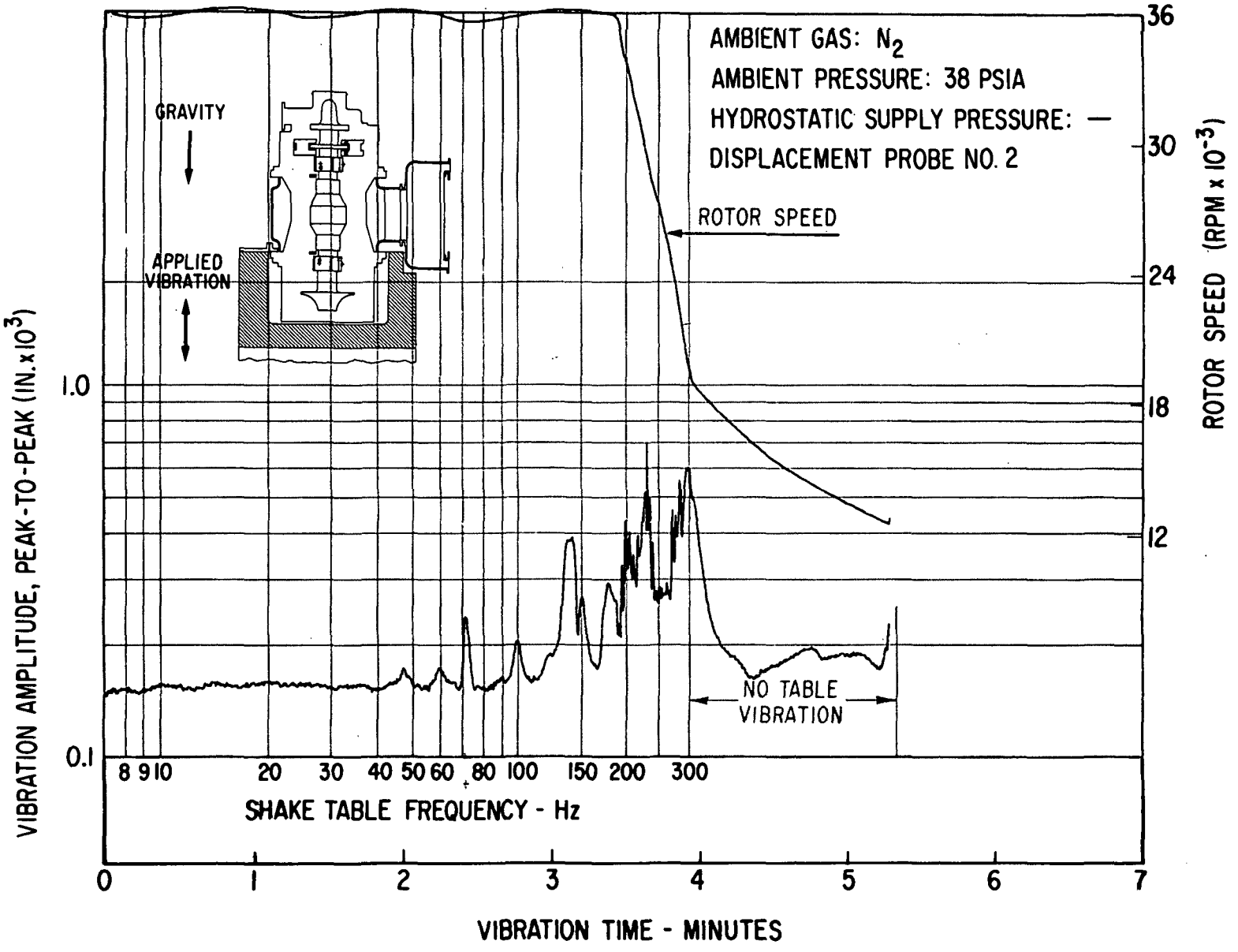

Fig. 67 Compressor Journal Amplitudes (Casing-To-Shaft; With Rub Occurring at 190 Hz) Under Externally-Imposed Sinusoidal Vibrations of 0.12 g Peak

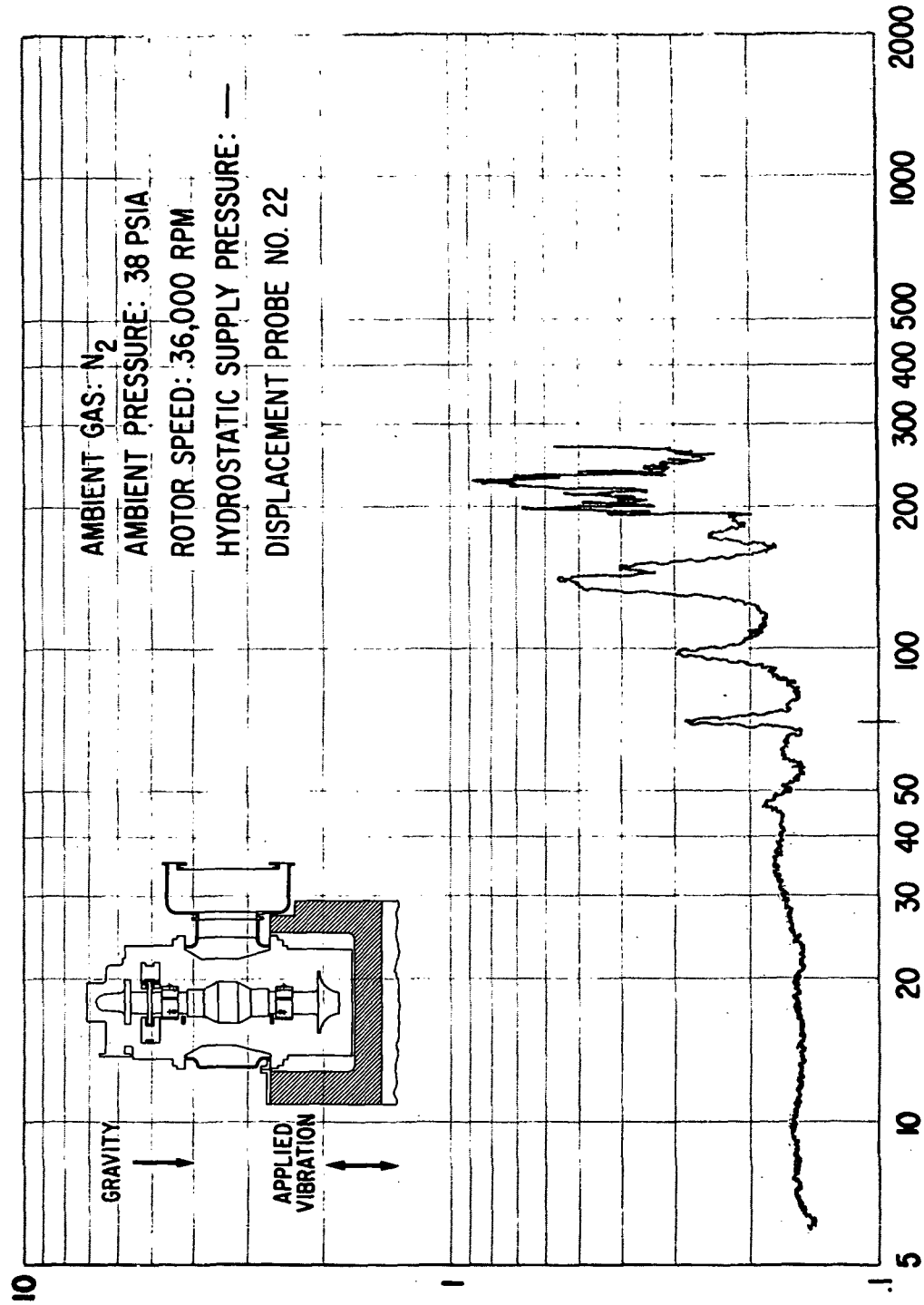

Fig. 68 Compressor Journal Flexure Amplitudes (With Rub Occurring at 190 Hz) Under Externally Imposed Sinusoidal Vibration of 0.12 g Peak

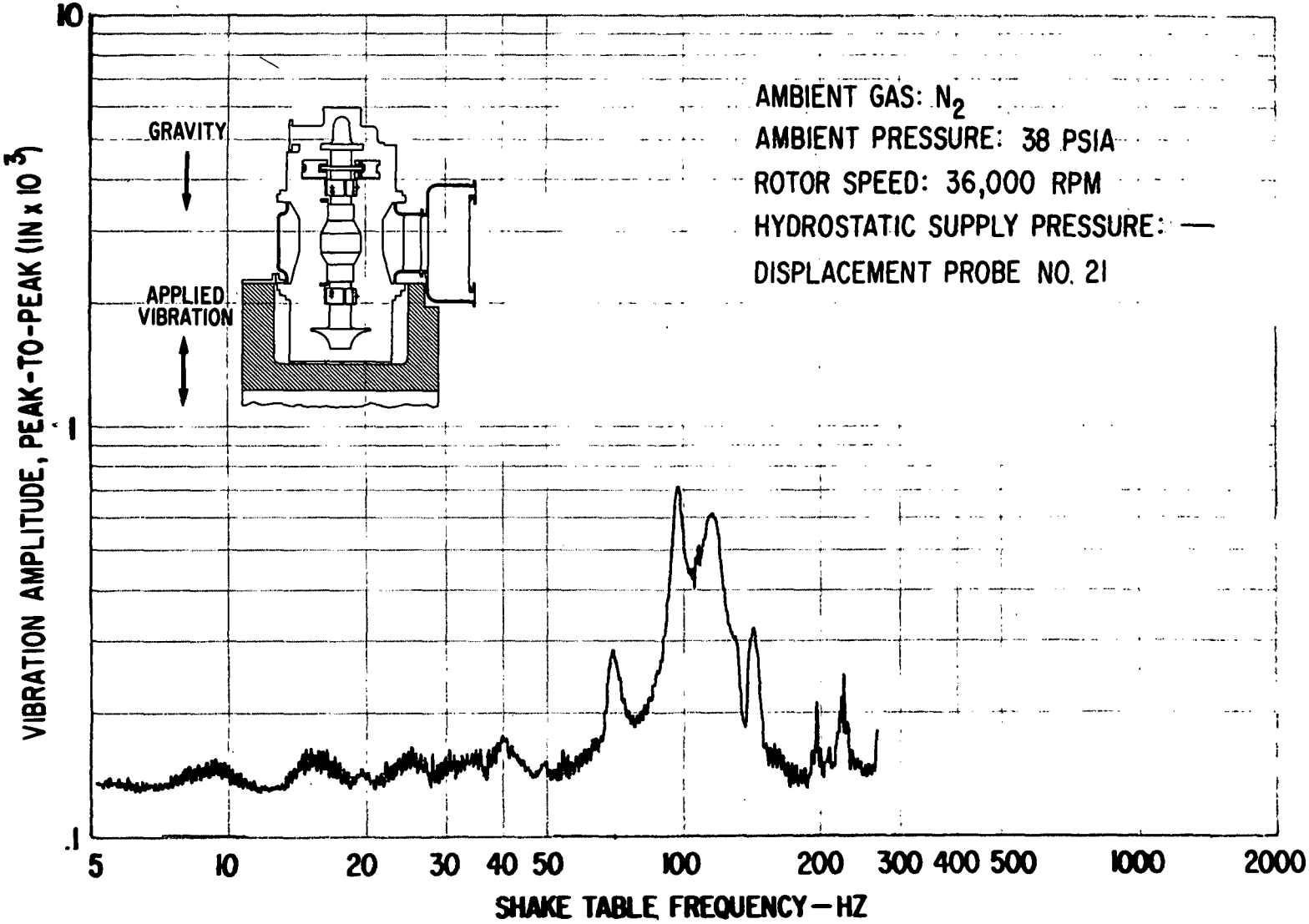

Fig. 69 Turbine Journal Flexure Amplitudes (With Rub Occurring at 190 Hz) Under Externally Imposed Vibration of 0.12 g Peak

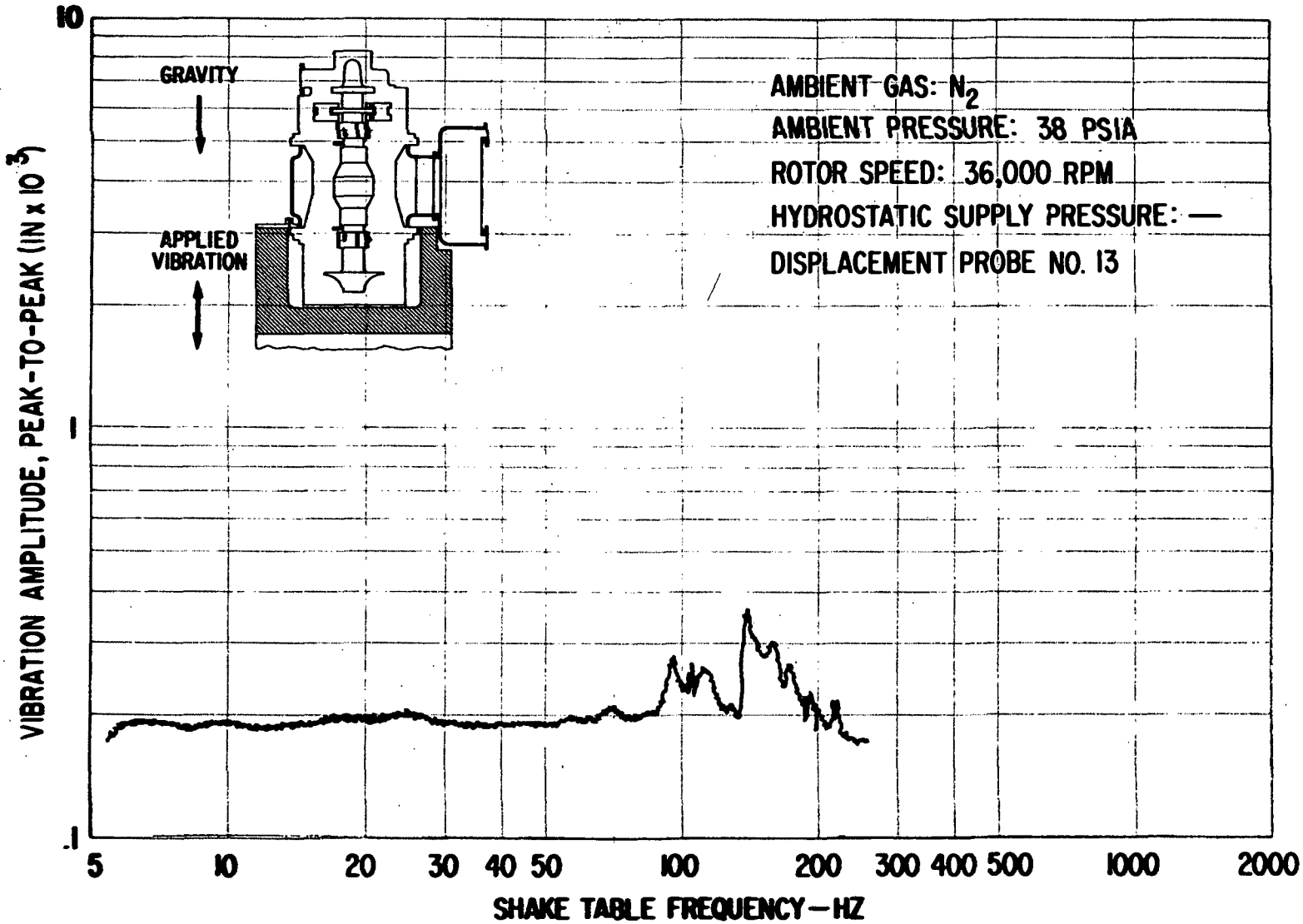

Fig. 70 Casing-To-Pad Leading Edge Amplitudes for Flex-Mounted Turbine Journal Bearing Pad (With Rub Occurring at 190 Hz) Under Externally-Imposed Vibration of 0.12 g Peak

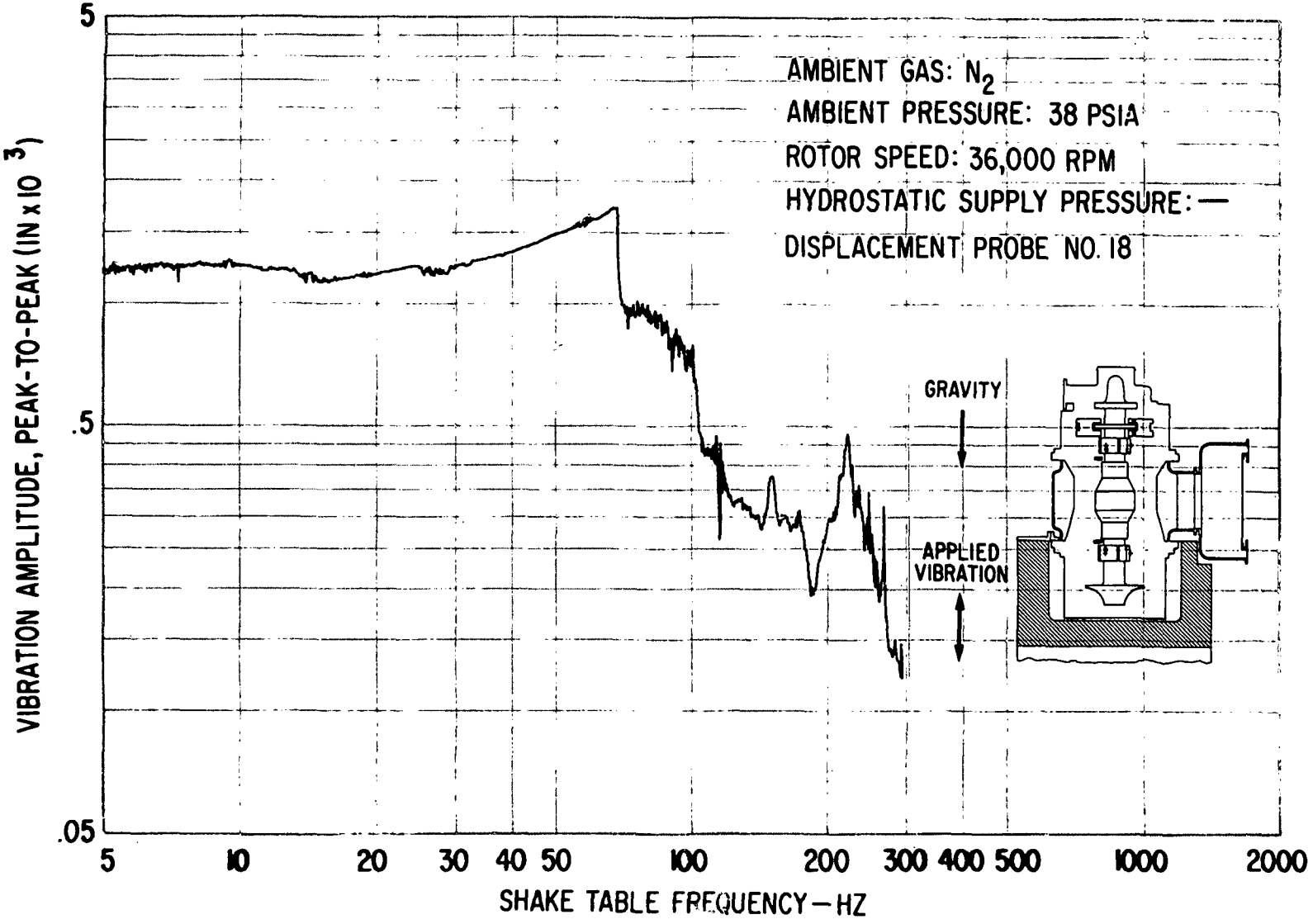

Fig. 71 Thrust Bearing Film Thickness Variation (With Rub Occurring at 190 Hz) Under Externally-Imposed Sinusoidal Vibration of 0.12 g Peak

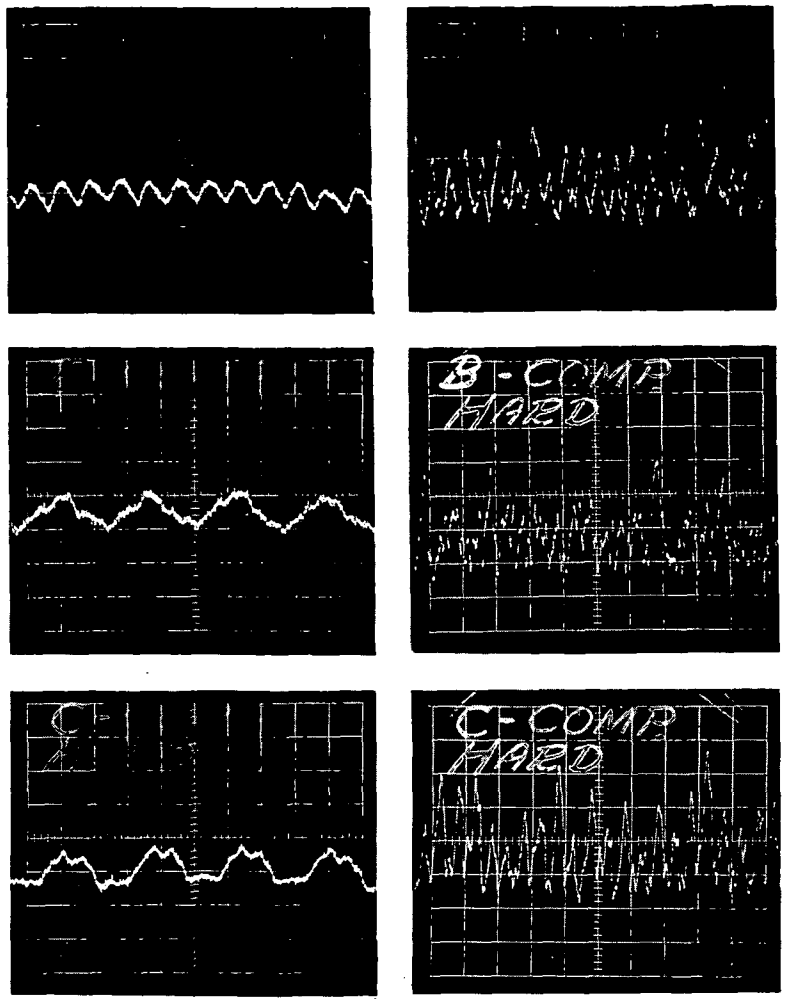

LEVEL OF APPLIED VIBRATION: 0.12 G SINE

ROTOR SPEED: 36,000 RPM

VIBRATION TABLE FREQUENCY WHEN CONTACT OCCURRED BETWEEN COMPRESSOR JOURNAL PADS AND SHAFT: 190 Hz

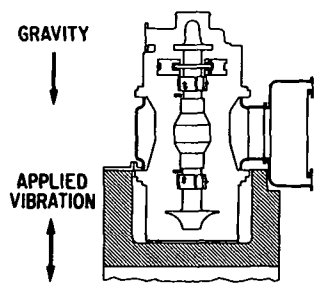

ig. 72 Pad-To-Shaft Pivot Film Thickness Variation For Compressor Journal Bearing Pads (With Rub Occurring at 190 Hz) Under Externally-Imposed Sinusoidal Vibration of 0.12 g Peak

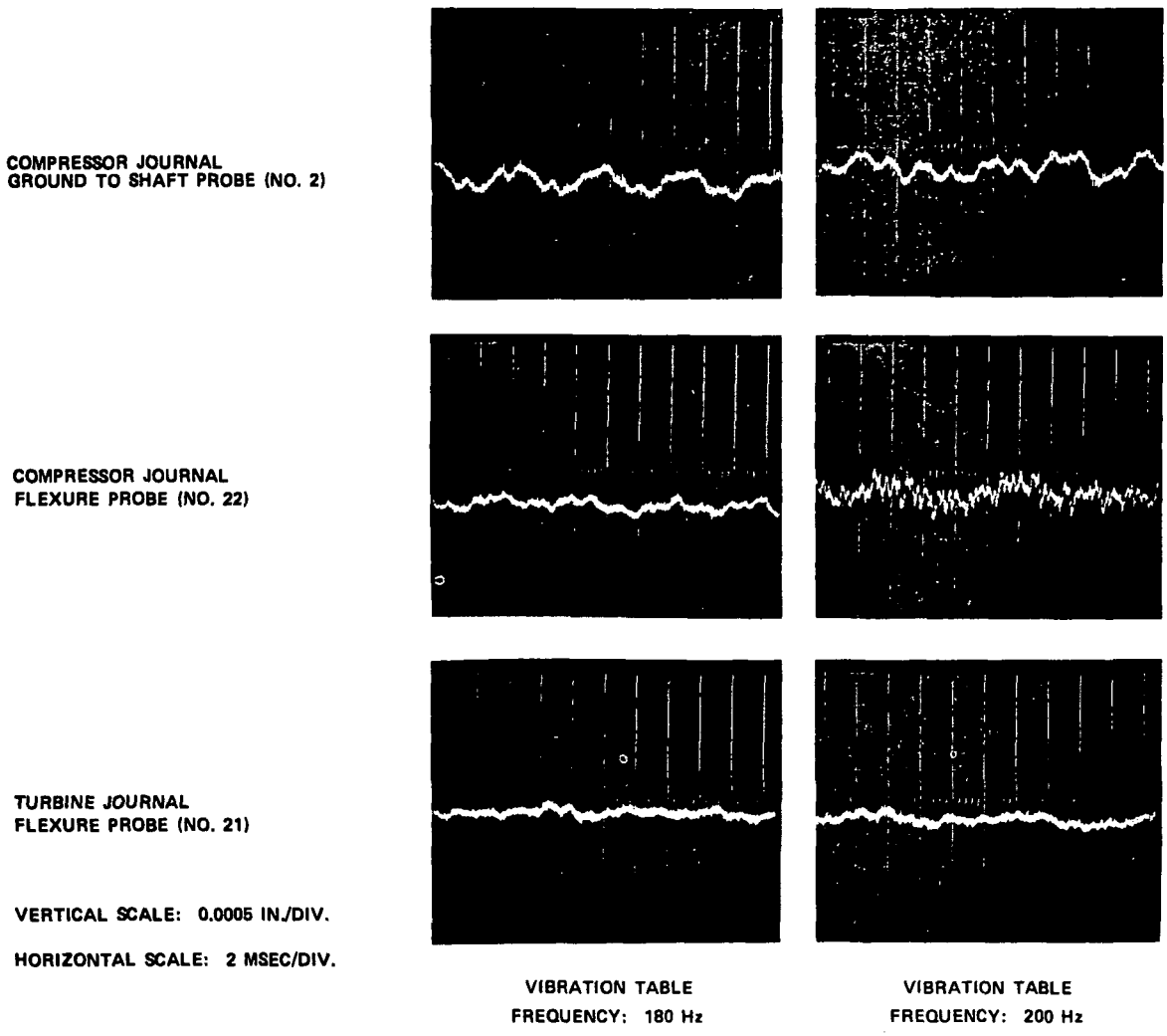

Fig. 73 Rotor and Flexure Amplitudes (With Rub Occurring at 190 Hz) Under Externally-Imposed Sinusoidal Vibration Of 0.12 g Peak

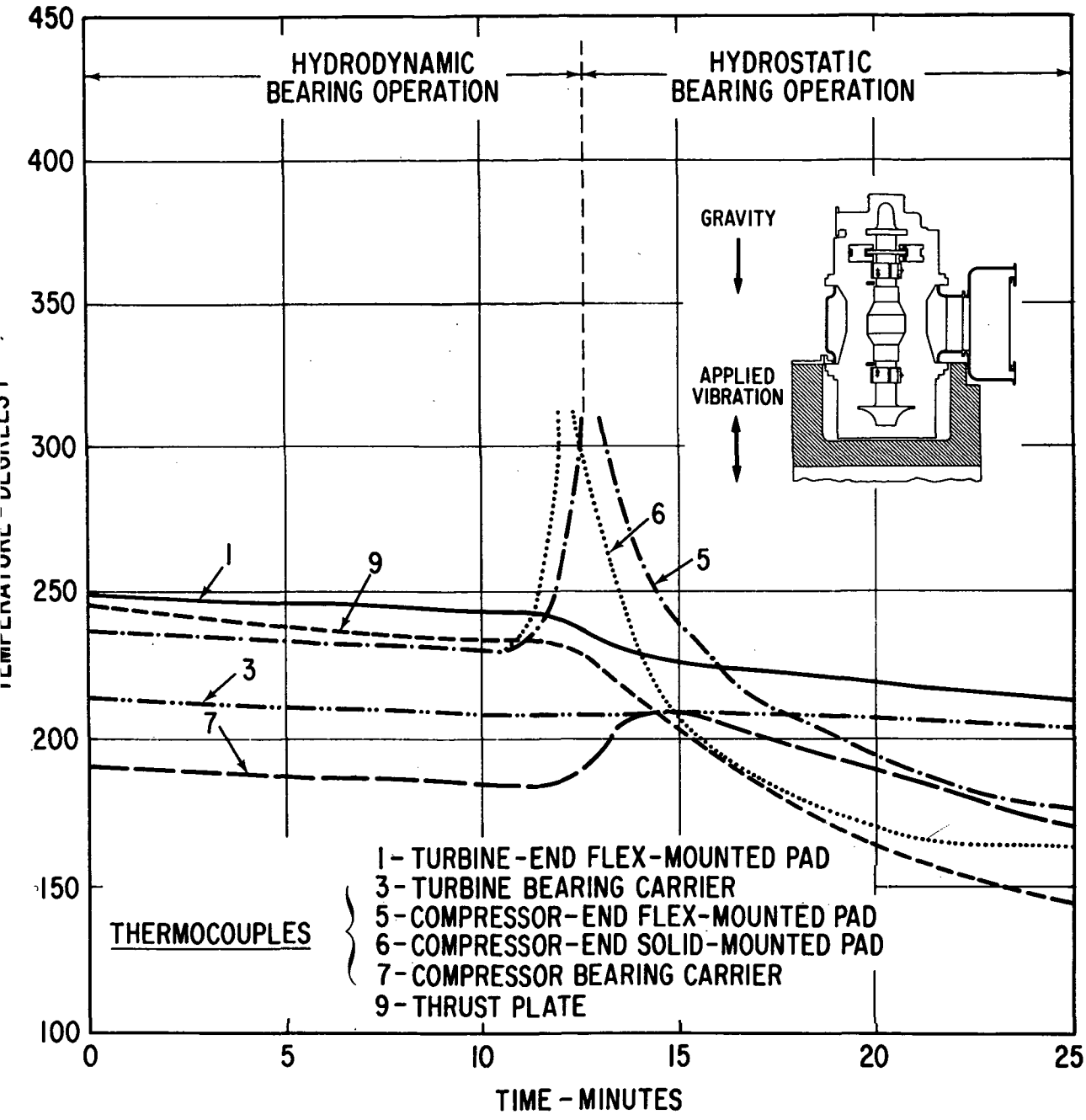

Fig. 74 Measured Temperatures In BRU Simulator Components (With Rub Occurring in Compressor-End Journal Bearing) Under Externally-Imposed Sinusoidal Vibration Of 0.12 g Peak

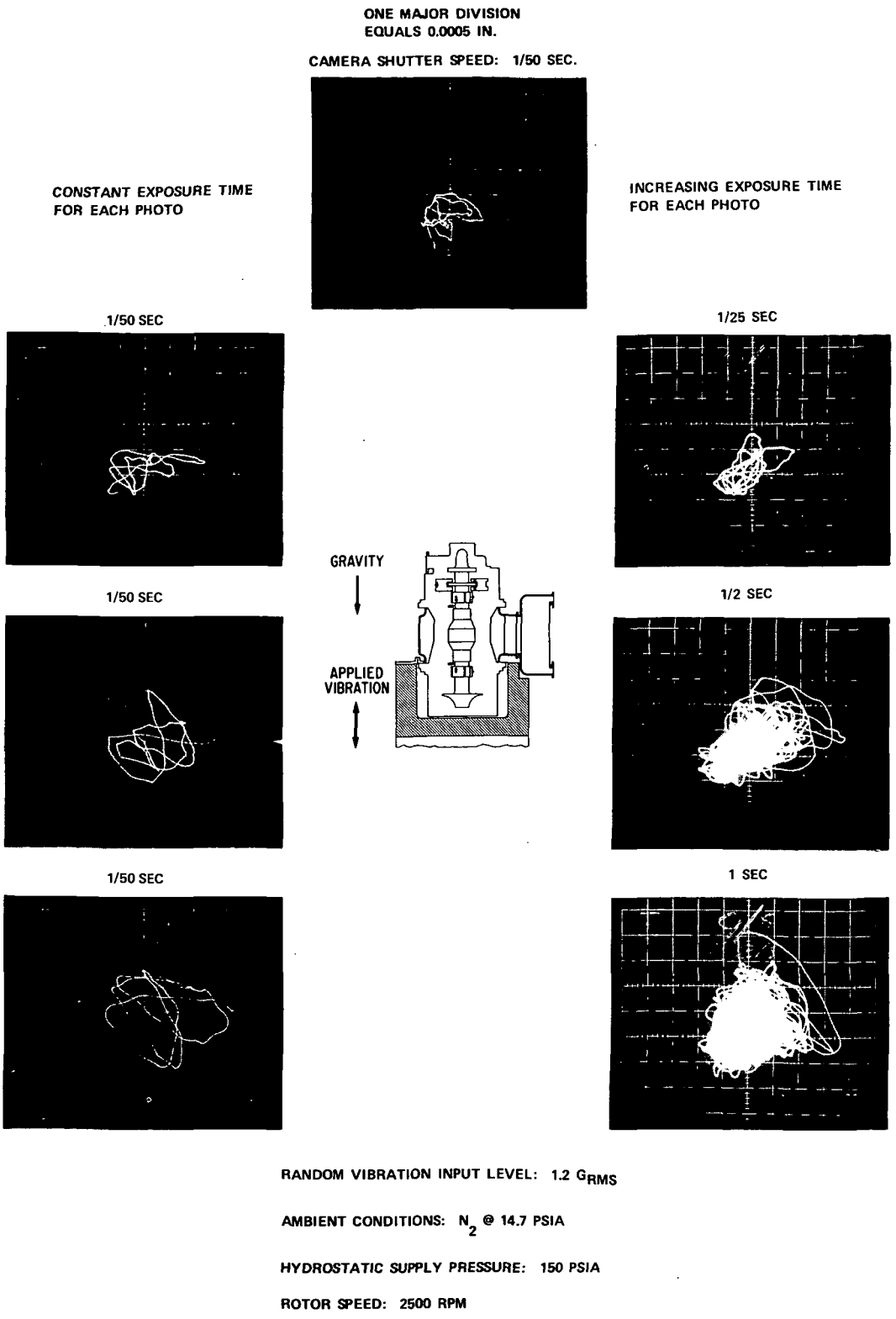

Fig. 75 Rotor Amplitudes (Casing-To-Shaft) Under Shaped Random Vibrations According To NASA Spec 417-2-C-3.5

UPPER TRACE: FLEX. MOUNTED PAD (D)
TURRINE JOURNAL

LOWER TRACE: FLEX. MOUNTED PAD (A)
COMPRESSOR JOURNAL

VERTICAL SCALE: 0.00025 IN./DIV.

HORIZONTAL SCALE: 20 MSEC/DIV.

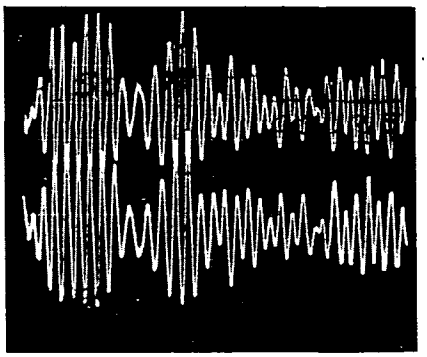

UPPER TRACE: SOLID MOUNTED PAD (F)
TURBINE JOURNAL

LOWER TRACE: SOLID MOUNTED PAD (C)
COMPRESSOR JOURNAL

VERTICAL SCALE: 0.00025 IN./DIV.

HORIZONTAL SCALE: 20 MSEC/DIV.

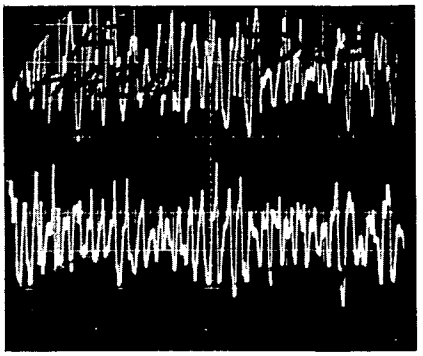

UPPER TRACE: COMPRESSOR JOURNAL
FLEXURE PROBE (NO. 22)

VERTICAL SCALE: 0.0005 IN./DIV.

LOWER TRACE: THRUST BEARING
GIMBAL PROBE (NO. 23)

VERTICAL SCALE: 0.00075 IN./DIV.

HORIZONTAL SCALE: 20 MSEC/DIV.

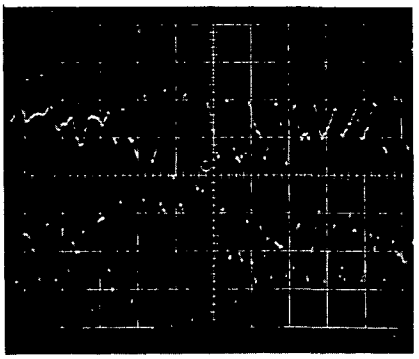

RANDOM VIBRATION INPUT LEVEL: 0.95 G_{RMS}

AMBIENT CONDITIONS: N_2 @ 14.7 PSIA

HYDROSTATIC SUPPLY PRESSURE: 150 PSIA

ROTOR SPEED: 2500 RPM

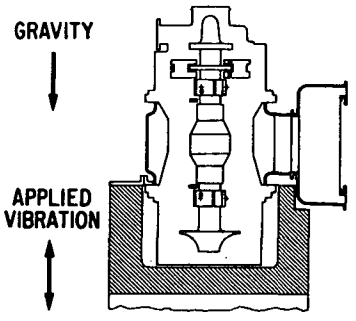

Fig. 76 Bearing Amplitudes Under Shaped Random Vibrations According To NASA Spec 417-2-C-3.5

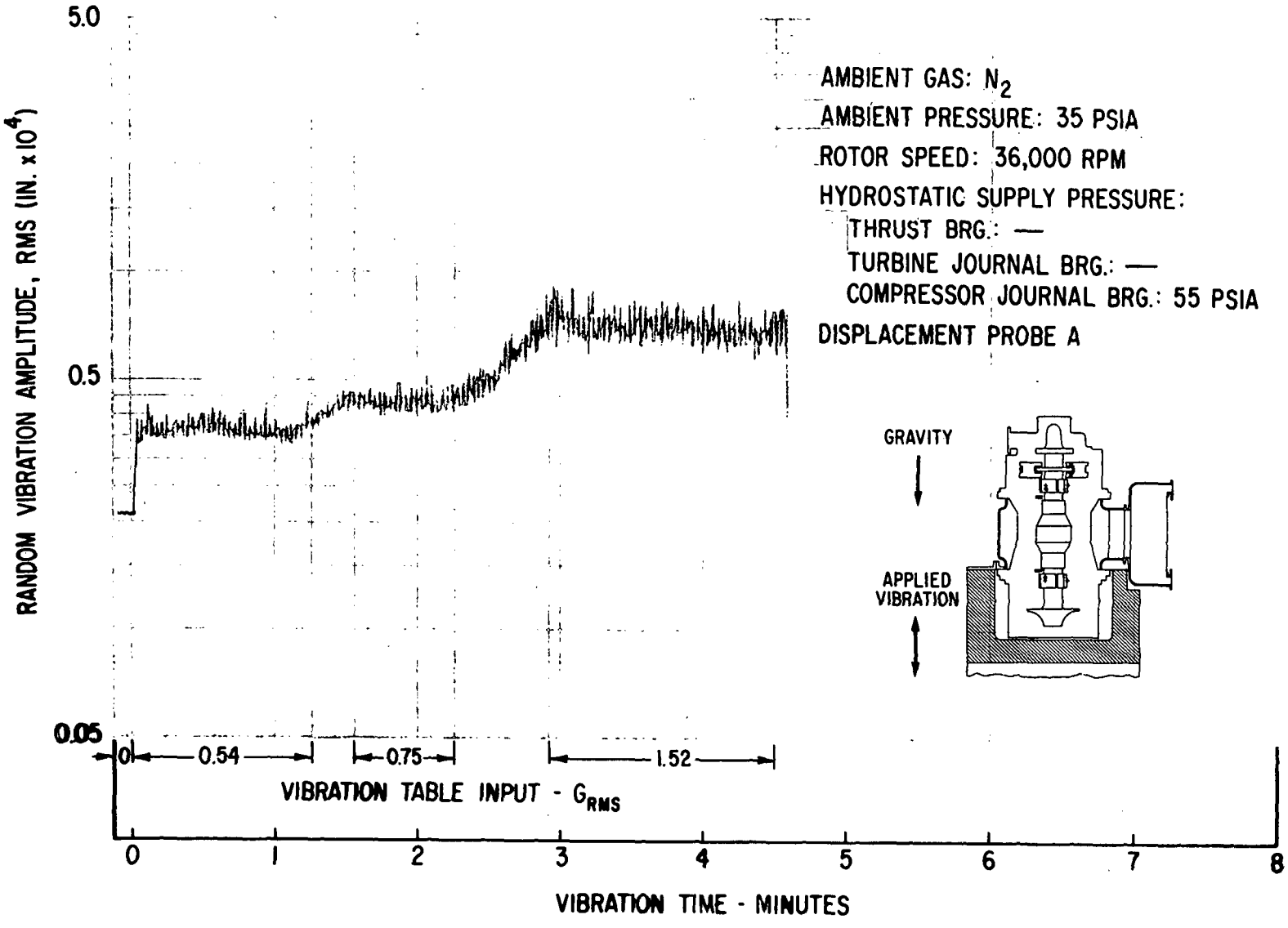

Fig. 77 Pad-To-Shaft Pivot Film Thickness Variation For Flex-Mounted Compressor Journal Bearing Pad Under Externally-Imposed Shaped Random Vibrations

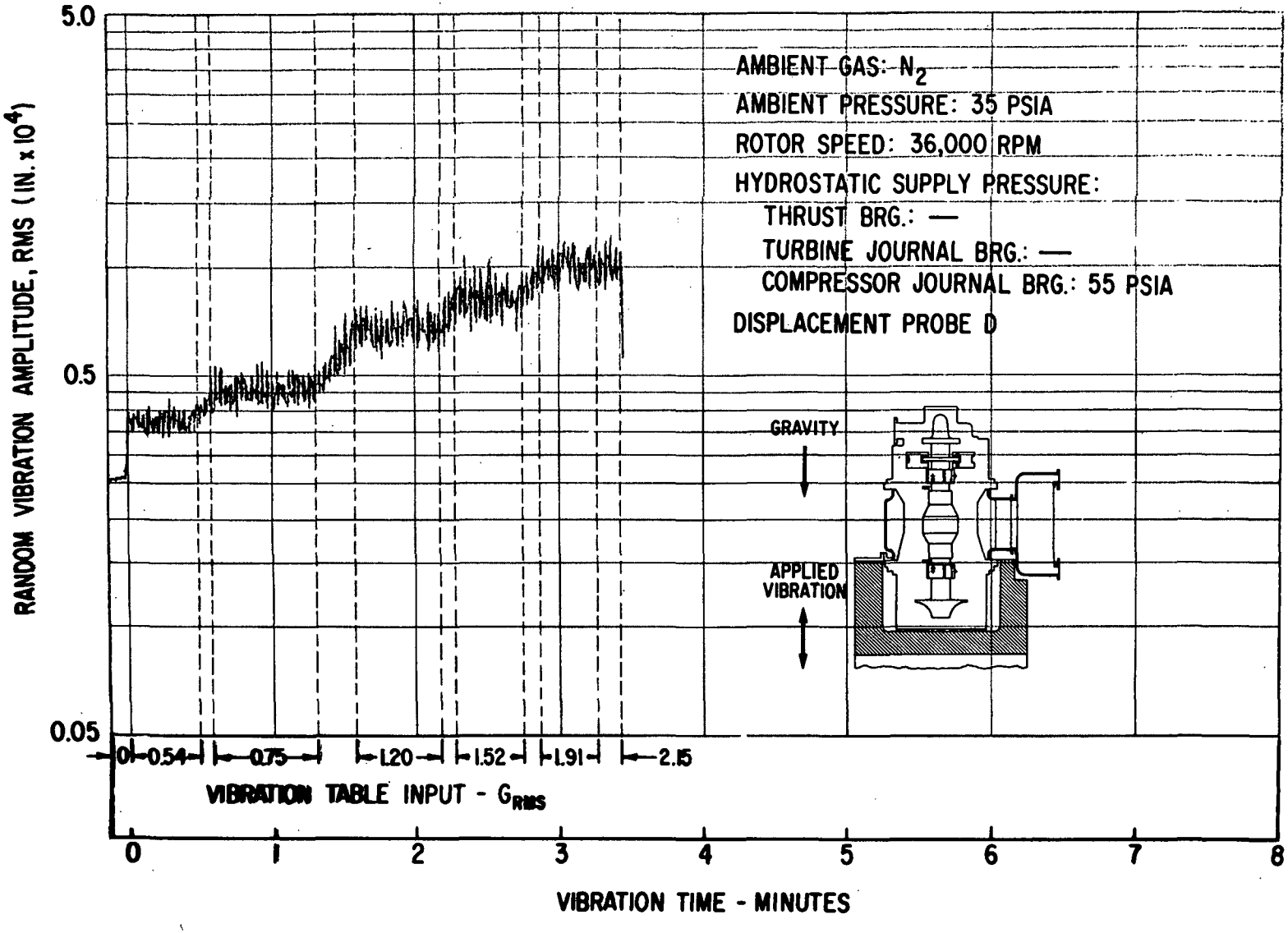

Fig. 78 Pad-To-Shaft Pivot Film Thickness Variation For Flex-Mounted Turbine Journal Bearing Pad Under Externally-Imposed Shaped Random Vibrations According To NASA Spec 417-2-C-3.5

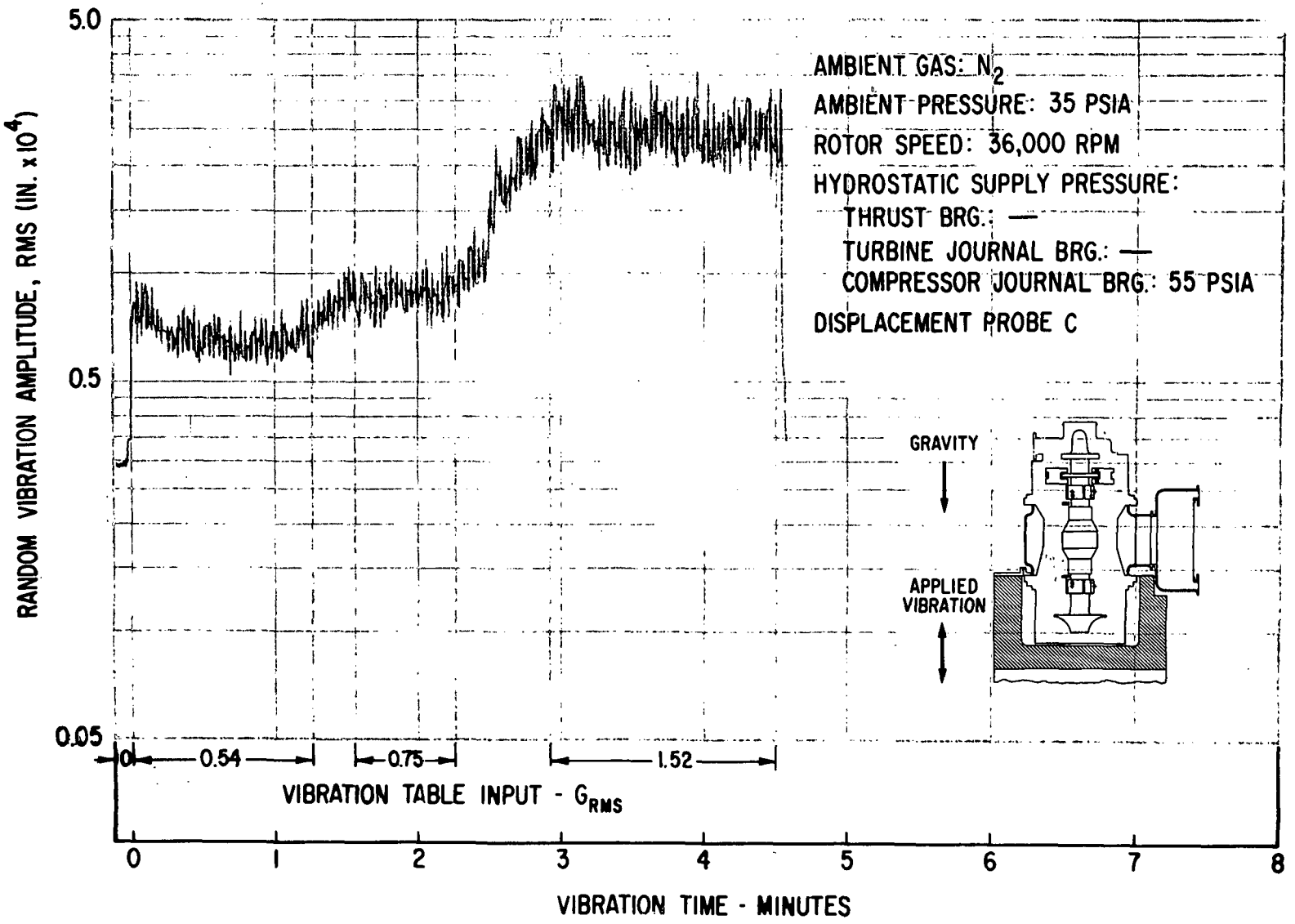

Fig. 79 Pad-To-Shaft Pivot Film Thickness Variation For Solid-Mounted Compressor Journal Bearing Pad Under Externally-Imposed Shaped Random Vibrations According To NASA Spec 417-2-C-3.5

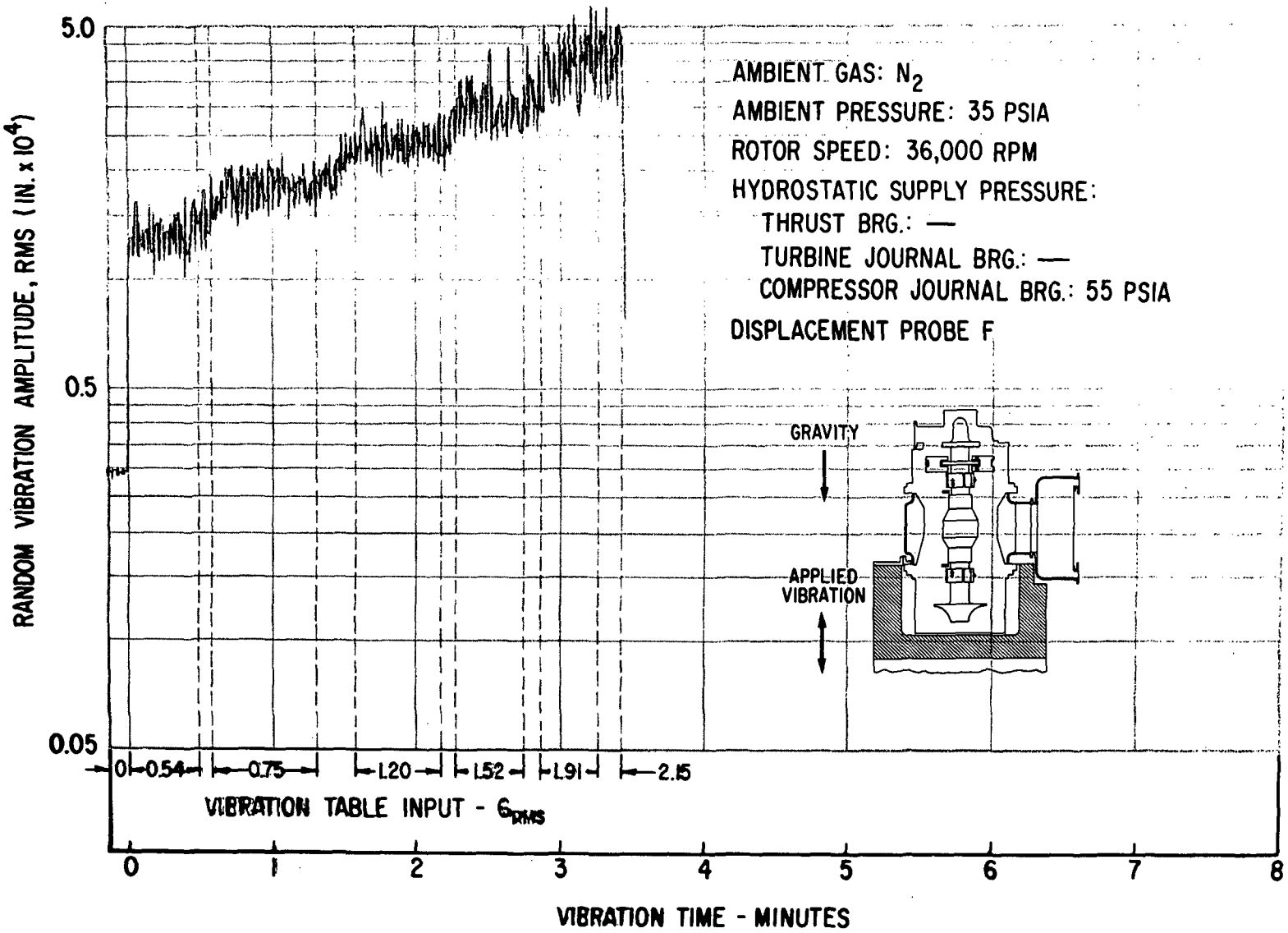

Fig. 80 Pad-To-Shaft Pivot Film Thickness Variation For Solid-Mounted Turbine Journal Bearing Pad Under Externally-Imposed Shaped Random Vibrations According To NASA Spec 417-2-C-3.5

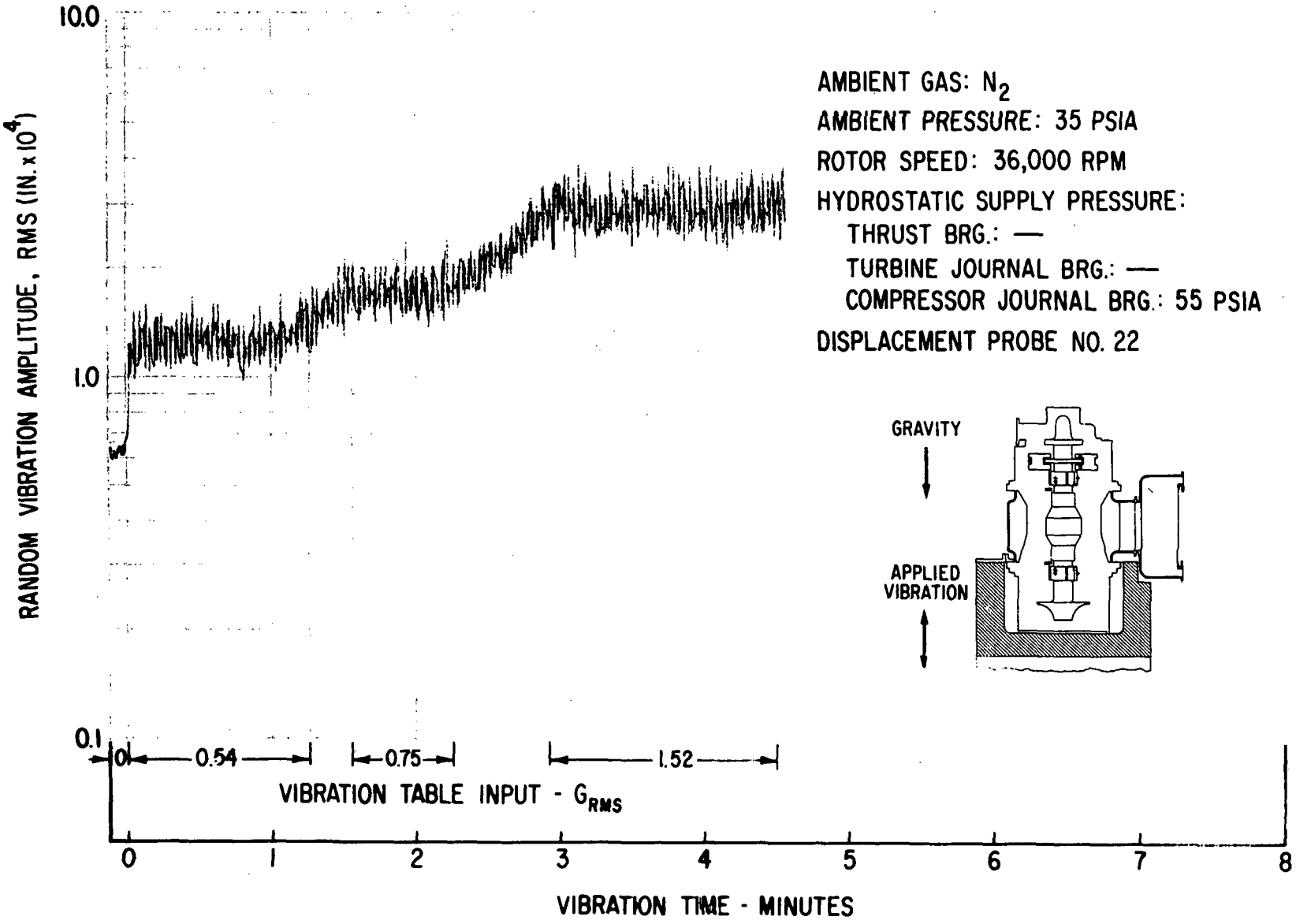

Fig. 81 Compressor Journal Flexure Amplitudes Under Shaped Random Vibrations According To NASA Spec 417-2-C-3.5

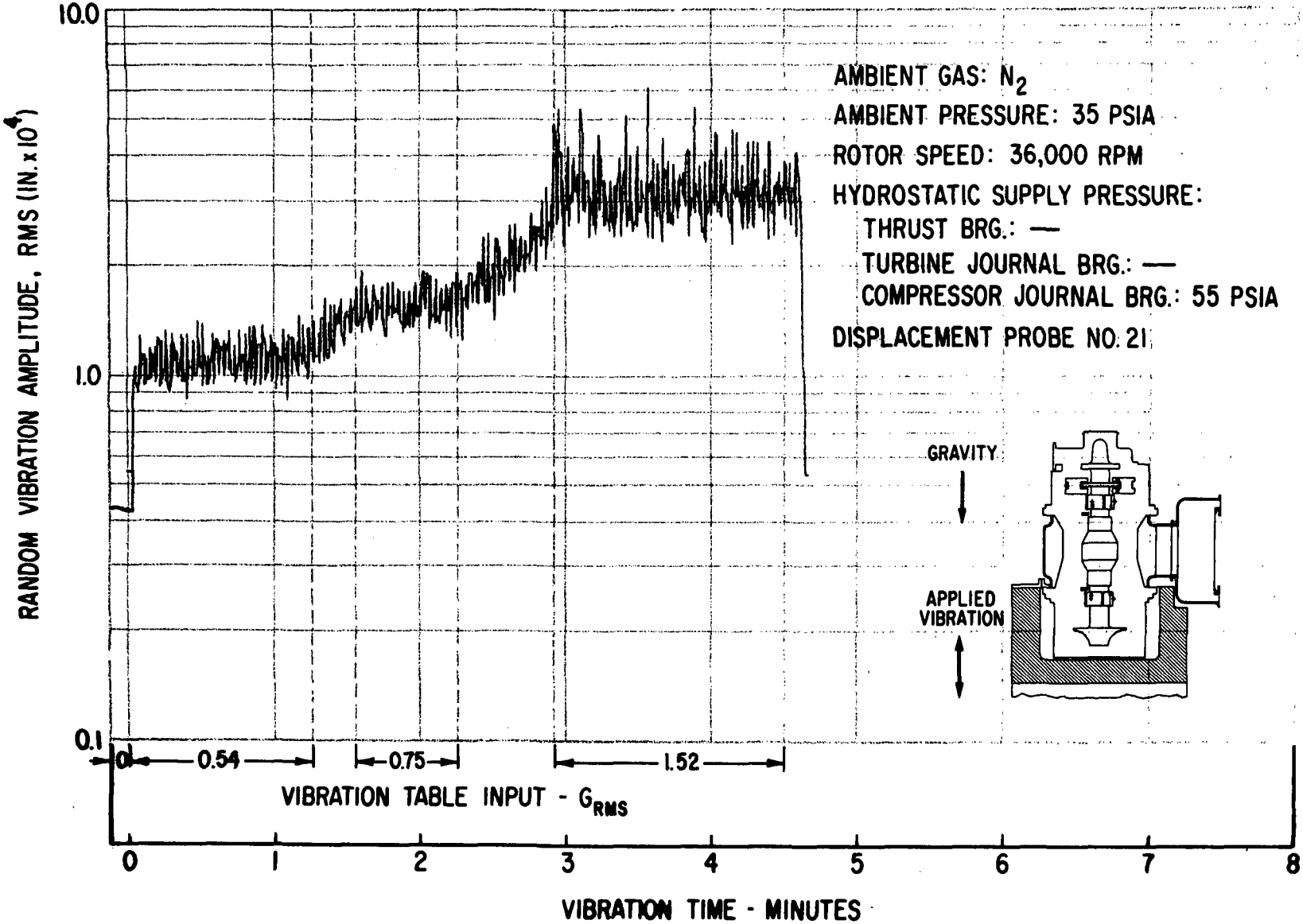

Fig. 82 Turbine Journal Flexure Amplitudes Under Shaped Random Vibrations According To NASA Spec 417-2-C-3.5

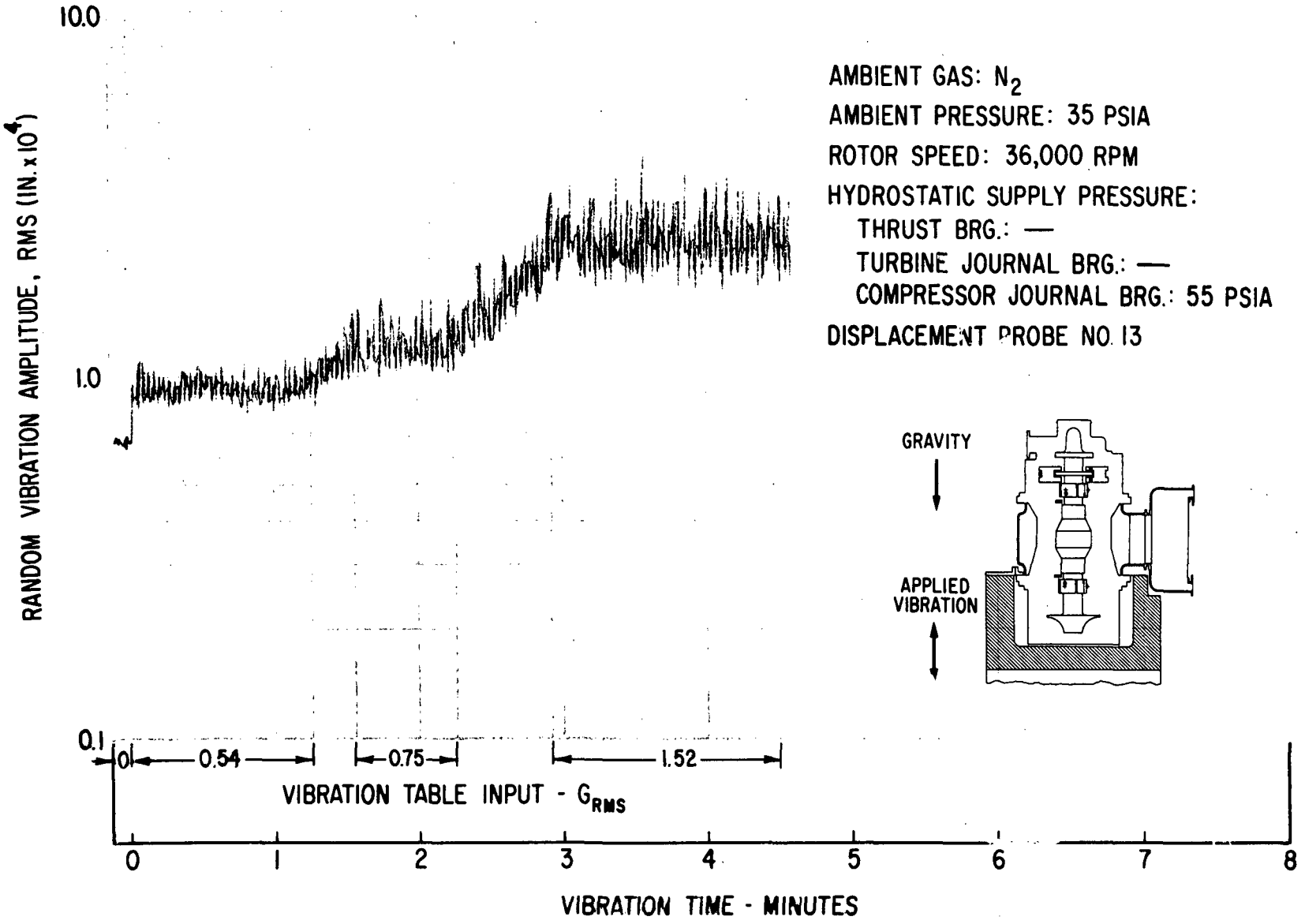

Fig. 83 Casing-To-Pad Leading Edge Amplitudes For Flex-Mounted Turbine Journal Bearing Pad Under Externally-Imposed Shaped Random Vibrations According To NASA Spec 417-2-C-3-5

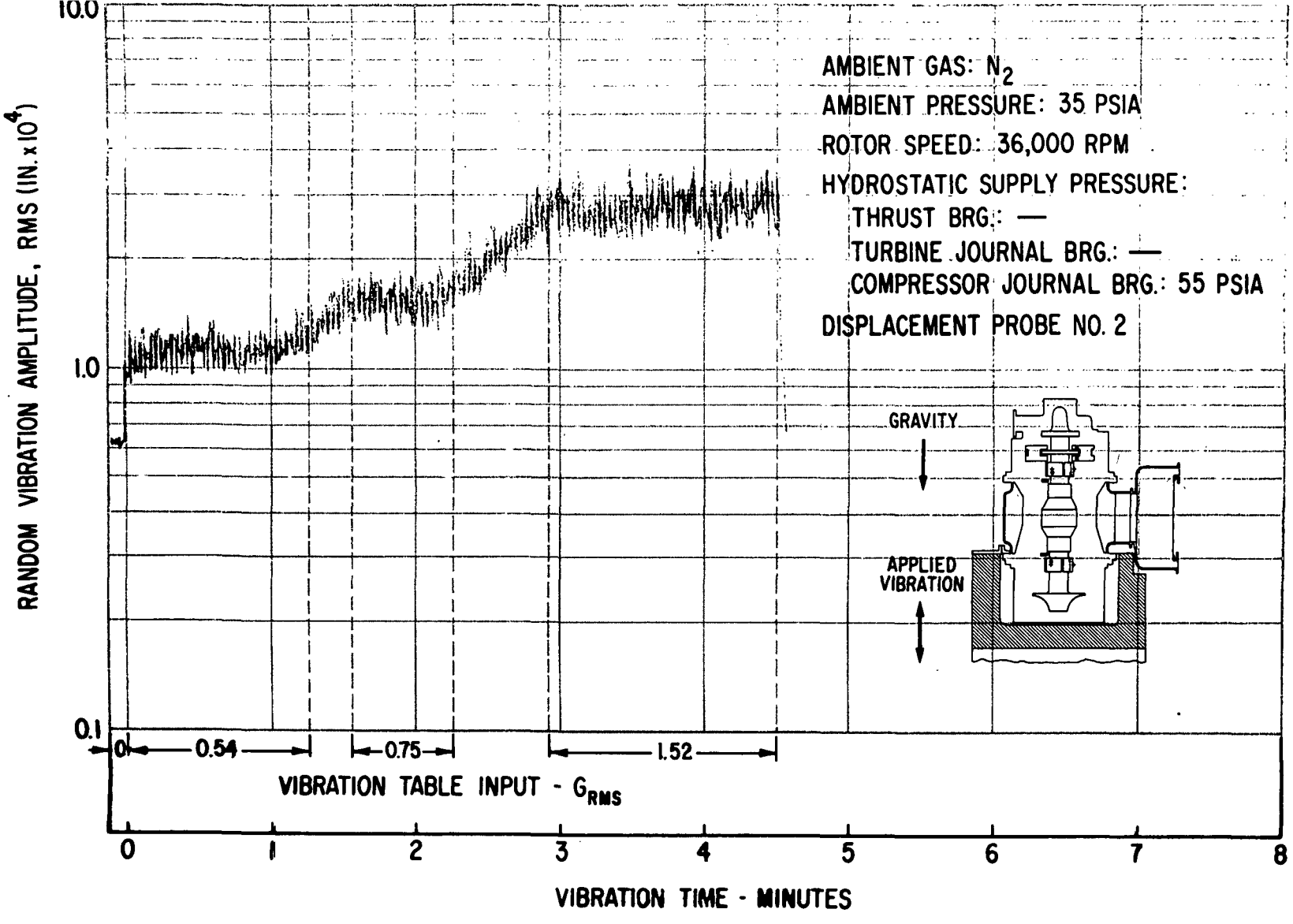

Fig. 84 Compressor Journal Rotor Amplitudes (Casing-To-Shaft) Under Shaped Random Vibrations According To NASA Spec 417-2-C-3.5

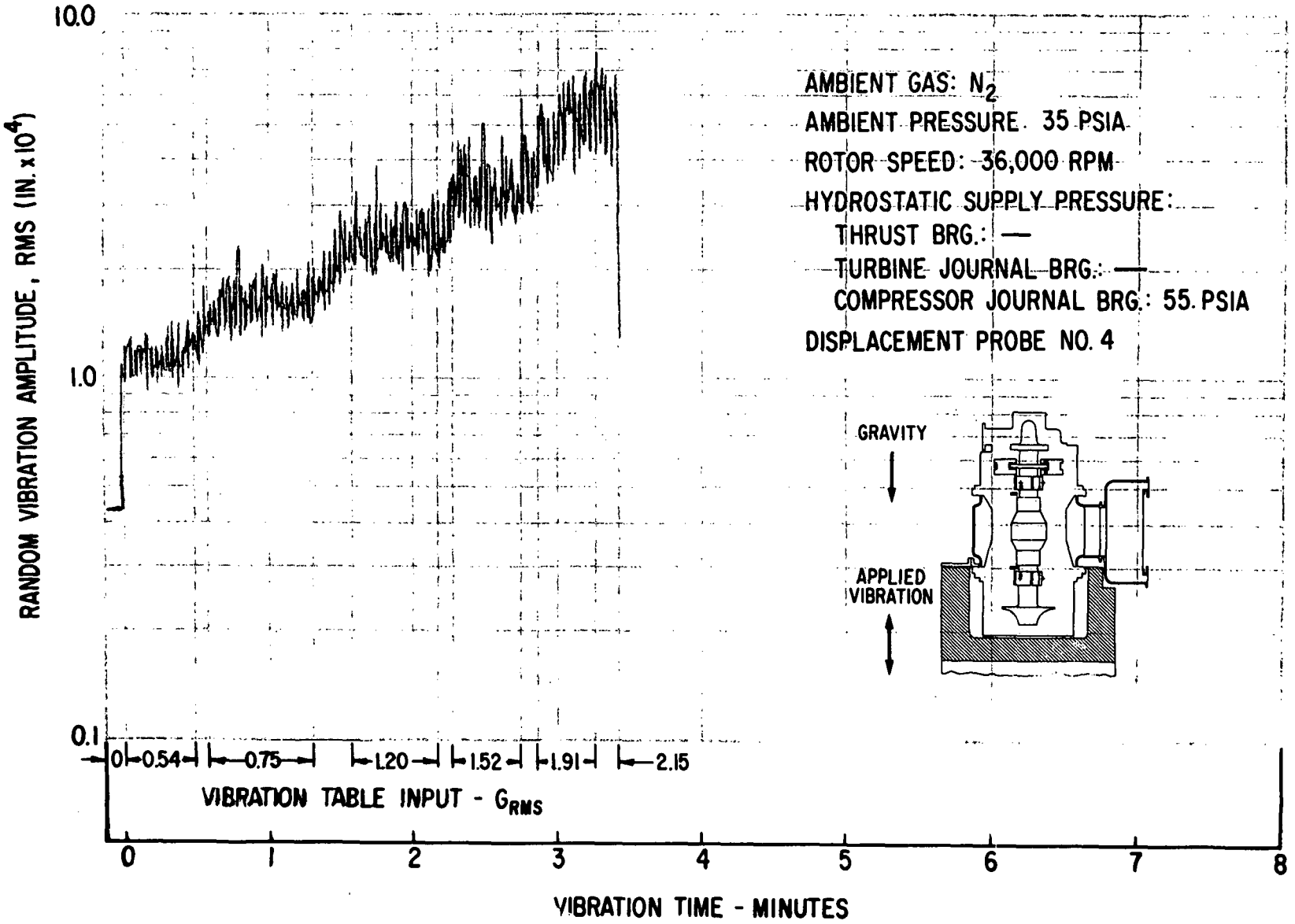

Fig. 85 Turbine Journal Rotor Amplitudes (Casing-To-Shaft) Under Shaped Random Vibrations According To NASA Spec 4[illegible]-2-C-3.5

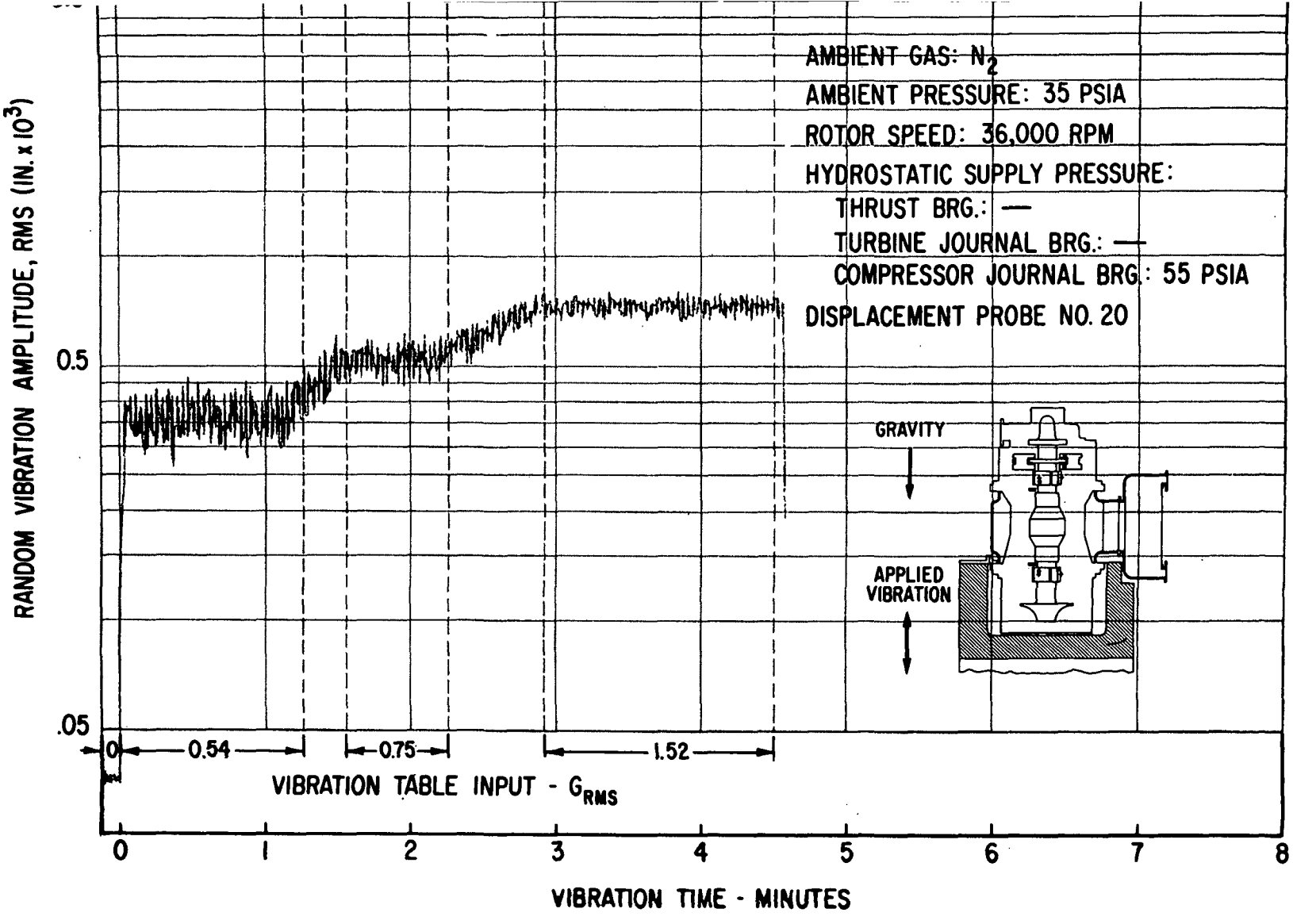

Fig. 86 Thrust Bearing Film Thickness Variation Under Externally-Imposed Shaped Random Vibrations According To NASA Spec 417-2-C-3.5

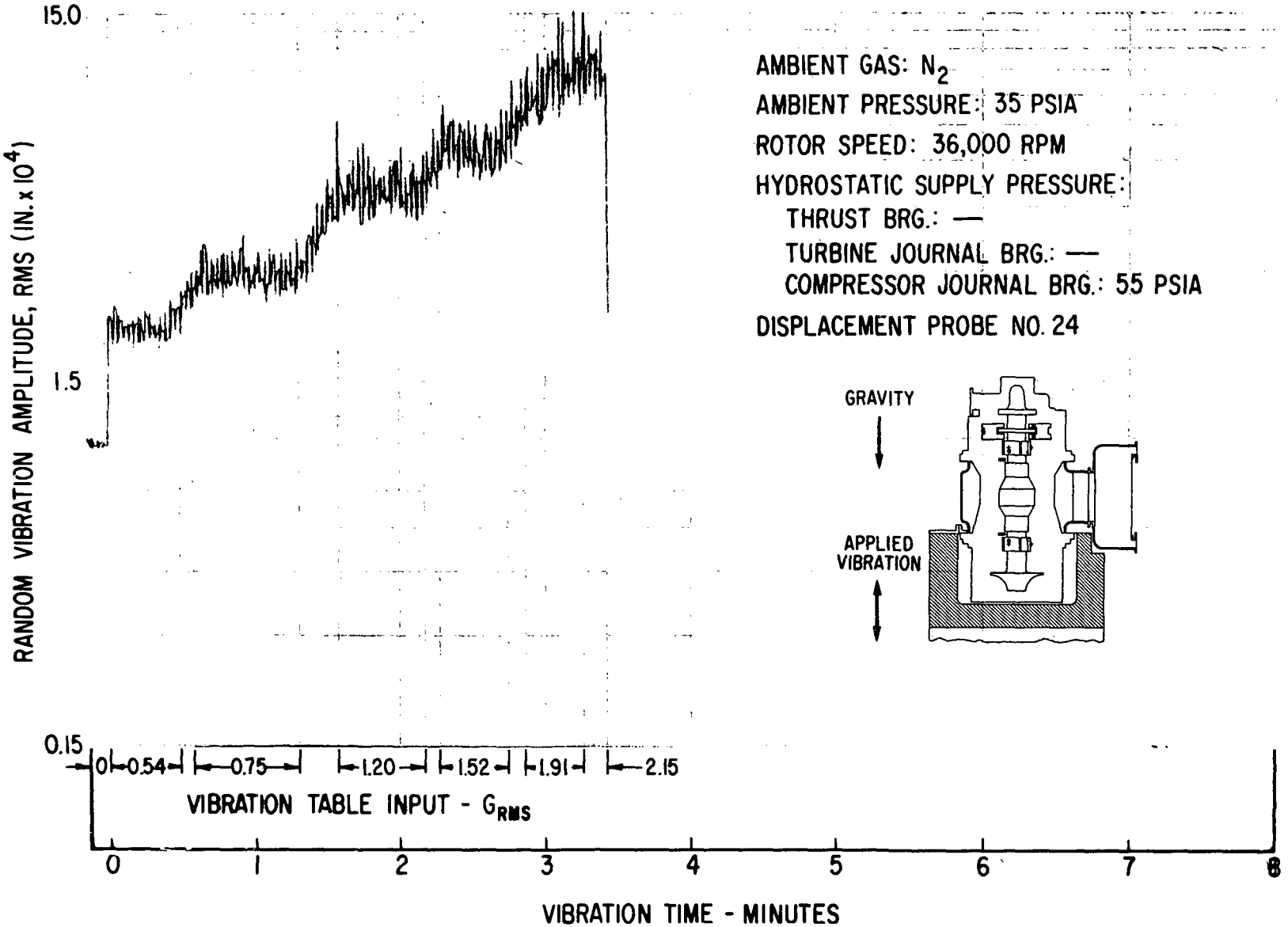

Fig. 87 Thrust Bearing Gimbal Amplitudes Under Shaped Random Vibrations According To NASA Spec 417-2-C-3.5

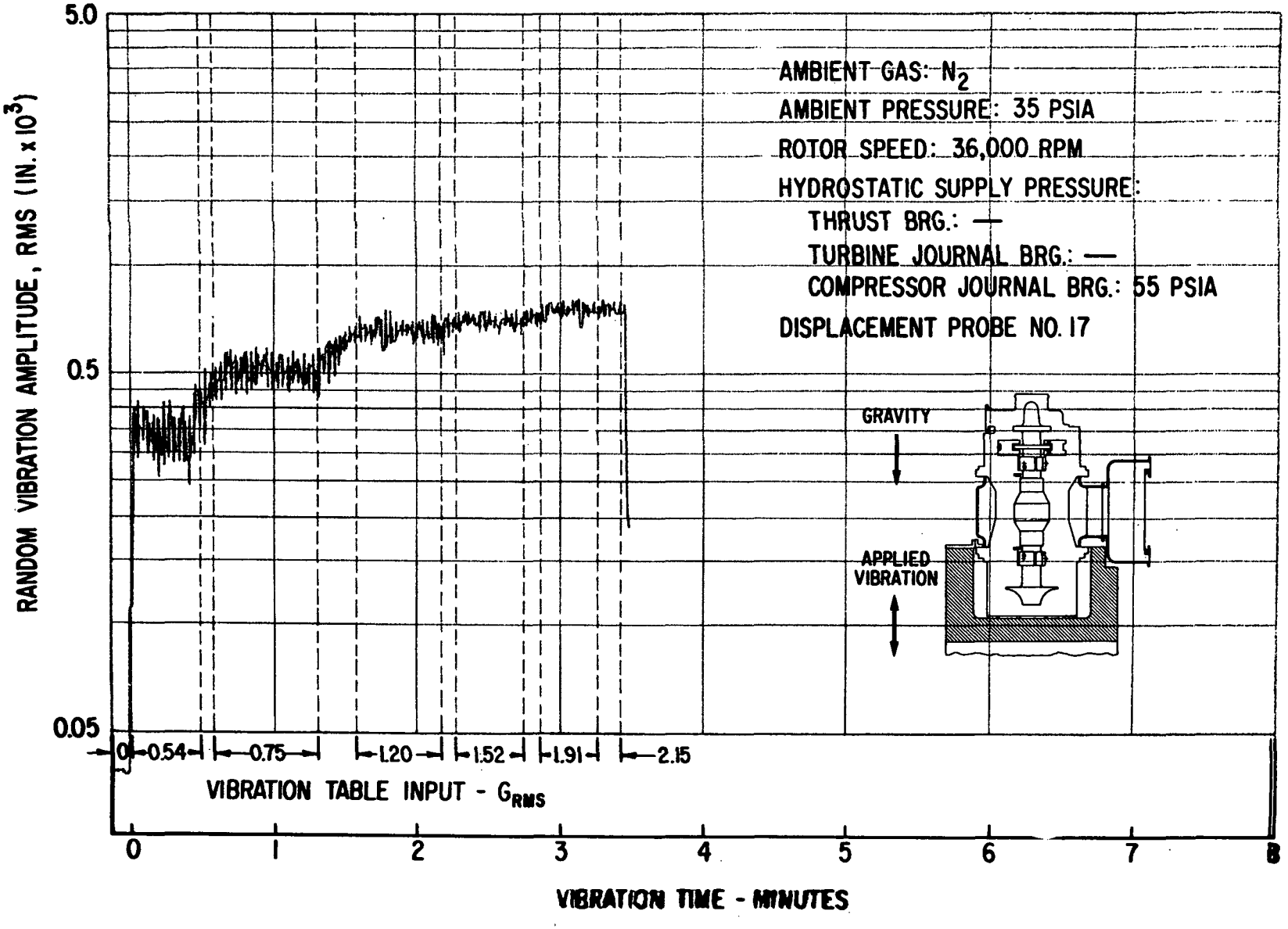

Fig. 88 Thrust Bearing Film Thickness Variation Under Externally-Imposed Shaped Random Vibrations According To NASA Spec 417-2-C-3.5

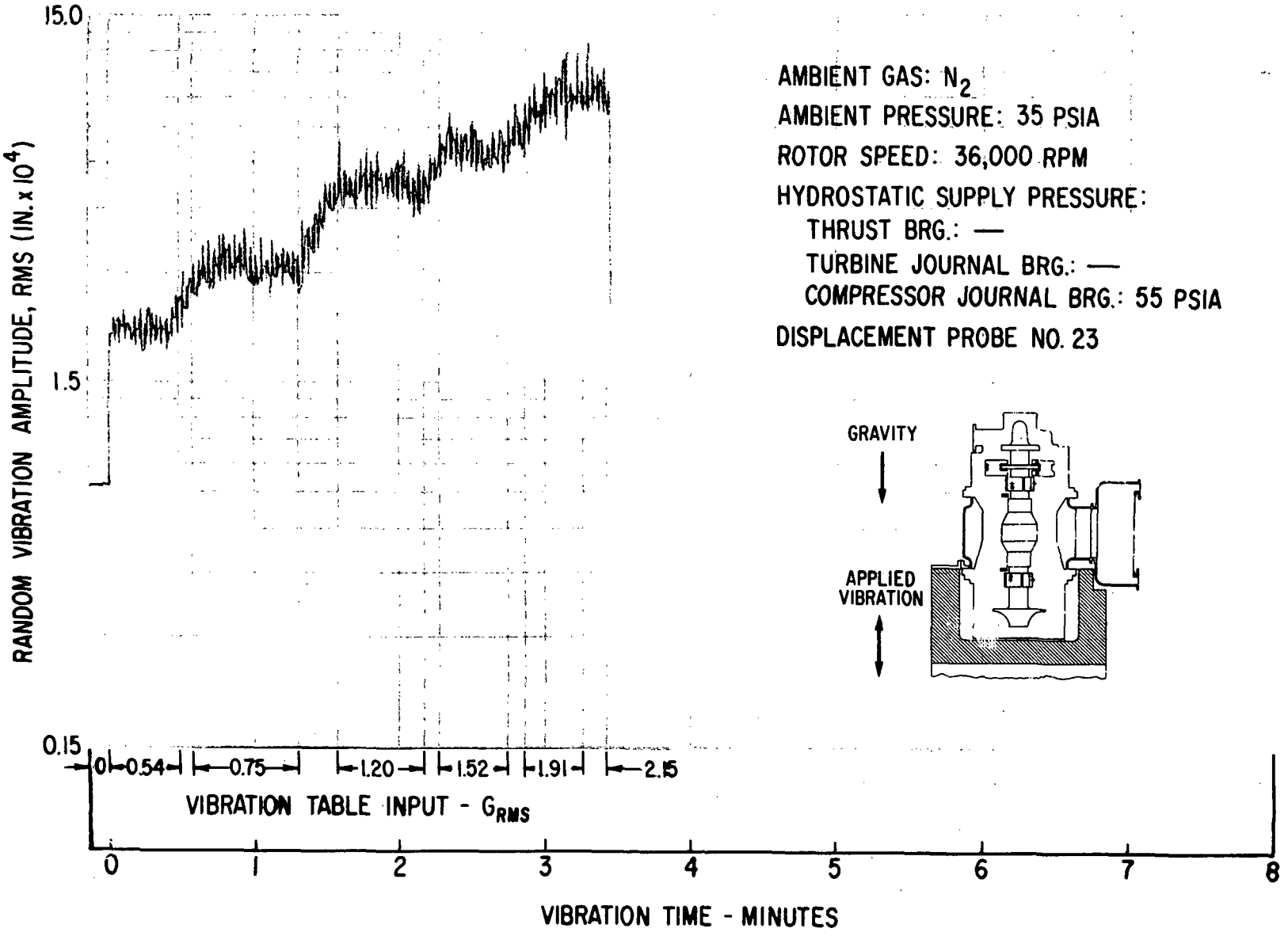

Fig. 89 Thrust Bearing Gimbal Amplitudes Under Shaped Random Vibrations According To NASA Spec 417-2-C-3.5

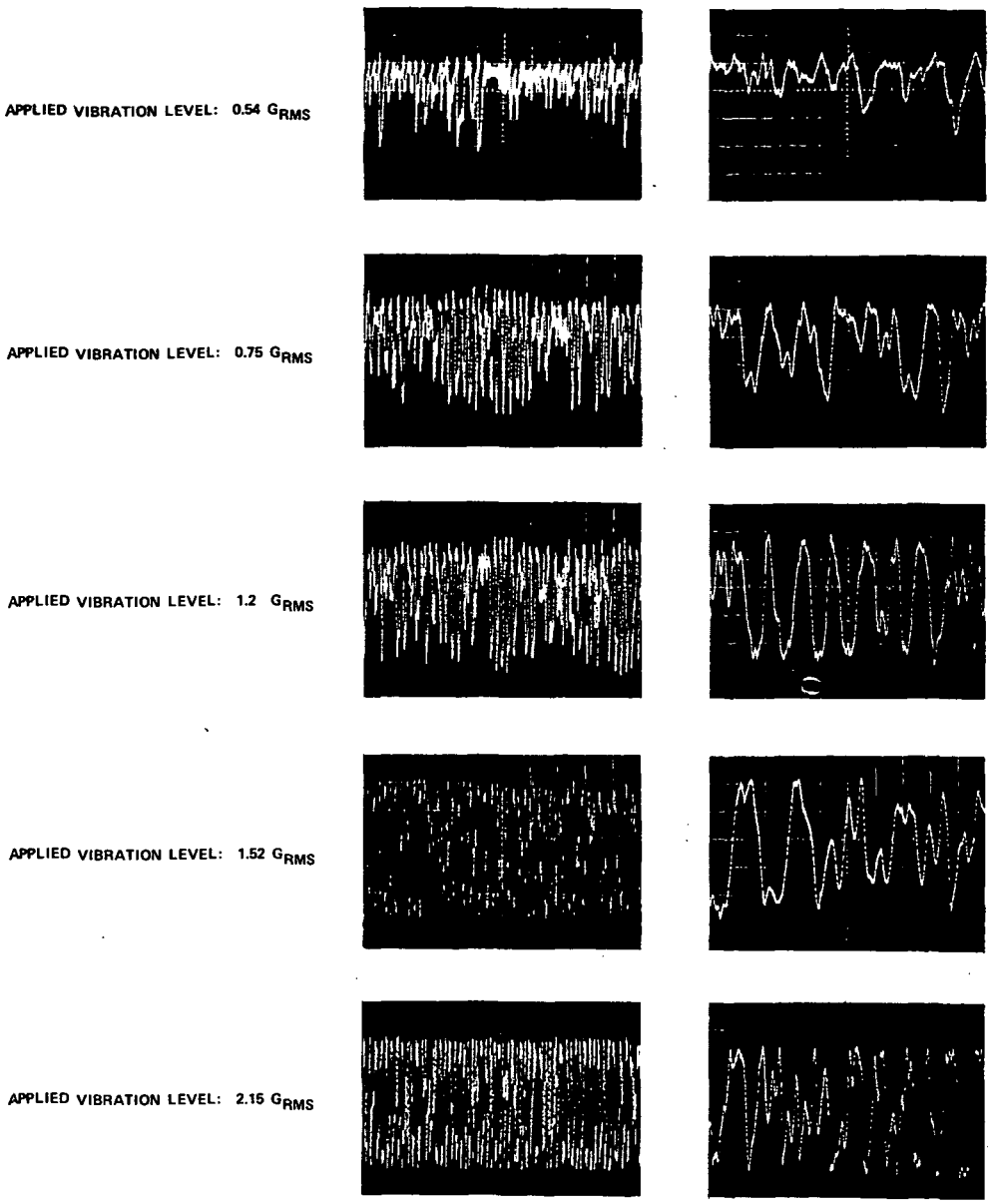

Fig. 90 BRU Simulator Thrust Bearing Gas Film Thickness Variations Under Shaped Random Vibrations According To NASA Spec 417-2-C-3.5

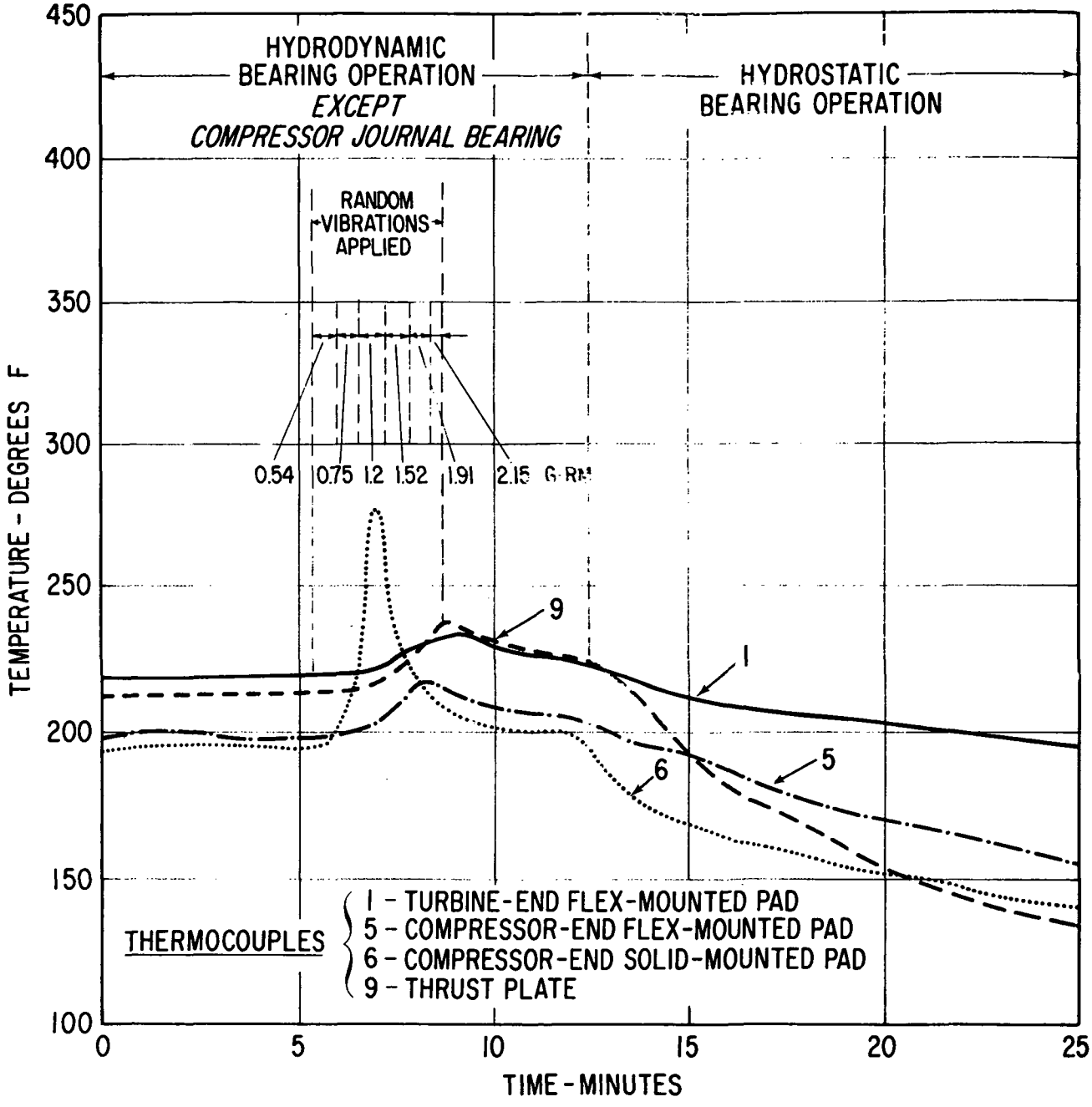

Fig. 91 Measured Temperatures in ERU Simulator Components With Axial Random Excitation (Shaft Speed 36,000 rpm)

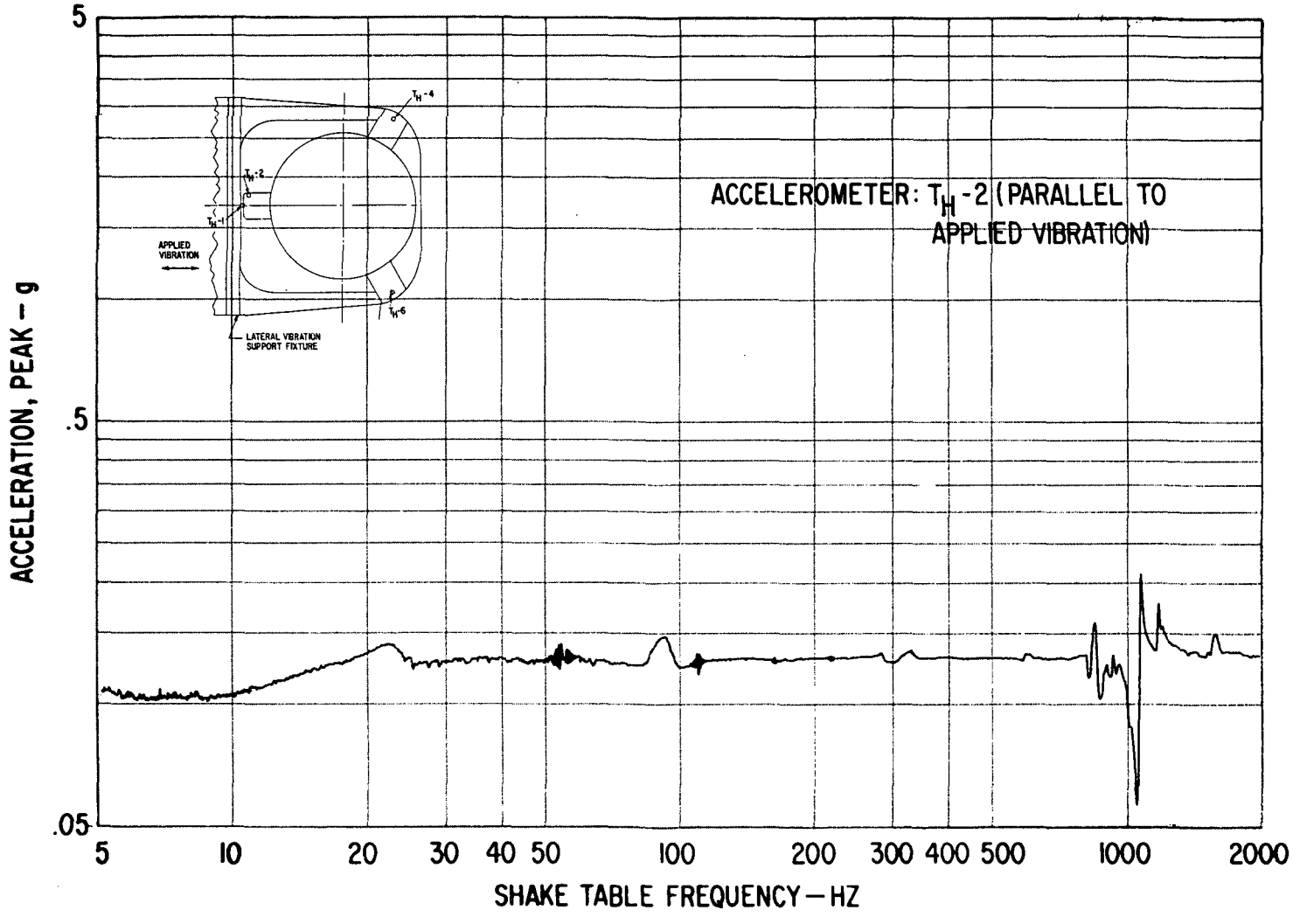

Fig. 92 Sinusoidal Acceleration of Transverse Vibration Test Support Fixture For BRU Simulator At 0.12 g Peak Shake Table Input

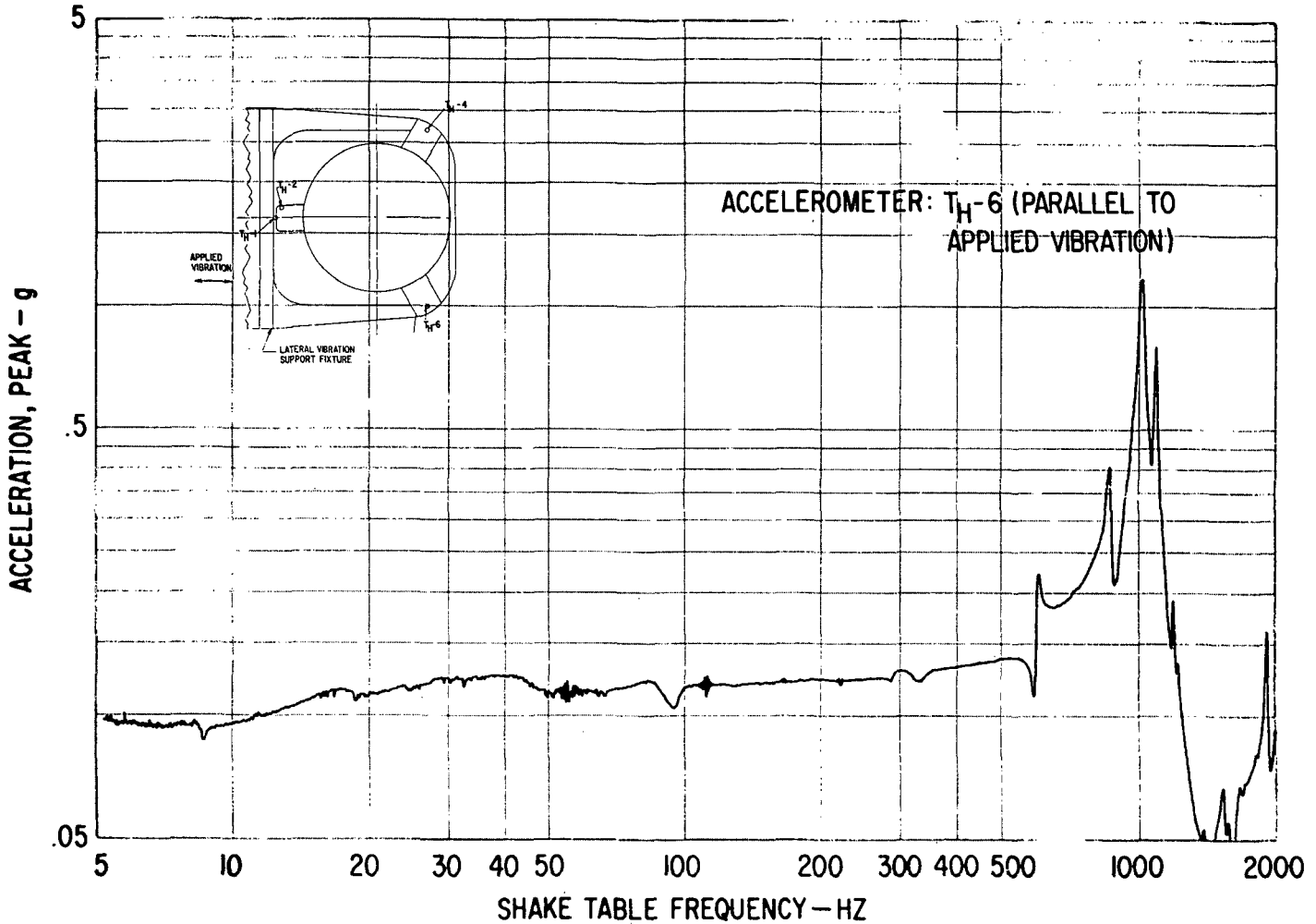

Fig. 93 Sinusoidal Acceleration of Transverse Vibration Test Support Fixture For BRU Simulator At 0.12 g Peak Shake Table Input

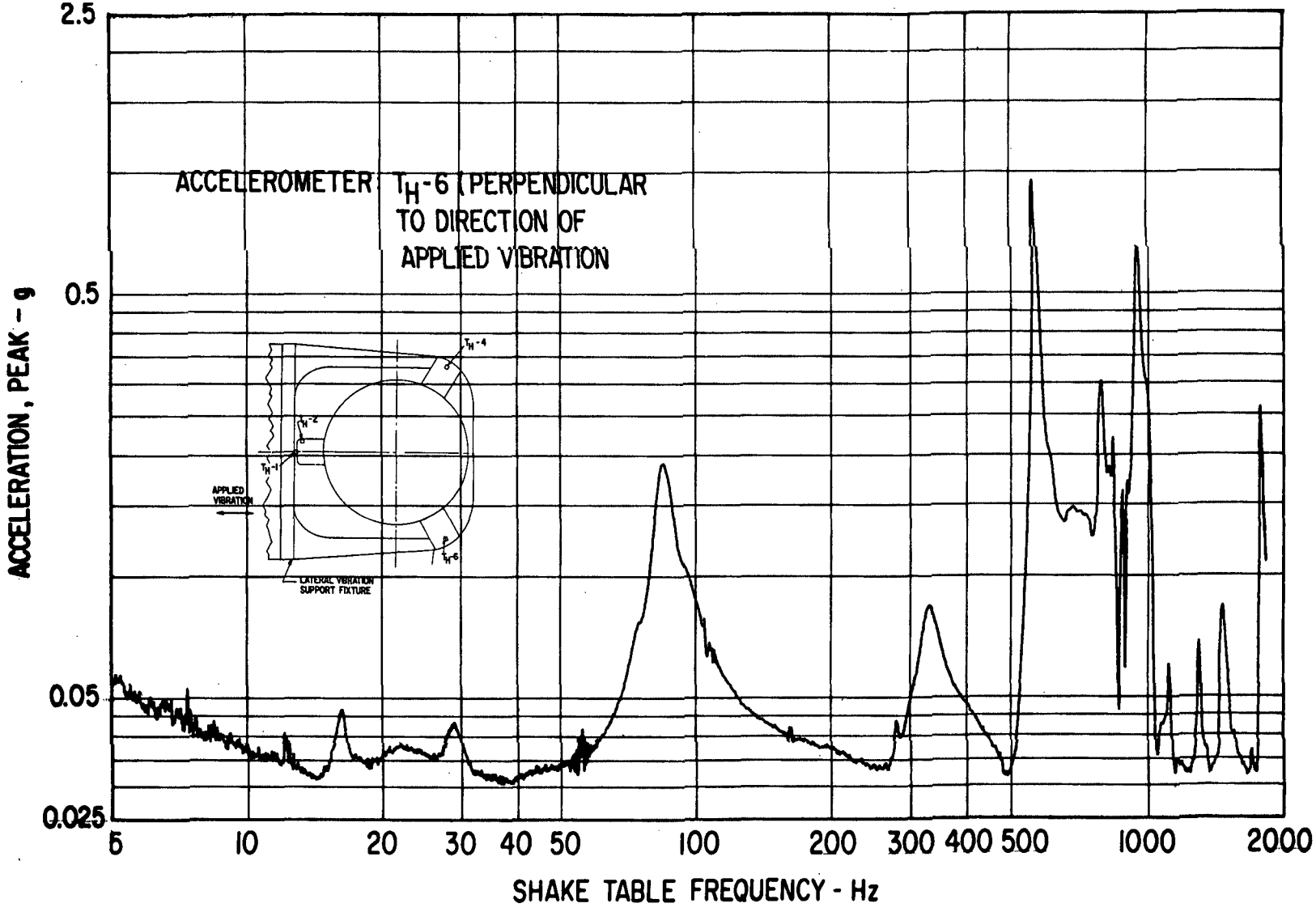

Fig. 94 Vertical Sinusoidal Acceleration of Transverse Vibration Support Fixture for BRU Simulator At 0.12 g Peak Shake Table Input

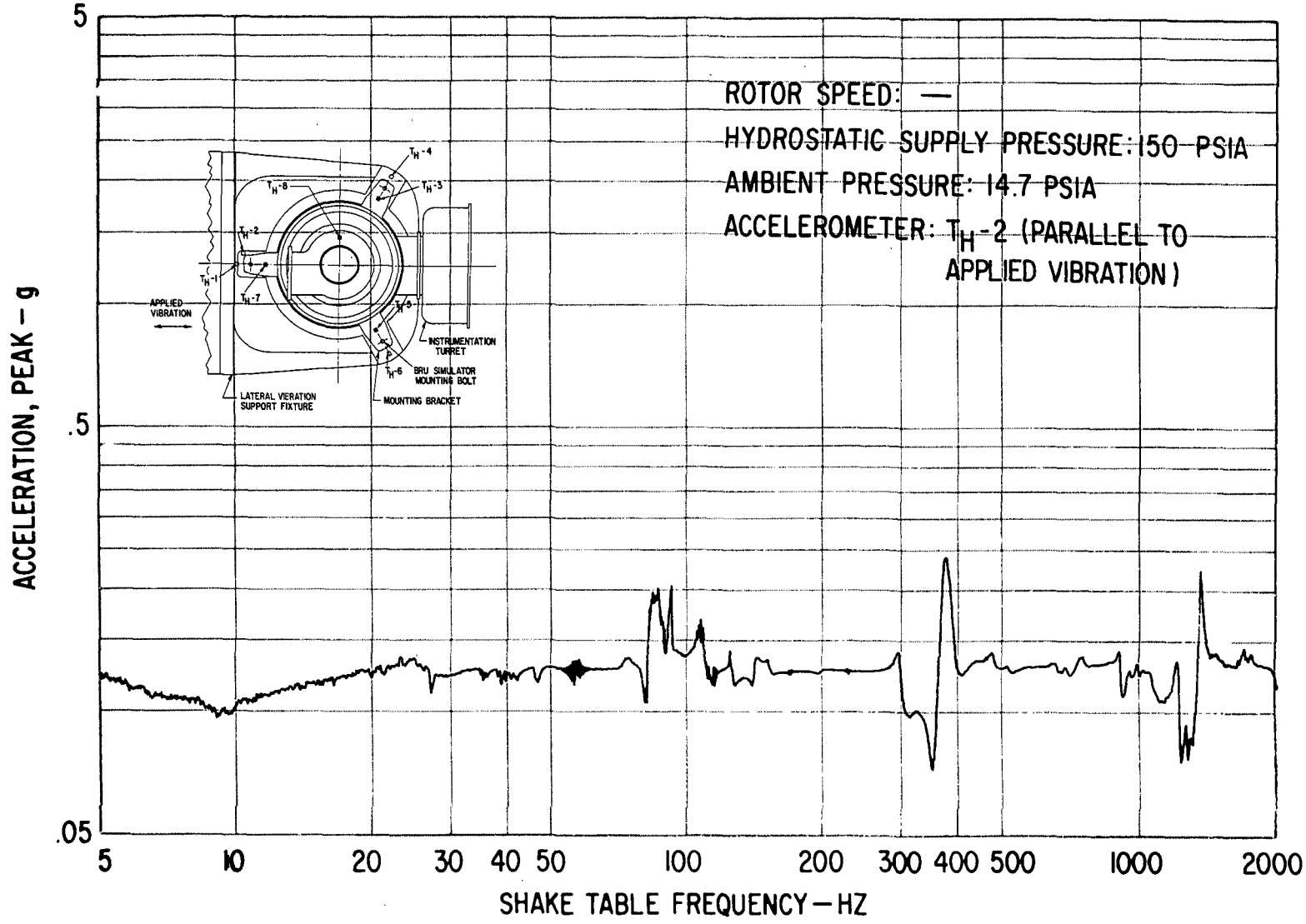

Fig. 95 Sinusoidal Acceleration of Transverse Vibration Test Support Fixture For BRU Simulator At 0.12 g Peak Shake Table Input (BRU Mounted in Fixture)

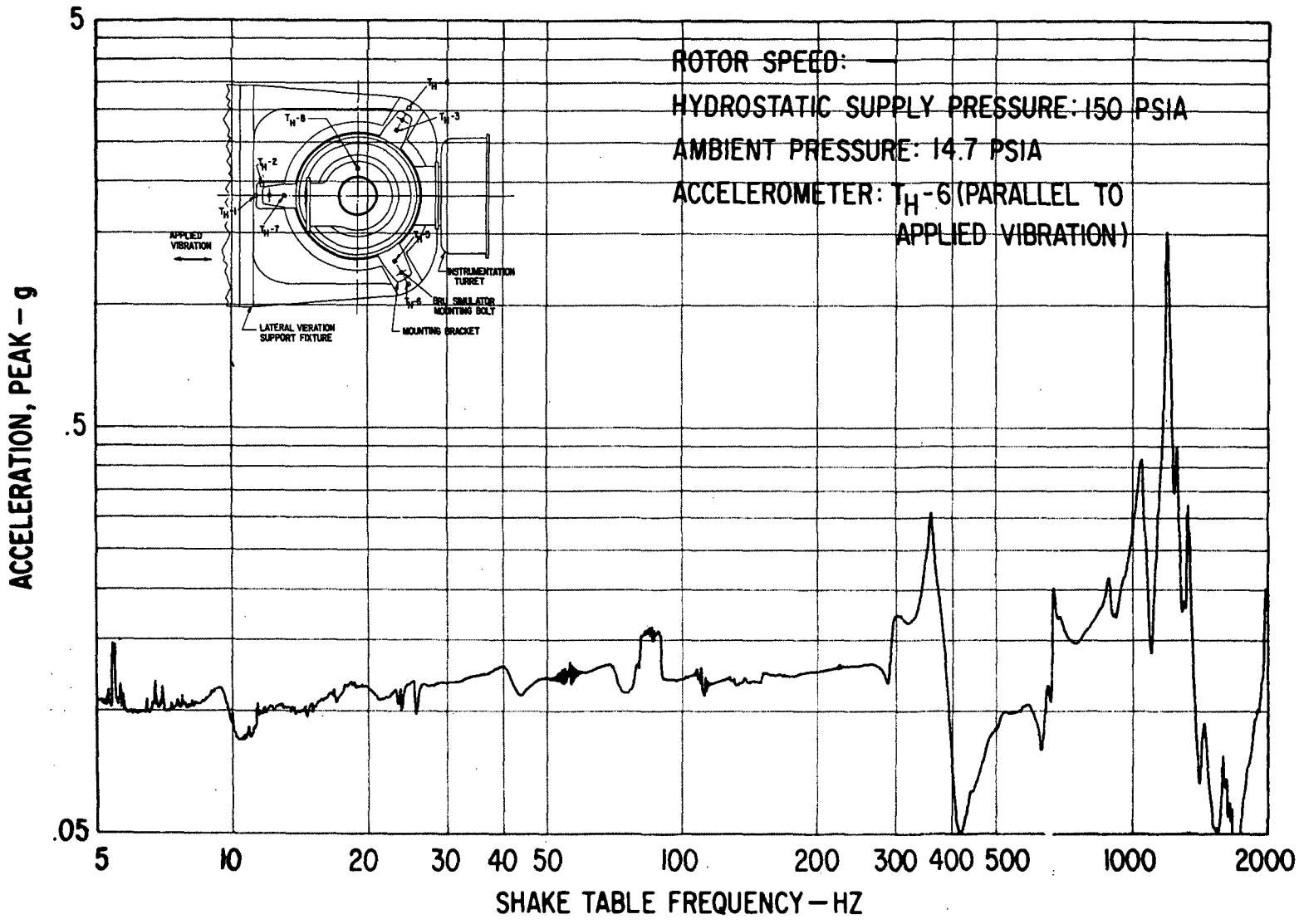

Fig. 96 Sinusoidal Acceleration of Transverse Vibration Test Support Fixture For BRU Simulator At 0.12 g Peak Shake Table Input (BRU Mounted in Fixture)

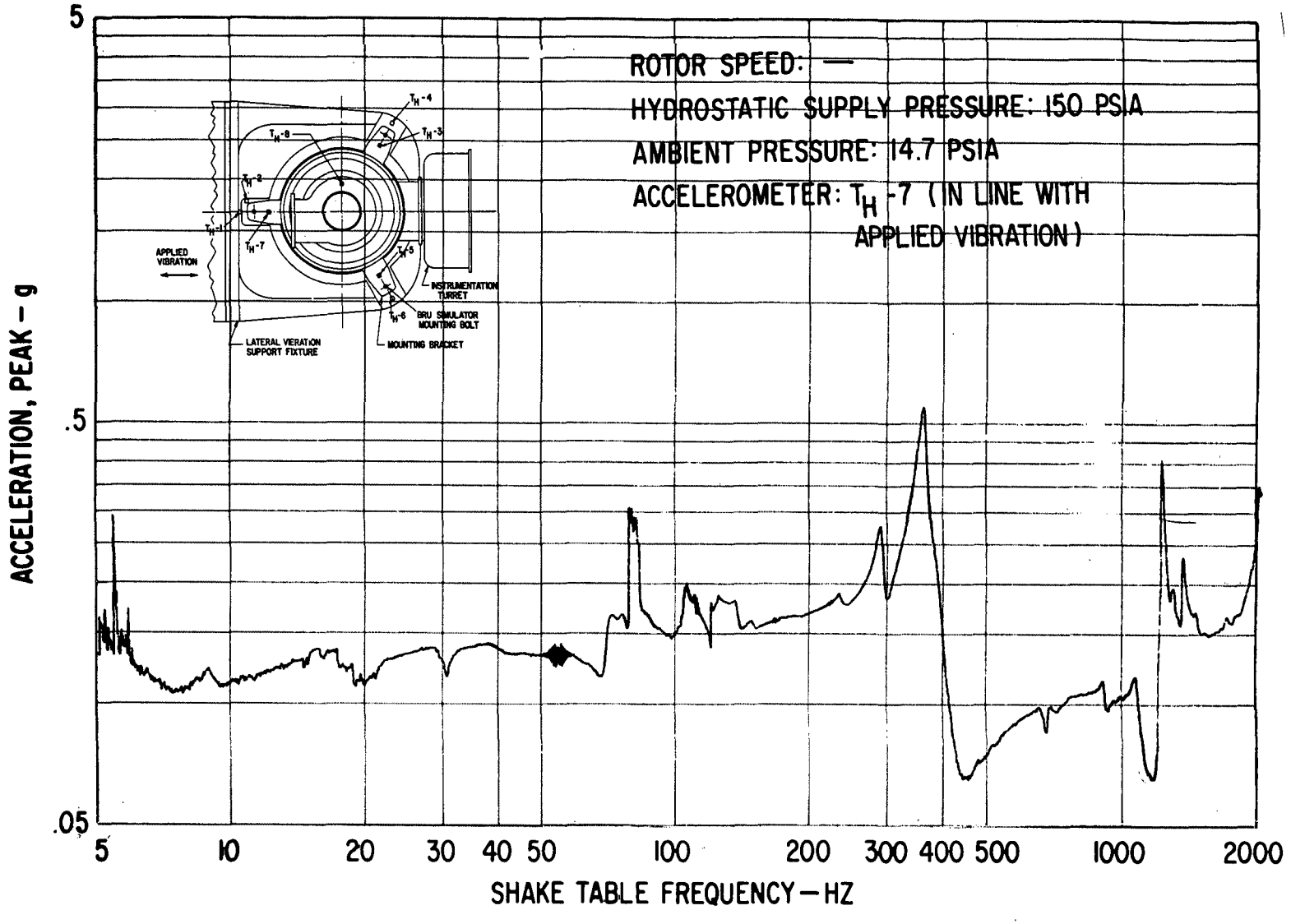

Fig. 97 Sinusoidal Acceleration On BRU Simulator Mounting Bracket Opposite From Turret, At 0.12 g Peak Shake Table Input

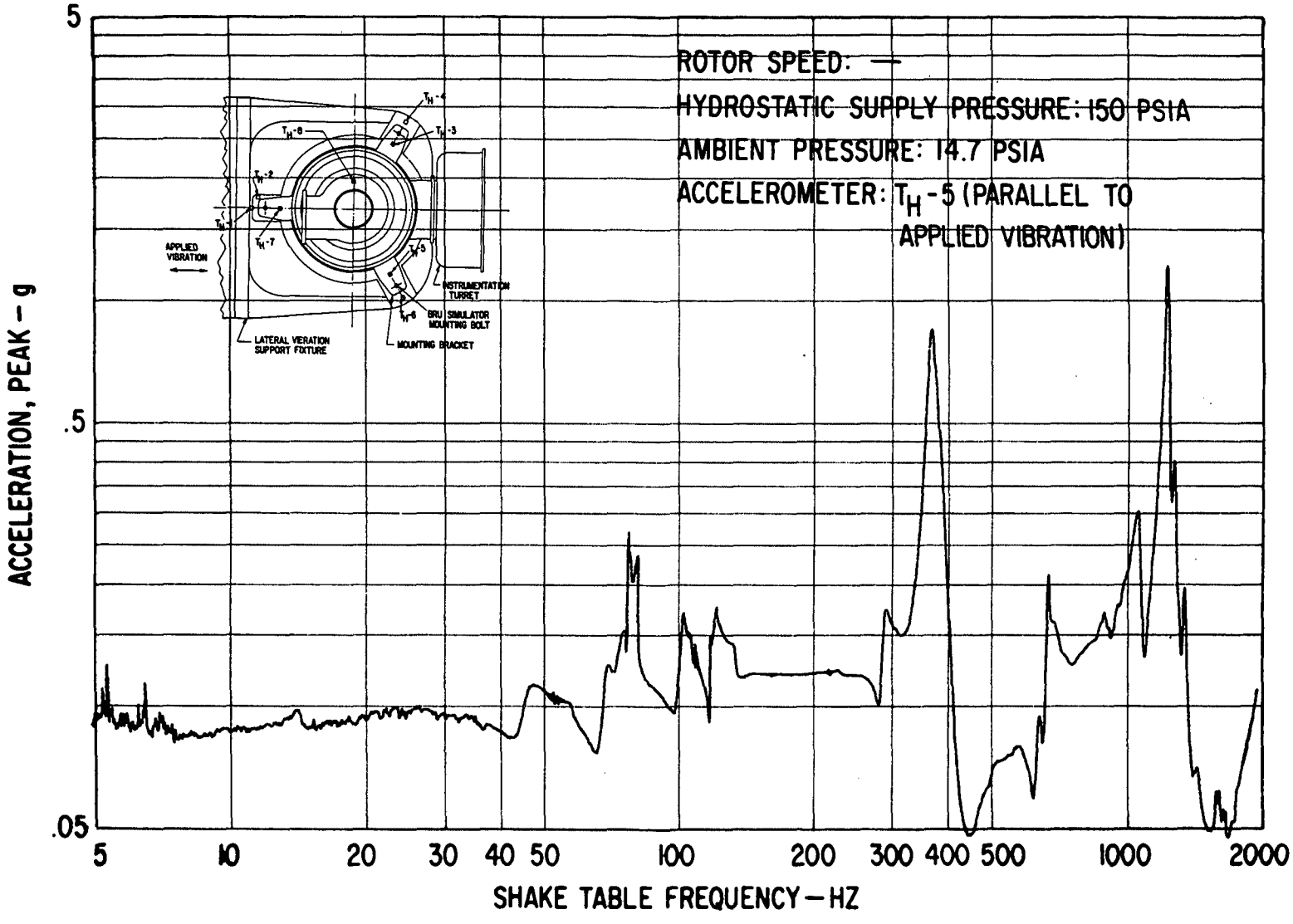

Fig. 98 Sinusoidal Acceleration On BRU Simulator Mounting Bracket, Counterclockwise From Turret, At 0.12 g Peak Shake Table Input

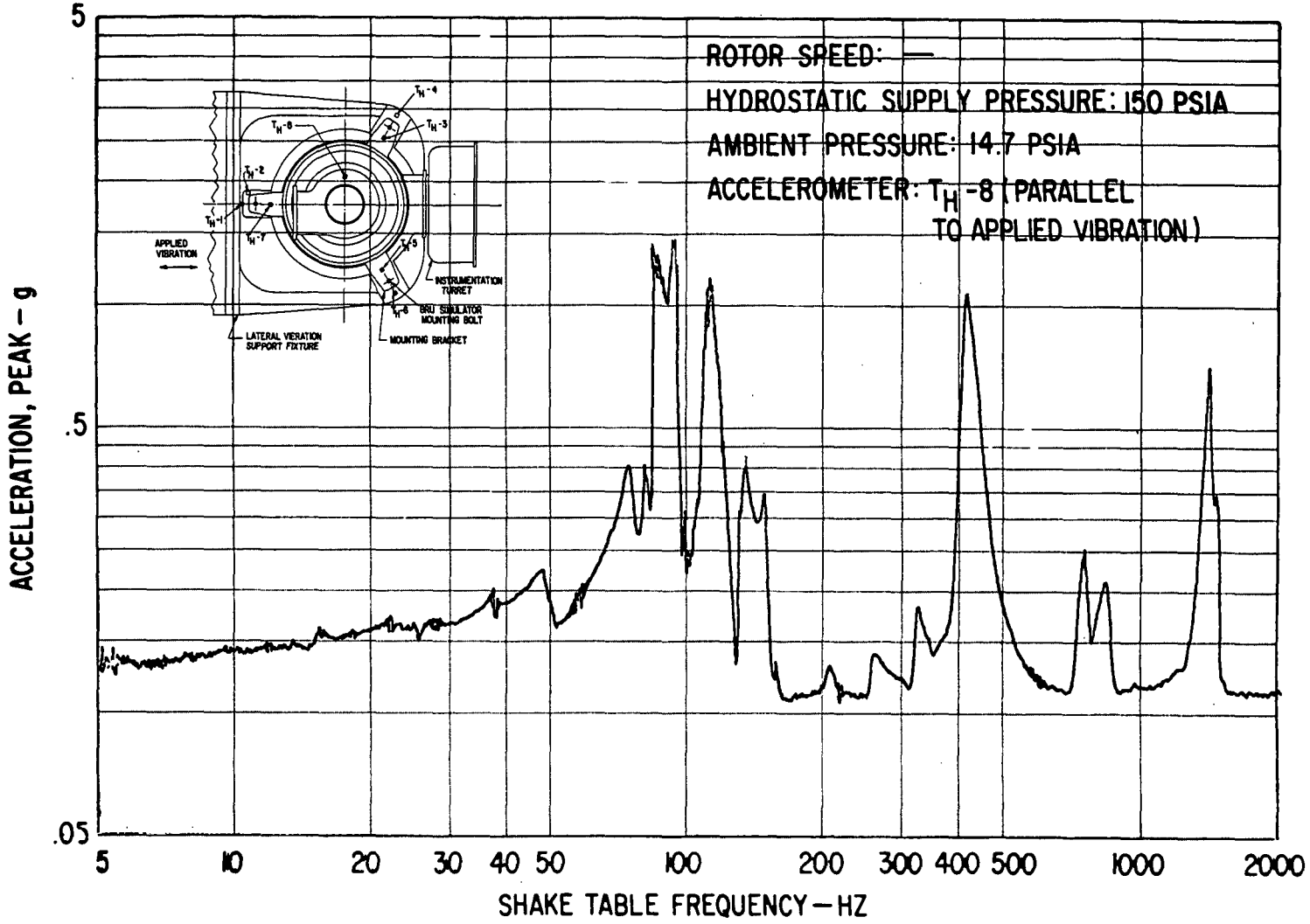

Fig. 99 Sinusoidal Acceleration On Top Of The BRU Simulator At 0.12 g Peak Shake Table Input

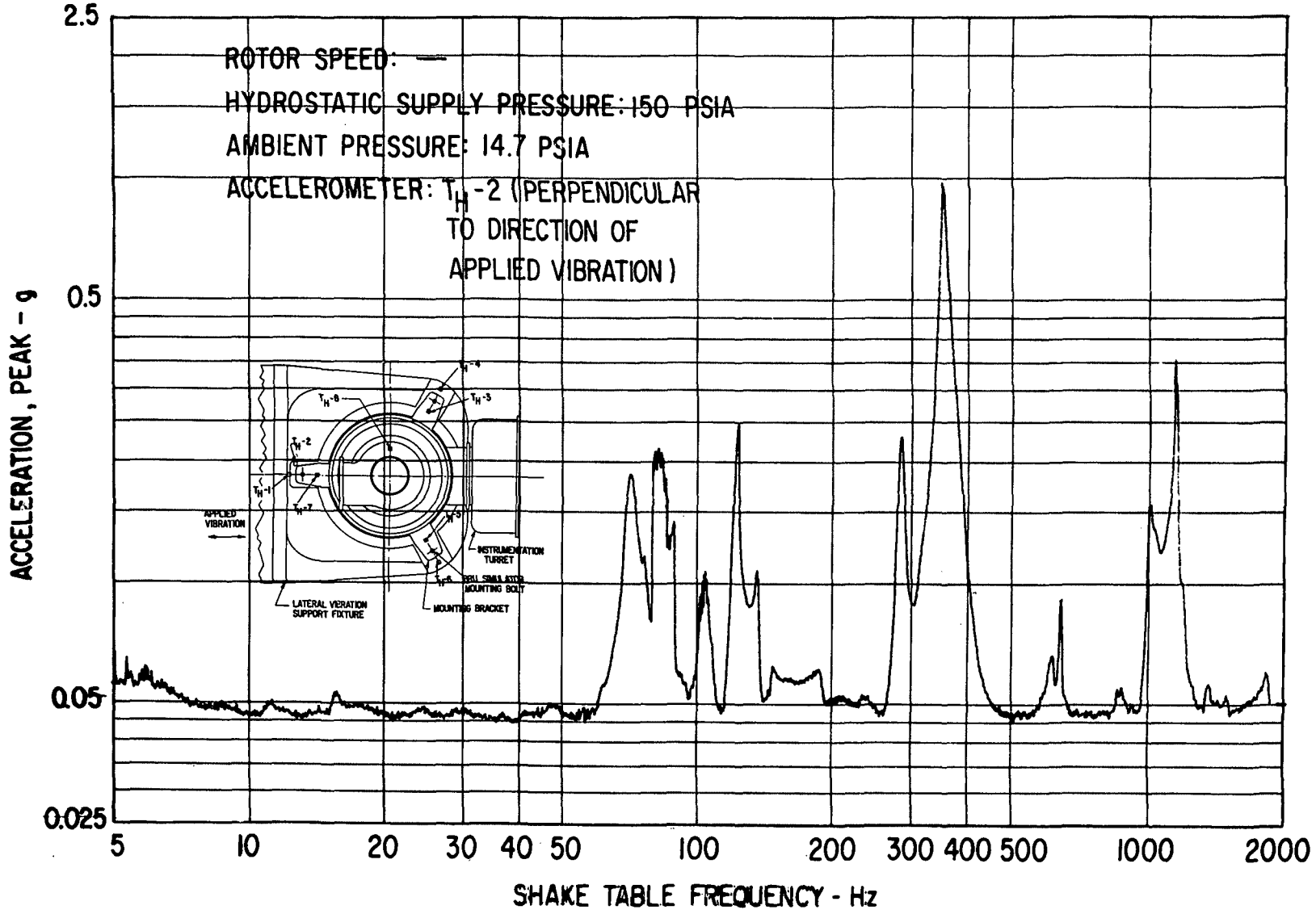

Fig. 100 Vertical Sinusoidal Acceleration of Transverse Vibration Support Fixture For BRU Simulator At 0.12 g Peak Shake Table Input (BRU Mounted In Fixture)

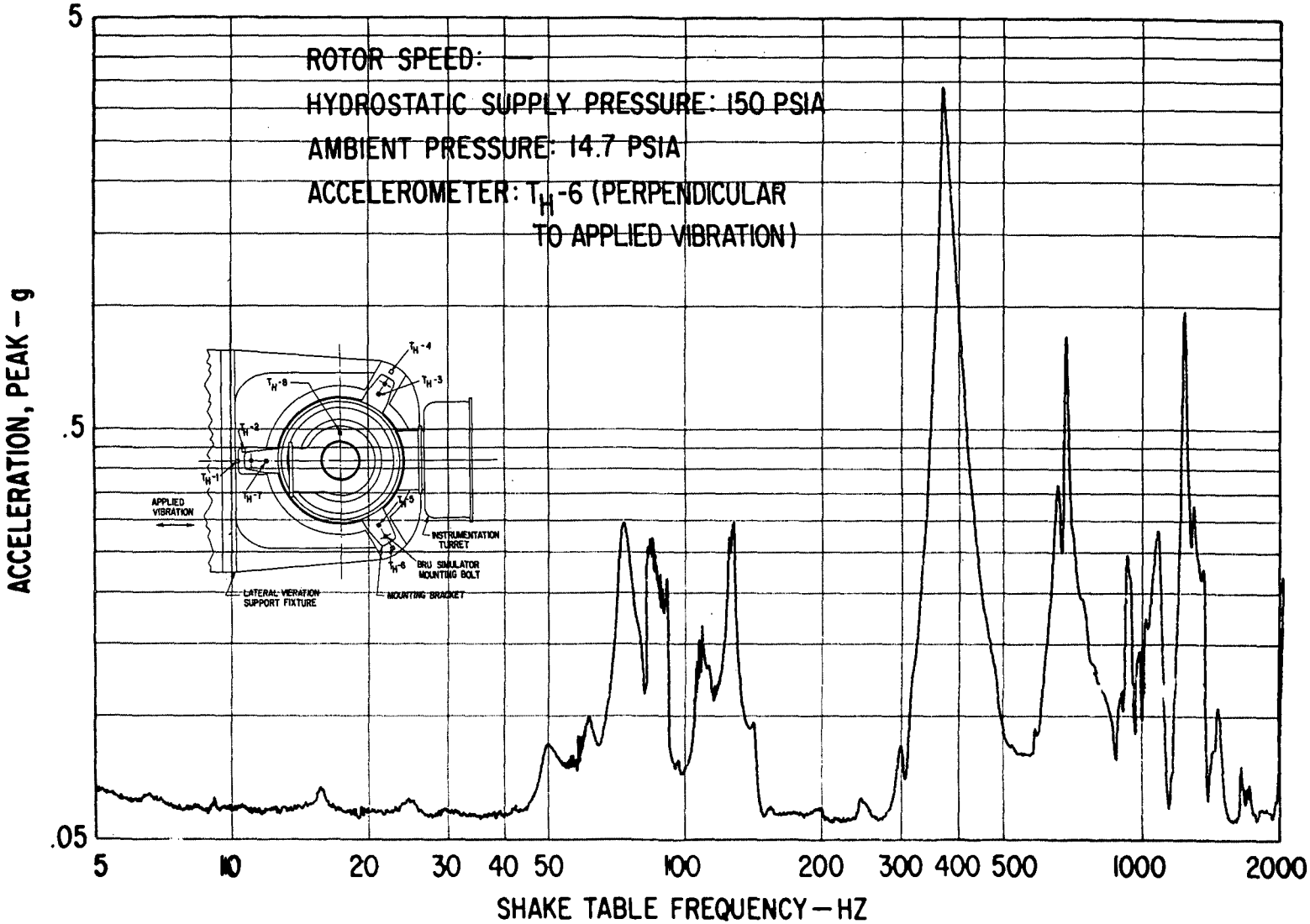

Fig. 101 Vertical Sinusoidal Acceleration of Transverse Vibration Test Support Fixture For BRU Simulator At 0.12 g Peak Shake Table Input (BRU Mounted In Fixture)

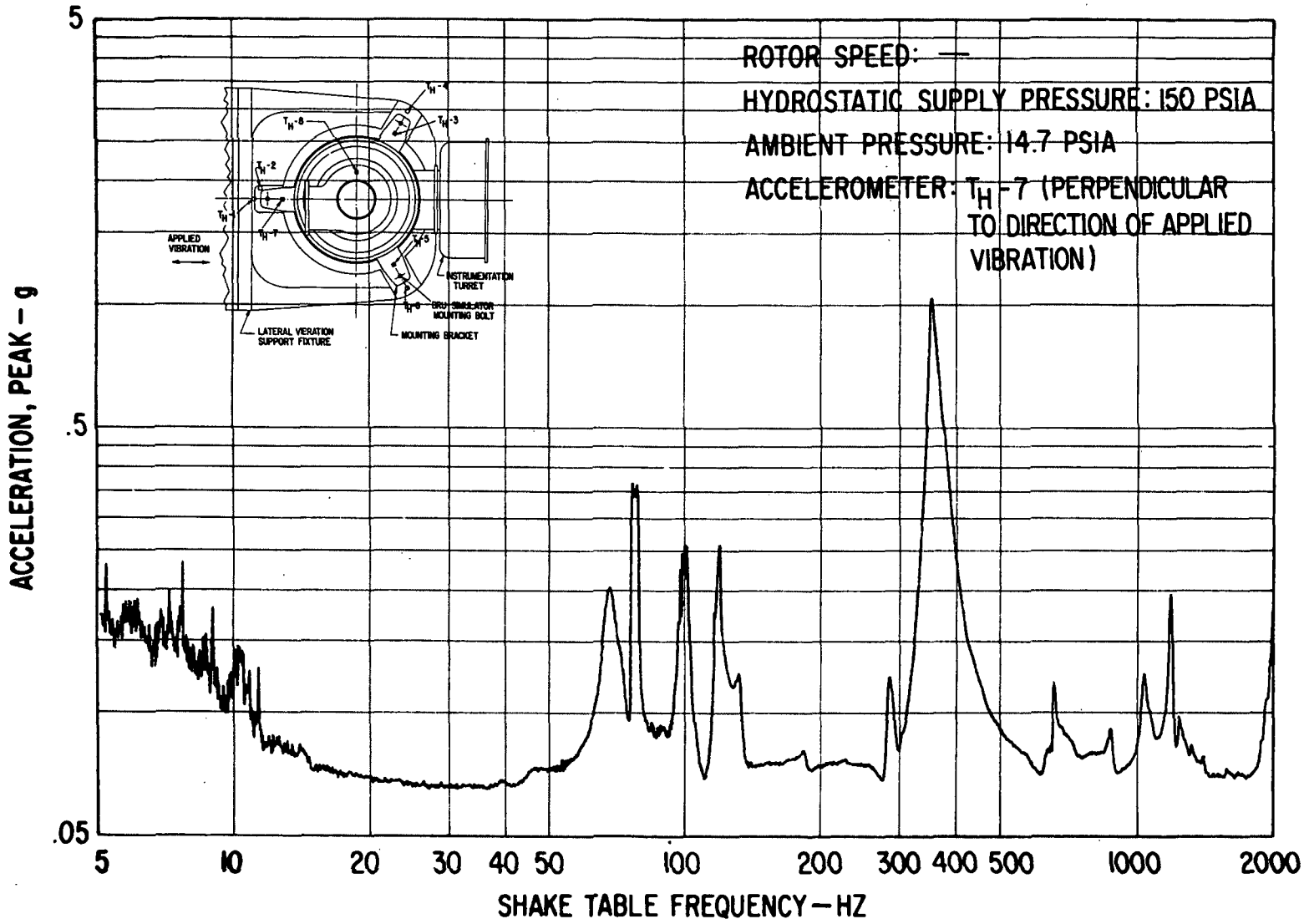

Fig. 102 Vertical Sinusoidal Acceleration On BRU Simulator Mounting Bracket Opposite From Turret, At 0.12 g Peak Shake Table Input

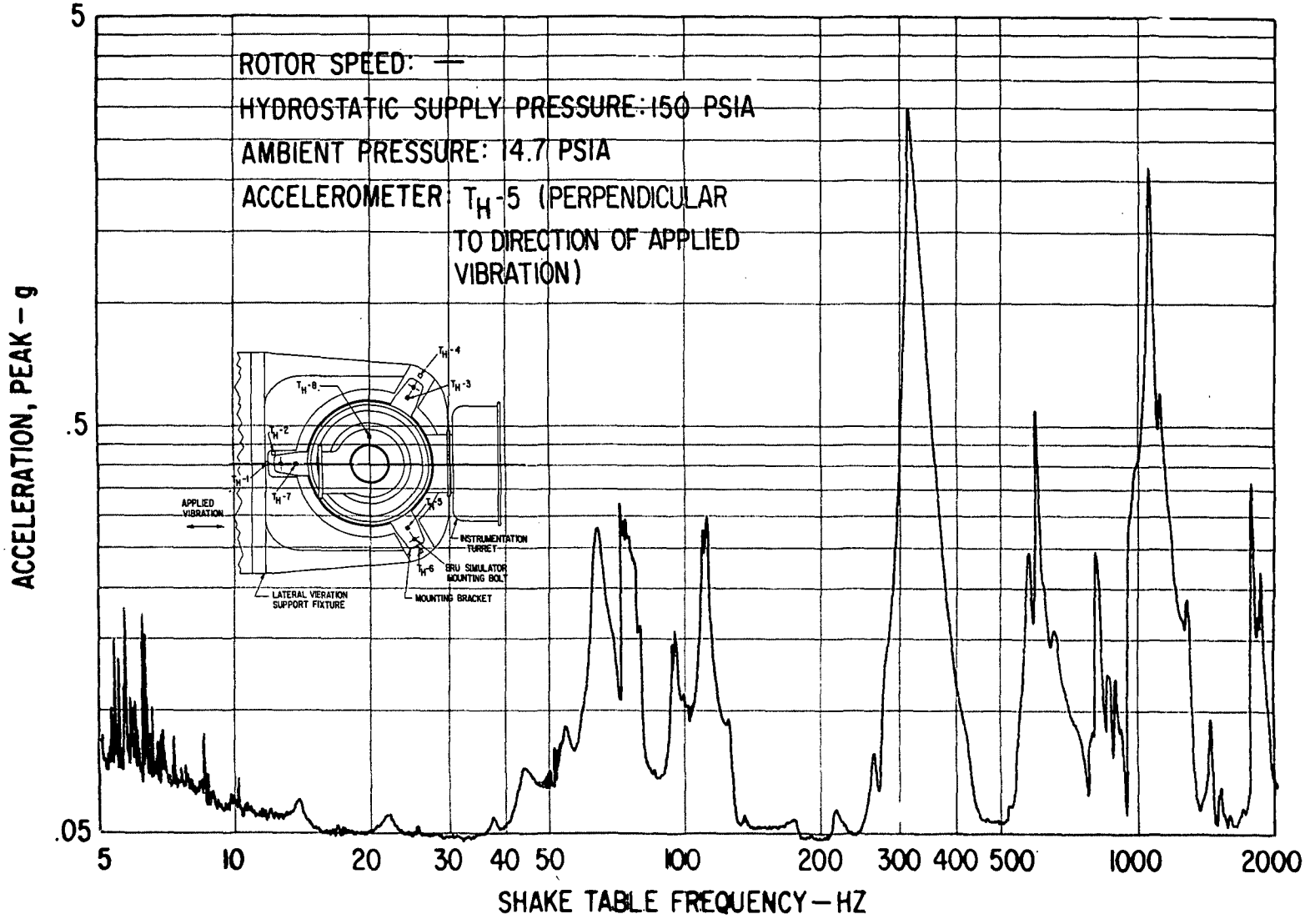

Fig. 103 Vertical Sinusoidal Acceleration On BRU Simulator Mounting Bracket Clockwise From Turret At 0.12 g Peak Shake Table Input

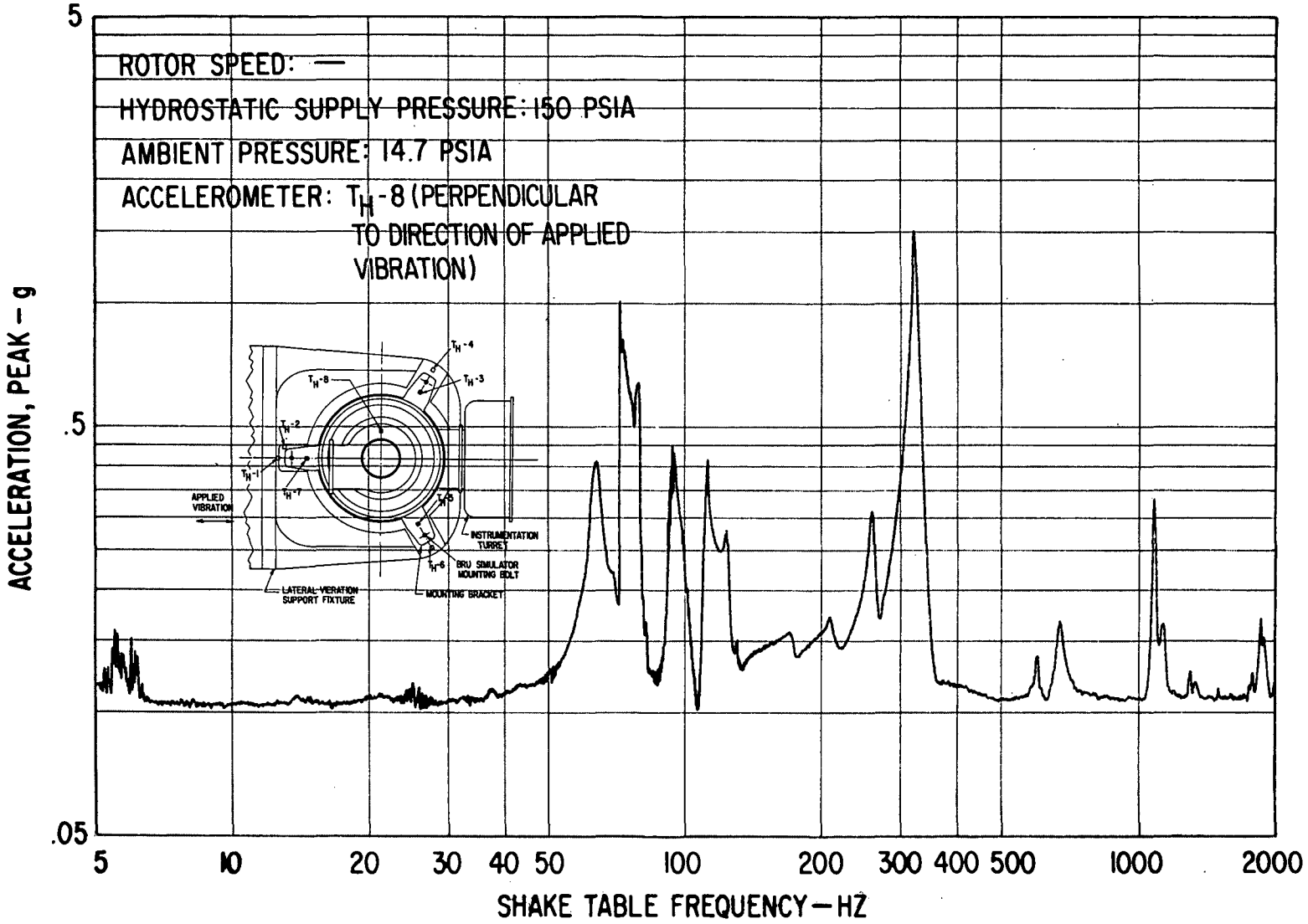

Fig. 104 Vertical Sinusoidal Acceleration At The Top Of The BRU Simulator At 0.12 g Peak Shake Table Input

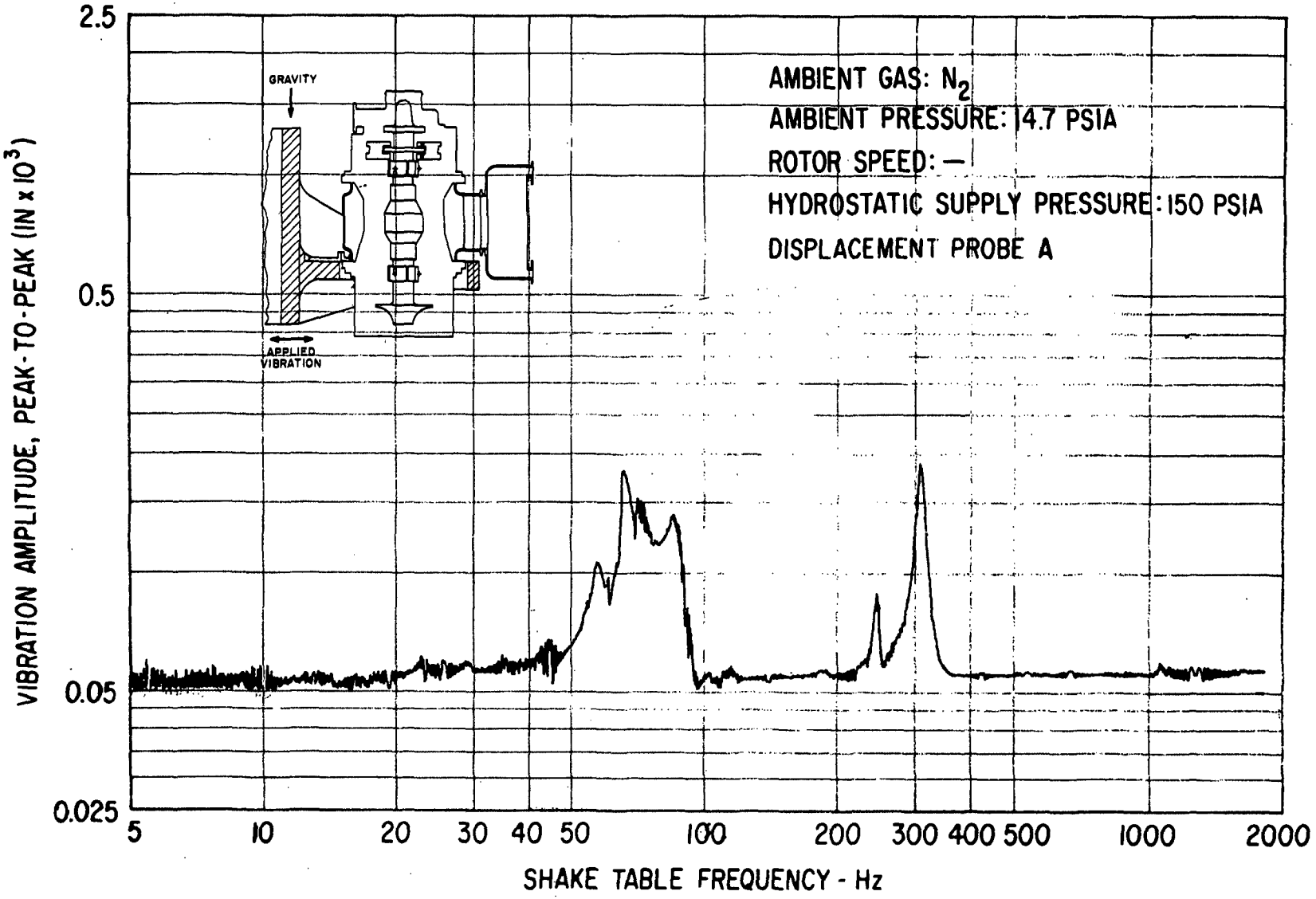

Fig. 105 Pad-To-Shaft Pivot Film Thickness Variation For Flex-Mounted Compressor Journal Bearing Pad Under Externally-Imposed Sinusoidal Vibration Of 0.12 x Peak

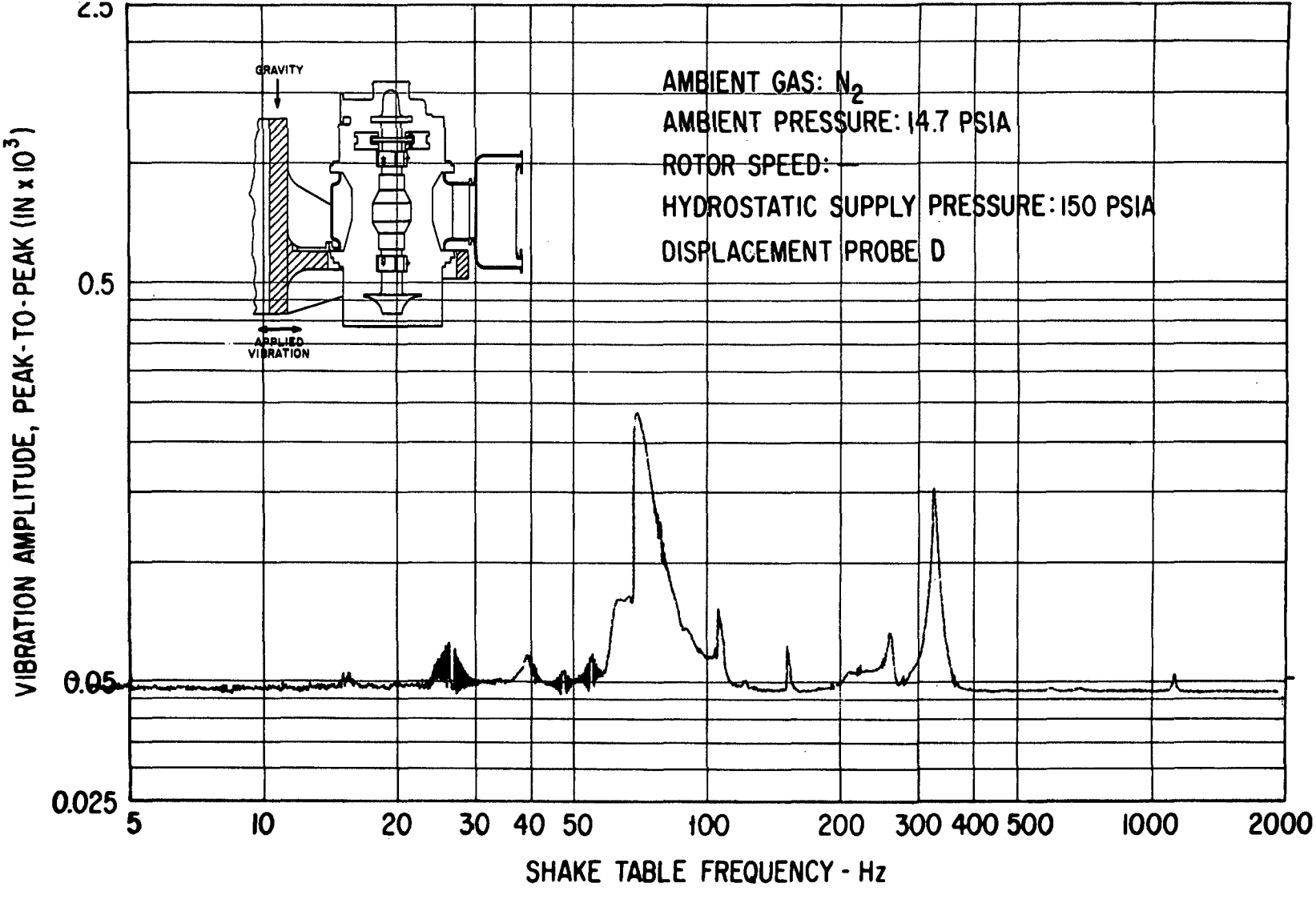

Fig. 106 Pad-To-Shaft Pivot Film Thickness Variation For Flex-Mounted Turbine Journal Bearing Pad Under Externally-Imposed Sinusoidal Vibration Of 0.12 g Peak

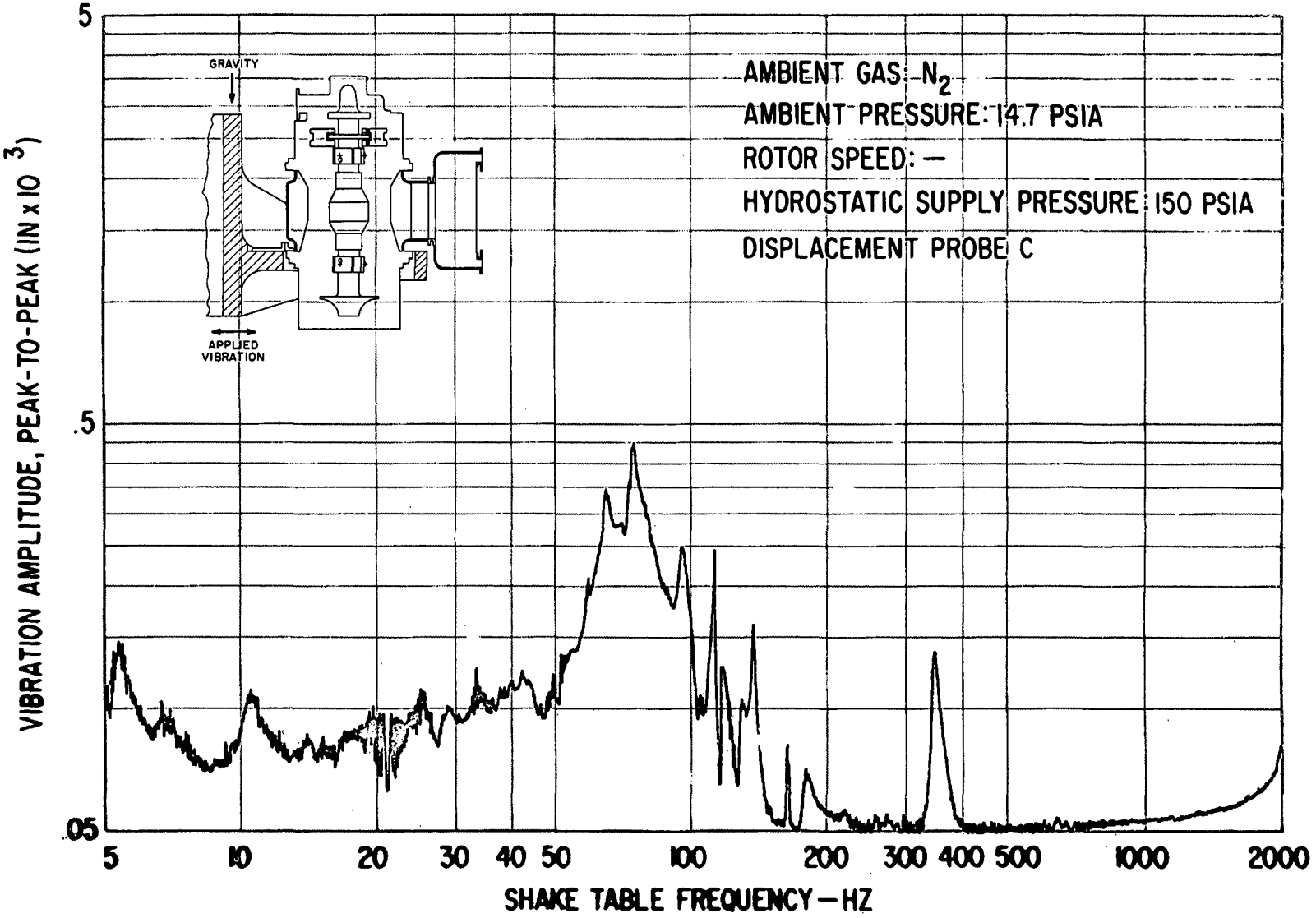

Fig. 107 Pad-To-Shaft Pivot Film Thickness Variation For Solid-Mounted Compressor Journal Bearing Under Externally-Imposed Sinusoidal Vibration Of 0.12 g Peak

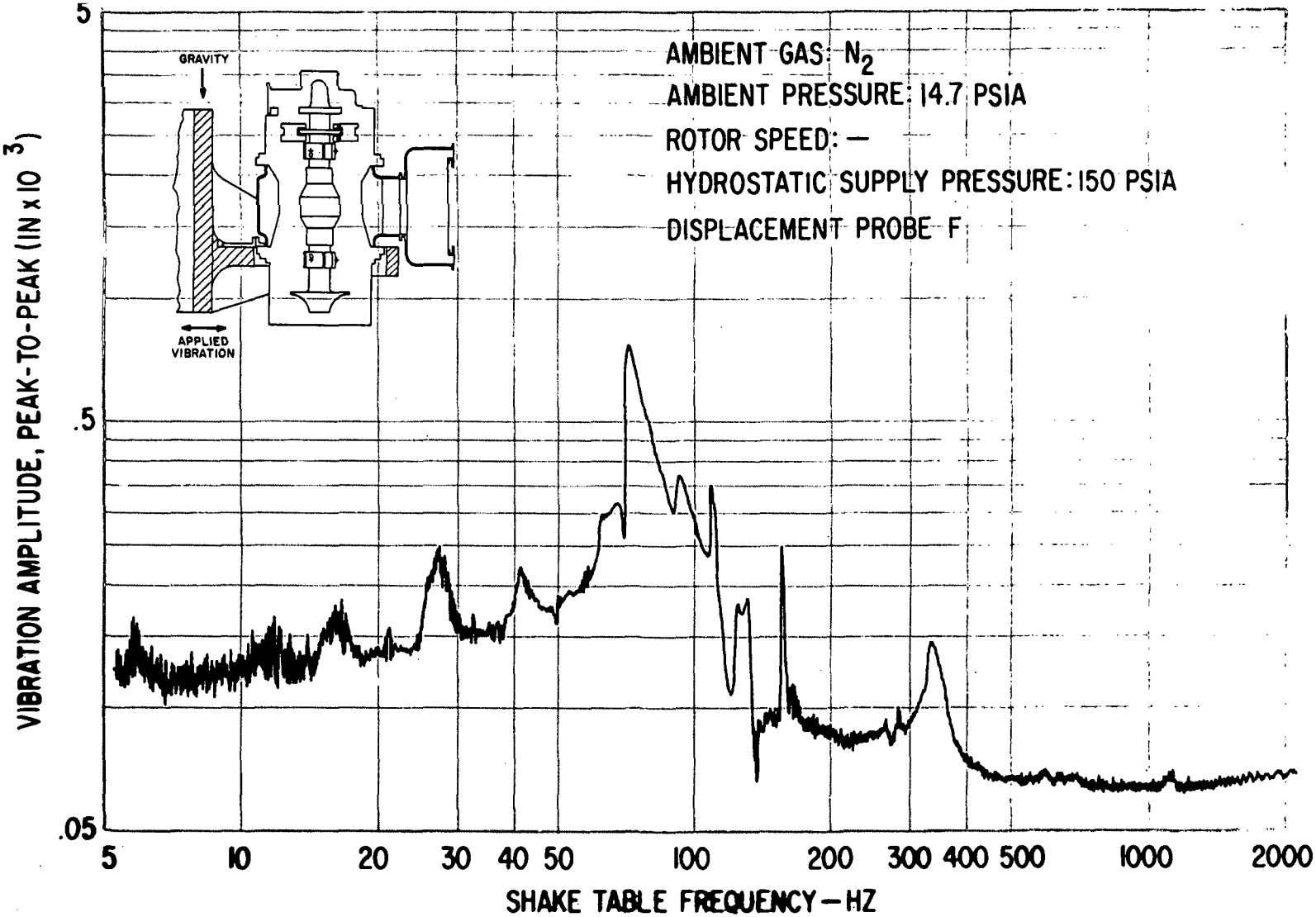

Fig. 108 Pad-To-Shaft Pivot Film Thickness Variation For Solid-Mounted Turbine Journal Bearing Under Externally-Imposed Sinusoidal Vibration Of 0.12 g Peak

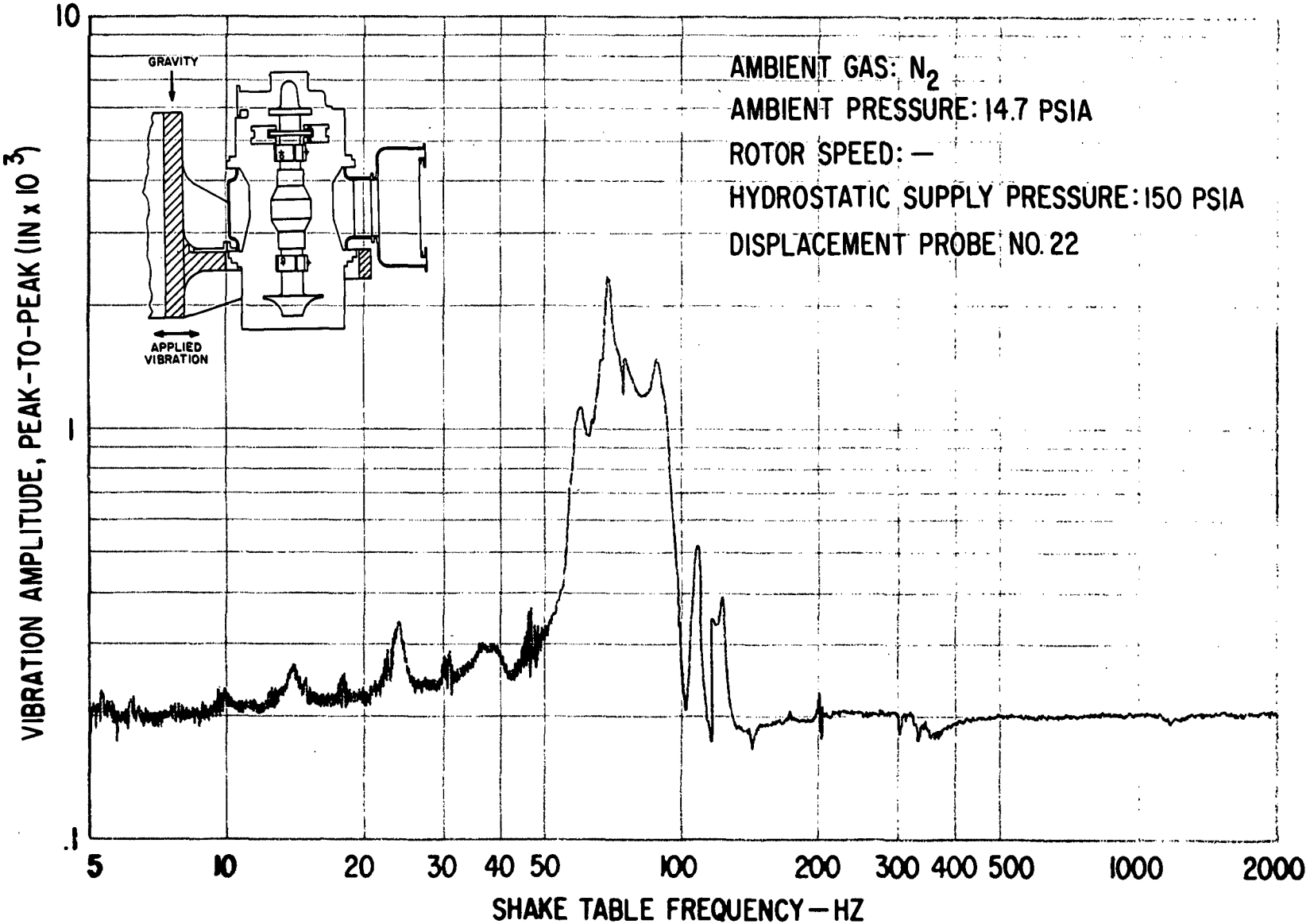

Fig. 109 Compressor Journal Flexure Amplitudes Under Externally-Imposed Sinusoidal Vibration Of 0.12 g Peak

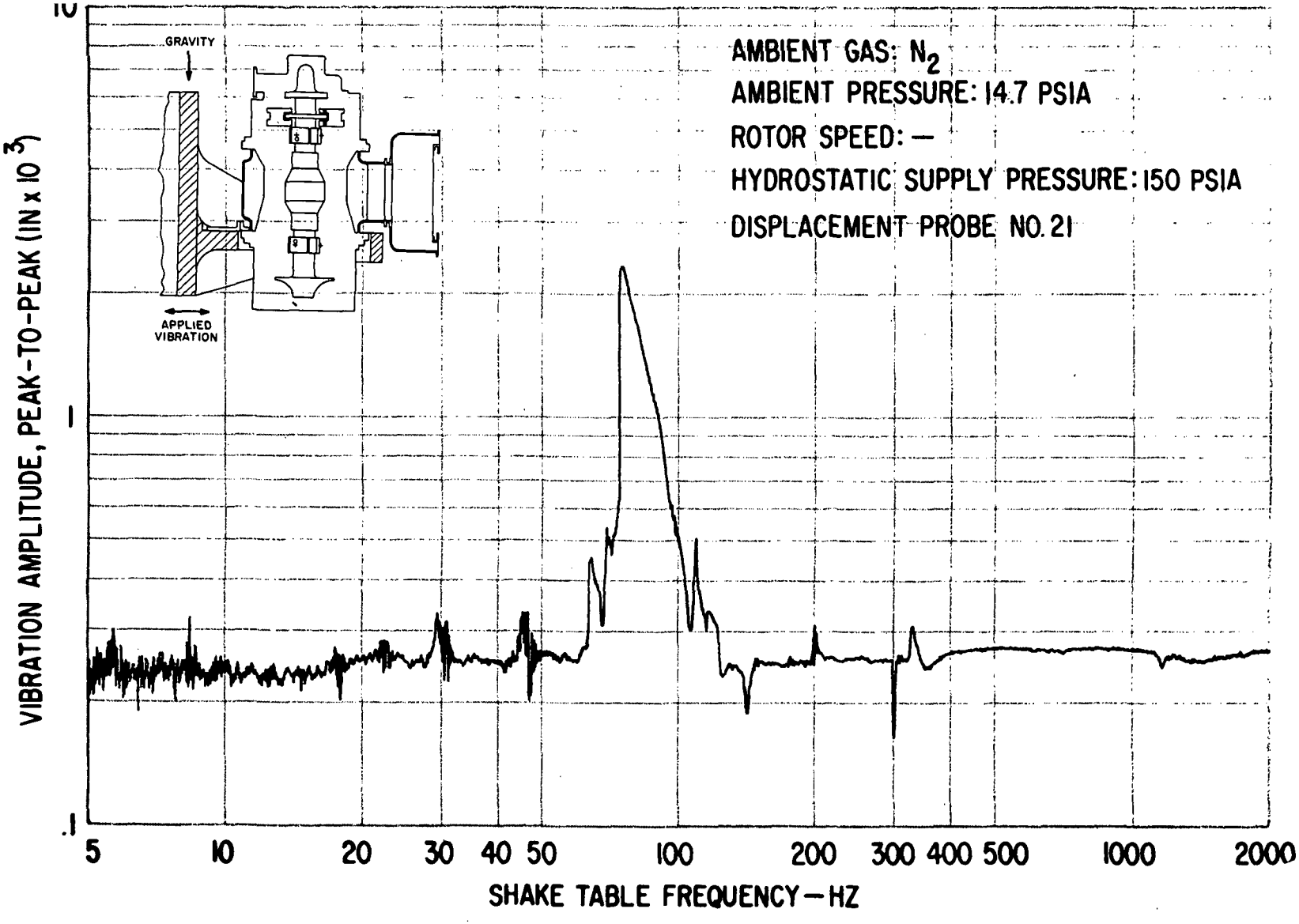

Fig. 110 Turbine Journal Flexure Amplitudes Under Externally-Imposed Sinusoidal Vibration Of 0.12 g Peak

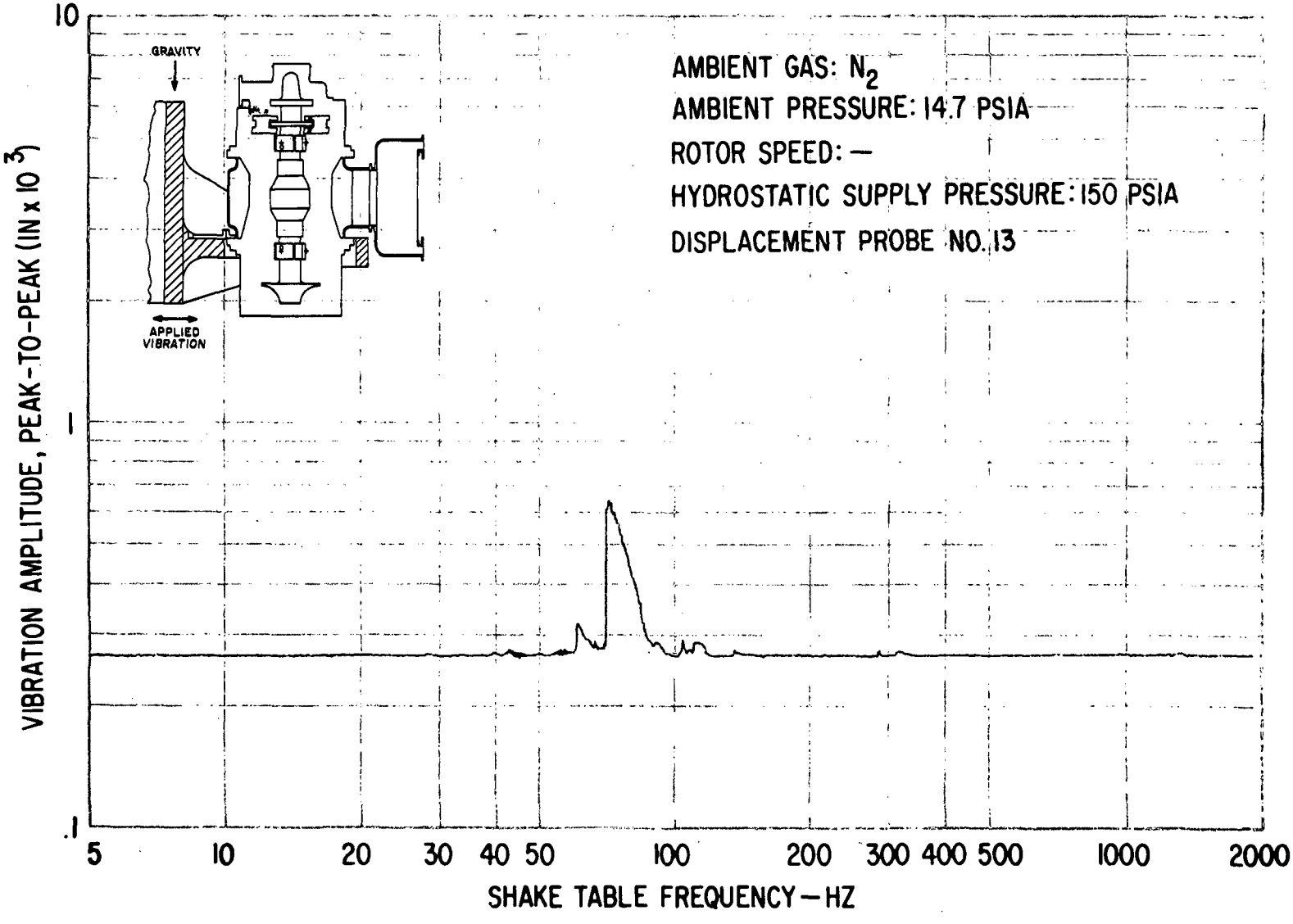

Fig. 111 Casing-To-Pad Leading Edge Amplitudes For Flex-Mounted Turbine Journal Bearing Pad Under Externally-Imposed Vibration Of 0.12 g Peak

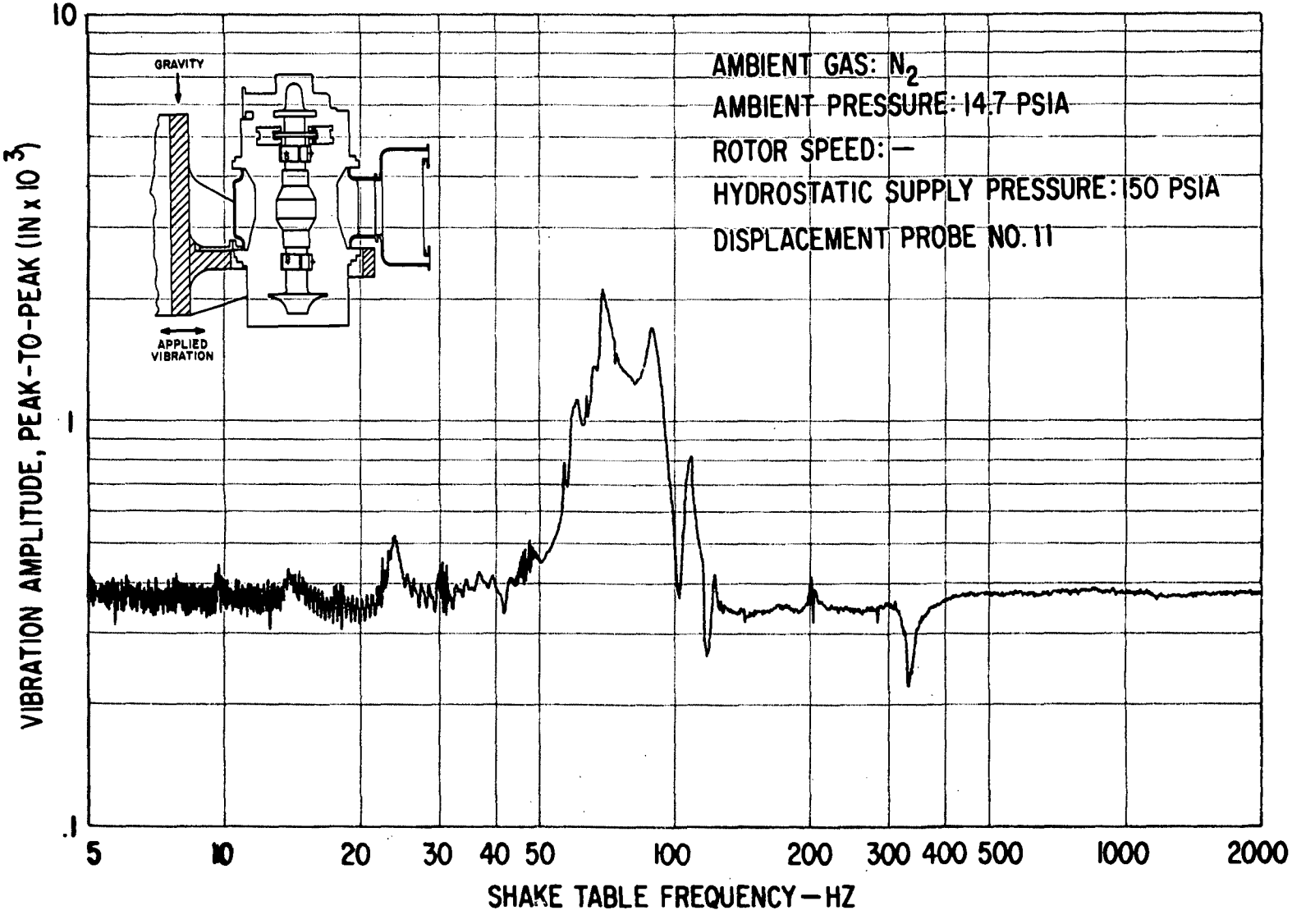

Fig. 112 Casing-To-Pad Leading Edge Amplitudes For Solid Mounted Compressor Journal Bearing Pad Under Externally-Imposed Vibration Of 0.12 g Peak

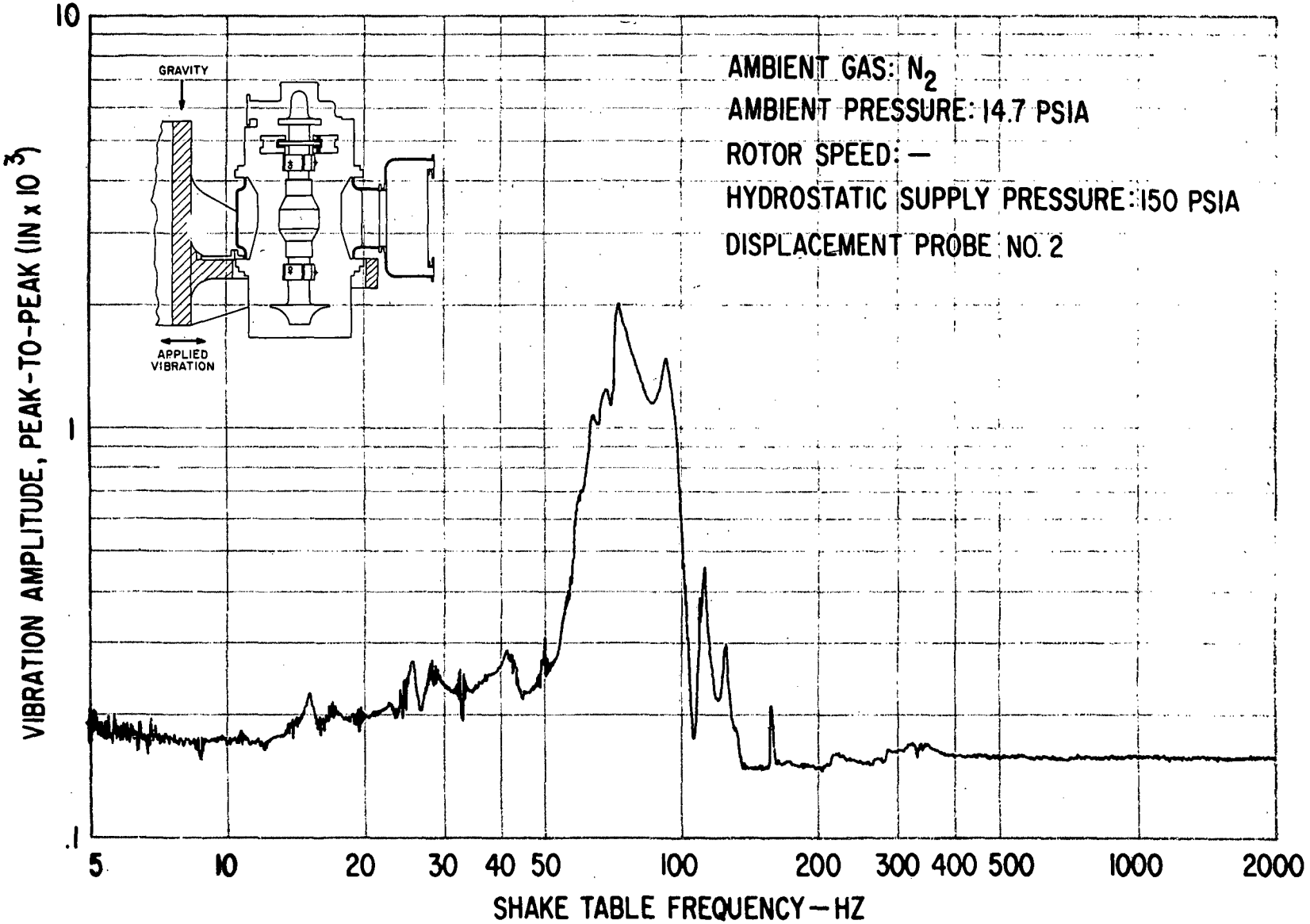

Fig. 113 Compressor Journal Rotor Amplitudes (Casing-To-Shaft) Under Externally-Imposed Sinusoidal Vibration Of 0.12 g Peak

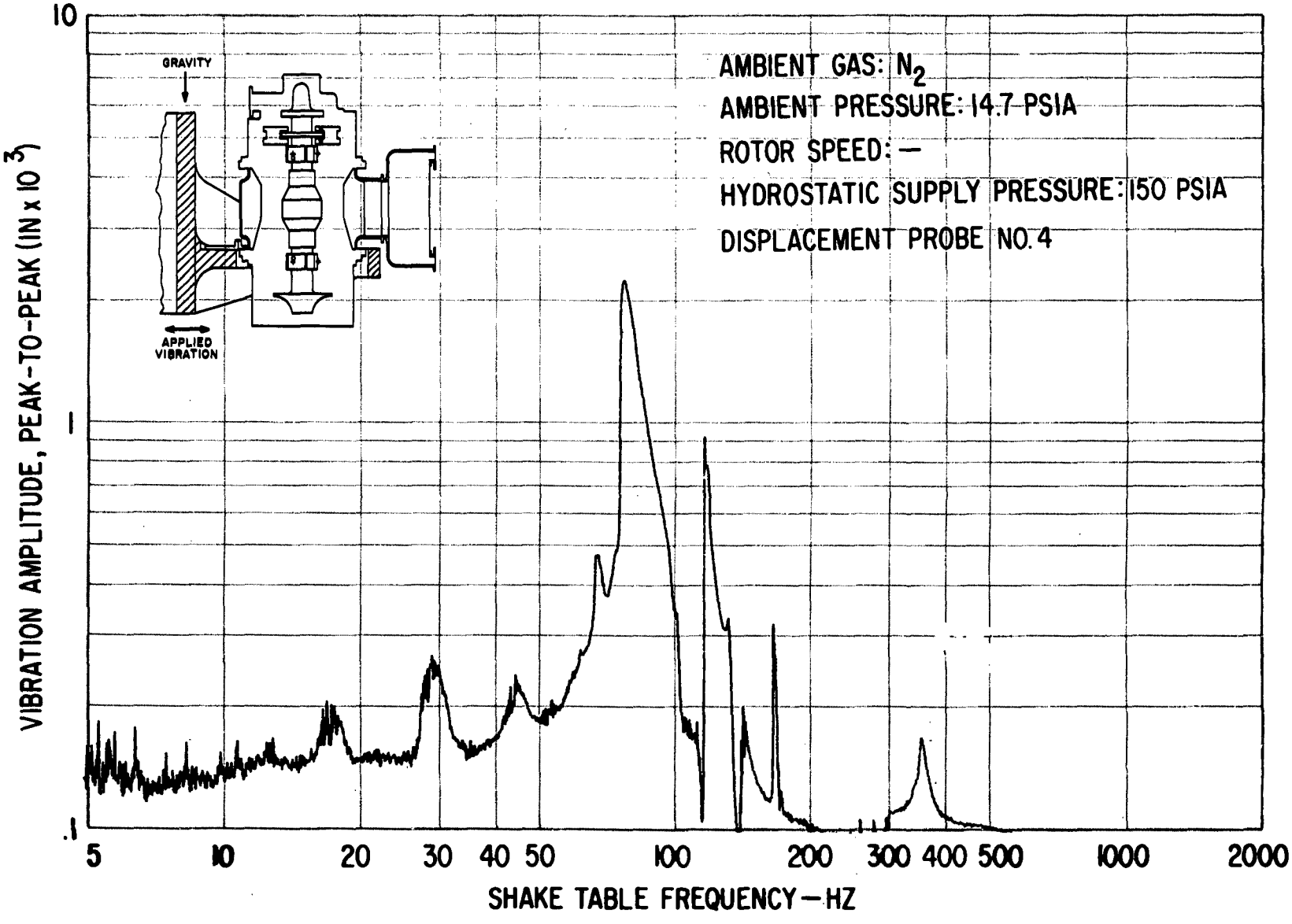

Fig. 114 Turbine Journal Rotor Amplitudes (Casing-To-Shaft) Under Externally-Imposed Sinusoidal Vibration Of 0.12 g Peak

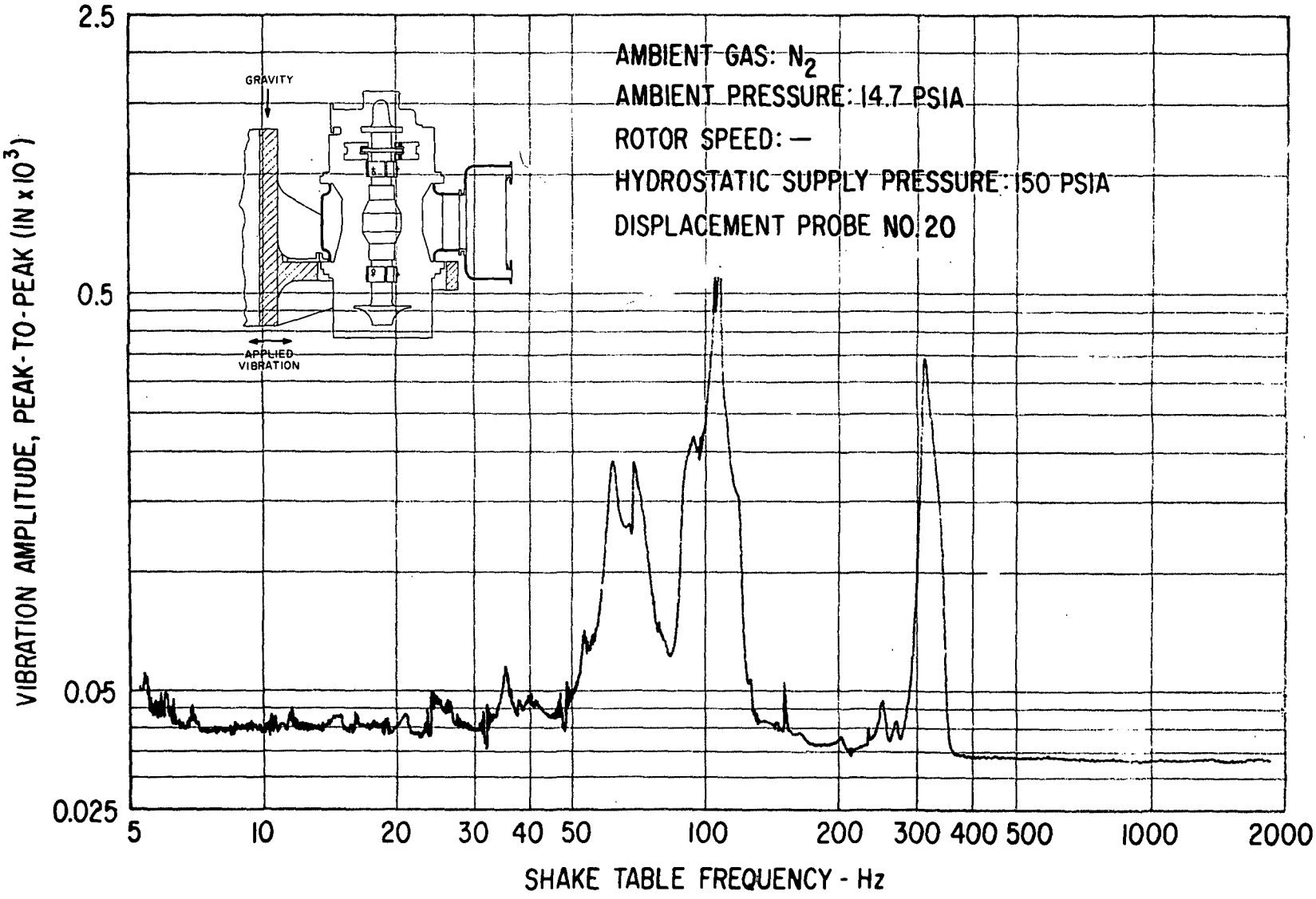

Fig. 115 Thrust Bearing Film Thickness Variation Under Externally-Imposed

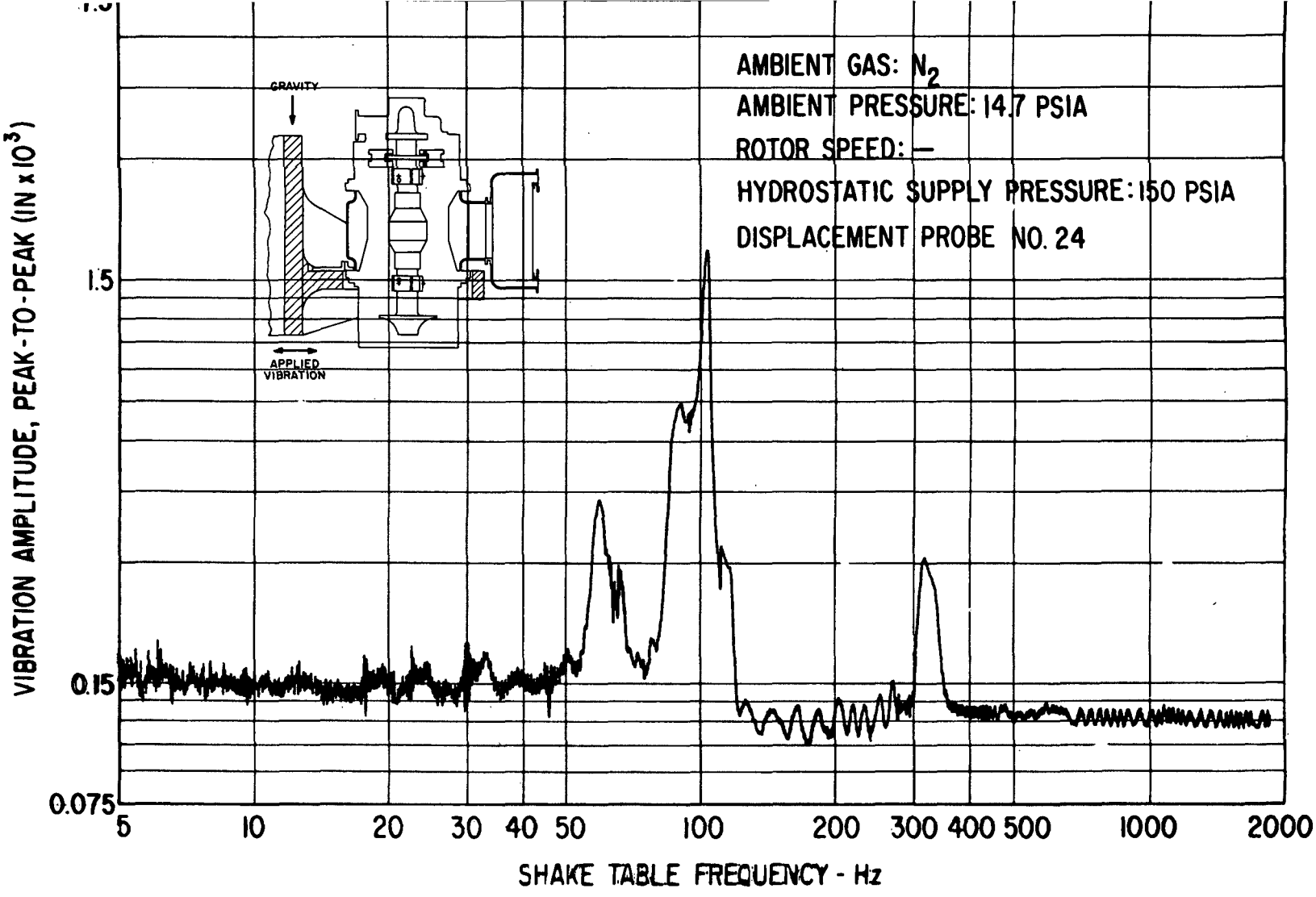

Fig. 116 Thrust Bearing Gimbal Amplitudes Under Externally-Imposed Sinusoidal Vibration Of 0.12 g Peak

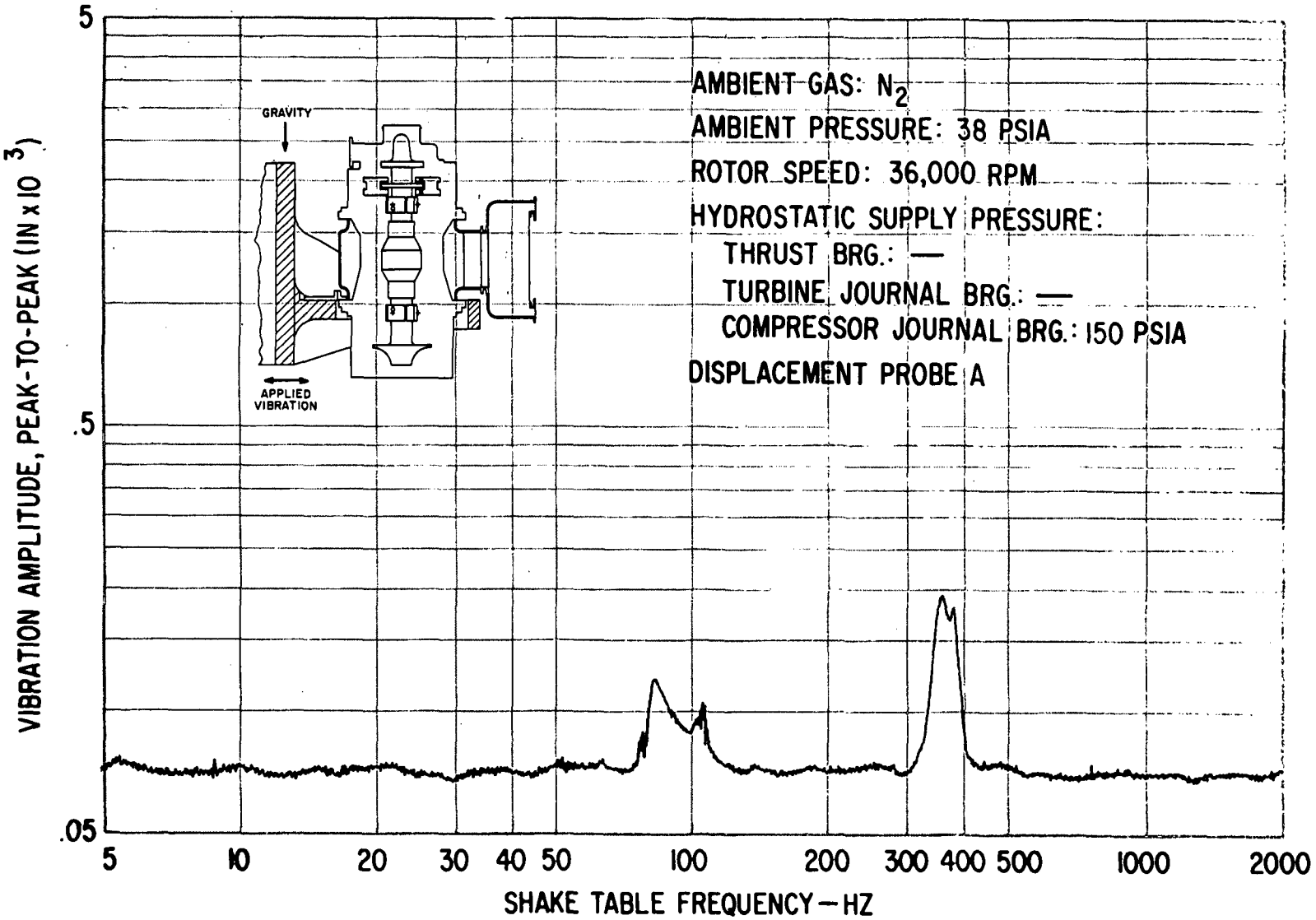

Fig. 117 Pad-To-Shaft Pivot Film Thickness For Flex-Mounted Compressor Journal Bearing Pad Under Externally-Imposed Sinusoidal Vibrations of 0.12 g Peak

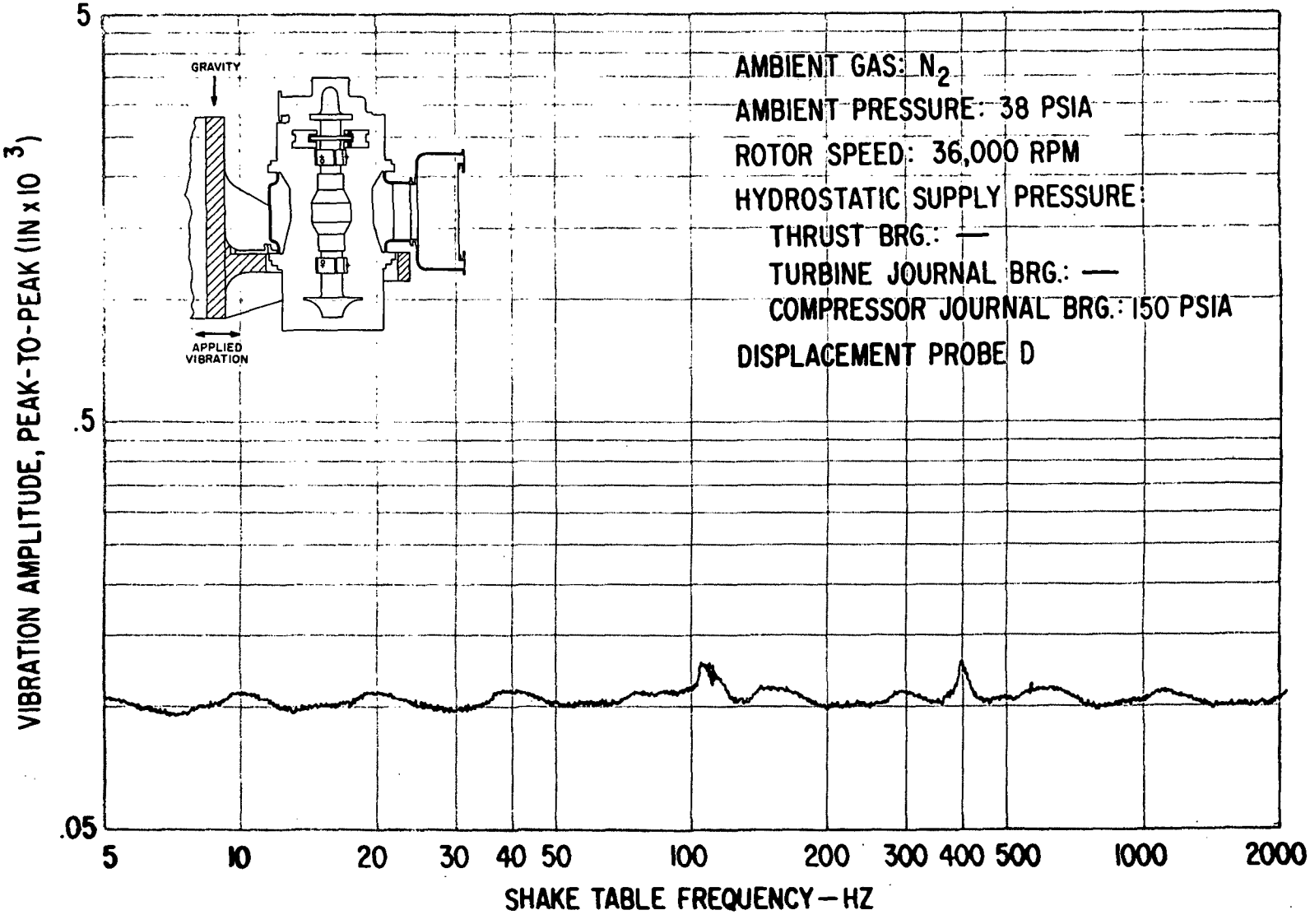

Fig. 118 Pad-To-Shaft Pivot Film Thickness Variation For Flex-Mounted Turbine Journal Bearing Pad Under Externally-Imposed Sinusoidal Vibration Of 0.12 g Peak

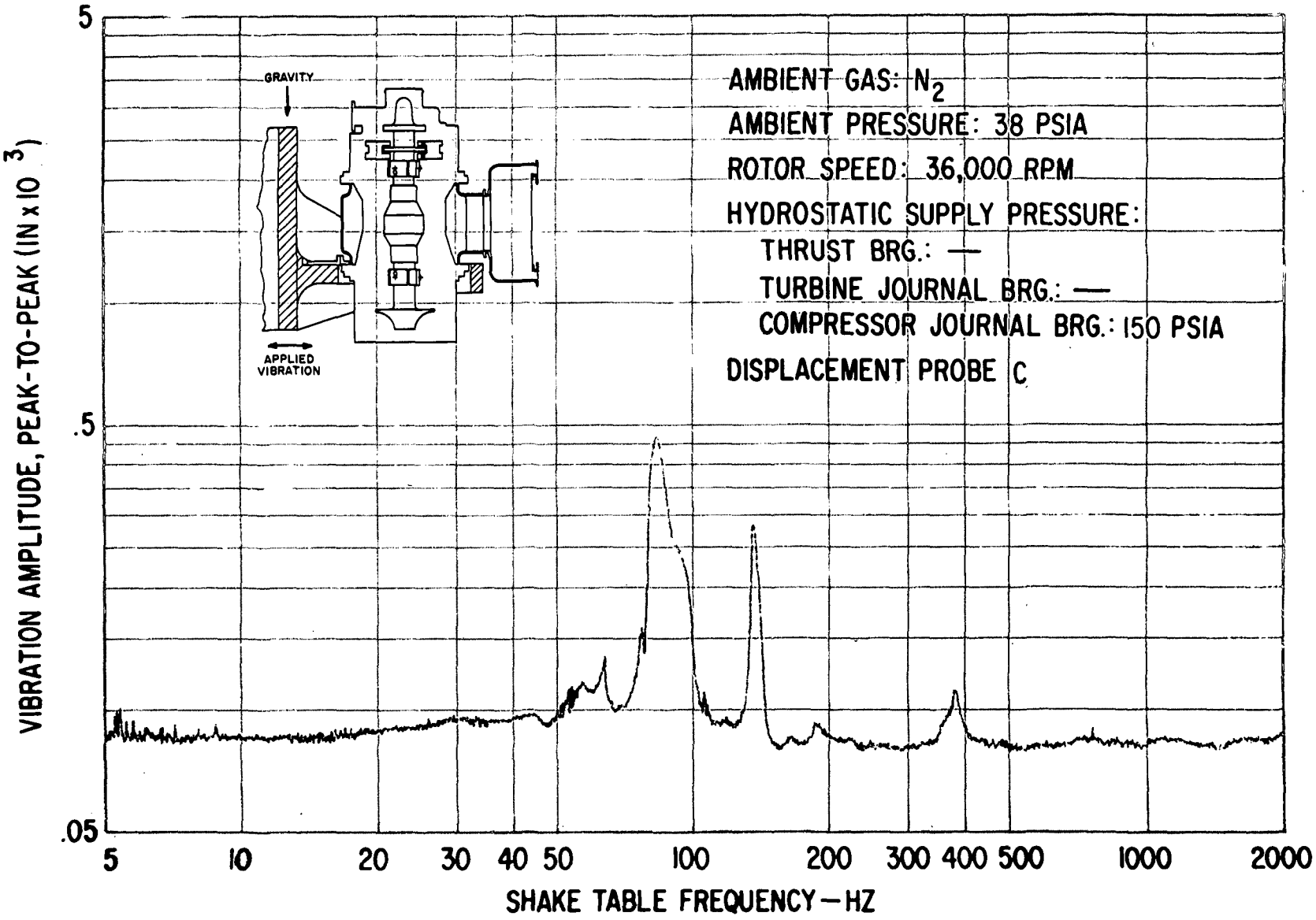

Fig. 119 Pad-To-Shaft Pivot Film Thickness Variations For Solid-Mounted Compressor Journal Bearing Pad Under Externally-Imposed Sinusoidal Vibrations Of 0.12 g Peak

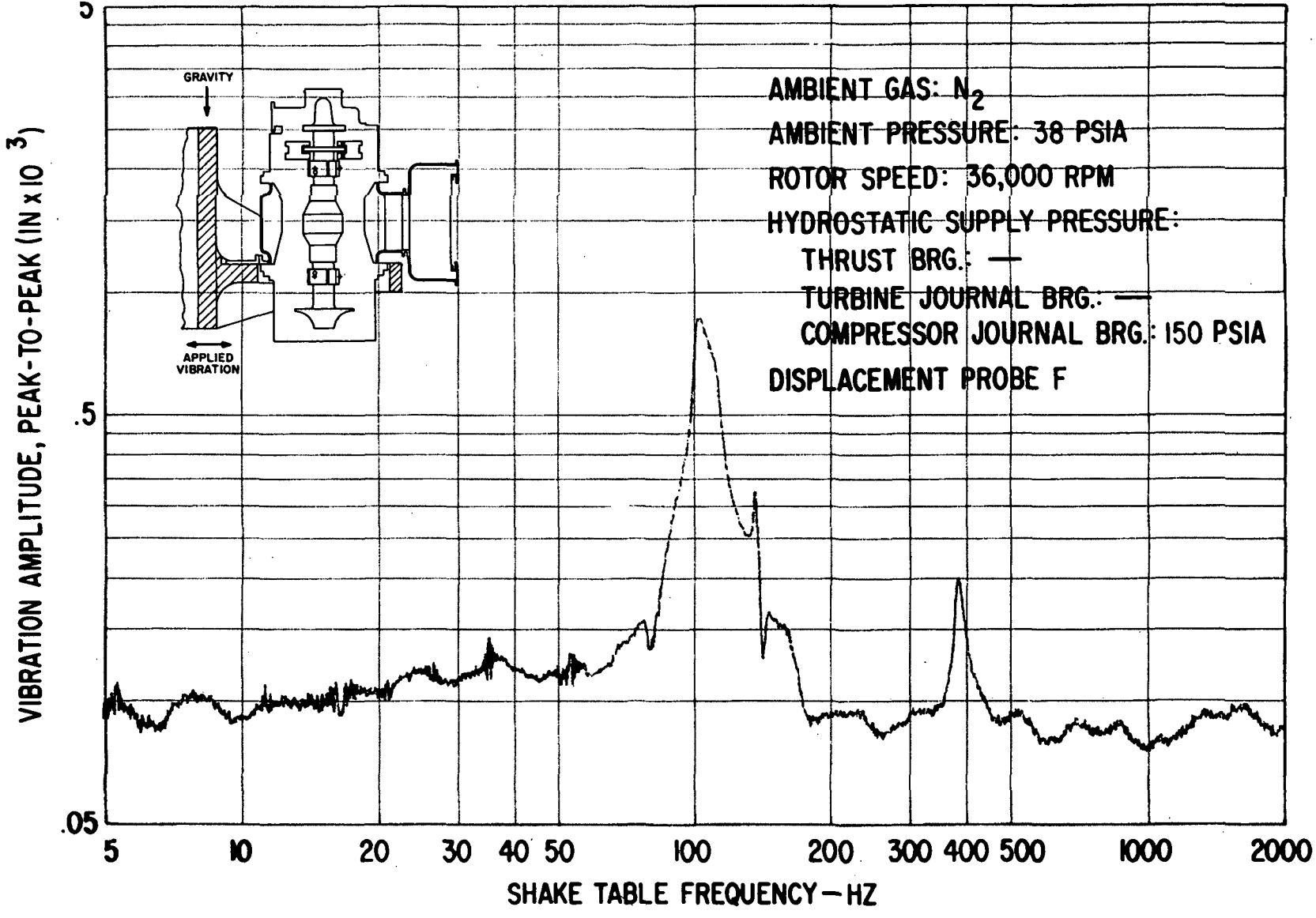

Fig. 120 Pad-To-Shaft Pivot Film Thickness Variation For Solid-Mounted Turbine Journal Bearing Under Externally-Imposed Sinusoidal Vibration Of 0.12 g Peak

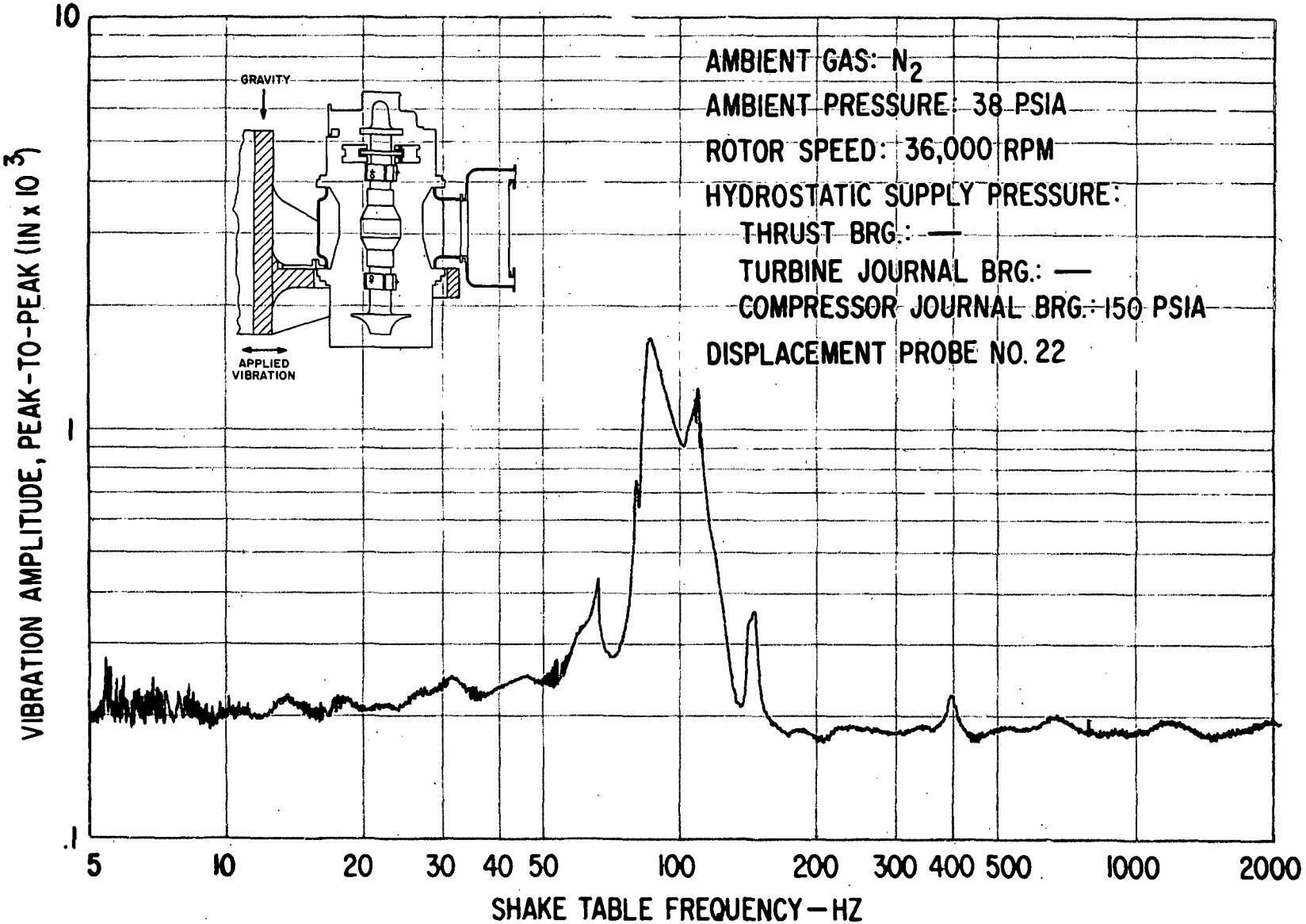

Fig. 121 Compressor Journal Flexure Amplitudes Under Externally-Imposed Sinusoidal Vibration Of 0.12 g Peak

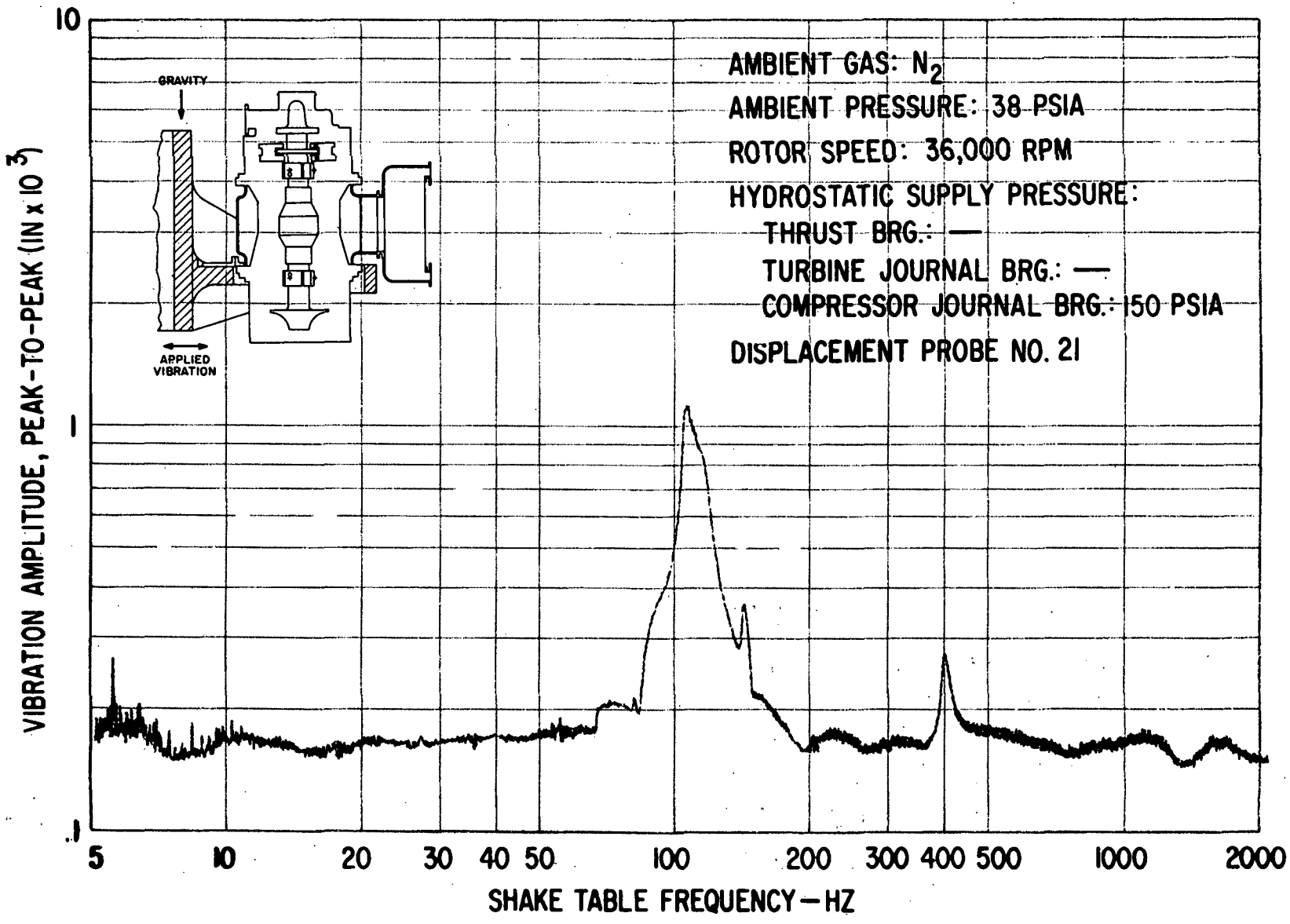

Fig. 122 Turbine Journal Flexure Amplitudes Under Externally-Imposed Sinusoidal Vibration Of 0.12 g Peak

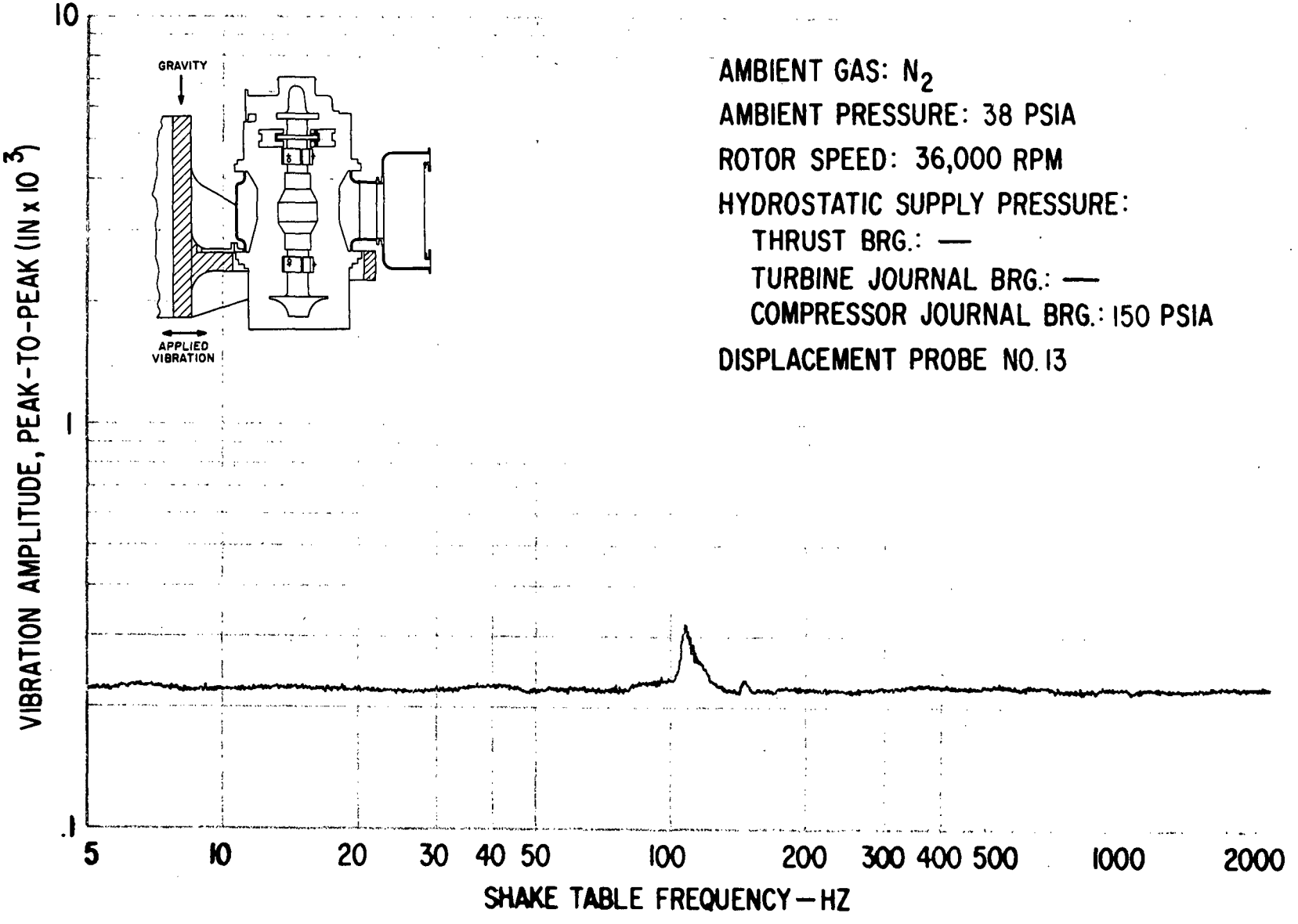

Fig. 123 Casing-To-Pad Leading Edge Amplitudes For Flex-Mounted Turbine Journal Bearing Pad Under Externally-Imposed Vibration Of 0.12 g Peak

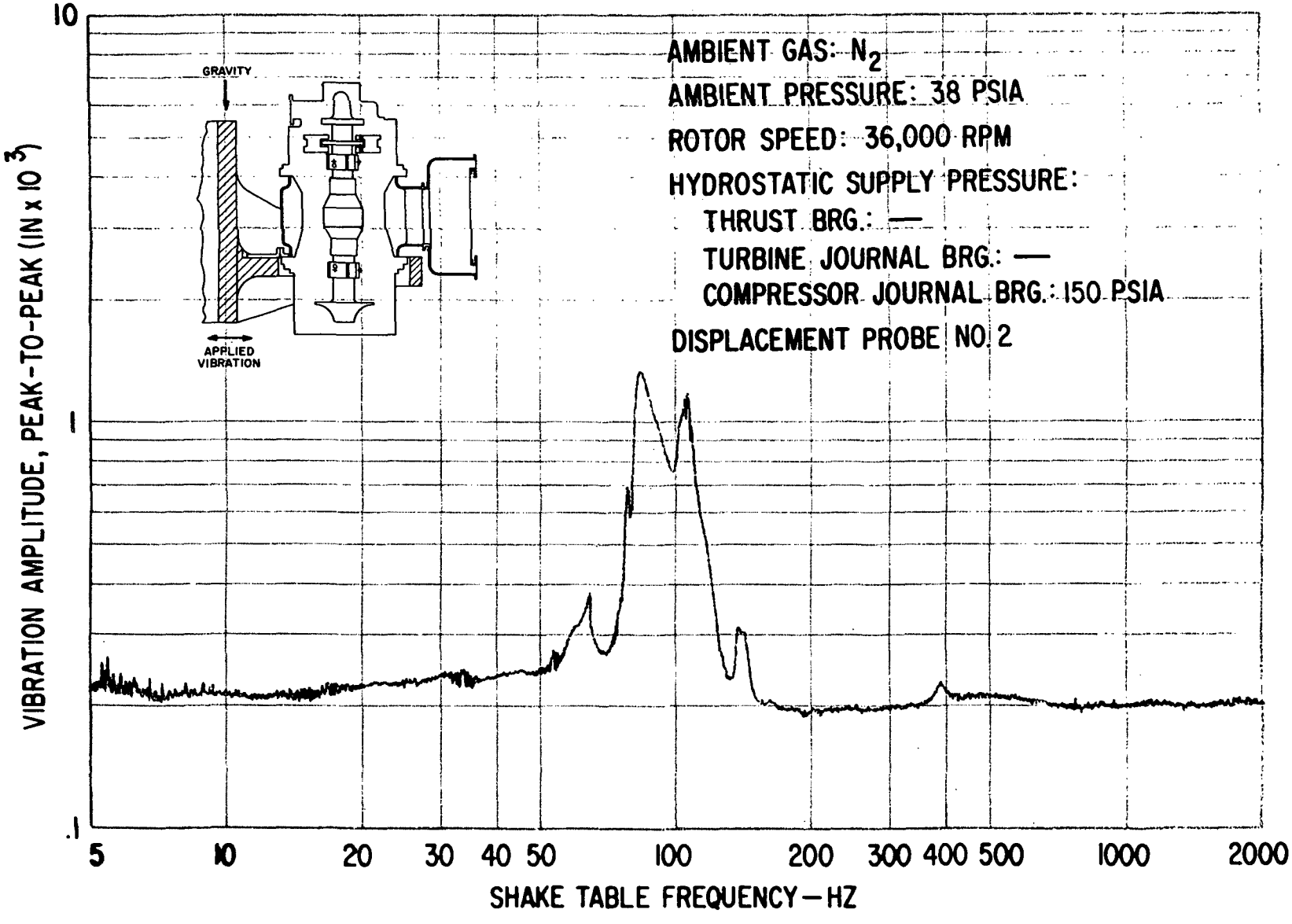

Fig. 124 Compressor Journal Rotor Amplitudes (Casing-To-Shaft) Under Externally-Imposed Sinusoidal Vibration Of 0.12 g Peak

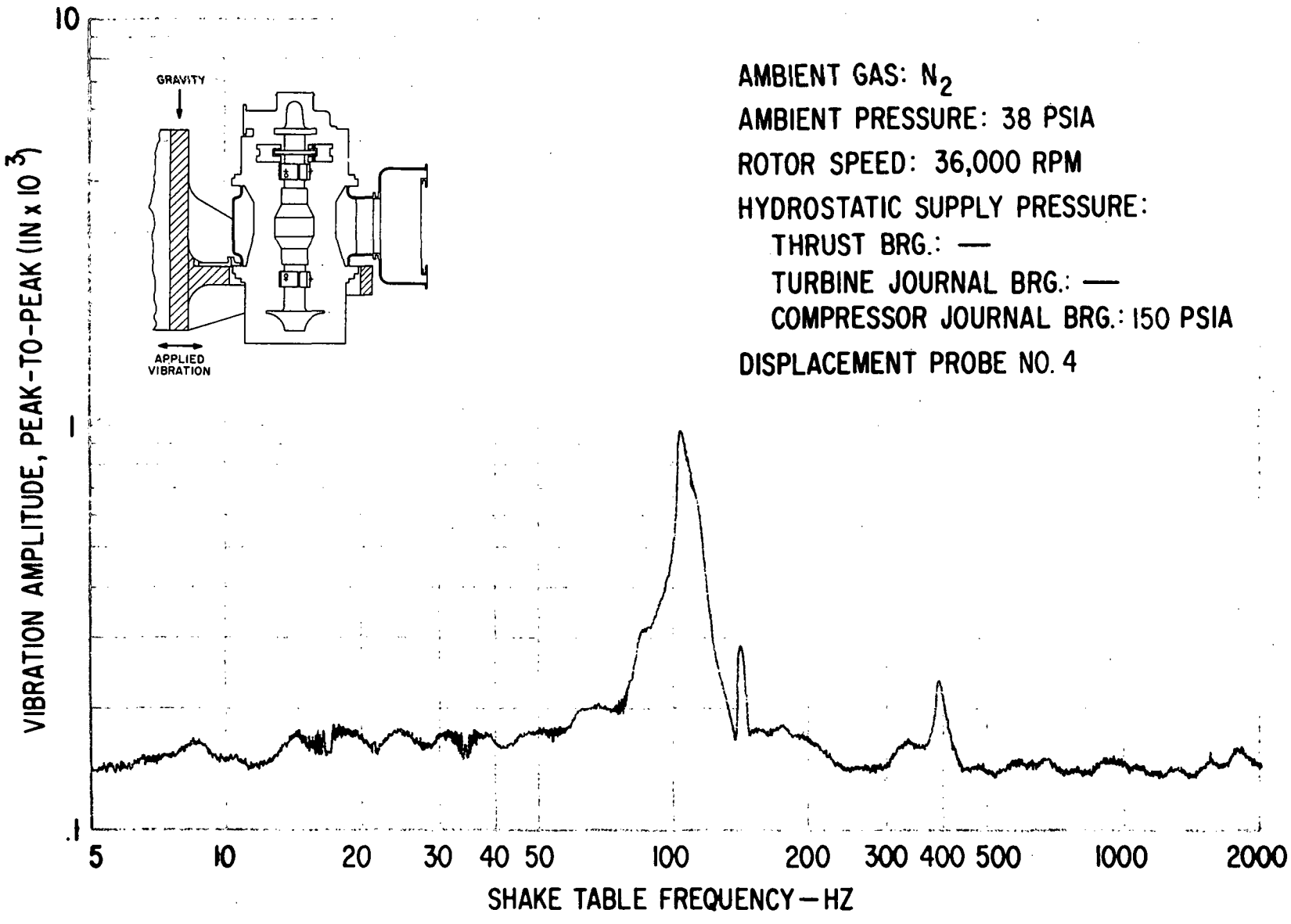

Fig. 125 Turbine Journal Rotor Amplitudes (Casing-To-Shaft) Under Externally-Imposed Sinusoidal Vibration Of 0.12 g Peak

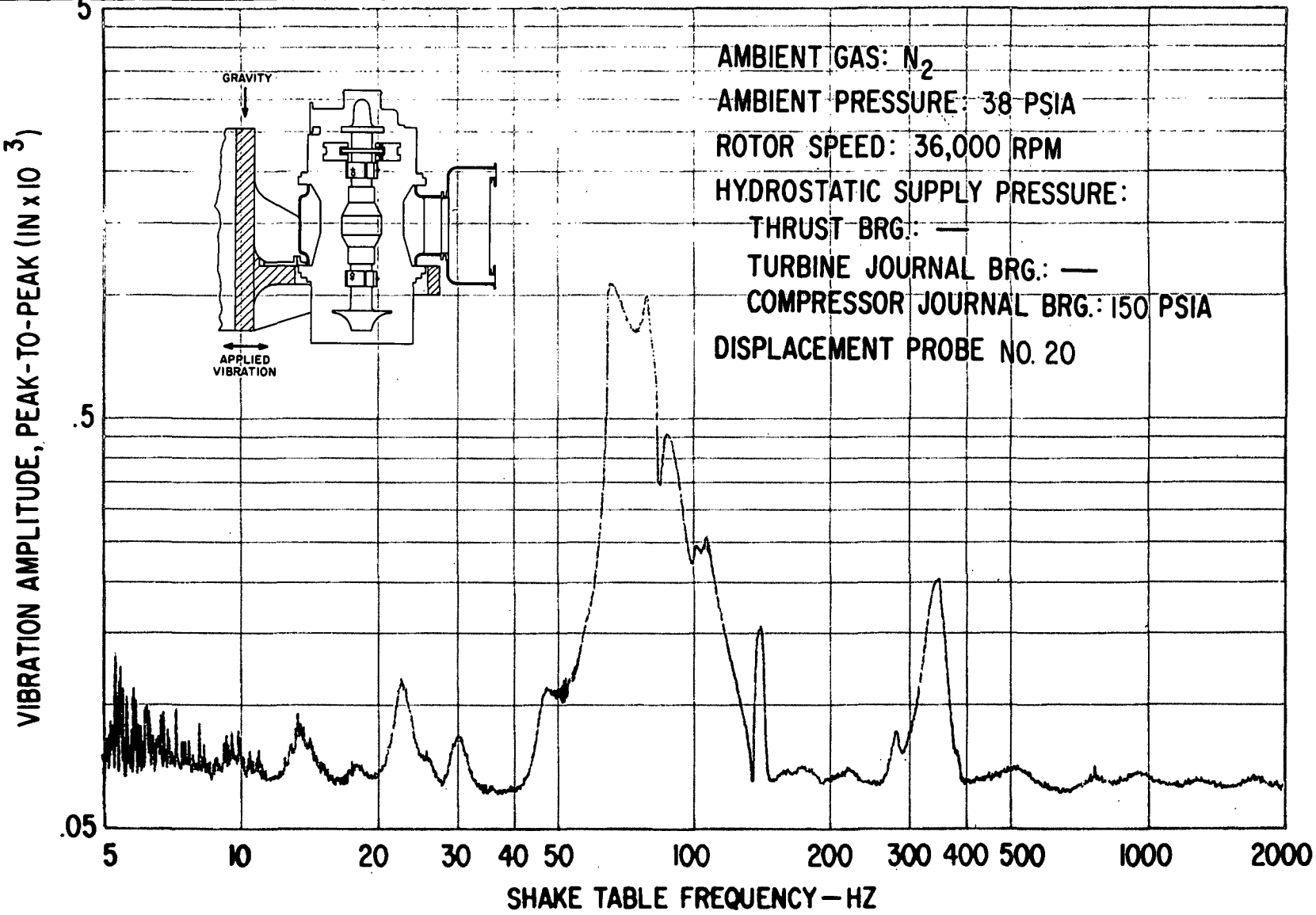

Fig. 126 Thrust Bearing Film Thickness Variation Under Externally-Imposed Sinusoidal Vibrations Of 0.12 g Peak

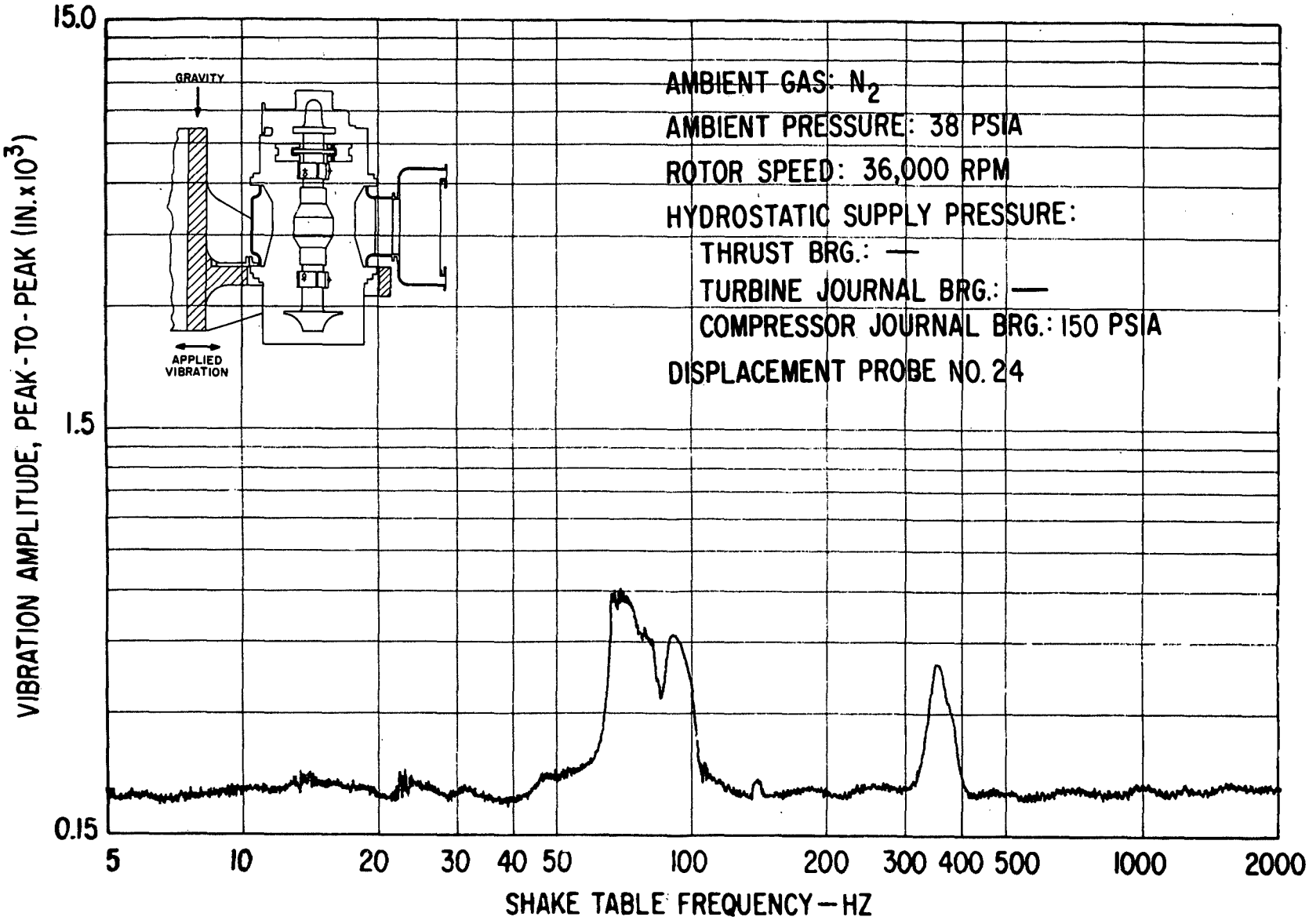

Fig. 127 Thrust Bearing Gimbal Amplitudes Under Externally-Imposed Sinusoidal Vibration at 0.12 g Peak

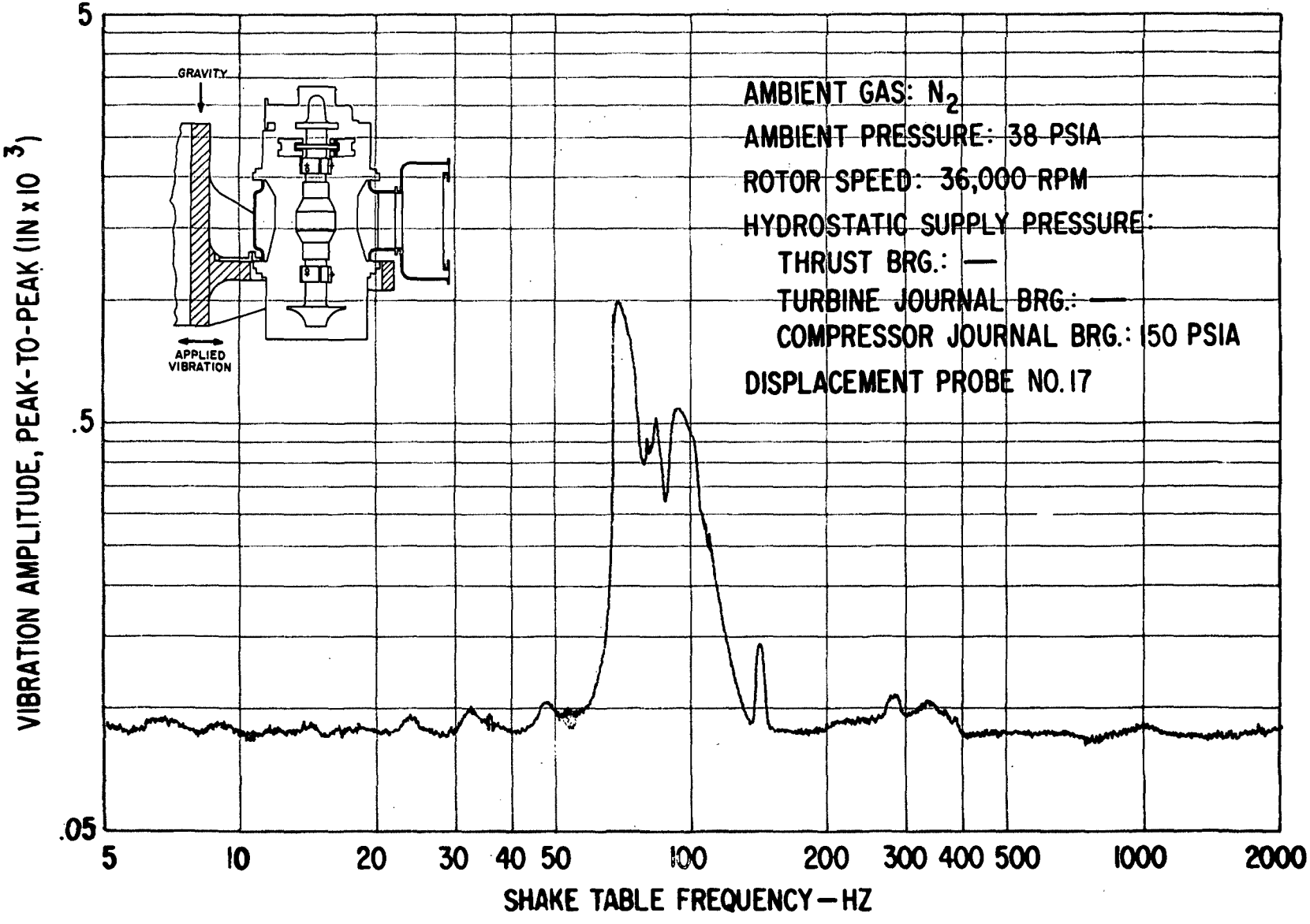

Fig. 128 Thrust Bearing Film Thickness Variation Under Externally-Imposed Sinusoidal Vibrations Of 0.12 g Peak

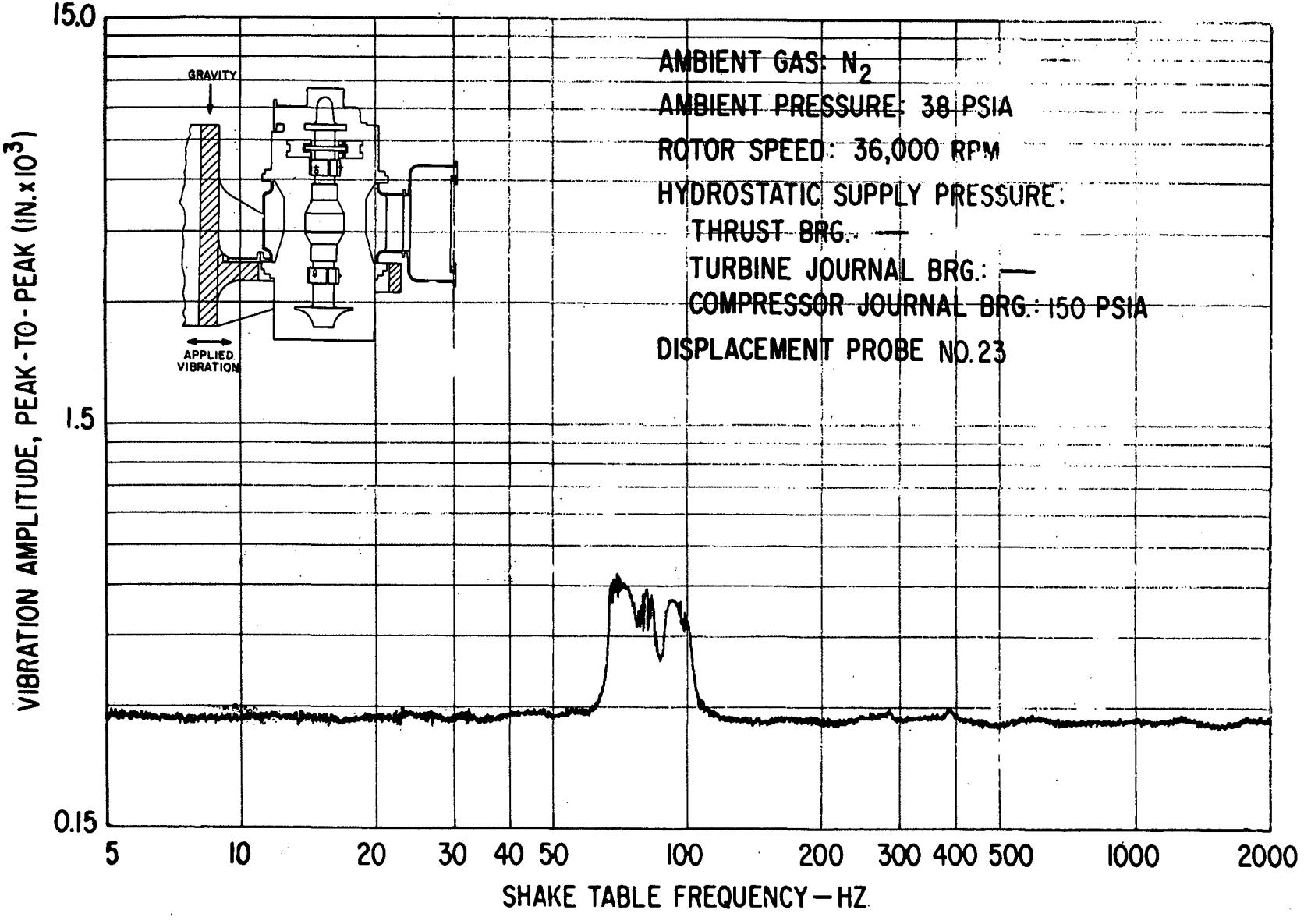

Fig. 129 Thrust Bearing Gimbal Amplitudes Under Externally-Imposed Sinusoidal Vibration Of 0.12 g Peak

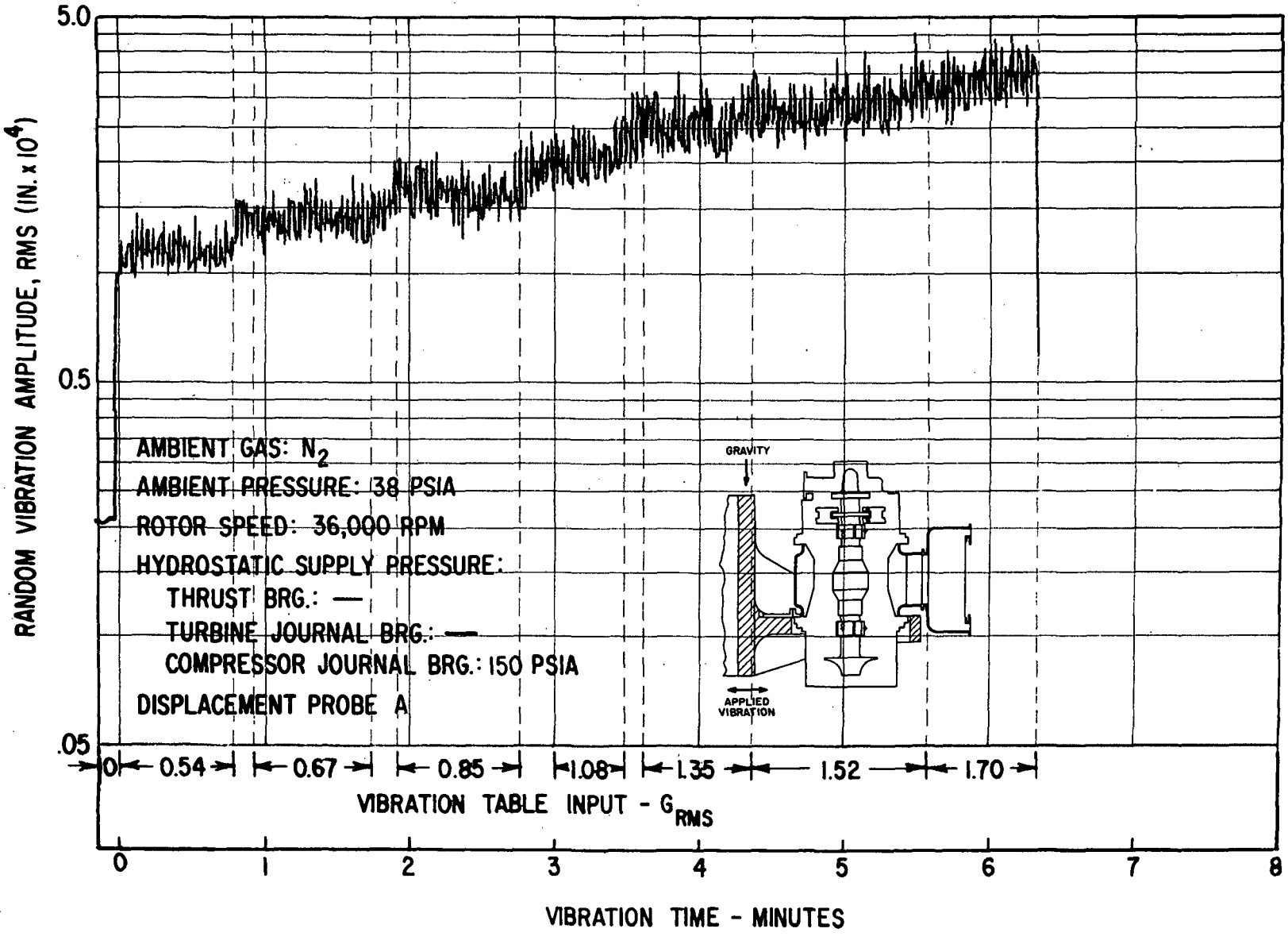

Fig. 130 Pad-To-Shaft Pivot Film Thickness Variation For Flex-Mounted Compressor Journal Bearing Pad Under Externally-Imposed Shaped Random Vibrations According To NASA Spec 417-2-C-3.5

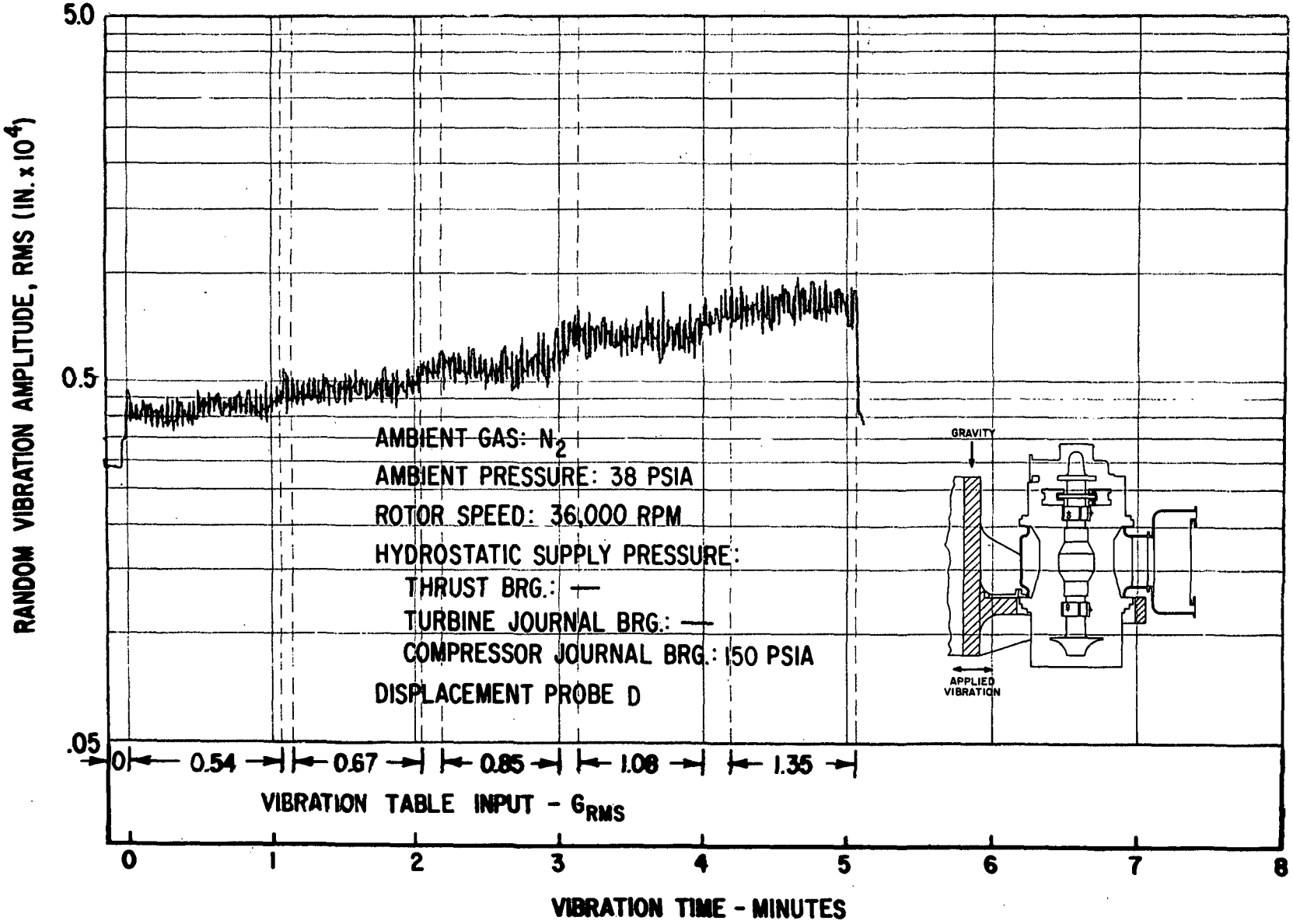

Fig. 131 Pad-To-Shaft Pivot Film Thickness Variation For Flex-Mounted Turbine Journal Bearing Pad Under Externally-Imposed Shaped Random Vibrations According To NASA Spec 417-2-C-3.5

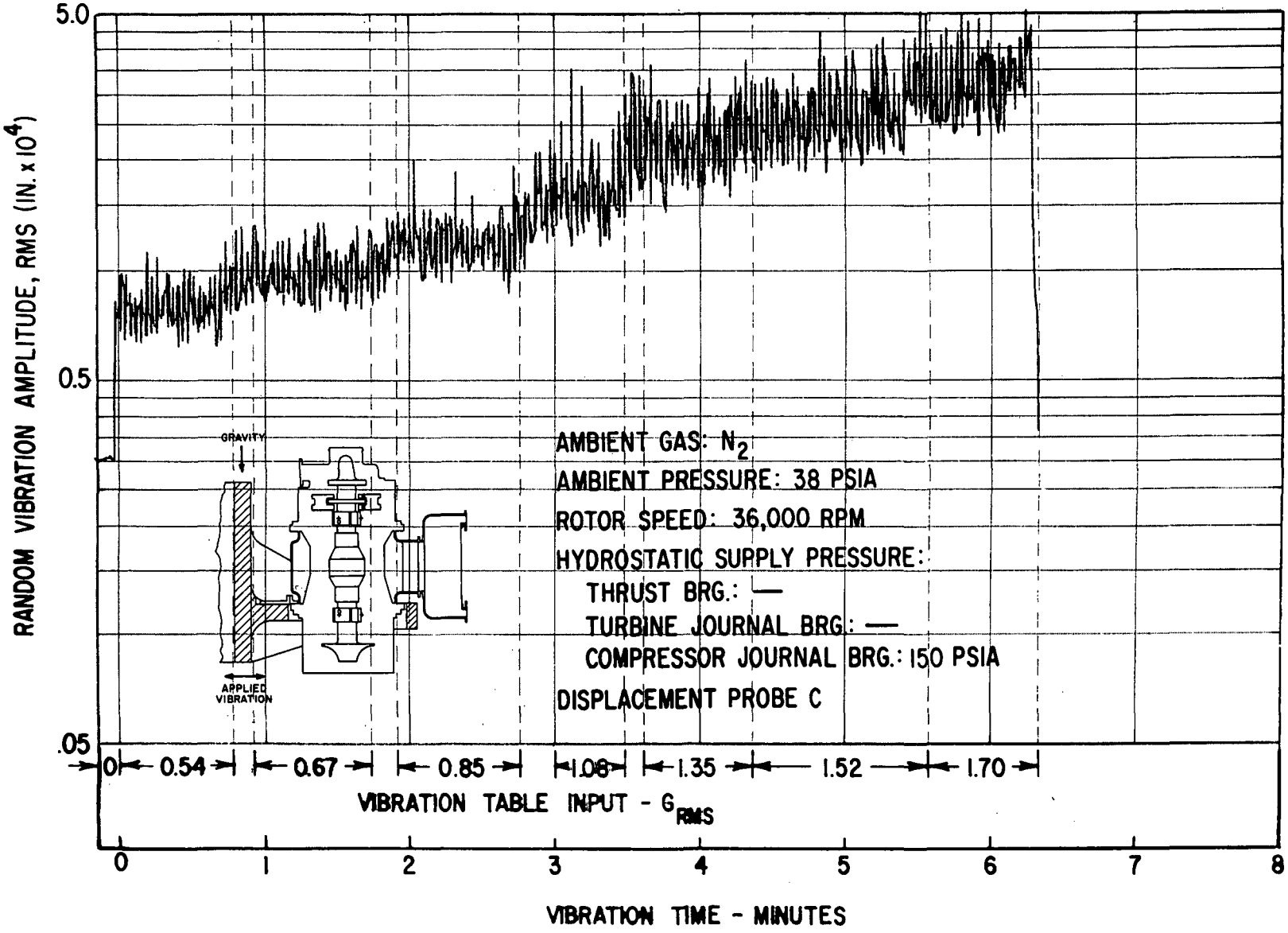

Fig. 132 Pad-To-Shaft Pivot Film Thickness Variation For Solid-Mounted Compressor Journal Bearing Pad Under Externally-Imposed Shaped Random Vibrations According To NASA Spec 417-2-C-3.5

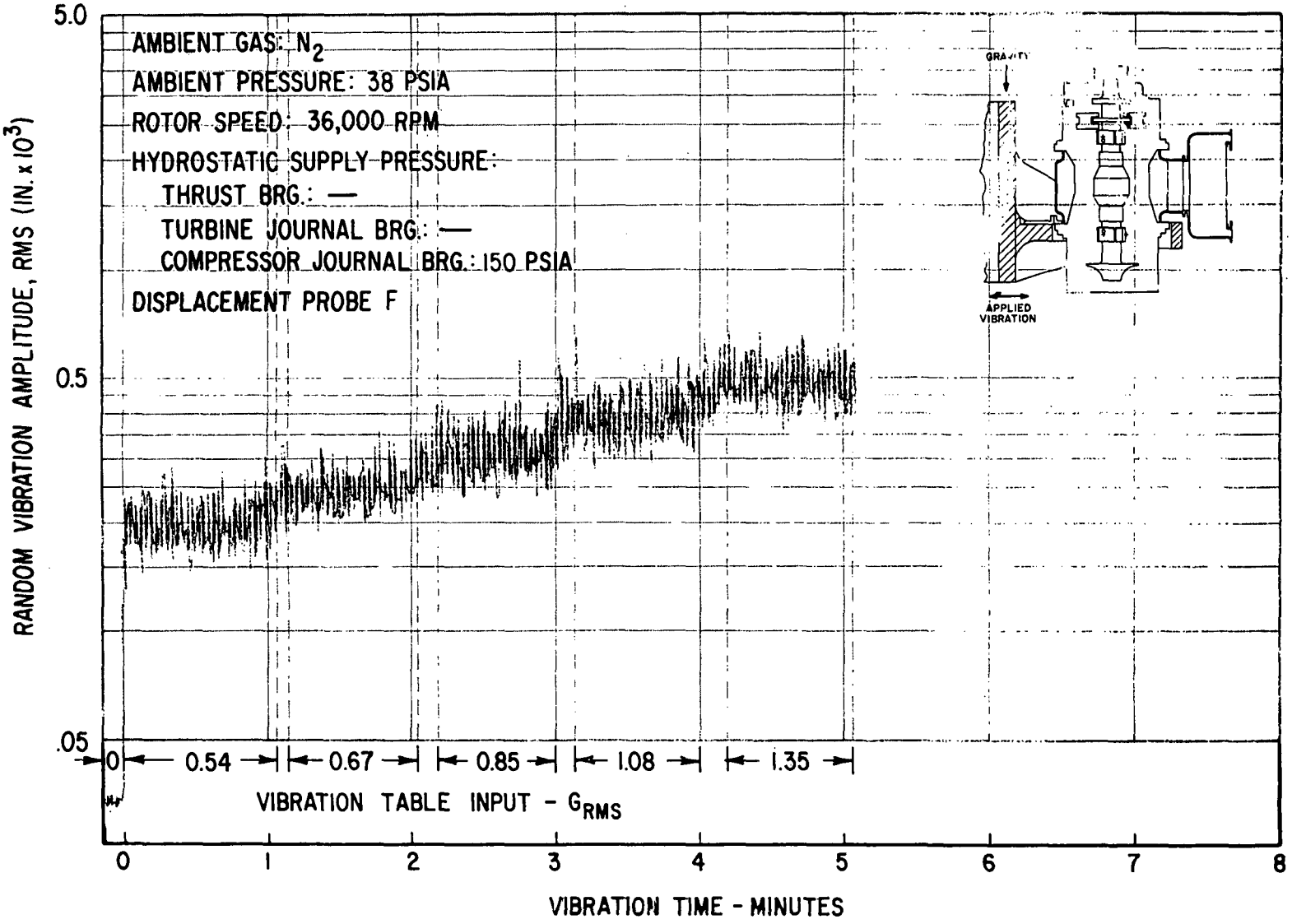

Fig. 133 Pad-To-Shaft Pivot Film Thickness Variation For Solid-Mounted Turbine Journal Bearing Pad Under Externally-Imposed Shaped Random Vibrations According To NASA Spec 417-2-C-3.5

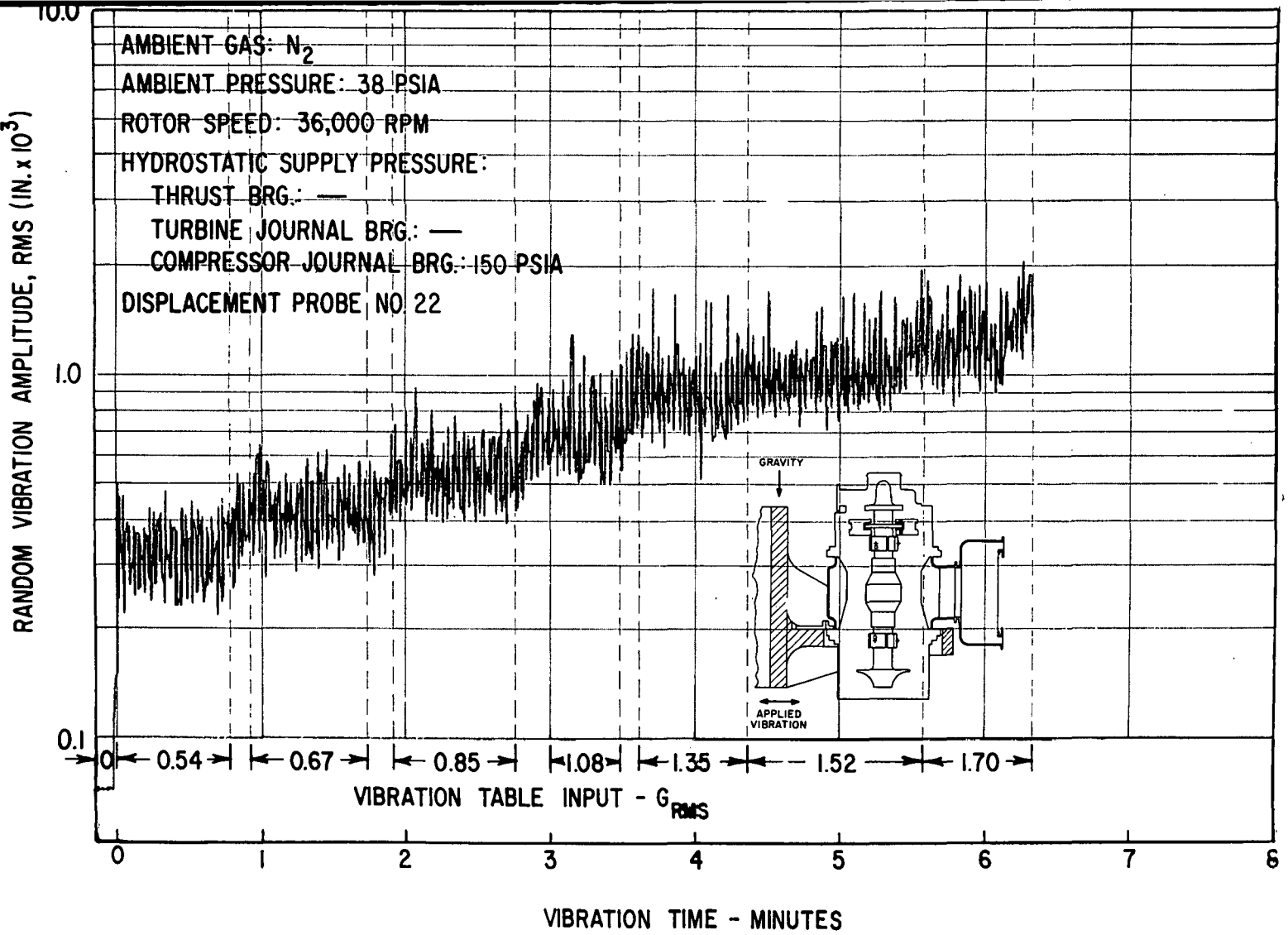

Fig. 134 Compressor Journal Flexure Amplitudes Under Shaped Random Vibrations According To NASA Spec 417-2-C-3.5

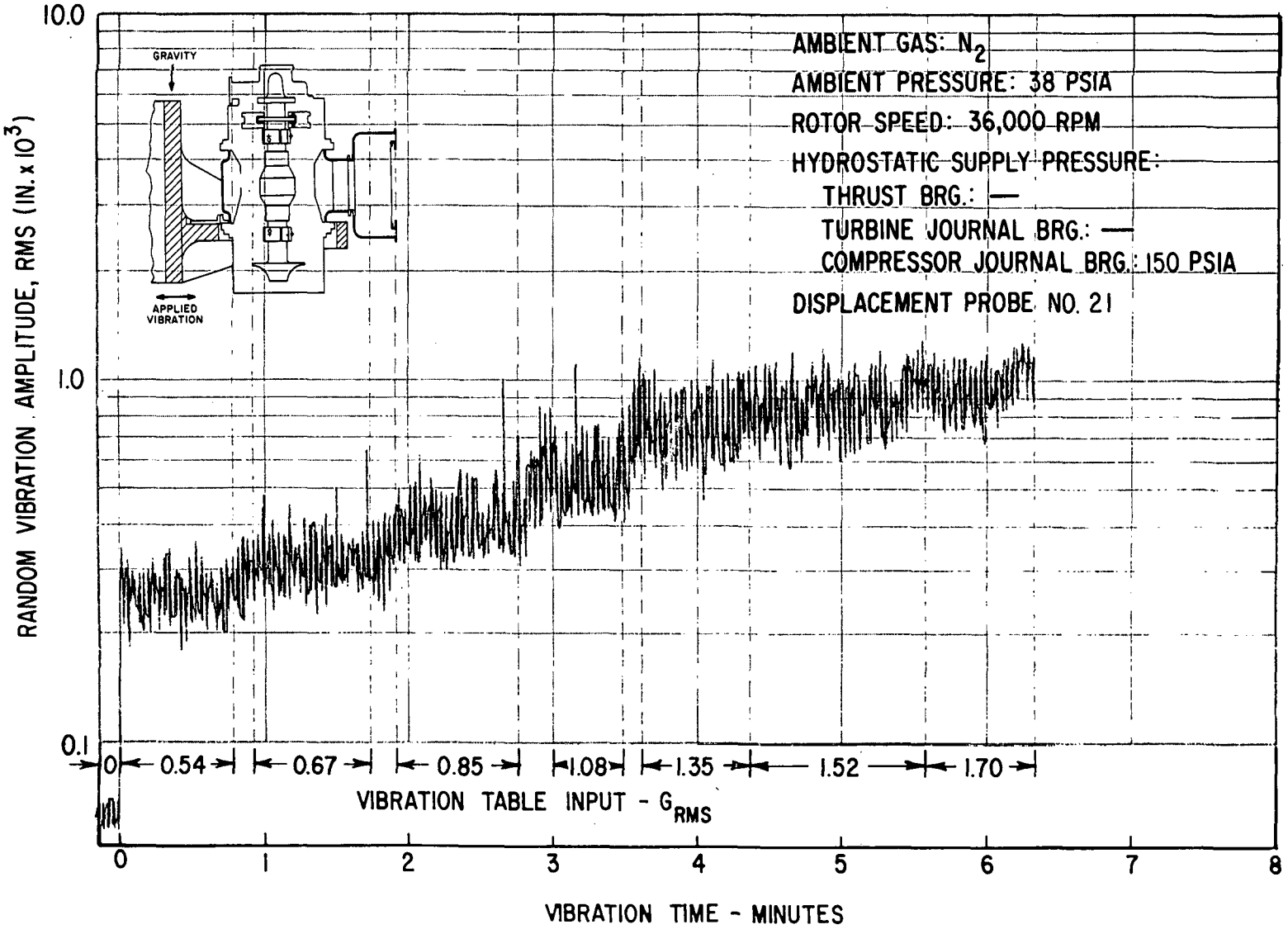

Fig. 135 Turbine Journal Flexure Amplitudes Under Shaped Random Vibrations According To NASA Spec 417-2-C-3.5

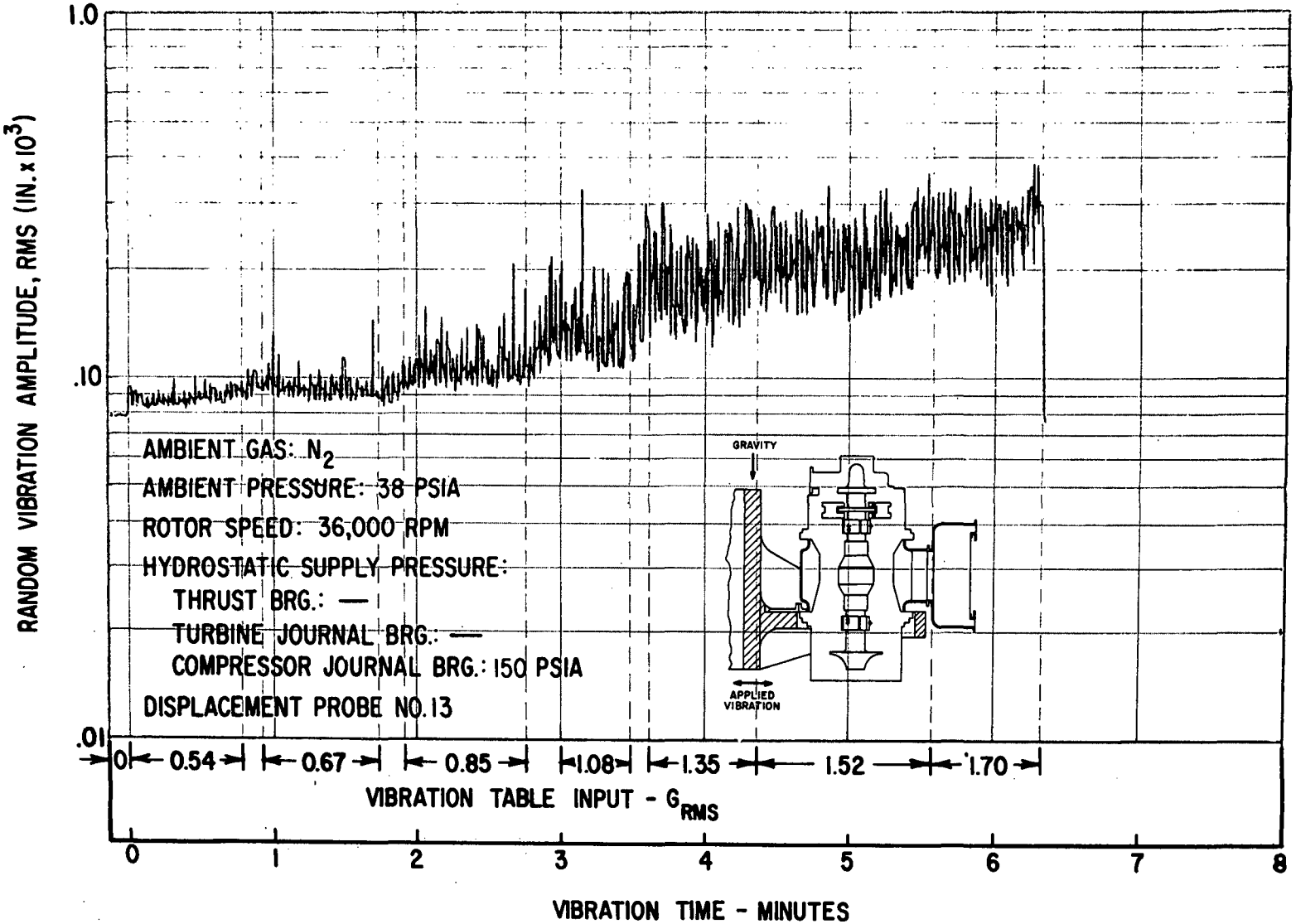

Fig. 136 Casing-To-Pad Leading Edge Amplitudes For Flex-Mounted Turbine Journal Bearing Pad Under Externally-Imposed Shaped Random Vibrations According To NASA Spec 417-2-C-3.5

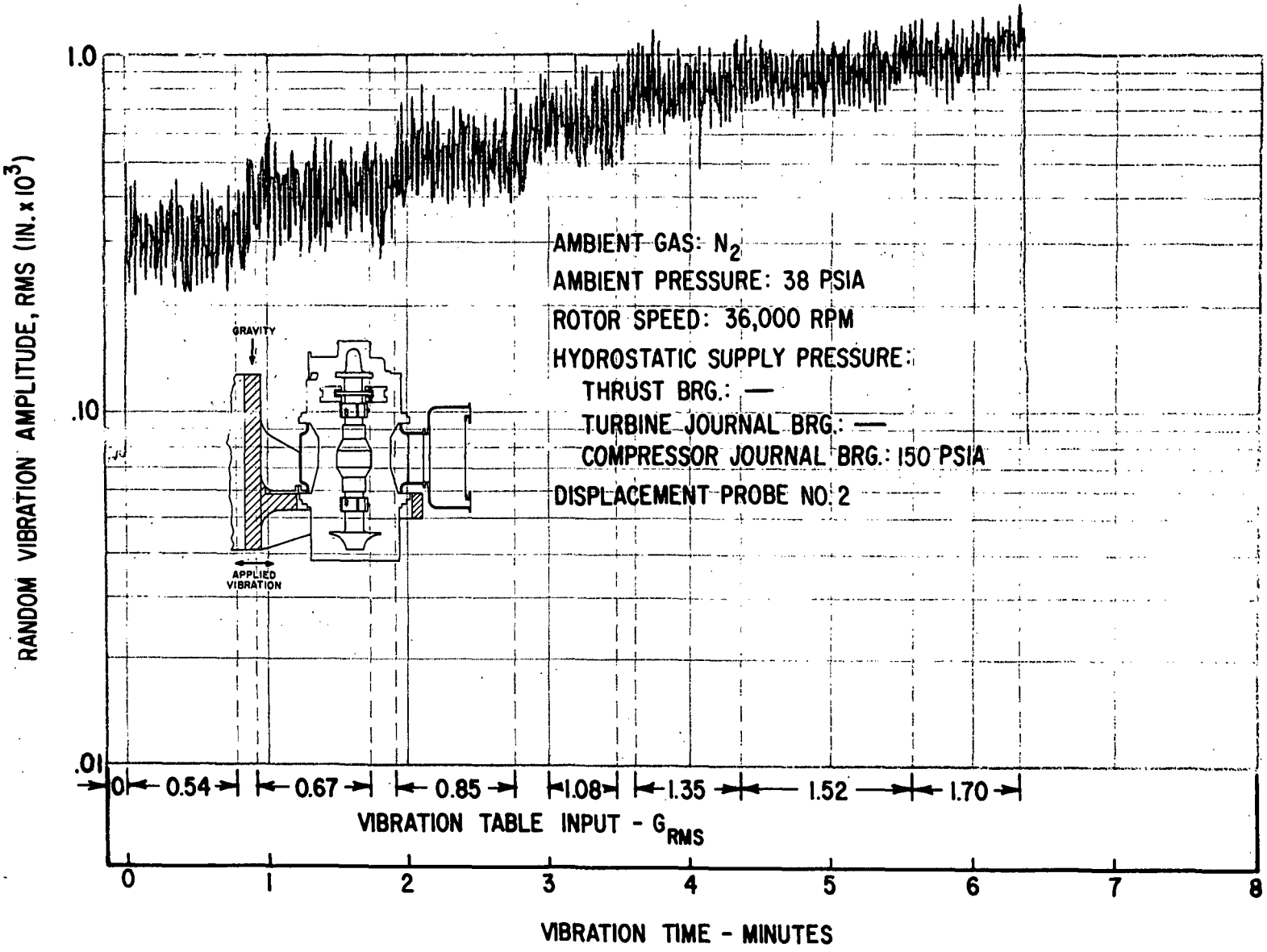

Fig. 137 Compressor Journal Rotor Amplitudes (Casing-To-Shaft) Under Shaped Random Vibrations According To NASA Spec 417-2-C-3.5

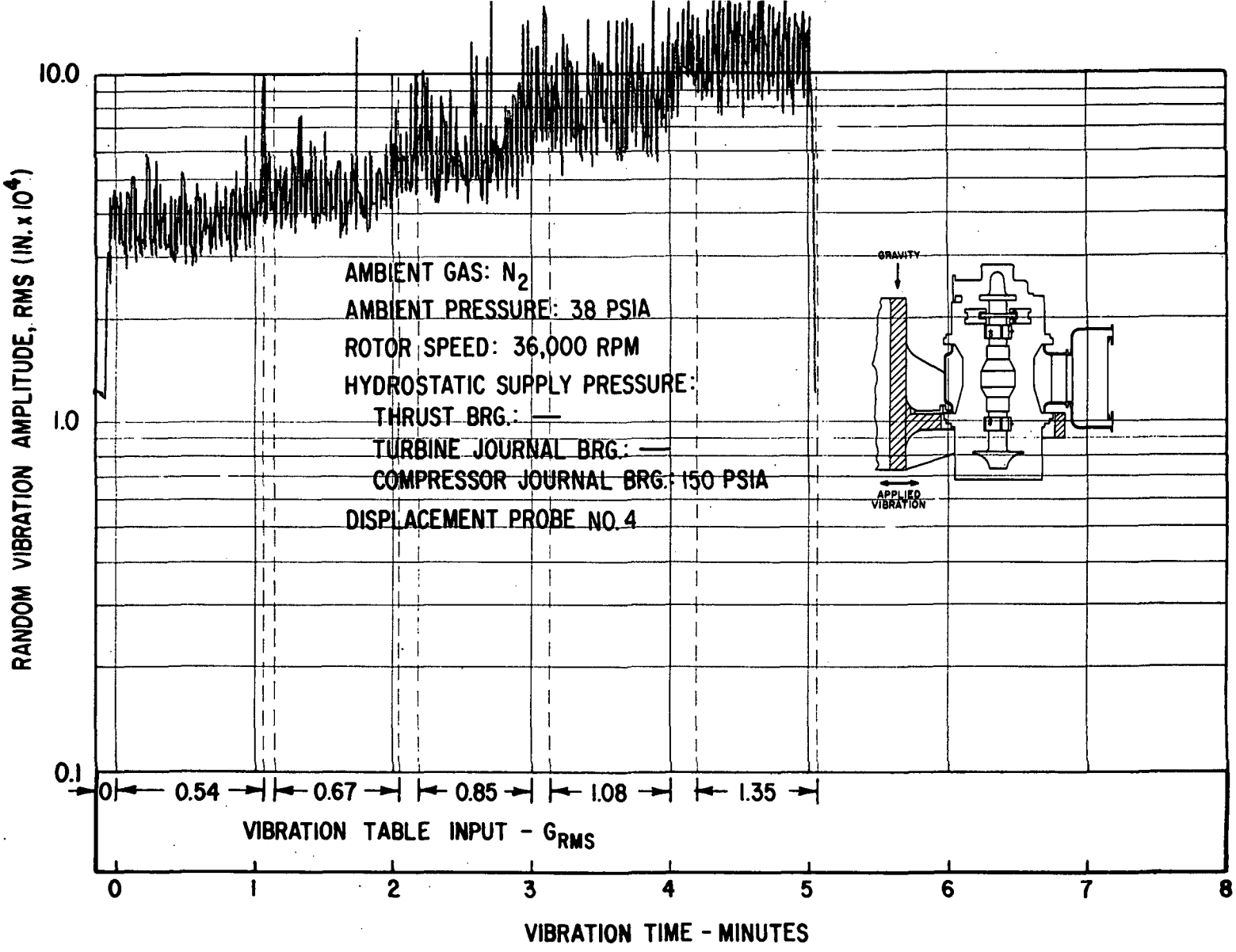

Fig. 138 Turbine Journal Rotor Amplitudes (Casing-To-Shaft) Under Shaped Random Vibrations According To NASA Spec 417-2-C-3.5

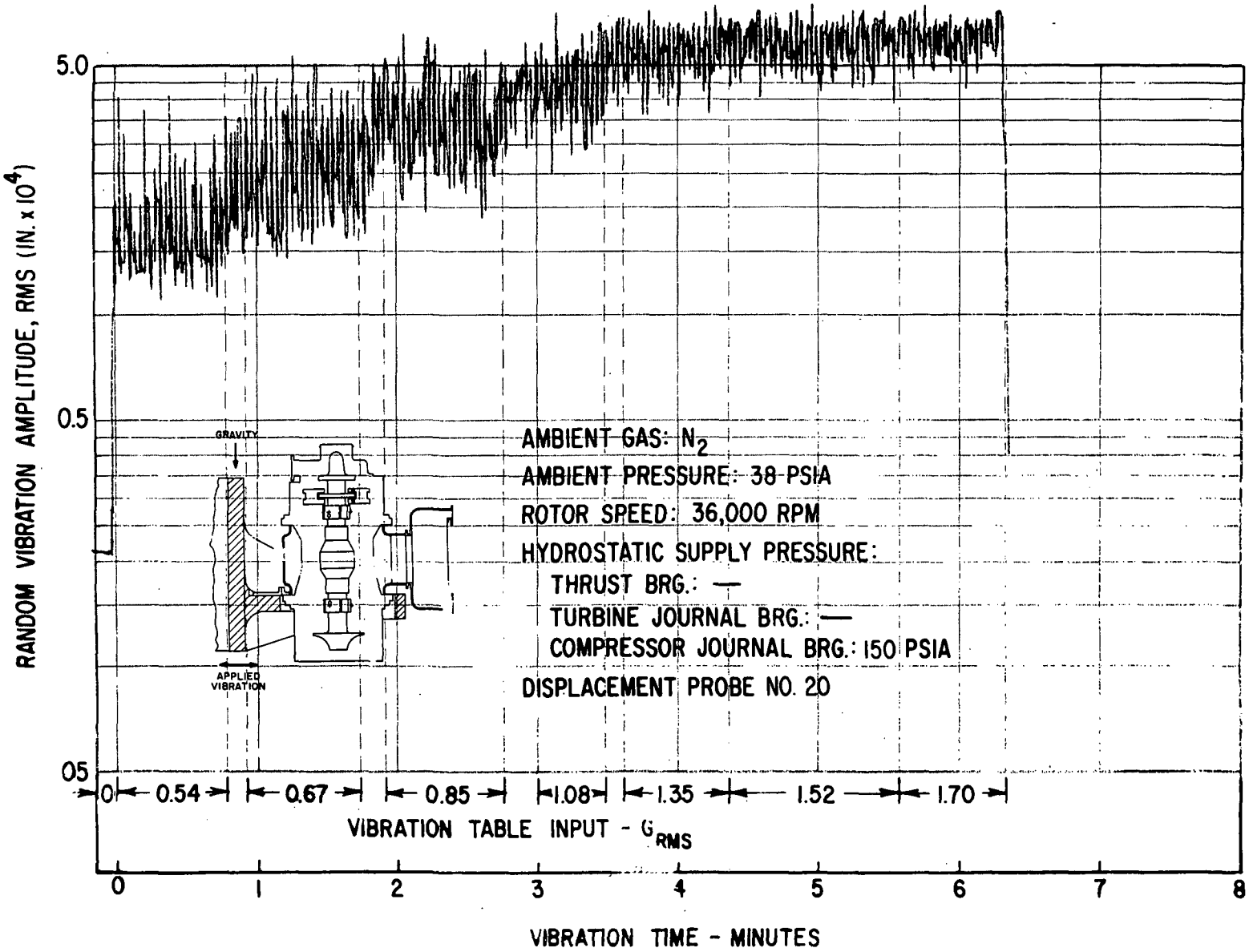

Fig. 139 Thrust Bearing Film Thickness Variation Under Externally-Imposed Shaped Random Vibrations According To NASA Spec 417-2-C-3.5

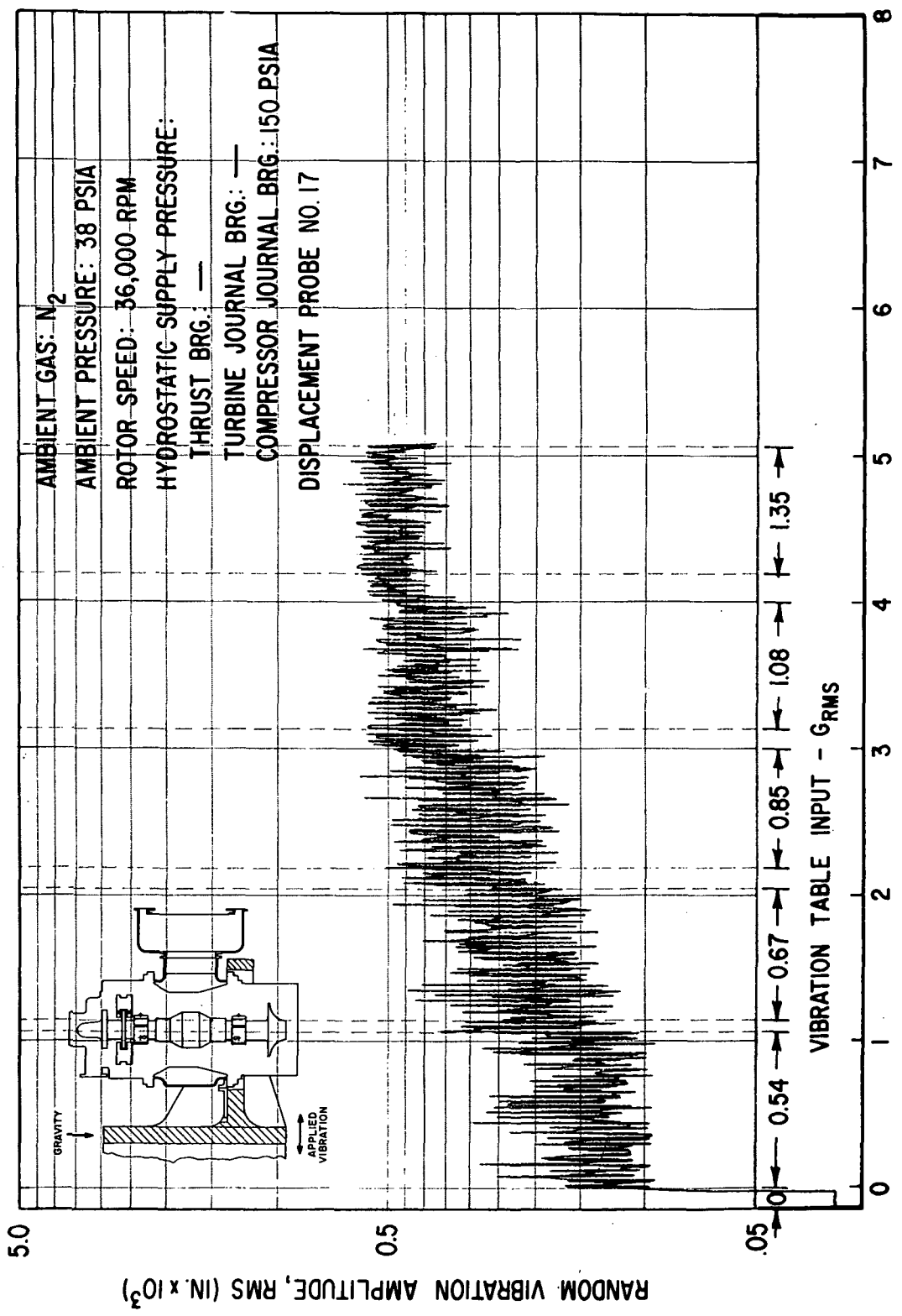

Fig. 140 Thrust Bearing Film Thickness Variation Under Externally-Imposed Shaped Random Vibrations According To NASA Spec 417-2-C-3.5

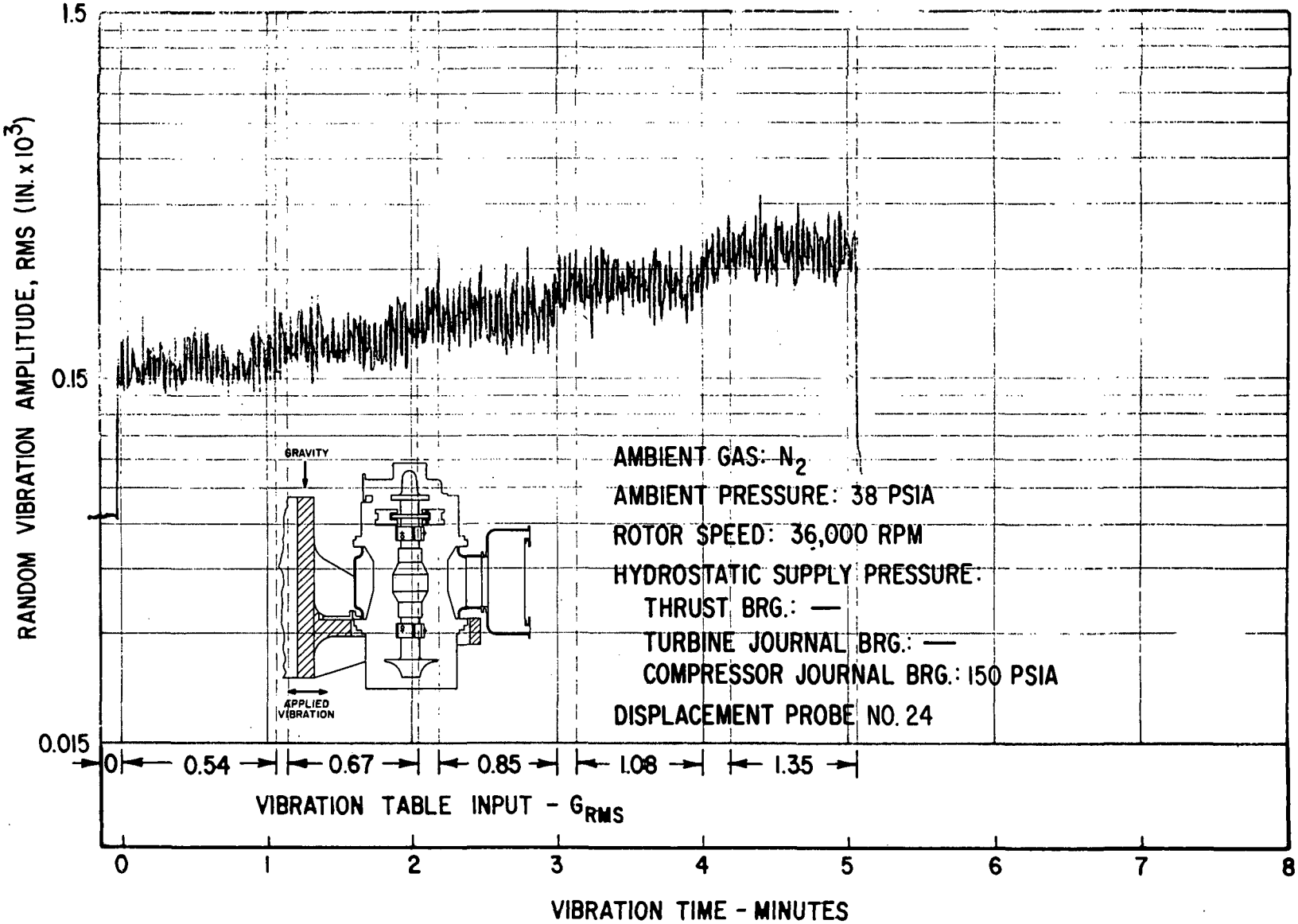

Fig. 141 Thrust Bearing Gimbal Amplitudes Under Shaped Random Vibrations According To NASA Spec 417-2-C-3.5

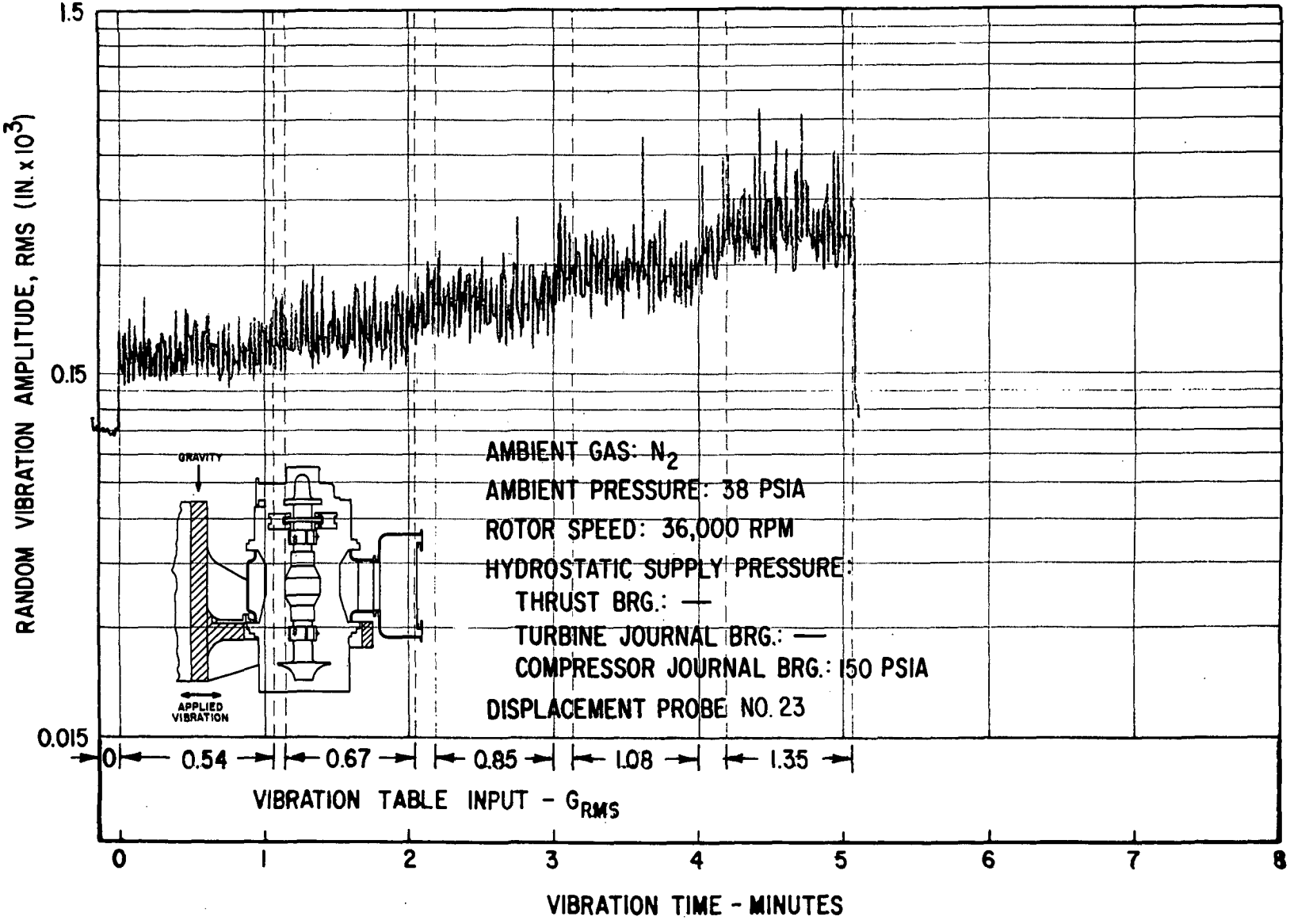

Fig. 142 Thrust Bearing Gimbal Amplitudes Under Shaped Random Vibrations According To NASA Spec 417-2-C-3.5

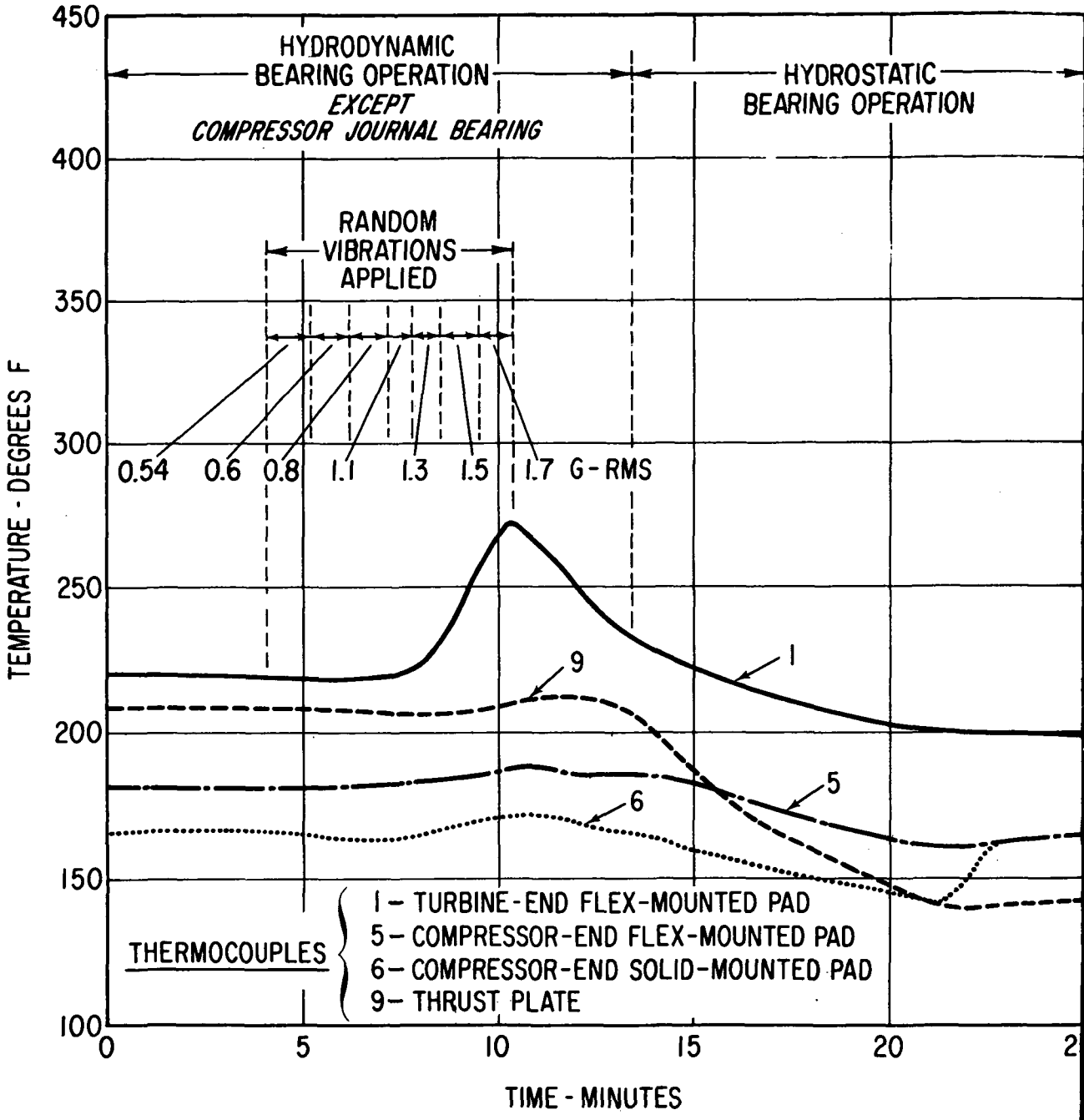

Fig. 143 Measured Temperatures In BRU Simulator Components With Transverse Random Excitation (Shaft Speed 36,000 rpm)

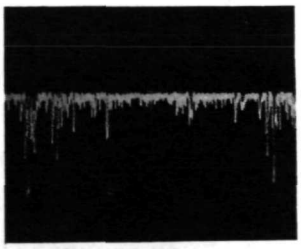

VERTICAL SCALE: 0.0005 IN./DIV.

DISPLACEMENT PROBE NO. 20

SEPARATION BETWEEN THRUST RUNNER AND THRUST PLATE

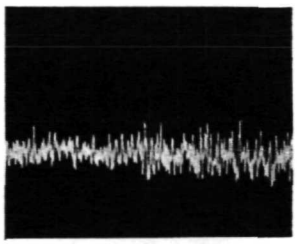

VERTICAL SCALE: 0.0015 IN./DIV.

DISPLACEMENT PROBE NO. 24

THRUST BEARING GIMBAL VIBRATIONS

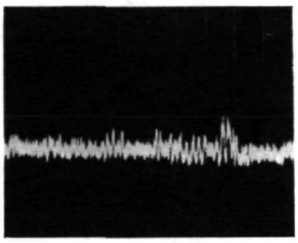

VERTICAL SCALE: 0.00025 IN./DIV.

DISPLACEMENT PROBE D

SEPARATION BETWEEN FLEX MOUNTED JOURNAL BEARING PAD AND ROTOR, TURBINE END

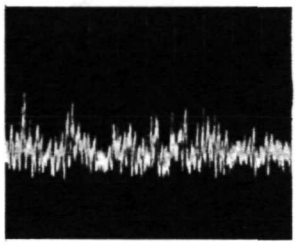

VERTICAL SCALE: 0.00025 IN./DIV.

DISPLACEMENT PROBE F

SEPARATION BETWEEN SOLID MOUNTED JOURNAL BEARING PAD AND ROTOR, TURBINE END

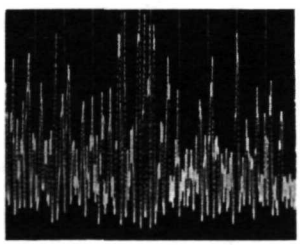

VERTICAL SCALE: 0.001 IN./DIV.

HORIZONTAL SCALE: 50 MSEC/DIV.

DISPLACEMENT PROBE NO. 21

FLEXURE VIBRATION, TURBINE END

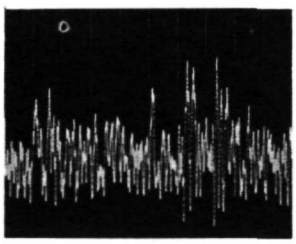

VERTICAL SCALE: 0.001 IN./DIV.

HORIZONTAL SCALE: 50 MSEC/DIV.

DISPLACEMENT PROBE NO. 3

VIBRATION OF ROTOR RELATIVE TO CASING, TURBINE END

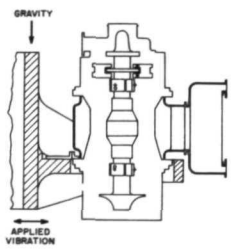

RANDOM VIBRATION INPUT LEVEL: 0.54 G_{RMS}

ROTOR SPEED: ZERO

HYDROSTATIC SUPPLY PRESSURE: –

Fig. 144 Rotor And Bearing Component Vibrations Under Shaped Random Vibrations According To NASA Spec 417-2-C-3.5

☆ U.S. GOVERNMENT PRINTING OFFICE: 1973 - 736-452, REGION NO. 3-II

"The aeronautical and space activities of the United States shall be conducted so as to contribute . . . to the expansion of human knowledge of phenomena in the atmosphere and space. The Administration shall provide for the widest practicable and appropriate dissemination of information concerning its activities and the results thereof."

—NATIONAL AERONAUTICS AND SPACE ACT OF 1958

NASA SCIENTIFIC AND TECHNICAL PUBLICATIONS

TECHNICAL REPORTS: Scientific and technical information considered important, complete, and a lasting contribution to existing knowledge.

TECHNICAL NOTES: Information less broad in scope but nevertheless of importance as a contribution to existing knowledge.

TECHNICAL MEMORANDUMS: Information receiving limited distribution because of preliminary data, security classification, or other reasons. Also includes conference proceedings with either limited or unlimited distribution.

CONTRACTOR REPORTS: Scientific and technical information generated under a NASA contract or grant and considered an important contribution to existing knowledge.

TECHNICAL TRANSLATIONS: Information published in a foreign language considered to merit NASA distribution in English.

SPECIAL PUBLICATIONS: Information derived from or of value to NASA activities. Publications include final reports of major projects, monographs, data compilations, handbooks, sourcebooks, and special bibliographies.

TECHNOLOGY UTILIZATION PUBLICATIONS: Information on technology used by NASA that may be of particular interest in commercial and other non-aerospace applications. Publications include Tech Briefs, Technology Utilization Reports and Technology Surveys.

Details on the availability of these publications may be obtained from:

SCIENTIFIC AND TECHNICAL INFORMATION OFFICE

NATIONAL AERONAUTICS AND SPACE ADMINISTRATION

Washington, D.C. 20546